An investigation into the role of Rab-Coupling Protein and EphA2 during cancer cell migration

Christine Gundry
MBiochem

Submitted in fulfilment of the requirements for the Degree of Doctor of Philosophy

Beaston Insitute for Cancer Research
College of Medical, Veterinary and Life Sciences
University of Glasgow

March 2015

Abstract

The gene encoding Rab-Coupling Protein (RCP), a Rab11 GTPase effector, is found on a chromosomal locus that is frequently amplified in cancer. We have previously shown that RCP drives $\alpha5\beta1$-integrin and EGFR recycling to the plasma membrane, thus contributing to the invasive migration of tumour cells. Using MALDI-TOF mass spectrometry, I have identified EphA2 and two Rab GTPases, Rab6 and Rab14, as novel RCP-associated proteins. Immunoprecipitation-based studies confirm these associations using several different cancer cell lines.

EphA2 is a receptor tyrosine kinase (RTK) that is required for contact inhibition of locomotion (CIL), and this process is thought to contribute to cancer cell invasion. To determine whether the EphA2-RCP association has functional significance, I tested whether RCP, Rab GTPases and other Rab11 effector proteins are required for CIL. siRNA knockdown of either RCP or Rab14 prevented efficient CIL, but depletion of Rab11 or Fip2 expression was ineffective in this regard. Likewise, HGF-induced scattering of cell colonies was opposed by suppression of EphA2, RCP or Rab14 expression. Since RCP and Rab14 are involved in RTK trafficking, EphA2 internalisation kinetics were investigated. HGF increased EphA2 trafficking in an RCP- and Rab14-dependent fashion. Live cell imaging demonstrated that EphA2 is delivered to an RCP and Rab14 positive compartment upon HGF treatment. Furthermore, HGF drove phosphorylation of RCP on Serine^{435}, which enhanced the association between EphA2, RCP and Rab14. Indeed, mutating the phosphor-acceptor site on RCP (RCP^{S435A}) reduced its association with EphA2 and Rab14, and blocked HGF-driven cell scattering.

EphA2 is frequently overexpressed in human pancreatic cancer and this is associated with poor patient prognosis. The role of EphA2 and RCP in metastasis was investigated in an autochthonous model of pancreatic ductal adenocarcinoma (PDAC) by crossing EphA2$^{-/-}$ and RCP$^{fl/fl}$ mice into the KPC (Pdx1-Cre, Kras$^{G12D/+}$, p53R$^{172H/+}$) PDAC model. Indeed, ablation of EphA2 or RCP expression in the mouse pancreas reduced the formation of liver metastases. Furthermore, PDAC lines from KPC EphA2$^{-/-}$ and KPC RCP$^{fl/fl}$ mice had a less scattered phenotype and were less invasive *in vitro* thus corroborating the observations indicating that EphA2 and RCP have an important role in cell-cell repulsion.

Table of Contents

List of Tables

List of Figures

List of Accompanying Material

Supplementary movies are provided as referred to in figures:

Figure 4.1 Suppression of RCP expression prevents efficient contact inhibition of locomotion – Movies 4.1 & 4.2

Figure 4.10 HGF-driven cell scattering is inhibited by depletion of EphA2 expression – Movies 4.3 – 4.6

Figure 4.12 HGF-driven cell scattering is inhibited by depletion of RCP expression – Movies 4.7 – 4.10

Figure 4.24 HGF increases the co-localisation between GFP-EphA2 and mCherry-RCP in vesicles – Movies 4.11& 4.12

Figure 4.26 HGF increases the co-localisation between GFP-EphA2 and mCherry-Rab14 in vesicles – Movies 4.13 & 4.14

Acknowledgements

I would like to thank Jim Norman for supporting and teaching me, and always being available to discuss my work with me. Kurt Anderson gave me helpful guidance as my advisor. Also, thanks to Karen Vousden for her support. I was financially supported by Cancer Research UK.

Many thanks to those I have collaborated with: Mary McCaffrey and Eoin Kelly for the Rab14 work and supplying reagents and plasmids; Patrick Caswell and Andrew Campbell for their help and expertise on phospho-RCP; Bryan Miller, Jen Morton, Joan Grindlay and Louise Mitchell for their contribution to the *in vivo* work; and Anna Hogeweg who was a Master's student who worked with me on a phospho-RCP project. I would like to express my gratitude to many people I have had interesting discussions with at the Beatson Institute, including Patricia Muller and members of the R20 lab. Many thanks to the Beatson service staff for their help, especially those in the Beatson Advanced Imaging Reseource.

During my studies I was diagnosed and successfully treated for mouth cancer and I would like to thank all those who have helped me get through my treatment, in particular my medical team in the Maxillofacial Department at the Southern General Hospital. Thanks to my friends in Glasgow, many of whom work at the Beatson Institute, who have encouraged me and helped me through the difficult days. Lastly, I'd like to thank my family, especially my husband, Adam.

This thesis is dedicated to the memory of Esther White, who asked big questions and had an infectious smile.

Author’s Declaration

I declare that I am the sole author of this thesis, except where explicit reference is made as to the work of others.

Abbreviations

ADAM	a disintegrin and metalloproteinase
AEBSF	4-(2-Aminoethyl)benzynesulphonyl fluoride
ALDH	aldehyde dehydrogenase
AMPA	α-amino-3-hydroxy-5-methyl-4-isoxazolepropionic acid receptor
ALLN	acetyl-Leu-Leu-Norleu
BSA	bovine serum albinum
CDM	cell derived matrices
CFTR	cystic fibrosis transmembrane conductance regulator
CIL	contact inhibition of locomotion
CYS	cysteine
BLAST	basic local alignment search tool
CUB	complement component Clr/Cls, Uegf, and bone morphogenic protein
DAG	diacylglycerol
DGK	diacylglycerol kinase
DMEM	dulbecco's modified eagle medium
ECM	extracellular matrix
EE	early endosomes
EEA1	early endosome antigen 1
ECL	enhanced chemiluminescence
EGFR	epidermal growth factor receptor
EHD	EPS15 homology domain-containing protein
ELISA	enzyme-linked immunosorbent assay
EMT	epithelial mesenchymal transition
Fc	Fragment crystallised (region of an antibody)
FN	fibronectin
FIP	family of interacting proteins
FRAP	fluorescence recovery after photobleaching
GFP	green fluorescent protein
GFPf	farnesylated green fluorescent protein
GPI	glycophosphatidylinositol
H & E	hematoxylin and eosin
HDF	human dermal fibroblasts
HGF	hepatocyte growth factor
HIF	hypoxia-inducible factor
IAA	iodoacetamide
IB	immunoblot
IgG	immunoglobulin G
IP	immunoprecipitate
IF	immunofluorescence
KPC	Pdx1-Cre, $Kras^{G12D/+}$, $p53^{R172H/+}$
LB	lysogeny broth
LCCL	*Limulus* factor C, cochlear protein (Coch-5b2) and late gestation lung protein (Lgl1)
LBD	ligand binding domain
LE	late endosomes
LMTK	lemur tyrosine kinase
LMW-PTP	low molecular weight – protein tyrosine phosphatase
MALDI-TOF	matrix-assisted laser desorption - ionization-time of flight
MAPK	mitogen-activated protein kinase

MDCK	Madin-Darby canine kidney
MES	2-(*N*-morpholino)ethanesulfonic acid
MesNa	sodium 2-mercaptoethanesulfonate
MOPS	3-(N-morpholino)propanesulfonic acid
MT1-MMP	membrane-associated, type 1 transmembrane matrix metalloprotinase
NCC	neural crest cells
NDLB	non-denaturing lysis buffer
NP-40	nonylphenoxy polyethoxy ethanol
NS	not statistically significant
NSCLC	non-small cell lung carcinoma
NT	non-targeting
OPA	ortho-phenylenediamine
OPN	osteopontin
PA	phosphatidic acid
PAGE	polyacrylamide gel electrophoresis
PBM	PDZ domain binding motif
PBS	phosphate buffer saline
PCP	planal cell polarity
PCR	polymerase chain reaction
PDAC	pancreatic ductal adenocarcinoma
PDZ	post synaptic density protein (PSD95), drosophila disc large tumor suppressor (Dlg1), and zonula occludens-1 protein (zo-1)
PFA	paraformaldehyde
PNRC	perinuclear recycling compartment
PQ	primaquine
PRR	proline rich region
PVDF	polyvinylidene fluoride
RBD	rab binding domain
RC	recycling compartment
RCP	rab coupling protein
RTK	receptor tyrosine kinase
SAM	sterile alpha motif
SEM	standard average of the mean
SER	serine
SDS	sodium dodecyl sulphate
SOC	super optimal broth with catabolite repression
SP	smart pool
TBS	tris-buffered saline
Tfn-R	transferrin receptor
TM	transmembrane
TNF	tumour necrosis factor
TK	tyrosine kinase
THR	threonine
TYR	tyrosine

1 Introduction

1.1 Cancer metastasis

1.1.1.1 The hallmarks of cancer

Cancer is an ancient disease dating back to the dinosaur era (Rothschild et al., 2003) and which now occurs in the majority of multicellular organisms. Carcinomas are the most common form of human cancer. They arise from epithelial cells and account for 80% of cancer deaths (Weinberg, 2007). Other types of tumour include sarcomas, which arise from mesenchymal cells; haemopoietic cancers, which arise from immune cells; and neuroectodermal tumours, which arise from the nervous system and melanomas (Weinberg, 2007). Cancer can be compared to a complex organ, since it is comprised of many different cells co-operating together. Each tumour has its own array of developing genetic mutations and epigenetic changes, and adapts to its surroundings in a similar fashion to Darwinian evolution but at a much more rapid pace. In 2000, Hanahan and Weinberg categorised 6 key features that tumour cells must acquire to render them malignant, termed the hallmarks of cancer (Hanahan and Weinberg, 2000). New studies have revealed other characteristics that tumour cells require for malignancy, which has increased the number of hallmarks of cancer to 10 (Hanahan and Weinberg, 2011). These hallmarks are: genome instability and mutation, sustaining proliferative signals, evading growth suppressors, enabling replicative immortality, avoiding immune destruction, tumour promoting inflammation, inducing angiogenesis, deregulating cellular energetics, resisting cell death and activating invasion and metastasis (Hanahan and Weinberg, 2011). As 90% of cancer deaths are caused by secondary tumours, which have arisen from primary tumours (Leber and Efferth, 2009), it is apparent that metastasis is important to investigate.

1.1.1.2 Metastasis in human cancer

Metastasis is a complex process, which has been described as a cascade divided into five key steps (**Figure 1.1**) (Leber and Efferth, 2009). First, cancer cells detach from the primary tumour, secrete proteases to degrade the extracellular matrix and activate cell migration. Second, intravasation occurs in which cancer cells migrate into the lumen of a blood or lymphatic vessel. Third, the tumour

cell travels through the circulation system to a distant site. For a cancer cell to survive in the circulation it must overcome anoikis (anchorage-dependent cell death) and survive high shear forces. Fourth, extravasation occurs in which the cancer cell leaves the blood vessel. This can occur by two mechanisms; either the cell proliferates in the vessel until the vessel wall is destroyed, or the cell degrades the endothelium and basement membrane in a similar fashion to intravasation (Leber and Efferth, 2009). The final step is colonisation of the new site, which requires cell proliferation, angiogenesis and survival in the new environment. There is clear evidence that tumours metastasise to particular sites, for example pancreatic cancer tends to metastasise to the liver, lung and peritoneum. Metastasis via blood or lymphatic vessels is complex and the cancer cells have to adapt to several environmental changes and unfavourable conditions to survive. There is increasing evidence that some types of cancer, such as leukemias and ENT tumours, metastasise via perineural invasion of nerves (Liebig et al., 2009), and more work is required to understand this route of metastasis.

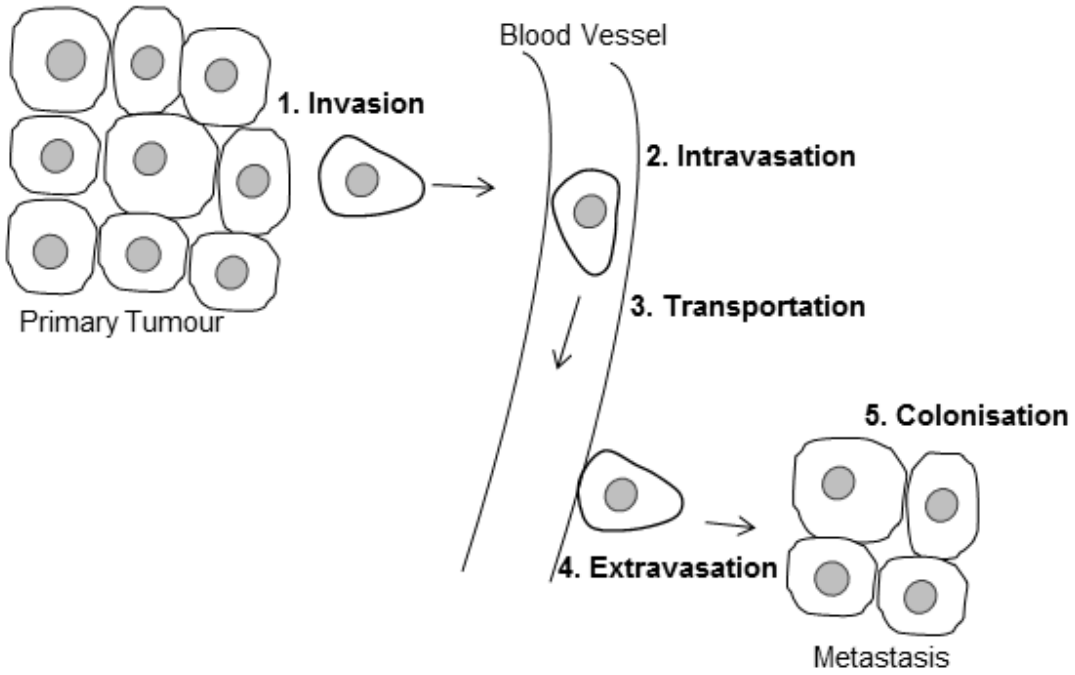

Figure 1-1 Cancer metastasis cascade
Cancer metastasis is a multi-step process: tumour cells invade neighbouring tissue, intravasate into blood vessels, are transported in the blood, extravasate out of the vessel and colonise another tissue.

1.1.1.3 Complexity of cell migration in metastasis

Successful metastasis requires cancer cells to migrate in different environments, therefore, they must adapt to their surroundings. Cancer cell migration *in vivo* is complex and controlled by many mechanisms. Despite this, many findings in cell migration *in vitro* are also apparent *in vivo*. Cancer cell migration may be determined by a number of factors. First, the complement of misregulated and mutated genes will define how a cancer cell migrates and responds to different environmental cues. The tumour microenvironment encompasses both the extracellular matrix (ECM) and other cells. The ECM is composed of a complex mix of proteins, such as fibronectin and collagen. Its components and stiffness can affect cell migration (Levental et al., 2009). Cells neighbouring cancer cells (such as stromal cells) can promote cancer cell invasion, for example, cancer associated fibroblasts (Kalluri and Zeisberg, 2006). These cells and the cancer cells themselves can secrete soluble factors, such as growth factors, that can stimulate the cancer cells to migrate. Also, cancer cell migration will depend on whether contact with other cancer cells or stromal cells promotes cell-cell adhesion or repulsion (**Section 1.1.3**). All these factors will determine whether a cancer cell invades and which mechanism it will adopt.

1.1.2 Cell migration

Cell migration is essential for normal physiological processes such as embryonic development, wound healing and immune response as well as during cancer cell metastasis. Cell migration is dependent on molecular parameters, physical forces and the microenvironment and can be divided into two broad categories: collective cell migration and single cell migration.

1.1.2.1 Collective cell migration

Cells migrate collectively in several physiological processes, such as mammary gland branch morphogenesis, wound healing, vascular sprouting and neural crest migration (Carmona-Fontaine et al., 2008; Ewald et al., 2008). While these processes are fairly well understood *in vitro*, the mechanisms and kinetics of collective migration *in* vivo are less well understood. Collective invasion of this type is observed by histology in many tumour types, such as breast, prostate and pancreatic cancer (Christiansen and Rajasekaran, 2006). During collective cell

migration, some carcinoma cells can continue to assume a more epithelial-type morphology (Christiansen and Rajasekaran, 2006), whilst maintaining functional cell-cell contacts, such as tight and adherence junctions (Theveneau and Mayor, 2012). In contrast, some cancers including melanoma and breast cancer contain small strands of migrating cells with the cytoskeleton of each cell acting independently (Hegerfeldt et al., 2002; Roussos et al., 2011). The organisation of collective cell migration is maintained by cell adhesion to the ECM, guided by growth factors and proteolysis (Friedl et al., 2012). There is evidence that during this migration there are leading cells that degrade the ECM and following cells that increase the diameter of the gap in the ECM allowing more cells to follow (Wolf et al., 2007). Indeed, cancer-associated fibroblasts can lead the invasive process of cancers that retain epithelial traits (Ewald et al., 2008).

1.1.2.2 Single cell migration

Once separated from their neighbours, cancer cells can migrate individually via several different mechanisms. The strategy of single cell migration depends on the strength of cell adhesion with the ECM, cytoskeleton contractibility, and the capability of remodelling and clearing a path in the ECM (Ridley et al., 2003). Two main types of single cell migration have been identified, mesenchymal and amoeboid, however, this is probably an over-simplification. Mesenchymal migration is characterised by cell elongation and requires extracellular proteolysis, while in amoeboid migration the cell is rounded, less dependent on proteolysis but has an elevated contractility of the actin cytoskeleton (Sanz-Moreno and Marshall, 2010). Cancer cells originating from different tissues often employ different modes of migration, for example, sarcomas and carcinomas normally migrate mesenchymally (Davies et al., 2005b), while, haematopoietic cancer cells adopt amoeboid migration (Friedl et al., 2001). Cancer cells can switch between different types of single cell migration, depending on the relative activities of Rho GTPase sub-families, which enables cancer cells to adapt and migrate in the appropriate way for their environment (Sanz-Moreno et al., 2008).

1.1.3 Contact inhibition of locomotion (CIL)

1.1.3.1 Historical perspective

Contact inhibition of locomotion (CIL) was defined by Michael Abercrombie in 1979 as: 'the stopping of the continued locomotion of a cell in the direction which has produced a collision with another cell' (Abercrombie, 1979). His studies on the social behaviour of cells were performed by placing two explants of chicken embryonic cells close together and observing fibroblast migration when they collide with each other (Abercrombie and Heaysman, 1954). CIL can occur between the same cell type (homotypic) or between different cell types (heterotypic) (Abercrombie, 1970). More recently a typical sequence of events has been used to define reciprocal CIL: two migrating cells collide into each other, protrusions at the site of contact are inhibited, new protrusions form at a new site away from the collision point and the cells migrate in the direction that the new protrusions have formed (**Figure 1.2A**) (Carmona-Fontaine et al., 2008). This description includes not just contact inhibition, but also includes subsequent cell-cell repulsion. However, some cells respond differently, and fail to form a new protusion and migrate after collisions.

Since Abercrombie's initial explant experiments, several different techniques have been developed to analyse CIL. CIL can be measured between two single cells in culture. Simple methods to quantify CIL on 2D surfaces include measuring the time cells remain in contact during collisions (Stramer et al., 2010), comparing the position of cells before and after a collision (Matthews et al., 2008) or illustrating the positions of *de novo* versus existing protrusions after CIL (Kadir et al., 2011). More recently, several studies have used the contact acceleration index (Cx) to quantify CIL (Astin et al., 2010; Sugiyama et al., 2013), by tracking each cell's migratory path before and after the collision. This index represents the difference between where the cell would have progressed if there had been no collision and where the cell has actually migrated. To determine how collisions have altered the cell's path, Cx is compared between colliding and free-moving cells. There are several limitations to using Cx, including the fact that the cells stay in contact for different periods of time and often rotate whilst in contact, thus altering the direction of subsequent cell migration. Also, cells have a stronger repulsive response in head-on collisions

(leading edge to leading edge) compared to side-on collisions (leading edge to cell body) (Abercrombie and Dunn, 1975), so it is essential to carefully compare like-for-like collisions when analysing this data. It is best to use a combination of methods to analyse CIL, as all of them have different drawbacks.

1.1.3.2 The functions of contact inhibition of locomotion

To date a variety of proteins have been shown to be required for CIL (**Table 1.1**), however further work is required to achieve a better mechanistic understanding of CIL. CIL is thought to contribute to several processes, such as development, axon guidance and angiogenesis, and I have summarised these in the following sections.

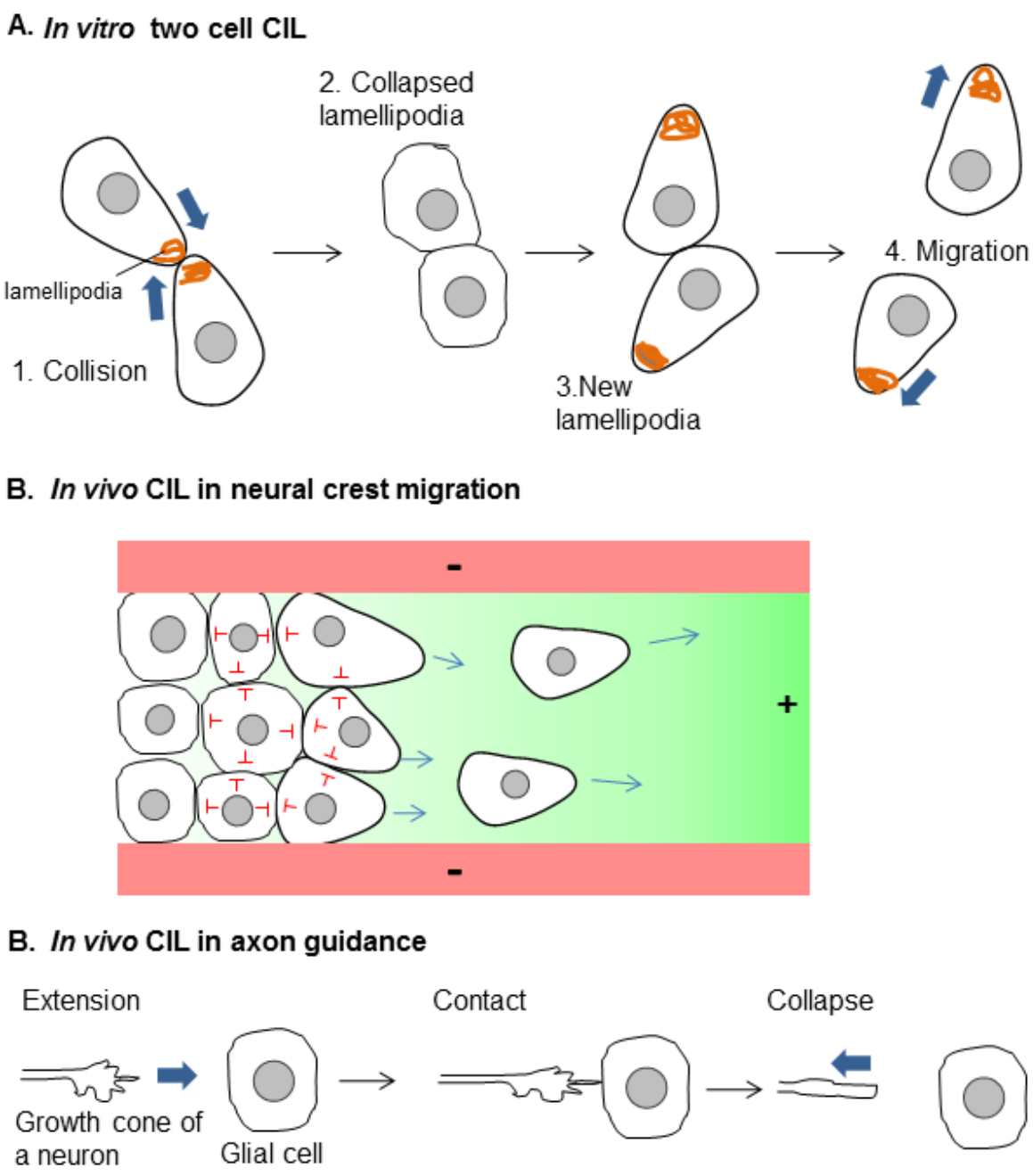

Figure 1-2 Contact inhibition of locomotion *in vitro* and *in vivo*
A. *In vitro* contact inhibition of locomotion occurs when two migrating cells collide. Their lamellipodia collapse upon contact and then the cells form new lamellipodia away from the site of collision. The cells migrate away from each other. B. Neural crest cell migration is regulated by contact inhibition of locomotion and chemotactic signals (represented with + and -). Cells surrounded by others, undergo CIL preventing the formation of lamellipodia (red inhibition signs), however, cells at the front form lamellipodia and can migrate away (blue arrows). C. During axon guidance the growth cone extends and comes into contact with other cells. If it is an unfavourable cell, upon contact, the growth cone collapses and moves away from the cell.

Protein	Role in contact inhibition of locomotion (CIL)
Cadherins	Downregulation of E-cadherin reduces CIL in epithelial cells (Bracke et al., 1997), while in myoblasts overexpressing N-cadherin prevents repulsion after a cell-cell collision (Huttenlocher et al., 1998).
Cdc42	Cdc42 is activated by EphB3/B4 in heterotypic collisions between fibroblasts and PC3 cells resulting in defective CIL (Astin et al., 2010).
Ephs and Ephrins	EphA4/B1 and EphrinB1 are expressed in distinct cell populations in embryonic development. Disrupting this expression results in failure of CIL and cells migrate into different territories (Smith et al., 1997). Several different Ephs and Ephrins are expressed in prostate cancer cells in which they have a role in CIL, influencing invasion and metastasis (Astin et al., 2010).
Integrin	Ectopically expressing α5-integrin in myoblasts inhibits migration upon cell-cell contact, resulting in aggregates of cells. Without cell-cell contact these cells migrate normally (Huttenlocher et al., 1998).
Microtubules	Microtubules de-stabilise at the cell-cell contact site and stabilise in the new lamellipodia in macrophages colliding *in vitro* (Kadir et al., 2011). Disruption of microtubules in haemocytes prevent CIL *in vivo* during embryogenesis (Stramer et al., 2010).
Nectins	Necl-5 is localised in the lamellipodia of fibroblasts. Upon collision it associates with Nectin-3, resulting in Necl-5 downregulation and reducing cell movement (Fujito et al., 2005; Takai et al., 2008).
Notch	Notch is found on growth cones while its ligand Delta is expressed on neighbouring cells. This guides the growth cone to repel or adhere its neighbouring cells (Crowner et al., 2003; Šestan et al., 1999).
Par3	Par3 is essential for CIL in neural crest migration. It reduces microtubule catastrophe at the contact site (Moore et al., 2013).
Rac1	Dominant negative Rac1 expression results in defective heterotypic CIL in fibroblast explant experiments by altering RhoA activation (Anear and Parish, 2012).
RhoA	RhoA is required for efficient CIL in neural crest cells (Carmona-Fontaine et al., 2008) and in fibroblasts (Kadir et al., 2011).
ROCK	Inhibition of ROCK in fibroblasts prevents CIL and cell-cell repulsion by mediating the microtubule cytoskeleton (Kadir et al., 2011). In PC3 cell retraction, EphAs signal to ROCK, which regulates actomyosin contractibility (Astin et al., 2010).
Semaphorins	Semaphorins and their receptors, neuropilins and plexins, have a role in growth cone guidance (Koropouli and Kolodkin, 2014) and development. Sema3F and Npn2 are expressed in distinct cell populations, which is required for cranial neural crest development (Gammill et al., 2007).
Wnt	Inhibition of the non-canonical Wnt and PCP pathway prevents efficient CIL and directionality of neural crest cell migration *in vivo*. Wnt is found at the cell-cell contact site, which activates RhoA (Carmona-Fontaine et al., 2008; Matthews et al., 2008).

Table 1-1 Role of proteins in contact inhibition of locomotion

Development

CIL has a role in development and has been most studied in neural crest cell (NCC) migration in *Xenopus*, *Zebrafish*, Chick and *Drosophila* embryogenesis (Davis et al., 2012; Kulesa and Fraser, 2000; Teddy and Kulesa, 2004). NCCs are highly migratory and are capable of differentiating into many different cell types, including neurons, Schwann cells, melanocytes and odontoblasts. *In vitro* studies have shown that NCCs undergo homotypic CIL, but not heterotypic CIL with mesodermal cells (Carmona-Fontaine et al., 2008). *In vivo*, CIL and chemotaxis work together so that NCCs migrate in a coordinated fashion through the embryo (**Figure 1.2B**). CIL inhibits trailing cells from forming protrusions and migrating away from the pack, while inhibitory signals prevent cell dispersal into the surrounding area. In contrast, CIL promotes the formation of protrusions and migration of the leading cells away from each other (Carmona-Fontaine et al., 2008). External signals promote migration of the leader cells in one particular direction, thus it is through a combination of chemotaxis and CIL that NCCs migrate in such a coordinated fashion. Furthermore, *in vivo* studies in *Drosophila* embryos, in which haemocytes are fluorescently labelled and tracked in real time, demonstrate that CIL is required to form the distinct pattern of haemocyte dispersal during embryogenesis (Davis et al., 2012; Stramer et al., 2010).

Axon guidance

Growth cones at the tips of axons travel long distances to find the correct target cell to form a synapse (**Figure 1.2C**). This is highly regulated and is thought to be controlled by a number of mechanisms, including chemo-attraction, chemo-repulsion, contact-mediated attraction or contact-mediated repulsion with other cells or the ECM (Mueller et al., 2006). The latter mechanism is reminiscent of CIL. A study was performed *in vitro* with embryonic chick retinal and sympathetic neurons (Kapfhammer and Raper, 1987). When these neurons are grown separately, their growth cones locate other neurons and form connections. However, when these neurons are co-cultured and a retinal growth cone contacts a sympathetic neuron, the growth cone collapses, extends in a different direction, and no connections are formed (Kapfhammer and Raper, 1987). Furthermore, a similar phenomenon has been observed in motor neurons from chick embryos, which form contacts with the anterior sclerotome, but avoid the posterior sclerotome (Oakley and Tosney, 1993). Interestingly, many of

the proteins required for axon guidance are also thought to have a role in CIL in cancer cells.

Angiogenesis

New blood vessels are formed by angiogenic sprouting. The basement membrane is degraded by proteases secreted by endothelial cells and these cells migrate into the connective tissue, proliferate and tubulate to form a new vessel with a lumen (Ribatti and Crivellato, 2012). In a newly formed vessel, it is thought that there are two types of cells: 'tips' that migrate into new regions and 'stalks' that proliferate providing the cells for new vessels (Gerhardt et al., 2003). New sprouts form in response to mechanical or chemical stimulation, such as VEGF (Ribatti and Crivellato, 2012). During the migrating phase of angiogenesis, protrusions on stalk cells are inhibited whereas on tip cells they are promoted, in a process that is reminiscent of the type of CIL that occurs during neural crest migration. Indeed, VE-cadherin, a key component of endothelial cell-cell junctions, prevents stalk cell sprouting and Rac1 driven migration by inhibiting VEGFR signalling (Abraham et al., 2009). As tip cells express less VE-cadherin than stalk cells, VEGF is then able to drive migration via Rac1 activation. Fibroblasts have been shown to have a role in angiogenesis (Orimo et al., 2005). Co-cultures of endothelial cells and heart fibroblasts in fibrin gels demonstrate that when the density of fibroblasts is low the endothelial cells form sprouts and grow, while, in higher fibroblast densities sprout formation is inhibited leading to endothelial cell retraction (Nehls et al., 1998).

1.1.3.3 CIL in cancer

As far back as 1979 Michael Abercrombie postulated that CIL may be important in cancer cell invasion and metastasis. He cultured two non-cancerous explants side by side, and the cells segregated via heterotypic CIL. However, when one explant contained cancerous cells it invaded into the other explant in which the cells failed to undergo heterotypic CIL (Abercrombie, 1979). Accumulating observations indicated that genes involved in development, which are often required for CIL, are frequently misregulated in cancer (Hanahan and Weinberg, 2011). Indeed, large scale genetic analysis of many human pancreatic ductal carcinomas (Biankin et al., 2012) and lung cancers (Nasarre et al., 2010) have

revealed that many genes involved in axon guidance were altered, many of which have a role in CIL.

During cancer metastasis, cancer cells must become motile and invade into the surrounding tissue. Thus neighbouring cells must no longer prevent the invasion of the cancer cells into their territory. Therefore, it is likely that both homotypic and heterotypic collisions will be relevant here. Indeed a situation has been envisaged in which homotypic collisions occur (allowing cancer cells to break away from the primary tumour and disperse), while heterotypic collisions are prevented (allowing cancer cells to continue to migrate into the surrounding tissue)(Astin et al., 2010; Mayor and Carmona-Fontaine, 2010; Paddock and Dunn, 1986; Veselý and Weiss, 1973). Evidence supporting this has been observed in invasive prostate cancer cell lines (Astin et al., 2010). These studies demonstrate an important role of Ephs/Ephrins and Rho GTPases in CIL (Astin et al., 2010) (**Section 4.1**), but more work is required to uncover the mechanism of CIL in cancer and to determine whether the mechanisms that control CIL can influence metastasis *in vivo*.

1.2 Ephs and Ephrins

Ephrins are a family of membrane-anchored proteins that act as ligands for their cognate receptors the Ephs, which are a subfamily of receptor tyrosine kinases (RTKs). Ephs and Ephrins are involved in a plethora of functions, including axon guidance, development, angiogenesis, and organisation of the crypt-villus axis, and these are frequently misregulated in cancer. It is thought that Ephs and Ephrins contribute to processes by regulating whether cells adhere or repel each other.

1.2.1 Historical perspective

The Ephrin receptor, EphA1 was discovered in 1987 during a search for tyrosine kinases in EPH cells (Erythropoietin-Producing Hepatocellular carcinoma) (Hirai et al., 1987). Ephs are highly conserved in metazoans and the human genome contains 14 members of the Eph subfamily, making this the largest subfamily of RTKs (Drescher, 2002). The ligands for Ephs, the Ephrins, are normally tethered by GPI linkages to the plasma membrane of adjacent cells, although some

Ephrins may be cleaved and shed from the cell surface to act as soluble ligands (Wykosky et al., 2008). The Ephs are divided into two subclasses based on Ephrin binding: the 9 EphAs are receptors for 5 GPI membrane-anchored EphrinAs, and the 5 EphBs associate with 3 transmembrane-anchored EphrinBs. There is mounting evidence that some EphAs associate with EphrinBs and vice versa, and EphA4 is particularly promiscuous (Qin et al., 2010).

1.2.2 Eph structure and clusters

Eph structure is conserved, and all the family members possess multiple domains both sides of the plasma membrane, which are connected by a single spanning hydrophobic transmembrane helix (**Figure 1.3**). Eph ectodomains contain a ligand binding domain (LBD), a Cys rich region composed of a Sushi, EGF-like and two fibronectin type 3 domains. The intracellular portion contains a small juxtamembrane region, a tyrosine kinase domain, a sterile-α motif and often a Psd-95, Dlg and ZO1 (PDZ) domain binding motif (PBM). Although the whole molecule has not been crystallised, the structures of the ectodomain and SAM domain have been solved (Himanen et al., 1998; Himanen and Nikolov, 2002; Thanos et al., 1999). Indeed, several Eph ectodomains have been crystallised in association with Ephrins, revealing a heterotetrameric complex with two ligands and receptors. In the LBD a class-specific loop has been identified, which differs in EphAs and EphBs, perhaps allowing specificity of ligand binding (Himanen et al., 2001; Xu et al., 2013).

One major factor determining whether Ephs will stimulate adhesion or repulsion is the degree of Eph/Ephrin clustering. Upon activation by engagement with Ephrins expressed on neighbouring cells, Eph/Ephrin tetramers recruit more Ephs, without further ligand association to form large clusters (Lane et al., 1998; Wimmer-Kleikamp et al., 2004). These clusters can contain multiple different Eph subtypes, which modulate downstream signalling (Jørgensen et al., 2009). Indeed, it has been shown that ectopic expression of soluble EphA7 associates with EphA2 and inhibits its signalling (Oricchio et al., 2011). Furthermore, most cells express both Ephs and Ephrins, which can also associate on the same membrane in ‘cis’ (Yin et al., 2004), to inhibit ‘trans’ activation of Ephs by Ephrins on neighbouring cells (Falivelli et al., 2013). In summary, association of

different Ephs and Ephrins in 'cis' or 'trans' can alter downstream signalling resulting in different cellular responses.

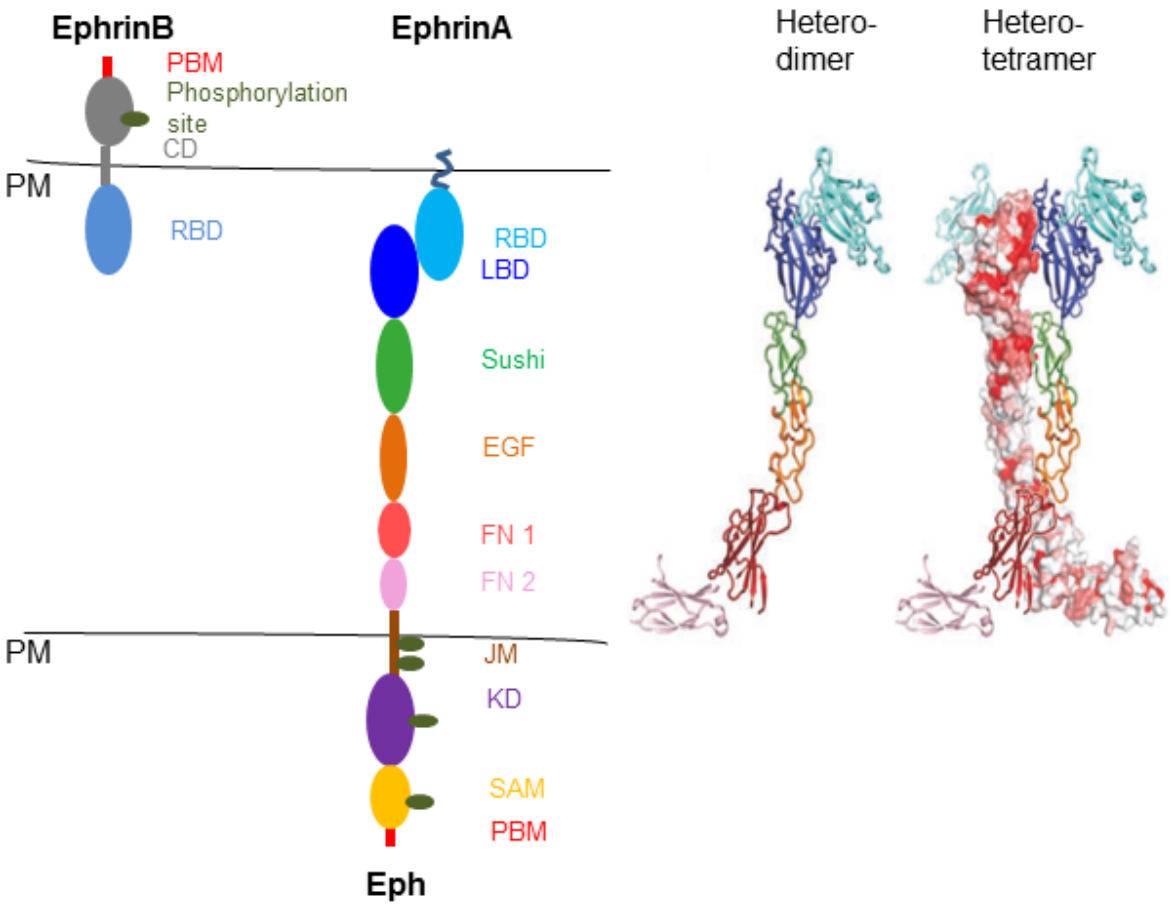

Figure 1-3 Structure of Eph and Ephrin
EphrinB is a transmembrane protein with a Receptor Binding Domain (RBD), Cytoplasmic Domain (CD) which contains phosphorylation sites and a PDZ binding motif (PMB). EphrinA is a GPI anchored protein with an extracellular RBD. Ephs contain many domains: a Ligand Binding Domain (LBD), Sushi domain and EGF-like domain, two fibronectin type3 domains (FN), a single spanning transmembrane region, juxtamembrane region (JM), kinase domain (KD), sterile α-motif (SAM) and a PBM. The structure of EphA2 and EphrinA5 are shown with the domains coloured the same as the schematic representation. This has been adapted from Seiradake *et al.* (2010)

1.2.3 Signalling

RTKs follow a classical cascade of activation: the ligand binds the receptor, the receptor autophosphorylates, signalling proteins associate and are phosphorylated, these signalling proteins activate other proteins and the cell responds to the signal. Ephs follow this activation cascade. However, Ephrins can also activate signalling proteins in neighbouring cells, which is called reverse

signalling. Ephs can influence a large array of signalling proteins and these pathways vary depending on cell type and the complement of Ephs and Ephrins expressed in the cell. Different intracellular domains of Ephs can influence signalling output. For example, the juxtamembrane region activates Src (Jørgensen et al., 2009), the kinase domain associates with and activates a Rho GEF, ephexin (Shamah et al., 2001), and the PDZ-binding motif can associate with PDZ binding proteins (Torres et al., 1998) potentially activating them.

1.2.3.1 Autophosphorylation

Upon ligand activation Ephs form large clusters, bringing Ephs in close proximity, which promotes trans-phosphorylation of two highly conserved residues in the juxtamembrane region (Tyr^{588} and Tyr^{594} in EphA2). Phosphorylation of these residues relieves inhibitory interactions with the kinase domain leading to a structural rearrangement of this domain, resulting in activation of the kinase activity (Binns et al., 2000; Wybenga-Groot et al., 2001). Indeed, a study using FLIM-FRET between membrane-labelled RFP and GFP-EphA3 indicates that the kinase domain physically moves away from the juxtamembrane region upon activation (Janes et al., 2009). There is an activation loop in the Eph kinase domain that also has a phosphor-acceptor tyrosine. Phosphorylation of this residue activates the kinase as the loop no longer blocks the active site. Although mutating this tyrosine in EphA4 prevents activation (Binns et al., 2000), further work is required to determine whether this loop is required for activation of other Ephs.

1.2.3.2 Forward signalling

Ephs can activate a variety of downstream signalling pathways that are required for their functions (**Figure 1.4**). The major signalling pathways downstream of Eph activation will be outlined. It is worth noting that different studies often show conflicting results with regards to Eph signalling, perhaps owing to difference in cell type and the microenvironment.

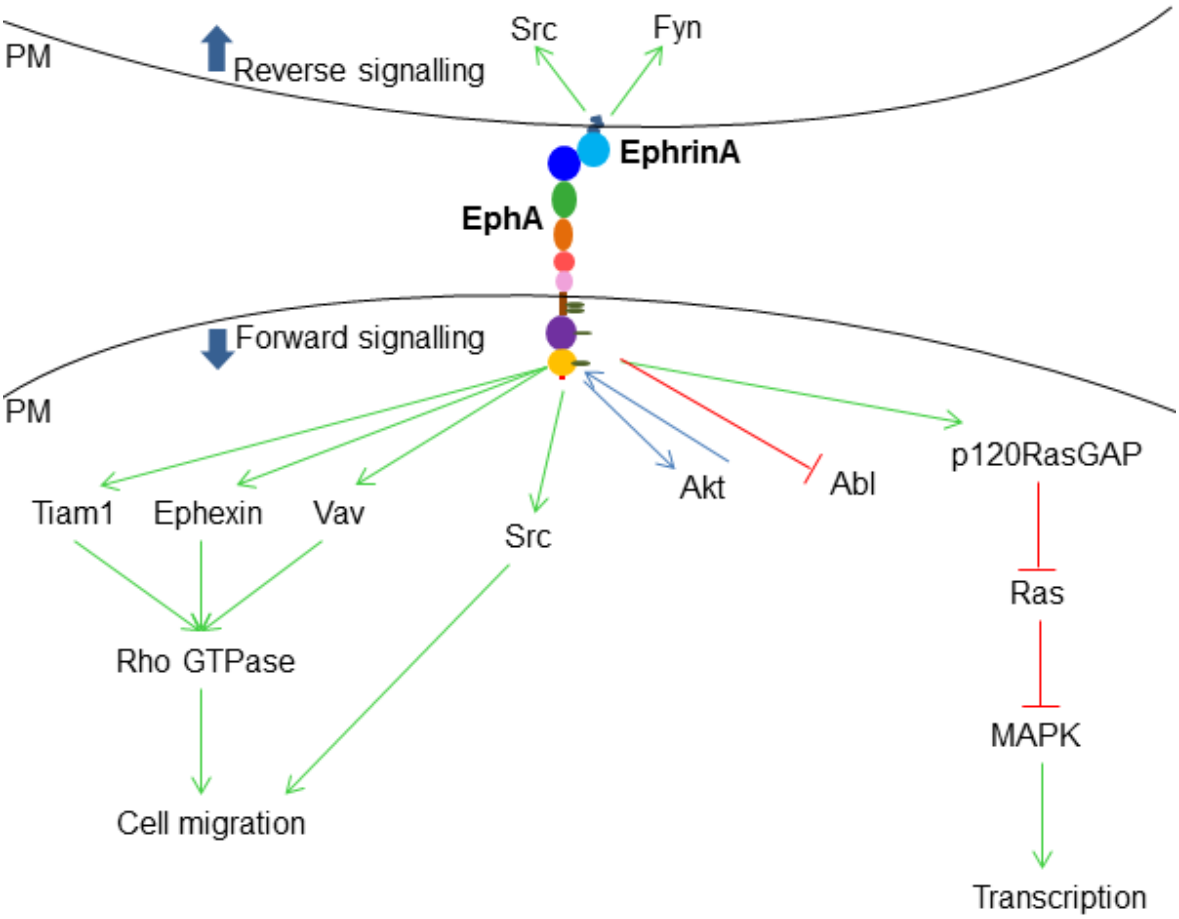

Figure 1-4 EphA and EphrinA Signalling
EphAs and EphrinAs are activated upon binding, which activates many signalling pathways. EphrinA reverse-signals to the Src family of kinases. EphA can inhibit Abl and the Ras-MAPK pathway, whilst activating Src and several Rho-GEFs (Tiam1, Ephexin and Vav), which can promote cell migration via Rho GTPases. Akt phosphorylates unbound EphA, but upon ligand association Eph negatively regulates Akt.

Rho GTPases

Rho, Ras and Rab GTPases are found in both active GTP-bound and inactive GDP-bound states, and this is controlled by GEFs (guanine nucleotide exchange factors) that exchange GDP with GTP, and GAPs (GTPase activating proteins) that promote hydrolysis of GTP to GDP. Prominent members of the Rho GTPases are: RhoA, which promotes contraction of the actin cytoskeleton and the formation of stress fibres; Rac1, which promotes formation of lamellipodia; and Cdc42, which promotes the formation of filopodia. Active Ephs have been shown to signal to Rho-GTPases during axon guidance and CIL (**Figure 1.4**) (Astin et al., 2010; Wahl et al., 2000). The GEFs, Ephexin and two of the Vav family are required for Ephs to activate RhoA and Rac1 to initiate growth cone collapse

(Cowan et al., 2005; Shamah et al., 2001). Other GEFs, such as Kalirin, Tiam1 and Intersectin are thought to have a role downstream of EphA2 in regulating dendritic spine morphogenesis (Irie and Yamaguchi, 2002; Penzes et al., 2003; Tolias et al., 2007). In prostate cancer cells, EphinA1 stimulation decreases cell adhesion via Rac1 inhibition and RhoA activation (Astin et al., 2010). Furthermore, Eph-Ephrin association activates LMW-PTP, which in turn dephosphorylates and inactivates its substrate p190RhoGAP, to drive RhoA activation leading to de-adhesion and promoting cell rounding (Buricchi et al., 2007). It is likely that EphA function in cancer may be dependent on Rho GTPases. Further work is required to understand Eph signalling to these GTPases and the functional responses downstream of this.

Ras-MAPK

Ras activates the MAP kinase pathway, which is important for transcriptional regulation, cell migration and axon guidance (Forcet et al., 2002). Indeed, EphA2 is a direct transcriptional target of this pathway (Macrae et al., 2005). Ephs can negatively regulate Ras in many cell lines, for example in epithelial, endothelial and tumour cells (Miao et al., 2001). It has been shown that p120RasGAP, which converts Ras into its inactive GDP-bound form, can mediate Eph's inhibition of Ras (Elowe et al., 2001). Ephs can act as a tumour suppressors by suppressing Erk1/2 activation, which is stimulated by other RTKs (Macrae et al., 2005). Despite this, in some instances Ephs activate the MAPK pathway. For example, EphB2 has been shown to activate Erk, which promotes cell-cell repulsion (Poliakov et al., 2008), and EphB1 activates Ras via the adaptor, Grb2, which promotes cell migration (Vindis et al., 2003). In summary, Eph signalling to the MAPK pathway is complex and may differ in different cell types.

Akt

Akt is a serine/tyrosine kinase that is typically activated by PI3Kinase and signals to downstream proteins such as mTOR. Eph signalling can both activate and deactivate Akt and this depends on the cell type. In some studies, Eph activation was found to indirectly de-phosphorylate and suppress Akt (Menges and McCance, 2008; Miao et al., 2009). Indeed, active EphB3 inhibits Akt activity in non-small-cell lung carcinoma cells. Nevertheless, Eph has also been shown to activate Akt in T-lymphocytes and pancreatic cancer cells (Chang et al., 2008; Maddigan et al., 2011). Interestingly, a recent report demonstrates crosstalk

between Akt and Eph signalling. Upon serum stimulation, Akt phosphorylates EphA2 at Serine-897 promoting cell migration (Miao et al., 2009). However, upon EphrinA1 stimulation EphA2 is dephosphorylated at this site, which dephosphorylates Akt, thus inactivating it and inhibiting cell migration (Miao et al., 2009).

Src and Abl

Ephs can signal to other downstream tyrosine kinases, such as Src and Abl, which regulates the actin cytoskeleton and cell migration (Kalo and Pasquale, 1999). Indeed, Fyn, a member of the Src family of kinases, is activated downstream of EphA8 (Choi and Park, 1999). In contrast, EphrinB1 stimulation of EphB2 decreases Abl activity (Yu et al., 2001).

1.2.3.3 Reverse signalling

Upon Eph association, Ephrins are activated and can influence signalling pathways in the cells in which they are expressed. This is defined as reverse signalling. Studies reveal that EphrinA can reverse-signal via association with other RTKs, for example, Ret (Bonanomi et al., 2012). It has been shown that upon Eph binding, EphrinAs are found in microdomains, which increases cell adhesion (Davy et al., 1999; Davy and Robbins, 2000). Several studies have shown that EphrinAs signal to Src kinases in these microdomains (**Figure 1.4**), for example, EphrinA5 activates Fyn (Davy et al., 1999). Indeed, over-expression of EphrinA5 increases cell invasiveness, which is blocked by the Src kinase inhibitor, PP2 (Campbell et al., 2006). EphrinBs can also reverse-signal via their cytoplasmic domain and C-terminal PDZ binding motif (PBM). Upon Eph binding, EphrinBs are phosphorylated by Src kinases, which enables them to activate signalling output (Cowan and Henkemeyer, 2001).

1.2.3.4 Modulation of Eph signalling

Eph signalling may be modulated by several different mechanisms, including: internalisation (examined in **Section 1.3.5**), cis-association with Ephrins and dephosphorylation by many different phosphatases. Indeed, it has been shown that EphA2 is dephosphorylated by LMW-PTP (Kikawa et al., 2002) and EphA3 is dephosphorylated by PTB1B. Both phosphatases attenuate Eph forward signalling. Furthermore, conserved phosphorylation sites in the juxtamembrane

domain of Eph can be de-phosphorylated by tyrosine phosphatase receptor type O (Shintani et al., 2006). Cis association between Eph and Ephrins can attenuate Eph forward signalling. Indeed, EphrinA5 can associate with the second FN type 3 domain of EphA3 in cis, which blocks the trans-association between EphA3 and EphrinAs (Carvalho et al., 2006).

Ephs are activated by ligand binding at the plasma membrane, where they are thought to activate downstream signalling pathways. Interestingly, a recent study showed that EphA2 remains phosphorylated once it is internalised into vesicles, suggesting that EphA2 could actively signal from an internal compartment. Boissier et al. (2013) demonstrated that phospho-Y594-EphA2 is located in EEA1-positive early endosomes after soluble EphrinA1 addition. To determine whether internalisation of Eph is required for its downstream signalling, further experiments should be conducted. For example, endocytosis inhibitors such as Dynasore could be used to determine whether endocytosis of Eph is required for Ephrin-induced cell rounding.

1.2.4 Ephs crosstalk with other membrane proteins

1.2.4.1 Ephs crosstalk with integrins

Integrins are cell-surface receptors that contain two subunits (α and ß), which associate with ECM proteins to mediate cell-matrix adhesion and to induce signalling to produce a variety of cellular responses. Numerous studies have shown that there is crosstalk between the Eph/Ephrin and integrin signalling pathways, and their interaction is proposed to contribute to the coordination of cell migration. Two studies have demonstrated a physical association between Ephs and integrins: EphA4 with ß3-integrin in platelets (Prévost et al., 2005) and EphrinAs/EphA2 with α3-integrin in a glioblastoma cell line (Makarov et al., 2013). Interestingly, internalised α3-integrin co-localises in vesicles with EphA2 (Makarov et al., 2013). The interaction of these pathways has been shown to have an important role in various cellular functions, including platelet activation (Prévost et al., 2005), structural organisation of dendritic spines in excitatory synapses (Bourgin et al., 2007), production of ECM (Jülich et al., 2009), and angiogenesis (Huynh-Do et al., 2002).

Ephs can promote integrin activation and signalling resulting in cell adhesion to the ECM. Eph/Ephrin signalling initiates integrin clustering during zebrafish somite morphogenesis (Jülich et al., 2009), while *in vitro* Ephs have been found to activate ß1-integrin signalling to increase cell adhesion to laminin (Huai and Drescher, 2001) and fibronectin (Davy and Robbins, 2000). Many signalling proteins activated by Eph have a role in activating integrins including: Src (Davy and Robbins, 2000), Paxillin (Vindis et al., 2004), the PI3K subunit—p110γ (Gu and Park, 2001), FAK (Carter et al., 2002; Parri et al., 2007), $p130^{Cas}$ (Carter et al., 2002) and p120 (Huai and Drescher, 2001). Nevertheless, numerous studies have shown that Eph can also inhibit integrin signalling resulting in a less adherent phenotype. Overexpression of EphB4 decreases adhesion independently of the ligand EphrinB2 (Noren et al., 2009), whilst ligand activated EphB2 triggers the phosphorylation of R-Ras, which attenuates integrin-mediated adhesion (Zou et al., 1999). Moreover, ligand-activated EphA2 may promote the inactive conformation of integrins to inhibit cell spreading (Miao et al., 2000). Focal adhesion kinase (FAK) associates with both integrins and EphA2. Upon Ephrin-A1 stimulation, SHP2 (a tyrosine phosphatase), is recruited to EphA2 and de-phosphorylates FAK, thereby inhibiting FAK kinase activity and suppressing integrin activity (Miao et al., 2000). Thus Ephs/Ephrins have been shown to both activate and deactivate integrins in different studies, perhaps due to differences in cell lines and the microenvironment (**Section 1.2.7**).

1.2.4.2 Ephs crosstalk with other receptor tyrosine kinases

RTKs are activated by external growth factors, which stimulate receptor dimerization, activation and autophosphorylation, resulting in a variety of cellular responses. Crosstalk between Ephs and several RTKs has been identified. In glioma cells an association between FGFR1 and EphA4 promotes FGFR1 signalling, thus increasing cell proliferation and migration (Fukai et al., 2008). EGFR and EphA2 can be co-immunoprecipitated and these co-localise in the plasma membrane. Indeed, suppression of EphA2 expression inhibits EGFR based motility (Larsen et al., 2007; Larsen et al., 2010). EphA2 depletion impairs breast cancer initiation and metastasis in models driven by overexpression of ErbB2, but not in those driven by polyomavirus middle T-antigen. Furthermore, in breast cancer cells ErbB2 was found associated with EphA2 and this enhanced RhoA and Ras-MAPK signalling (Brantley-Sieders et al., 2008). RTKs can also

crosstalk with Ephrins. Indeed, active FGFR phosphorylates EphrinB1 preventing it from signalling during *Xenopus* development (Lee et al., 2009). Interestingly, EphrinB2 promotes VEGFR2/3 internalisation and signalling during angiogenesis (Sawamiphak et al., 2010; Wang et al., 2010).

1.2.4.3 Ephs crosstalk with cadherins

Many studies demonstrate crosstalk between Ephs and cadherins. Indeed, E-cadherin increases EphA2 expression, surface localisation and EphrinA1-activated signalling (Orsulic and Kemler, 2000; Zantek et al., 1999). Moreover, EphA2 signalling increases E-cadherin dependent cell adhesion, indicating that the crosstalk between these two receptors can be bidirectional (Miura et al., 2009). In HT-29 colon cancer cells, EphB2 signalling increases E-cadherin membrane localisation and cell-cell adherence. However, if EphB2 is depleted in these cells, EphrinB1 induces cell separation and migration; suggesting EphB2 activation is required for E-cadherin dependent cell-cell adherence (Cortina et al., 2007). On the other hand, E-cadherin has an important role in Eph/Ephrin-driven cell segregation. Upon EphB activation by EphrinB, E-cadherin is cleaved by ADAM10, thus adherens junctions do not form between EphB and EphrinB-expressing MDCK cells (Solanas et al., 2011). Further work shows that Ephs and N-cadherins crosstalk. EphA4 is essential for N-cadherin driven EMT in developing zebrafish somites (Barrios et al., 2003) and EphA2 mutations in human cells or loss of EphA2 in mice disrupts N-cadherin junctions (Jun et al., 2009). Taken together, these studies demonstrate that bidirectional crosstalk between cadherins and Ephs may determine whether cells repel or adhere.

1.2.5 Eph and Ephrin functions

1.2.5.1 The role of Eph/Ephrin in neuronal patterning

In neuronal development Ephs and Ephrins are required for correct neuronal patterning. They are involved in growth cone guidance, axon branching, and dendritic branching. To study axon guidance, *in vitro* striping assays are used in which neural explants are grown next to strips of different substrates. If the molecules on the strips are attractive the axons move down the strips, however if they are repulsive the axons are repelled from the strips (Yates et al., 2001). Using this assay it has been shown that EphrinA5 acts as a growth cone repellent,

and EphA signalling in the growth cone is required for this repulsion (Drescher et al., 1995) Furthermore, EphA2-rich growth cones are repelled by EphrinA2 regions (**Figure 1.5A**) (Hansen et al., 2004). Striping assays are also used to monitor axon branching. Axons move into regions of high EphrinA concentration but axon branching is inhibited. At lower EphrinA concentration, axon branching is promoted (Yates et al., 2001). This demonstrates the importance of Ephs/Ephrins in axon branching and guidance. Knockout and knockin mice of various Ephs and Ephrins have been used to study topological defects *in vivo*. Indeed, EphA3 was ectopically expressed in a subset of retinal ganglion cells, which enhances a repulsive response to Ephrin, causing incorrect positioning of axons (Brown et al., 2000). Also, EphrinA2 and EphrinA5 knockout mice contain incorrectly targeted axons (Feldheim et al., 2000).

As well as axon guidance and branching, EphB signalling is involved in morphogenesis of dendritic spines (Ethell et al., 2001; Penzes et al., 2003). Upon EphrinB activation, EphB signalling recruits proteins required in the dendrites, allowing the formation of a synapse (Dalva et al., 2000). Interestingly, EphrinAs are expressed on glial cells that surround the synapse. They regulate dendritic spine density, which is required for learning (Murai et al., 2003).

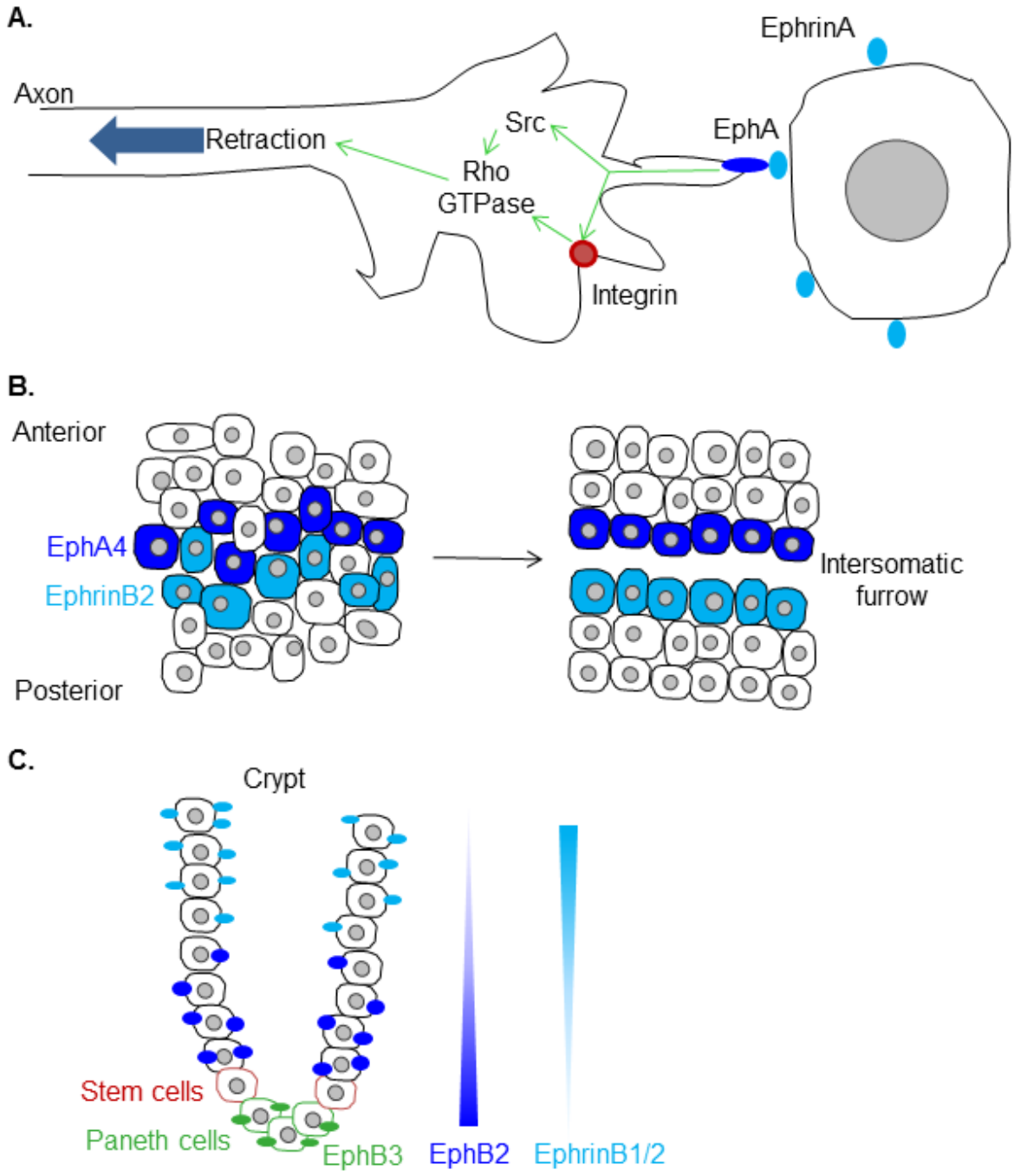

Figure 1-5 Eph and Ephrin functions
A. During axon guidance, the growth cone enriched with EphA extends and contacts an EphrinA positive cell. Upon Eph and Ephrin engagement, Eph is activated and signals to Src, Rho GTPases and β1-integrin, which stimulates rapid growth cone retraction. B. During somatogenesis, cells expressing EphA4 are found on the anterior half, whilst cells expressing EphrinB2 are found on the posterior half of the embryo. EphA4 and EphrinB2 interactions stimulate epithelisation forming the intersomatic furrow. C. Ephs and Ephrins are required for the organisation of the intestinal crypt. Paneth cells are found at the base of the crypt and have high EphB3 expression. EphB2 expression decreases up the crypt, whilst, EphrinB1/2 expression increases.

1.2.5.2 The role of Eph/Ephrin in development

Ephs/Ephrins have an important role in multiple stages of development. EphA1 and EphrinA1/A3 are expressed during the very early stages of embryogenesis, in somatogenesis (Duffy et al., 2006). Indeed, EphA4 is found expressed in the anterior region, while EphrinB2-positive cells reside on the posterior half of the embryo (Durbin et al., 1998). At the boundary, between EphA4 and EphrinA1/B2 positive cells, the ligand and receptor interact causing EphA4 and EphrinA1/B2 positive cells to detach from each other and undergo epithelisation to form the intersomatic furrow (**Figure 1.5B**) (Barrios et al., 2003). However, EphA4 knockout mice have no defects in somatic segmentation indicating a possible redundancy with other Ephs.

Neural crest cells (NCCs) migrate from the dorsal region of the neural tube to populate the embryo and in doing so can differentiate into many cell types. Ephs and Ephrins spatially restrict the migration of these cells. EphrinBs are expressed in the posterior region of the somite, and this acts as a repulsive cue for the EphB expressing neural crest cells (Krull et al., 1997; Wang and Anderson, 1997). Neural crest cells that are specified as neurons and glia migrate ventrally, while those specified as melanoblasts migrate in the dorsolateral pathway. EphrinBs are expressed in the dorsolateral pathway and if this expression is disrupted neural crest cells migrate incorrectly along the dorsolateral pathway (Santiago and Erickson, 2002). *In vitro* migration assays demonstrate that melanoblasts migrate towards EphrinB1 and express EphBs (Santiago and Erickson, 2002). Therefore, EphrinB is acting as an inhibitory migration signal to neuron-specified neural crest cells, while promoting the migration of melanoblasts.

1.2.5.3 The role of Eph/Ephrin in epithelial cell segregation and migration

As well as a role in developmental cell segregation, Ephs and Ephrins are thought to have a role in epithelial cell segregation. *C.elegans* only express one Eph and one Ephrin, and disrupting either of these causes defects in the ventral closure of the epidermis (George et al., 1998). In adult tissue, epithelial cell segregation is best studied in the context of mammary gland branching-morphogenesis and in the generation of the crypt-villus axis. In the mammary gland, EphB4 is expressed in myoepithelial cells, while EphrinB2 is expressed in luminal

epithelial cells. This expression pattern is regulated by the oestrous cycle (Munarini et al., 2002) and its disruption results in carcinogenesis (Nikolova et al., 1998). Also, Ephs/Ephrins prevent intermingling of distinct cell populations in the intestinal crypt. Paneth cells are found at the base of the crypt and have high EphB3 expression. As proliferative cells migrate up the crypt they commit to different lineages, such as absorptive and goblet cells (**Figure 1.5C**). In these cells, EphB2 expression decreases with progress up the crypt, while, EphrinB1/B2 levels increase. This expression pattern is under the control of Wnt (van de Wetering et al., 2002). Disrupting *EPHB2* or *EPHB3* genes in mice results in loss of organisation in the crypt and intermingling of different cell populations (Batlle et al., 2002), thus suggesting that Ephs and Ephrins have an important role for the cellular organisation of intestinal crypts.

1.2.5.4 The role of Eph/Ephrin in vasculogenesis

Ephs and Ephrins have an important role in the development and maintenance of blood vessels. In mouse embryos EphB4 is expressed on primordial veins (Gerety et al., 1999), while EphrinB2 is expressed on primordial arteries. (Wang et al., 1998) Indeed, null mutations in either EphB4 or EphrinB2 cause embryonic lethality. Other Ephs and Ephrins are co-expressed on arteries and veins leading to complex patterning. Ephs and Ephrins are also involved in angiogenesis, which is best studied during tumourigenesis (**Section 1.2.6.3**).

1.2.6 The role of Ephs and Ephrins in cancer

1.2.6.1 Misregulation of Eph and Ephrin expression

Eph and Ephrin expression are frequently misregulated in cancer for a number of different reasons, including chromosomal addition or loss, epigenetics, alterations in mRNA stability and transcriptional changes (Arvanitis and Davy, 2012). Some Ephs are upregulated, while others are downregulated. For example, EphA2 is frequently upregulated and linked to poor prognosis in breast cancer (Wykosky et al., 2008), while EphA1 is downregulated in skin and colorectal cancers (Hafner et al., 2006; Herath et al., 2009). Indeed, in some cancers, inverse expression is seen for Ephs and Ephrins, for example in breast cancer cell lines EphA2 is often upregulated, while EphrinA1 is downregulated (Macrae et al., 2005). Most interestingly, in colorectal cancer, some EphBs are

initially overexpressed in tumourigenesis, but later repressed by hypermethylation (Herath and Boyd, 2010). It is rare that more than one Eph is significantly overexpressed in a tumour, suggesting altered expression of one Eph is sufficient for tumour cell evolution. Interestingly, the expression of Ephs and Ephrins on neighbouring cells may influence tumourigenesis. Indeed, EphrinA1 expression is upregulated in endothelial cells by VEGF, TNF or HIF2a that is secreted by cancer cells, thereby regulating tumour neovascularisation (Pandey et al., 1995; Yamashita et al., 2008).

1.2.6.2 Eph mutations

There is emerging evidence that Ephs are frequently mutated in cancer. *EPHB2* mutations have been identified in prostate, melanoma and colorectal cancer, (Alazzouzi et al., 2005; Pia et al., 2004; Prickett et al., 2009), while *EPHA3* and *EPHA5* are mutated in lung cancer (Davies et al., 2005a; Ding et al., 2008). These mutations are found throughout the protein and the effects of these mutations are largely unknown. EphA3 mutations are the best studied and many lead to loss of function (Lisabeth et al., 2012; Zhuang et al., 2012). EphA2 is less frequently mutated. Nevertheless, a mutation is found in its FN type 3 repeat in lung cancer that promotes cell invasiveness (Faoro et al., 2010). Interestingly, in human tumour samples multiple Ephs are mutated at once (Lisabeth et al., 2012). It would be interesting to thoroughly study these mutations and the consequences they have in tumourigenesis and metastasis.

1.2.6.3 The role of Ephs in tumourigenesis and metastasis

The role of Ephs and Ephrins in cancer is clearly not straightforward. They can act as both oncogenes and tumour suppressors, and are likely to have multiple functions in tumourigenesis and metastasis. In this section I will focus of EphA2 to outline the main functions of Ephs in cancer.

Stem cells

Cancer stem cells are self-renewing and thought to drive tumourigenesis, although the existence of such cells remains controversial. EphA2 is found overexpressed in glioblastoma stem cells and its expression correlates with tumour initiating properties (Binda et al., 2012). Indeed, suppressing EphA2 expression prevents stem cell renewal (Binda et al., 2012). Furthermore, in lung

cancer EphA2 expression correlates with the expression of stem cell markers such as ALDH (Song et al., 2014). Indeed, suppressing EphA2 expression in these cells inhibits the formation of spheroids *in vitro* (Song et al., 2014). EphA3 is also expressed in undifferentiated cancer cells (Day et al., 2013). The role of Ephs in cancer stem cells requires more thorough investigation.

Tumour angiogenesis

Tumours contain many blood vessels, which are required for supplying the cancer cells with nutrition and providing a route for metastasis. The involvement of Ephs and Ephrins in angiogenic sprouting is well studied. EphA2 is expressed in angiogenic sprouting cells, but is not detected in embryonic or adult endothelial cells. Nevertheless, EphA2 deficient mice have vessels with defective pericyte coverage (Okazaki et al., 2009). Ephrins expressed on cells adjacent to endothelial cells can promote repulsive signals that stimulate migration of the endothelial cells, which form sprouts. Indeed, EphrinA1-expressing tumour cells contain EphA2-expressing endothelial cells. Disruption of EphA2 prevents endothelial cells from assembling into vascular structures in response to pro-angiogenic EphrinA1 (Brantley-Sieders et al., 2004). Interestingly, when cancer cells were implanted subcutaneously into EphA2-deficient mice, angiogenesis was inhibited, thus suggesting that EphA2 expression in the endothelial cells, and not the cancer cells, is important for tumour angiogenesis (Brantley-Sieders et al., 2005). Furthermore, Ephs and Ephrins are required for maximal VEGF functions. VEGF increases EphrinA1 expression, which interacts with EphA2 and is required for endothelial cell migration and sprouting. Treatment with soluble EphA2 decreases neovascularisation by preventing endothelial cell migration (Cheng et al., 2002). EphBs/EphrinBs are also important for tumour angiogenesis. EphrinB2 is highly expressed on angiogenic vessels (Adams et al., 2001) and its reverse-signalling to Src is required for angiogenesis (Palmer et al., 2002). Indeed, in tumour angiogenesis EphrinB2 promotes sprouting in response to VEGF by inducing VEGFR internalisation and signalling (Sawamiphak et al., 2010; Wang et al., 2010).

Epithelial-mesenchymal transition

During carcinoma tumourigenesis, the cancer cells often change from an epithelial-type to a mesenchymal-type phenotype in a process that is termed epithelial-mesenchymal transition (EMT). During this process, cancer cells lose

epithelial polarity and E-cadherin junctions, and become more migratory. In gastric cancer, overexpression of EphA2 correlates with a more mesenchymal-type phenotype (Hou et al., 2012). Indeed, EphA2 can activate EMT signal transduction pathways (Hou et al., 2012). Furthermore, overexpression of EphA2 upregulates mesenchymal markers, such as N-cadherin and Snail, and downregulates epithelial markers, such as E-cadherin (Huang et al., 2014). Other Ephs have been linked to EMT, for example, EphB2 expression in cervical cancer cells promotes EMT (Gao et al., 2014). EMT and a migratory and invasive phenotype are closely linked; the latter will be examined next.

Cancer cell invasion and metastasis

Ephs have a conflicting role in invasion and metastasis, and opposing results are often reported. Normally, EphA2 overexpression correlates with increased metastasis, for example, in oesophageal squamous cell carcinoma high EphA2 expression correlates with lymph node metastasis (Miyazaki et al., 2003). Furthermore, *in* vitro work demonstrates that EphA2 overexpression increases cell invasion into Matrigel (Chen et al., 2014). Perhaps EphA2 is best studied in breast cancer, in which it is highly overexpressed and its levels correlate with poor prognosis (Brantley-Sieders et al., 2008). EphA2 drives metastasis via its association with ErbB2 and by forward signalling to Akt, Src and Rho GTPases. Indeed, in breast cancer EphA2 clusters with ErbB2, which enhances Ras and Rho signalling and drives cell migration (Brantley-Sieders et al., 2008).

In colorectal cancer EphA2 is overexpressed in the early stages of tumourigenesis but is lost as the tumour metastasises (Kataoka et al., 2004). Conversely, in melanoma distant metastases express much higher levels of EphA2 than the primary tumour (Easty et al., 1995). Interestingly, EphA2 is overexpressed in pancreatic cancer and expressed in lymph node, but not liver, metastases (Mudali et al., 2006). Together this suggests that EphA2 expression may vary during tumourigenesis and may be involved in targeting cancer cells to particular sites for metastases. Interestingly, it is not only tumour cells that have a role in metastasis but also the cells that the tumour cells come into contact with, such as stromal and endothelial cells. There is emerging evidence that tumour cells interact with stromal cells via Ephs and Ephrins (Astin et al., 2010). These interactions may determine whether cancer cells invade into their local environment via contact inhibition of locomotion (**Section 4.1.1**). Interestingly,

immunohistochemistry of human prostate cancer demonstrates that EphB4 is highly expressed in prostate cancer cells, while EphrinB2 is highly expressed in endothelial and smooth muscle cells (Astin et al., 2010). Further work is required to mechanistically understand the role of Ephs and Ephrins in metastasis.

1.3 Receptor trafficking in cancer

The endocytic trafficking pathway is composed of several distinct intracellular membrane compartments. Transmembrane proteins are internalised into vesicles via different mechanisms, including micropinocytosis, clathrin-mediated endocytosis or calveolar-mediated endocytosis. These proteins are transported to early endosomes and then sorted into recycling or degradation pathways (**Figure 1.6**). Recycled proteins can either be returned directly from early endosomes to the plasma membrane or indirectly via the peri-nuclear recycling compartment. Proteins targeted for degradation are transported through late endosomes into lysosomes, which are enriched with lysosomal hydrolases. Althernatively, proteins are delivered to multivesicular bodies that contain small vesicles in their lumen, enriched with ubiquitylated transmembrane proteins, which are either degraded (by fusion with lysosomes) or secreted in small vesicles called exosomes. Many proteins have been found to localise in distinct compartments along the endocytic pathway. Most interestingly, each compartment contains different members of the family of Rab-GTPases (**Figure 1.6**) (Zerial and McBride, 2001). Indeed, different Rab-GTPases can occupy different regions of the same compartment, for example, Rab4, Rab11 and Rab5 are found at distinct locations on the same early endosome (Sonnichsen et al., 2000), whilst Rab7 and Rab9 occupy distinct microdomains on late endosomes (Barbero et al., 2002). Perhaps, the pressence of multlpe Rabs on the same compartment may allow differential sorting of proteins internalised into the same compartment.

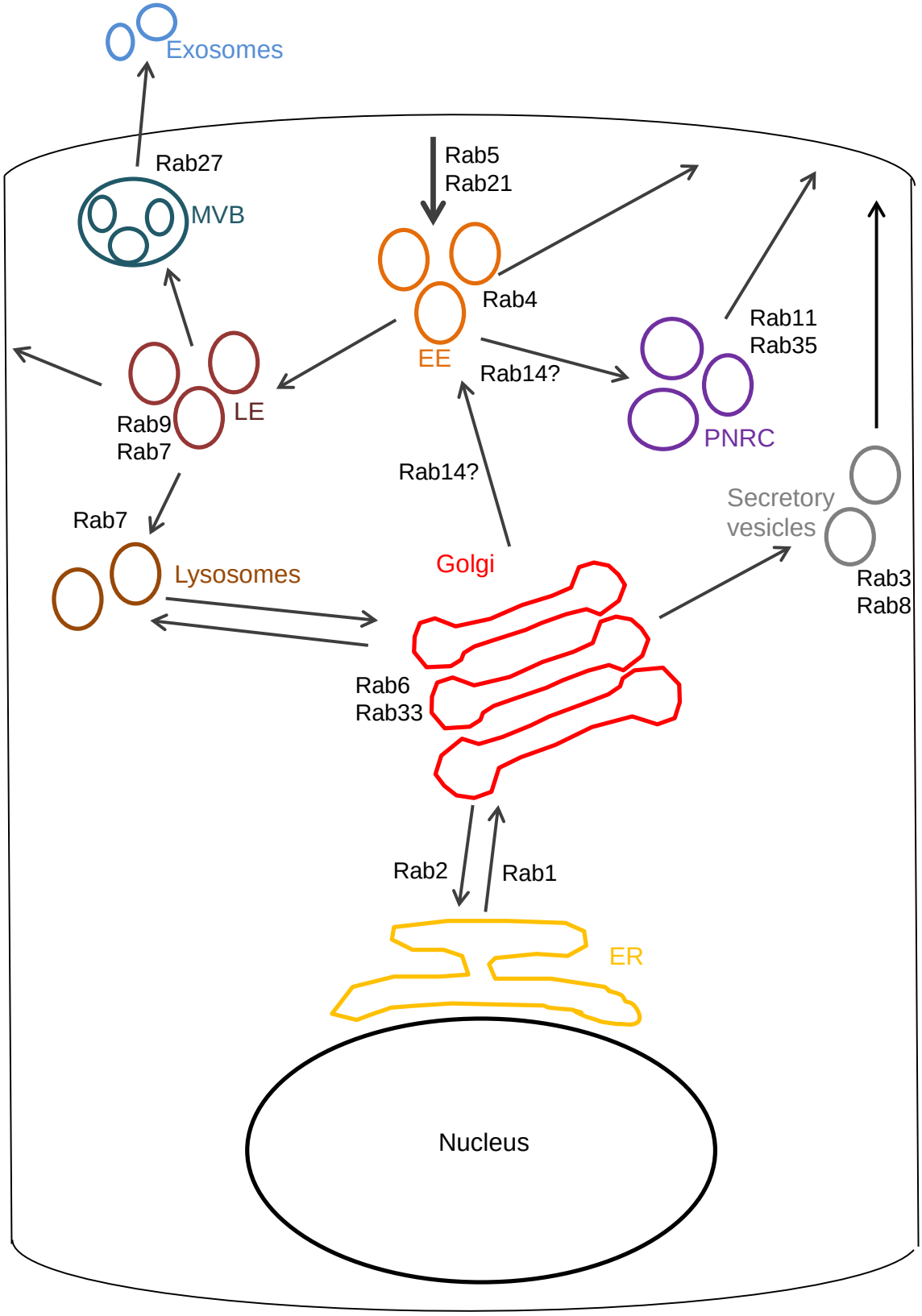

Figure 1-6 Intracellular localisation of RabGTPases
Membrane-bound proteins are synthesised in the ER (endoplasmic reticulum), trafficked through the Golgi apparatus and transported to the appropriate subcellular compartment. Internalised proteins are transported to the EE (early endosomes) where they are sorted for direct recycling, indirect recycling through the PNRC (peri-nuclear recycling compartment), or targeted for degradation via LE (late endosomes), the MVB (multi-vesicular body) and lysosomes. The localisation of key Rab-GTPases is indicated.

1.3.1 Rab GTPases

The human Rab GTPase family of proteins has over 60 members (Zerial and McBride, 2001). The best characterised role of Rab GTPases is in vesicular trafficking, including endocytosis and exocytosis, which requires the dynamic coupling of Rab proteins with vesicles to accurately deliver vesicular cargo to their appropriate destination (**Figure 1.6**). These monomeric GTPases act as molecular switches, which cycle between an active GTP-bound and inactive GDP-bound state (**Figure 1.7**). Key proteins involved in regulating this cycle include: guanine nucleotide exchange factors (GEF) which trigger GTP binding and GTP activating proteins (GAP) which increase hydrolysis of bound GTP. Disruption of this cycle often alters the subcellular localisation of the Rab-GTPases and the morphology of the compartment, for example mutant GTP-locked Rab5 enlarges early endosomes, whilst the GDP-locked mutant has the opposite effect (Stenmark et al., 1994). More recently, Rab-GEFs have been shown to have a role in targeting Rab-GTPases to their appropriate membrane (Blumer et al., 2013; Gerondopoulos et al., 2012). Rab-GDP dissociation inhibitors (GDI) can also relocate Rab-GTPases to different compartments, by associating with GDP-bound Rab proteins, and are capable of retrieving the Rab from intracellar membranes (Ullrich et al., 1993).

Rab effectors bind specifically to GTP-bound Rabs and have diverse roles in membrane trafficking (Grosshans et al., 2006). Some Rab effectors interact with components of the actin or microtubule cytoskeleton, such as Rabkinesin 6, a Rab6 effector, which acts as a microtubule motor aiding vesicular mobility during cytokinesis (Echard et al., 1998). Other effectors have been implicated in the tethering of vesicles and in membrane fusion such as the Rab5 effector, EEA1 (Christoforidis et al., 1999). The Rab GTPase cycle allows temporal and spatial association with various effectors, which regulate membrane trafficking by controlling vesicle budding, tethering, motility or fusion (Pfeffer and Aivazian, 2004). Several Rab-GTPases are investigated in this thesis, including Rab14 (**Section 3.2.2.1**), Rab6 (**Section 3.2.3.1**) and Rab11 (**Section 1.32)**.

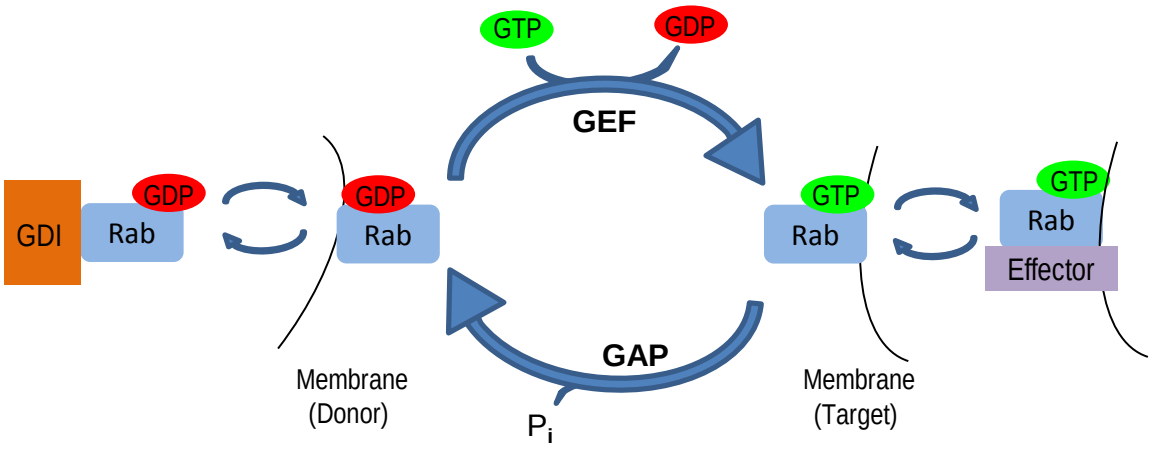

Figure 1-7 Rab-GTPase switch
Rab GEFs (guanine nucleotide exchange factors) trigger GTP binding to the Rab, which activates it and allows it to associate with effector proteins. Rab GAPs (GTPase activating proteins) hydrolyse the GTP into GDP, which dissociates the Rab effectors from the Rab. GDIs (GDP dissociation inhibitors) are found in the cytoplasm and can associate with GDP-bound Rabs.

1.3.2 The Rab11 family of GTPases

Rab11 has three isoforms, Rab11A, Rab11B and Rab11C/Rab25, which have a role in various trafficking pathways, including the secretory pathway (Golgi to plasma membrane) (Jung et al., 2012), receptor recycling via the peri-nuclear recycling compartment (Caswell et al., 2008) and transcytosis in epithelial cells (Casanova et al., 1999). These Rab11 pathways are important for cell migration, cytokinesis, cilogenesis, oogenesis and neuritegenesis (Welz et al., 2014). Rab11 is of particular interest as it has been reported to act as both an oncogene and a tumour suppressor protein (Section 1.3.6), and has been shown to regulate the trafficking of integrins and RTKs during cancer cell migration (Caswell et al., 2008; Caswell et al., 2007).

Several Rab11 GAPs have been identified, including TBC1D11, TBC1D14 and Evi5. Indeed, GTP-bound Rab11 recruits Evi5 to the recycling endosome and Evi5 knockdown blocks receptor recycling and cell migration (Laflamme et al., 2012). In contrast to the GAPs, few Rab11 GEF has been identified including Crag1, which has an important role in regulating rhodopsin recycling in *Drosophila (Xiong et al., 2012).* Rab11 has been shown to associate with several motor proteins, such as Myosin Vb, allowing the transportation of Rab11-positive vesicles along the cytoskeleton (Lapierre et al., 2001).

1.3.3 Rab11-Fips

A number of Rab11 effectors have been identified, including Rabphilin-11 (Mammoto et al., 1999) and the Rab11-Fips (Rab11-family of interacting proteins) (Hales et al., 2001). Rab11-Fips have a conserved Rab binding domain (RBD) at their C-terminus, which contains a YID (tyrosine-isoleucine-aspartic acid) motif. Mutating these residues significantly reduces the ability of Rab11-Fips to interact with Rab11a (Lindsay and McCaffrey, 2004). Interestingly, the structure of the RBD from Fip2 bound to Rab11-GTP has been solved, and found to form a heterotetramer with a central dimer of Fip2-RBD forming an amphipathic alpha helix embedded between two Rab11 molecules (Jagoe et al., 2006).

The Rab11-Fip family contains five members, which can be divided into two sub-classes, class I and class II (**Figure 1.8**). Class I Rab11-Fips include Rab Coupling Protein (RCP/Fip1), Fip2 and Rip11/Fip5, which have a conserved C2 domain at the N-terminus that interacts with phospholipids (Lindsay and McCaffrey, 2004). All three Class I Rab11-Fips localise to the perinuclear recycling compartment (PNRC), although a recent paper demonstrates that they localise in distinct regions within this compartment (Baetz and Goldenring, 2013). Class I Rab11-Fips regulate receptor recycling, for example, Rab11-Fip2 is involved in returning internalised transferrin receptor to the plasma membrane (Fan et al., 2004). Furthermore, Fip2 has been shown to associate with EHD proteins, which control the exit of internalised proteins (Naslavsky et al., 2006) and with Myosin5b, which regulates the movement of vesicles (Schafer et al., 2014).

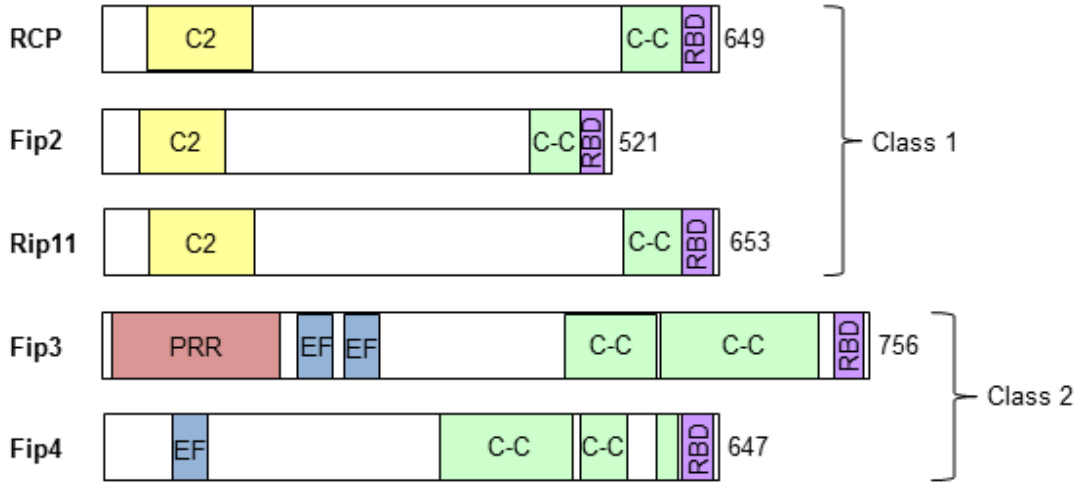

Figure 1-8 Schematic representation of the Rab11-Fips
Rab11-Fips are split into 2 classes: class I Rab11-Fips contain a C2 domain and include RCP, Fip2 and Rip11, and class II Rab11-Fip2 contain an EF hand and include Fip3 and Fip4. (RBD: Rab binding domain, C-C: coiled-coiled domains, EF: EF hand, PRR: proline rich region)

There are two members of the class II Rab11-Fips, Fip3 and Fip4, which contain a proline-rich region and an ERM (erzin/radixin/moesin) domain. Some members of this family have been shown to interact with the Arf (ADP ribosylation factor) subfamily of GTPases as well as Rab11, for example Fip3 associates with both Rab11 and Arf6 (Shiba et al., 2006). Both Fip3 and Fip4 are thought to have a role in delivering membrane from recycling endosomes to the cleavage furrow, and are required for cytokinesis (Fielding et al., 2005). Interestingly, more recently Fip3 has been reported to have a role in the development of dendritic spines in neurons (Yazaki et al., 2014) and is required for breast cancer cell (MDA-MB231) motility in the control of Rac1 activity (Jing et al., 2009).

1.3.3.1 RCP

RCP was named as it was initially thought to interact with both Rab4 and Rab11 and thus potentially couple the two GTPases (Lindsay et al., 2002). However, a subsequent study only detected a weak interaction between RCP and Rab4 *in vitro* and no interaction *in vivo*, indicating that RCP does not act as a Rab4 effector, at least in this cell type (Peden et al., 2004). The gene that encodes for RCP is alternatively spliced producing eight different gene transcripts that are differentially expressed in various cell types (Jin and Goldenring, 2006).

Indeed, some variants lack the RBD so may not be involved in Rab11 functions (Jin and Goldenring, 2006). The exact role of these transcripts remains elusive. At least one of the RCP gene transcript products is involved in trafficking from the PNRC to the plasma membrane, Rab11-Fip1c, which is the most abundant. This isoform is the one commonly referred to as RCP and has been shown to regulate transferrin trafficking (Peden et al., 2004) and in macrophages is thought to regulate recycling from phagosomes (Damiani et al., 2004). More recent work demonstrates the involvement of RCP in EGFR and $\alpha5\beta1$-integrin trafficking, which has an important role in cancer cell migration (Caswell et al., 2008).

1.3.4 Integrin trafficking

Integrin trafficking is complex and has been well studied. Integrin heterodimers are internalised via various pathways, including: clathrin-dependent, clathrin-independent and caveolar mechanisms (Caswell and Norman, 2006). Rab21 is known to contribute to the internalisation of the heterodimers and it associates with the cytoplasmic tail of integrin α-subunits in early endosomes (Pellinen et al., 2006). Once they have reached the early endosomes, internalised integrins can be sorted three ways: into vesicles to the plasma membrane, recycling endosomes or late endosomes (**Figure 1.9**). $\alpha v\beta3$-integrin is trafficked directly from the early endosomes back to the plasma membrane in the rapid route under control of Rab4 (Parker et al., 2004). $\alpha v\beta3$-integrin recycling via this pathway is promoted by growth factor induced autophosphorylation of PKD1, which enables the recruitment of this kinase to the $\beta3$ cytoplasmic tail (Roberts et al., 2004). Indeed, mutating the Serine^{916} autophosphorylation site on PKD1 inhibits recycling of $\alpha v\beta3$-integrin (White et al., 2007).

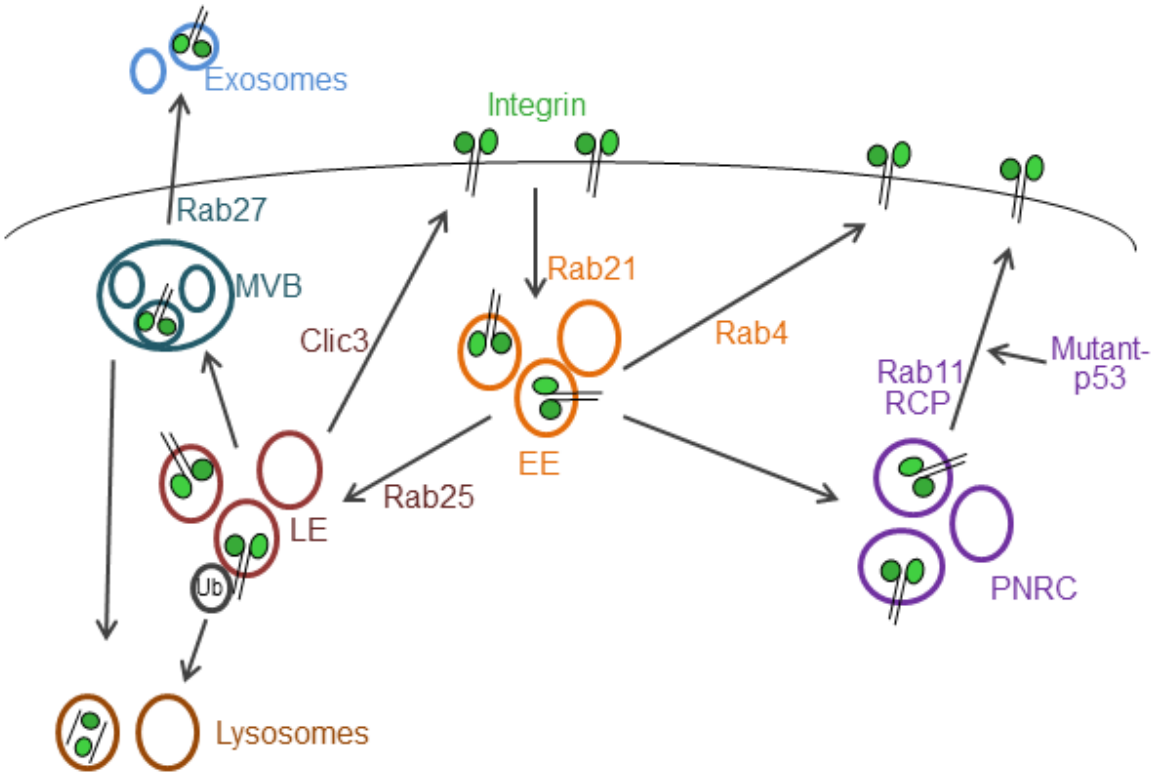

Figure 1-9 Rab GTPase control of integrin trafficking
Integrins are internalised into early endosomes (EE) via several mechanisms, which can be regulated by Rab21. In early endosomes, integrins can be recycled straight back to the plasma membrane in Rab4 positive vesicles or via the perinuclear recycling compartment (PNRC) in RCP/Rab11 positive vesicles. Alternatively, integrin can be trafficking to the late endosome (LE) in which they are either: recycled back the plasma membrane in a Rab25 dependent fashion, are secreted in exosomes via the multivesicular body (MVB) or are ubiquitylated and targeted for lysosomal degradation.

In contrast, many different integrin heterodimers are sorted from early endosomes into recycling endosomes before returning to the plasma membrane via the Rab11-dependent route (**Figure 1.9**). For example, α5β1 (Roberts et al., 2001), αvβ3 (Roberts et al., 2001), αLβ2, α6β1 (Strachan and Condic, 2004) and α6β4 (Yoon et al., 2005) are recycled this way. Numerous pro-migratory kinases are thought to have a regulatory role in this recycling pathway; PKCε phosphorylates vimentin (Ivaska et al., 2005) to release β1 integrin vesicles from the PNRC, and PKB/Akt phosphorylates GSK-3 (Roberts et al., 2004) and ACAP1 (Li et al., 2007) to stimulate β1 delivery from the PNRC to the plasma membrane. Furthermore, RCP regulates α5β1-integrin and EGFR delivery to the plasma membrane. Upon mutant-p53 overexpression or inhibition of αvß3-integrin, RCP's association with α5ß1-integrin and EGFR is enhanced and drives recycling of α5ß1 to the plasma membrane, which drives cancer cell invasion (**Section 3.1**) (Caswell et al., 2008).

Lastly, integrins can be transported from early endosomes into late endosomes (**Figure 1.9**). Indeed, immunogold staining demonstrates that α5β1-integrin localises to late endosomes (Lobert et al., 2010). Furthermore, in ovarian cancer cells α5β1-integrin has to be bound to its ligand, fibronectin, for it to reach the Rab25-positive late endosomes (Dozynkiewicz et al., 2012). Ubiquitylation sites have been identified on both integrin subunits, which can target α5β1-integrin for lysosomal degradation (Böttcher et al., 2012; Lobert et al., 2010). Alternatively, α5β1-integrin can be recycled back to the plasma membrane from late endosomes in a Rab25 and CLIC3 dependent fashion (Demory Beckler et al., 2013; Dozynkiewicz et al., 2012). Lastly, late endosomes can mature into multi-vesicular bodies (MVB) with integrins localised in the intraluminal vesicles, which can be secreted from the cell as exosomes (Vesiclepedia - http://microvesicles.org).

1.3.5 Trafficking of Receptor Tyrosine Kinases

The traditional view of RTK trafficking is that the ligand binds the receptor, the receptor auto-phosphorylates and activates downstream signalling pathways, meanwhile the receptor is ubiquitylated, internalised and degraded. However, recent reports suggest this situation is more complex and that RTKs can be recycled. For example, EGFR is internalised and recycled with α5β1-integrin via the RCP/Rab11 compartment and this is enhanced in cells expressing mutant-p53 ($p53^{175H}$ or $p53^{273H}$) (Caswell et al., 2008). Furthermore, it has been shown that EGFR internalises via clathrin-independent routes resulting in its degradation, and via clathrin-dependent routes resulting in its recycling and prolonged signalling (Sigismund et al., 2008).

cMet is the receptor for HGF and diverges structurally from most RTKs as it is a heterodimer linked by a disulphide bond with an extracellular α-subunit and a transmembrane ß-subunit, which contains an intracellular tyrosine kinase domain (Giordano et al., 1989). Upon HGF stimulation, cMet undergoes rapid internalisation (**Figure 1.10**). The E3 ubiquitin ligase, Cbl, can ubiquitylate cMet, which internalises and targets the receptor for lysosomal degradation (Petrelli et al., 2002). Nevertheless, it has been shown that internalisation and sorting into signalling endosomes is important for cMet signalling. Indeed, this is essential for downstream Erk1/2 signalling, which is dependent on microtubules

and PKCα (Kermorgant et al., 2004). There is emerging evidence that cMet is also recycled (**Figure 1.10**). Indeed, it has been shown that cMet is recycled through a Rab4 endosome, which is regulated by Arf6, and is required for Erk1/2 signalling (Parachoniak et al., 2011). In cancer cells, mutations have been found in cMet that promote recycling and downstream signalling to Rac1 and increase tumourigenesis and metastasis *in vivo* (Joffre et al., 2011). Furthermore, tumour cells that express mutant-p53 have increased c-Met recycling, which is required for mutant-p53 driven cell scatter and invasion (Muller et al., 2013). These studies demonstrate that perturbed RTK trafficking can influence tumourigenesis and metastasis.

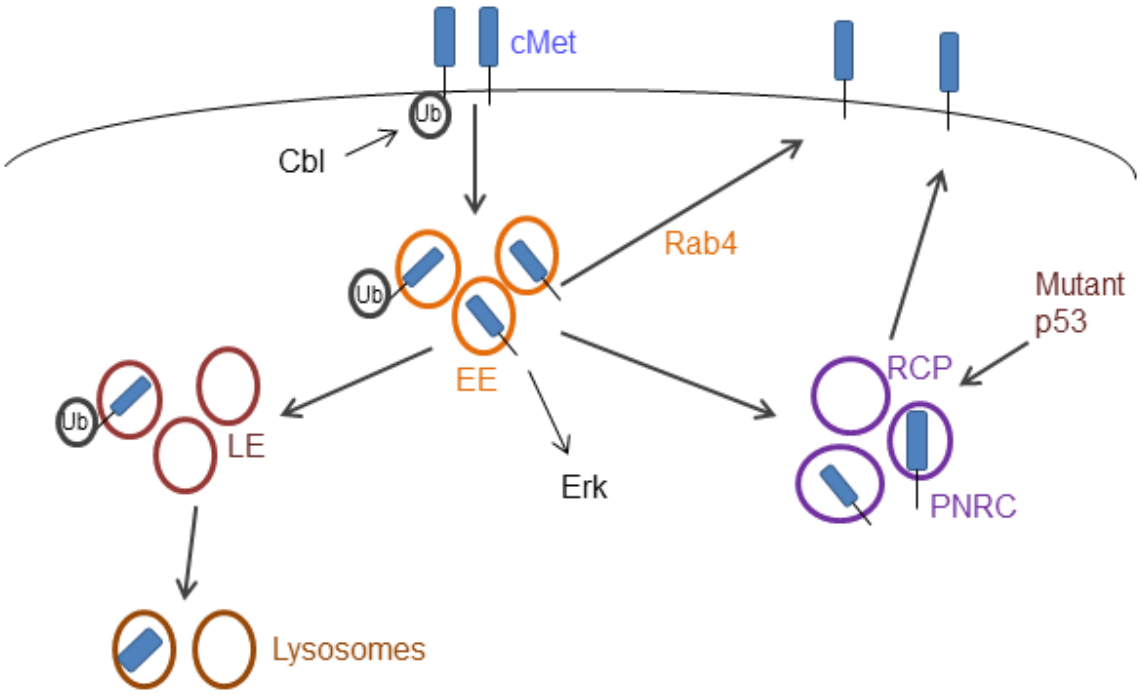

Figure 1-10 cMet trafficking
cMet is rapidly internalised upon ligand activation into EE (early endosomes), which can activate Erk signalling. cMet can be recycled back to the plasma membrane via Rab4 vesicles, while in cancer cells mutant-p53 can promote RCP dependent recycling of cMet. Alternatively, Cbl can ubiquitylate cMet targeting it for lysosomal degradation.

1.3.6 Eph Trafficking

1.3.6.1 Eph and Ephrin detachment

As Eph is normally associated with its cognate ligand on a neighbouring cell, it can only be internalised once the ligand is cleaved by proteolysis or the Ephrin can be internalised with the receptor via trans-endocytosis. Ephs and Ephrins can be proteolytically cleaved by ADAM metalloproteases, γ-secretase proteases and MT1-MMP. ADAM10 is a membrane protein that acts as a sheddase and can cleave many membrane proteins. The ADAM10 cleavage site sequence is conserved in all vertebrate Ephrins. ADAM10 is found loosely associated to EphA3 (Janes et al., 2005). EphrinA2 binding stimulates autophosphorylation of the juxtamembrane region of EphA3 causing a structural rearrangement (Janes et al., 2009), which positions the proteinase domain of ADAM10 onto EphrinA2, stimulating its cleavage (**Figure 1.11A**). Two other members of the ADAM protease family are thought to cleave Ephrins: Kuzbanian cleaves EphrinA2, which is required for axon withdrawal (Hattori et al., 2000), and ADAM12 cleaves EphrinA1 (Ieguchi et al., 2014). EphrinAs are GPI-anchored proteins so cleavage generates an extracellular protein, which can be internalised with the Eph on a neighbouring cell or that can be released to act in a paracrine fashion. Indeed, GFP-EphrinA2 has been shown to be locally dispersed from cells after detachment from their neighbours (Hattori et al., 2000). Secreted EphrinA1 has been shown to disrupt EphA1/EphrinA1 associations on neighbouring cells, causing lung hyperpermeability and promoting the spread of cancer cells (Ieguchi et al., 2014). In contrast, EphrinBs are transmembrane proteins that are cleaved in the extracellular domain leaving a truncated form of activated EphrinB in the plasma membrane. It has been shown that γ-secretase cleaves EphrinBs a second time, after the cleavage by a metalloprotease, and the remaining truncated protein activates Src reverse-signalling (Georgakopoulos et al., 2006; Tomita et al., 2006).

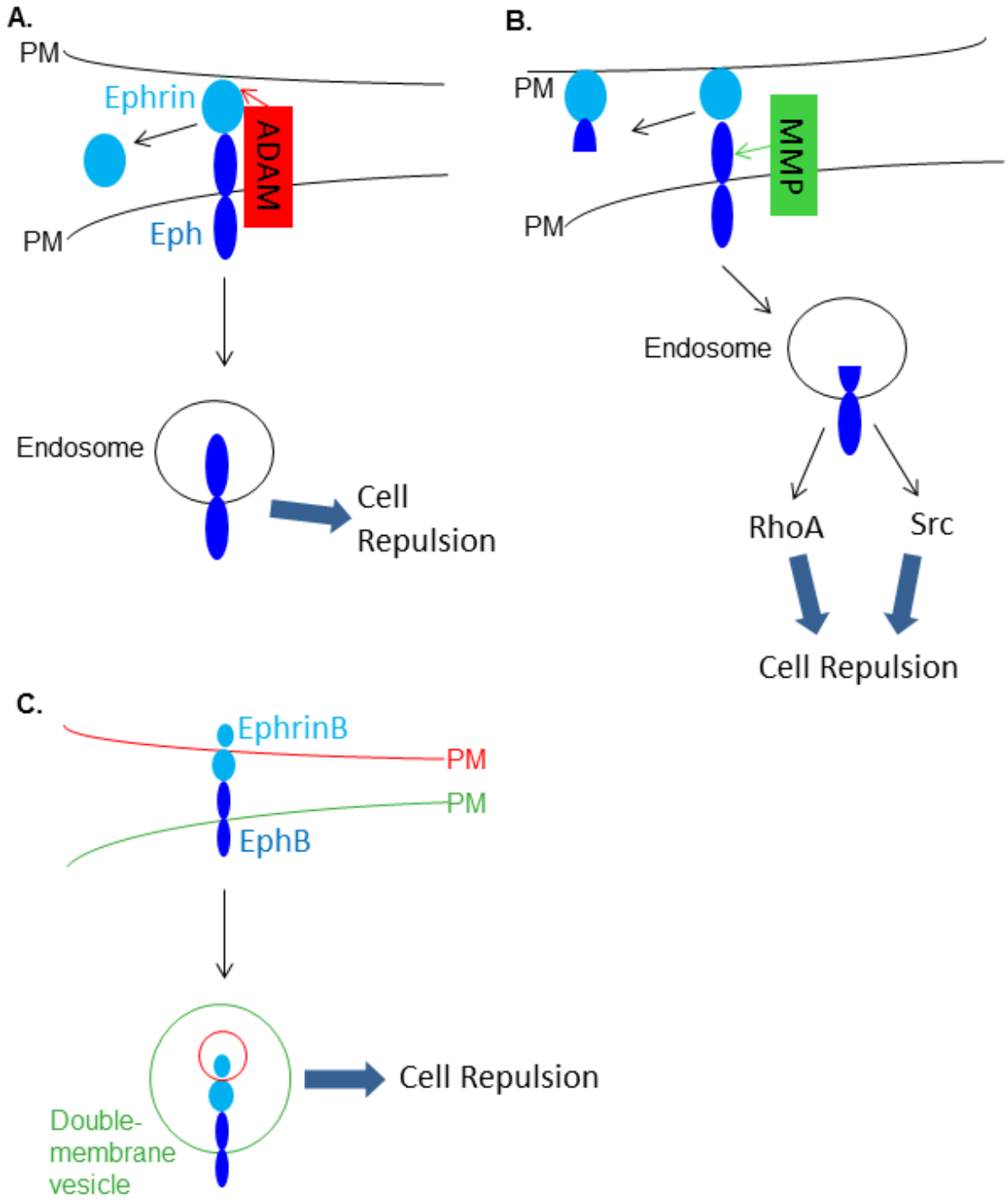

Figure 1-11 Eph and Ephrin detachment
A. ADAM proteases can associate with EphA/EphrinA complexes and cleave Ephrin. The Eph can then internalise and the Ephrin is released, stimulating cell-cell repulsion. B. MT1-MMP proteases can associate with EphA/EphrinA complexes and cleave EphA in its FN type 3 repeat. The transmembrane EphA product is internalised and activates Src kinases and Rho GTPases, which promote cell-cell repulsion. C. EphB/EphrinB can internalise, while associated, by transendocytosis forming a double membrane vesicular structure, which stimulates cell-cell repulsion.

There is some evidence that Ephs can be cleaved in a similar fashion to Ephrins. EphA4 is cleaved by γ-secretase (Inoue et al., 2009) and EphA2 is cleaved in its fibronectin type 3 repeats by MT1-MMP (Sugiyama et al., 2013). MT1-MMP cleavage of EphA2 triggers internalisation of the membrane bound cleaved product, which activates Src and RhoA in a vesicular compartment (**Figure 1.11B**) (Sugiyama et al., 2013). These studies demonstrate that proteolytic cleavage of Ephs/Ephrins may be an important step in cell-cell repulsion.

Ephs and Ephrins are internalised together into one of the cells in a double-membrane vesicle. This poorly understood mechanism is termed trans-endocytosis and has only been reported to occur with the B subgroup of Ephs and Ephrins (**Figure 1.11C**). Marston *et al.* showed in both fibroblasts and primary endothelial cells that EphrinB4 associates with EphB2 and they internalise together into EphB2-positive cells. The double-membrane vesicles contains phosphorylated EphB2 that remains bound to EphrinB4 and is therefore capable of signalling (Marston et al., 2003). In primary neurons EphB2 and EphrinB1 were found to trans-endocytose into either cell; this was required for efficient growth cone retraction (Zimmer et al., 2003). Furthermore, double membrane vesicles were observed by electron microscopy *in vivo* in the rat hippocampus (Spacek and Harris, 2004).

1.3.6.2 Eph internalisation

Ephs are endocytosed via clathrin-dependent and independent mechanisms. Purified clathrin-positive vesicles are enriched in EphA4 (Bouvier et al., 2010) and EphA8 co-localises with clathrin heavy chain in HEK293 cells (Yoo et al., 2010). EphA2 and EphB1 colocalise with caveolin1 and, upon ligand stimulation, these Ephs physically associate with caveolin1 (Vihanto et al., 2006). Several studies have demonstrated that internalised Ephs co-localise with early endosome antigen (EEA1) (**Figure 1.12**) (Parker et al., 2004; Yoo et al., 2010). EphrinBs internalise via Clathrin dependent mechanisms (Parker et al., 2004) and in raft microdomains (Brückner et al., 1999).

Several proteins have been identified as positive or negative regulators of Eph endocytosis. Two proteins have been found that promote Eph endocytosis: Rin1 and Vav2. Rin1 is a Rab5-GEF that promotes EphA4 endocytosis into Rab5-

positive vesicles in postnatal amygdala neurons, which is thought to have an important role in synaptic plasticity (Deininger et al., 2008). Vav2 is a Rho-GEF that is transiently activated upon EphinA1 stimulation. Vav2 depletion inhibits EphA4 internalisation resulting in defects in growth cone repulsion (Cowan et al., 2005). Also, two proteins have been found that negatively regulate Eph internalisation: Tiam1 and SHIP2 (Src homology 2 domain-containing phosphoinositide 5-phosphatase 2). SHIP2 is recruited to the SAM domain of EphA2 upon ligand stimulation, and this is thought to attenuate EphA2 receptor endocytosis (Zhuang et al., 2007). Tiam1 is a Rac-GEF that associates with the juxtamembrane region of EphA8. Suppression of Tiam1 expression inhibits the internalisation of EphA8 (Yoo et al., 2010). More work is required to determine whether these proteins have a role of regulating Eph endocytosis in cancer cells.

1.3.6.3 Eph degradation

Ligand activated Ephs are ubiquitylated and targeted for lysosomal degradation (**Figure 1.12**). Cbl is an E3 ubiquitin ligase, which associates and ubiquitylates both EphA2 and EphB1 (Fasen et al., 2008; Wang et al., 2002). Blocking lysosomal degradation with lysosomotropic agents such as bafilomycin, inhibits EphB1 degradation upon stimulation with EphrinB1 (Fasen et al., 2008). Eph degradation is thought to be a control mechanism to terminate Eph signalling. For example, an Ank family protein, Odin, is found associated with the SAM domain of EphA2 and EphA8, which protects these proteins from being ubiquitylated (Kim et al., 2010). In contrast to Ephs, EphrinBs have been shown to be ubiquitylated by Smurf E3 ligases, which regulates EphrinB degradation (Hwang et al., 2013).

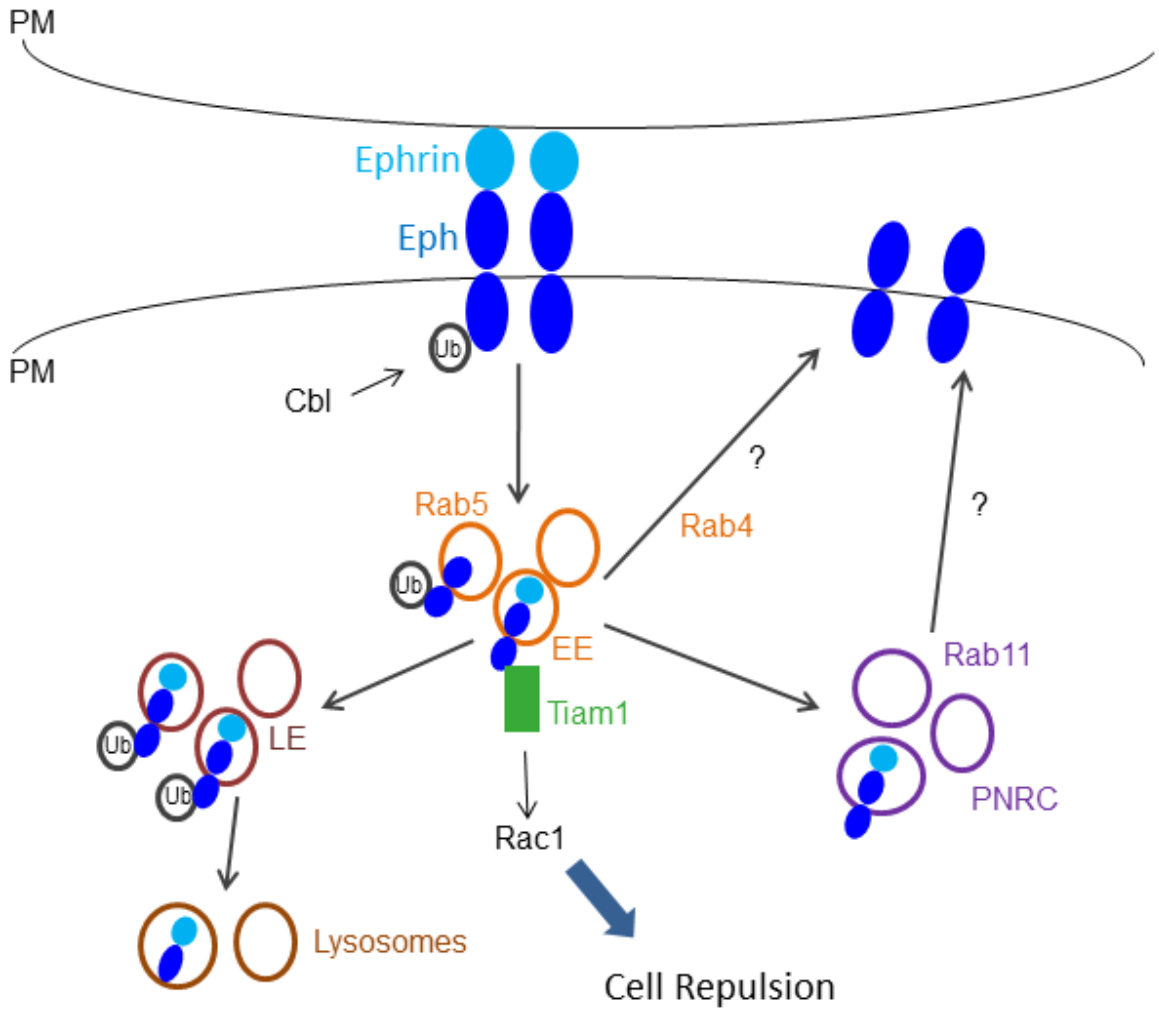

Figure 1-12 Eph trafficking
Upon Ephrin binding, Ephs are internalised into a Rab5 and EEA1 positive early endosome (EE). In early endosomes Ephs can activate Tiam1, which activates cell-cell repulsion. Ephs colocalises with Rab4 and Rab11 in vesicles and are recycled back to the plasma membrane. Ephs can be ubiquitylated by Cbl at the plasma membrane, which targets them for lysosomal degradation.

1.3.6.4 Eph recycling

Only one study has been published on Eph recycling. Upon EphrinA2 stimulation 40% of EphA2 is internalised and 30% of this internalised protein is recycled back to the plasma membrane (Boissier et al., 2013). At early time points after EphrinA1 stimulation, EphA2 co-localises with Rab4 and at later times with Rab11 (**Figure 1.12**). EphA2 remains ligand-associated and phosphorylated in vesicles where it associates with Tiam1 (a cytosolic Rho-GEF), while EphA2 remaining at the cell surface did not associate with Tiam1 (Boissier et al., 2013). Suppression of Tiam1 expression with siRNA inhibited EphA2 internalisation and EphrinA1-induced Rac1 activation, which triggered cell-cell repulsion. This

demonstrates the potential impact of EphA2 trafficking on its downstream signalling (Boissier et al., 2013).

1.3.6.5 Ephs and Ephrins regulate the trafficking of other growth factor receptors

Ephs/Ephrins have an important role in regulating the internalisation and signalling of other growth factor receptors and vice versa. This has been shown in several biological settings, for example EphB2 activation stimulates phosphorylation of synaptojanin-1, a phosphatase, which is important for clathrin-mediated endocytosis. Thus, upon EphrinB2 stimulation EphB2 activation promotes internalisation of TfnR in HEK 293 cells and AMPA in hippocampal neurons (Irie et al., 2005). In vascular smooth muscle cells depletion of Ephrin-B2 redistributes PDGFRβ from caveolin to clathrin associated membrane fractions, which enhances PDGFRβ internalisation and activates MAPK and JNK signalling, while impairing TIAM1-Rac1 signalling (Irie et al., 2005). EphrinB2 also regulates endothelial sprouting by controlling VEGRF2 or VEGFR3 internalisation, which regulates downstream signalling to Rac1, Akt and Src (Sawamiphak et al., 2010; Wang et al., 2010). Indeed, suppressing EphrinB2 expression impairs tumour vascularisation and growth (Sawamiphak et al., 2010). In glioma cell lines EphrinA5 enhances Cbl binding to EGFR and promotes its internalisation and degradation (Li et al., 2009).

1.3.7 Receptor trafficking in cancer

Receptor trafficking is often perturbed in cancer, which often increases RTK signalling and promotes tumourigenesis and metastasis. For example, mutations in cMet promote recycling and prolonged signalling, while inhibiting degradation, which increases tumourigenesis and metastasis *in vivo* (Joffre et al., 2011). Altered expression of several Rab GTPases, such as Rab5, Rab20, Rab23, Rab25 and Rab34, has been identified in tumours (Chia and Tang, 2009). Rab25 is the most studied Rab in cancer and has an interesting and complex role. Its mRNA levels are significantly increased in 89% of ovarian cancers (Schaner et al., 2003) and in 67% of breast cancers (Sorlie et al., 2003) and patients with high Rab25 expression have a poor rate of survival (Cheng et al., 2005). Overexpression and siRNA studies demonstrate that Rab25 accelerates the growth and aggressiveness of breast and ovarian tumours via a mechanism that is likely to involve the

activation of PKB/Akt signalling (Cheng et al., 2005; Wei et al., 2001). Rab25 directly associates with the cytoplasmic tail of β1-integrin. Overexpression of Rab25 increases α5β1-integrin recycling from late endosomes, which increases cell invasion into fibronectin-rich 3D matrices (Caswell et al., 2007; Dozynkiewicz et al., 2012). Conversely, Rab25 also has tumour suppressor functions. In some breast cancer cells, Rab25 expression is lost (Cheng et al., 2006) and re-expressing Rab25 reduces tumour growth and invasion *in vivo* (Cheng et al., 2010). Furthermore, Rab25 expression is lost in colonic neoplasms and colonic adenocarcinomas, which is associated with poor survival (Goldenring and Nam, 2011). More work is required to determine how other Rab GTPases contribute to carcinogenesis.

Not many studies have investigated the role of Rab effectors in tumourigenesis. However, it has been reported that the RCP gene is amplified breast tumour cases (Garcia et al., 2005), small lung carcinomas (Balsara et al., 1997), colorectal cancers (Nakao et al., 2004) and urinary bladder tumours (Simon et al., 2001). As RCP expression is frequently misregulated in cancer (**Section 3.1.1**), it is an interesting and relevant protein to study to gain a better molecular understanding of its role in cancer.

1.4 Aims and preamble to results

RCP clearly contributes to cancer cell invasion by controlling the trafficking of adhesion receptors, such as α5β1-integrin, and RTKs, such as EGFR and cMet. However, it is likely that these receptors are not the only cargoes of RCP-mediated transport that have relevance to cancer cell migration and invasion. In this study I set out to use an unbiased proteomic approach to characterise RCP's interactome and in this way identify potential new cargo for RCP-regulated recycling pathways. Using this approach I have identified EphA2 as an RTK whose trafficking and function is controlled by RCP. I then proceeded to study the role played by RCP in influencing EphA2's ability to mediate contact inhibition of locomotion and cell-cell repulsion. In particular I have focused on how phosphorylation of RCP at a potential residue enables it to mediate EphA2-dependent cell-cell repulsion, thus describing a new pathway through which a Rab11 effector may contribute to the dissemination and metastasis of cancer.

2 Materials and Methods

2.1 Materials

2.1.1 Reagents

Reagent	Supplier
1kB ladder	Thermo Scientific
2% gelatin (in PBS)	Sigma
AEBSF	Melford
Agarose (high gel strength)	Melford Laboratories
ALLN	Calbiochem
Ampicillin	Sigma
Aprotinin	Sigma
Ascorbic Acid	Sigma
Bacto-trypton	Melford
BamH1	New England Biolabs
Benzamidine	Sigma
BL21(DE3)pLysS	Promega
Bradford (Coomassie plus) reagent	Thermo scientific
Bromo-phenol Blue	Sigma
BSA	First link
Calcein-AM	Life Technologies
Cilengitide	Bachem
Cirtrate retrieval buffer	Thermo scientific
Citric acid	Sigma
Collagen 1 (rat tail high concentration)	BD bioscience
Coomassie	Life Technologies
cRAD	Bachem
cRGD	Bachem
DH5α cells	Life Technologies
Dialysis cassettes	Pierce
DNAse1	Roche
dNTP (100mM)	Life Technologies
DTT	Melford
Dulbecco's Modified Eagle Medium (DMEM)	Gibco
Dynabeads anti-mouse	Life Technologies
Dynabeads anti-rabbit	Life Technologies
ECL Western blotting substrate	Pierce
EcoR1	New England Biolabs
EDTA	Sigma
EGF	Peprotech
EGTA	Sigma

EphrinA1-Fc	R & D systems
Ethidium Bromide	Sigma
Falcon tissue culture dishes (10 & 15cm^2)	BD Biosciences
Fc	Millipore
Fibronectin (1mg/ml soluble)	Sigma
Foetal Calf Serum	Autogen Bioclear
Fungizone	Sigma
Geltrex	Life Technologies
Glass bottom 3 cm^2 and 6 well plates	Maktek
Glutathione	Sigma
Glutathione (4% agarose beads)	GE Healthcare
Glycerol	Fisher Scientific
H_2PO_4	Sigma
HCL	Sigma
HGF	Sigma
Hybond-P PVDF membrane	GE Healthcare
Hydrogen peroxide	Fisher Scientific
Igepal CA-630	Fluka
IgG	Jackson immunoResearch
IHC Dako envision rabbit secondary	Dako
Iodoacetamide (IAA)	Sigma
IPTG	Melford
Kanamycin	Sigma
KCl	Fisher Scientific
Leupeptin	Melford
L-Glutamine (200mM)	Life Technologies
Lysozyme	Sigma
MatrigelTM Basement membrane mix	Becton Dickson
Maxisorp 96 well plates	Life Technologies
MesNa	Fluka
Milk powder	Marvel
Na_2CO_3	Fisher Scientific
Na_2HPO_4	Fisher Scientific
Na_3V0_4	Fisher Scientific
NaCl	Fisher Scientific
NaF	Sigma
$NAHCO_3$	Fisher Scientific
NaOH	Fisher Scientific
Nunc tissue culture plates	TCS biologicals
NuPAGE MES SDS running buffer	Life Technologies
NuPAGE MOPS SDS running buffer	Life Technologies
NuPAGE pre-cast gels (4-12%, 10, 12, 14 wells)	Life Technologies
NuPAGE sample buffer	Life Technologies

NuPAGE transfer buffer	Life Technologies
Osteopontin	Sigma
Parafilm wrap	Fisher Scientific
Paraformaldehyde	Electron microscopy sciences
PBS containing calcium and magnesium	Sigma
PD150606	Calbiochem
Penicillin/Streptomycin	Life Technologies
PLATINUM Taq DNA polymerase high fidelity	Life Technologies
Precision plus protein all blue standard	Biorad
Primaquine	Sigma
Propan-2-ol	Fisher
Protease inhibitor cocktail	Roche
Pst1	New England Biolabs
Rapid ligation buffer	Promega
RMPI-1640 medium	Gibco
Sal1	New England Biolabs
SDS	Fisher Scientific
siRNA	Dharmacon
SOC media	Life Technologies
Sulfo-NHS-SS-Biotin	Pierce
Super RX medical x-ray film	Fuji
T4 DNA ligase	Promega
TOP10 OneShot cells	Life Technologiesa
Transwell Permeable Support (8µm pore size)	Fisher Scientific
Tris HCl	Melford
Triton-X100	Sigma
Tween-20	Sigma
Vectashield mounting media (+/- DAPI)	Vector laboratories
Xho1	New England Biolabs
Yeast extract	Fisher Scientific
β-mercaptoethanol	Sigma

Table 2-1 Reagents and suppliers

2.1.2 Solutions

Solution	Recipe
Eluate buffer	50mM Tris-HCl (pH6.8), 92 mg/ml DTT, 10% SDS (w/v), 15% glycerol (w/v), 1% bromo-phenol blue (v/v)
Biotin reduction buffer	50mM Tris HCl (pH7.5), 10mM NaCl, add 10N HCl until buffer reaches pH8.6 (~1.4ml) at 4ºC
ELISA coating buffer	0.05M Na_2CO_3, pH9.6 at 4ºC
ELISA developing reagent	0.56 mg/ml ortho-phenylenediamine , 25.4mM Na_2HPO_4, 12.3mM citric acid, pH5.4 with 0.003% H_2O_2
LB agar	85mM NaCl, 1% bacto-trypton (w/v), 0.5% yeast extract (w/v), 1.5% agarose (w/v), +/- 100µg/ml ampicillin or 50µg/ml kanamycin
LB broth	85mM NaCl, 1% bacto-trypton (w/v), 0.5% yeast extract (w/v), +/- 100µg/ml Ampicillin or 50µg/ml Kanamycin
No detergent NDLB	50mM Tris HCl (pH7.0), 150mM NaCl, 10mM NaF, 1mM Na_3V0_4, 5mM EDTA, 5mM EGTA
PBS	170mM NaCl, 3.3mM KCl, 1.8mM Na_2HPO_4, 10.6mM H_2PO_4
PBS-T	PBS, 0.1% Tween-20 (v/v)
TBS	10mM Tris-HCl (pH7.4), 150mM NaCl
TBS-T	TBS, 0.1% Tween-20 (v/v)
Triton NDLB	No detergent NDLB lysis buffer, 1.5% Triton-X100 (v/v), 0.75% Igepal CA-630 (v/v)
Tween NDLB	No detergent NDLB lysis buffer, 0.15% Tween-20 (v/v)

Table 2-2 Recipes of solutions

2.1.3 Kits

Kits	Supplier
F-410 DyNAmo SYBR Green qPCR kit	Thermo Scientific
ImProm-IITM reverse transcription system	Promega
Nucleofector Kit T	Amaxa
Nucleofector Kit V	Amaxa
Pierce BCA protein assay kit	Thermo Scientific
Platinum PCR SuperMix High Fidelity	Life technologies
QIAGEN Plasmid maxi kit	Qiagen
QIAprep Spin miniprep kit	Qiagen
QIAquick gel extraction kit	Qiagen
QIAquick PCR purification kit	Qiagen
Quick ligation kit	NEB
RNeasy mini kit	Qiagen
Western Blotting equipment and solutions	Life Technologies

Table 2-3 Kits and suppliers

2.1.4 DNA Plasmids

Plasmid	Supplier/ Cloned by
pEGFP-C1-3	Clonetech
pEGFP-C2-Rab6A	Mary McCaffrey
pEGFP-C2-Rab6B	Christine Gundry
pEGFP-C3-Fip2	Mary McCaffrey
pEGFP-C3-Fip3	Mary McCaffrey
pEGFP-C3-Fip4	Mary McCaffrey
pEGFP-C3-Rab14	Mary McCaffrey
pEGFP-C3-RCP	Mary McCaffrey
pEGFP-C3-RCP$^{199-649}$	Mary McCaffrey
pEGFP-C3-RCP$^{2-199}$	Mary McCaffrey
pEGFP-C3-RCP$^{379-639}$	Mary McCaffrey
pEGFP-C3-RCP^{I621E}	Mary McCaffrey
pEGFP-C3-RCP^{S435A}	Patrick Caswell
pEGFP-C3-Rip11	Mary McCaffrey
pEGFP-farnesylated	Juliana Schwarz
p-EGFP-N1	Clonetech
pEGFP-N1-EphA2	Christine Gundry
pGEX-4T1	Pharmacia Biotech
pGEX-4T1- Rab6B	Christine Gundry
pmCherry	Roger Tsien
pmCherry-Rab14	Mary McCaffrey
pmCherry-RCP	Mary McCaffrey
pTRCHisA	Life technologies
pTRCHisA-RCP	Mary McCaffrey

Table 2-4 DNA plasmids and suppliers

2.1.5 Primers

Primer	Use	Sequence/ Company
Actin F & R	RT-PCR/PCR	Quantitect
EphA2 middle 1	Sequencing	ACTGTGCAGTGGATGGCG AGT
EphA2 middle 2	Sequencing	GAGTGTGGAAGTACGAGGTCAC
GAPDH F & R	RT-PCR	Quantitect
Fip2 F &R	RT-PCR	Quantitect
pEGFP-C2-Rab6B F	Cloning	AAAGAATTCATGTCCGCAGGGGGAGATTTTG
pEGFP-C2-Rab6B R	Cloning	TTTGTCGACGCTGGCCGGGGCTCCTGGGGT
pEGFP-N1-EphA2 F	Cloning	CCCGAATTCACATGGAGCTCCAGGCAGCCCGCGCCT
pEGFP-N1-EphA2 R	Cloning	GGGGTCGACAGGATGGGGATCCCCACAGTGTTCACC
Rab6A/A' F	PCR	ATGTCCACGGGCGGA
Rab6A/A' R	PCR	CTGAAGAAGGTTGAAGATG
Rab6B F	PCR	TCGACAACACATACCAGGCA
Rab6B R	PCR	TGCTTCACGTTGTAGCCAGT

Table 2-5 Primer uses and sequences
(F: forward, R: reverse)

2.1.6 Antibodies

Andibody	Species	Technique (dilution)	Supplier
Alexa-fluor 488 α-mouse	Goat	IF (1/300)	Life Technologies
Alexa-fluor 568 α-chicken	Goat	IF (1/300)	Life Technologies
Alexa-fluor 568 α-rabbit	Donkey	IF (1/300)	Life Technologies
cMet	Goat	ELISA (5µg/ml)	R & D Systems
EGFR	Mouse	IB (1/1K), ELISA (5µg/ml)	BD Pharmingen
EphA2	Mouse	IB (1/1K), IP (1.5µg/ml), IF (1/200), ELISA (5µg/ml)	Millipore
Fip2	Rabbit	IB (1/500)	Proteintech
Fip3	Rabbit	IB (1/500)	Mary McCaffrey
GFP	Mouse	IB (1/2K)	Abcam
GFP	Rabbit	IP (1.5µg/ml)	Abcam
HRP α-mouse	Goat	IB (1/3K)	Sigma
HRP α-rabbit	Goat	IB (1/3K)	Sigma
Phospho-RCP	Rabbit	IB (1/500)	Eurogentech
Rab11A	Rabbit	IB (1/1K), IF (1/100)	Zymed
Rab14	Rabbit	IB (1/500)	Abnova
Rab14	Rabbit	IB (1/500)	Abcam
Rab4	Rabbit	IB (1/1K)	Transduction labs
Rab5	Mouse	IB (1/1K)	Transduction labs
Rab6A	Rabbit	IB (1/1K)	Proteintech
RCP (human)	Chicken	IB (1/7K), IF (1/300)	Genway
RCP (human)	Rabbit	IB (1/1K), IF (1/300)	Eurogentech
RCP(mouse)	Rabbit	IB (1/1K), IHC (1/1.5K)	Eurogentech
RG-16	Rabbit	IP (1.5µg/ml)	Sigma
Tnf Receptor	Mouse	ELISA (5µg/ml)	BD Pharmingen
α5 integrin	Mouse	IB (1/1K)	BD Transduction
α5 integrin	Mouse	ELISA (5µg/ml)	BD Phamingen
β-tubulin	Mouse	IB (1/10K)	Sigma

Table 2-6 Antibodies
(IB: immunoblotting, IP: immunoprecipitation, IHC: immunohistochemistry, IF: immunofluorescence)

2.2 Methods

2.2.1 Cell culture

2.2.1.1 Cell lines

A2780-DNA3 and A2780-Rab25 cell lines were generated and donated by Professor Gordon Mills (Cheng et al., 2005). As I wanted to use the PC3 cell in which the Ephs and Ephrins have been characterised (Astin et al., 2010), Professor Kate Nobes kindly gave us their PC3 cells. Several cell lines were obtained from others at the Beatson Institute, including the H1299 cells (Patricia Muller) and the pancreatic ductal adenocarcinoma (PDAC) mouse lines (Bryan Miller/Jen Morton).

2.2.1.2 Cell cultivation

The cell lines were grown at 37ºC and 10% CO_2 in a humidified incubator. A2780 and PC3 cells were cultured in RMPI-1640 media, whilst H1299 cells and the PDACs were cultured in DMEM media. All media was supplemented with 10% foetal calf serum, 2mM L-glutamine, 100IU/ml penicillin, 100µg/ml streptomycin and 250µg/ml fungizone. Cells were split once they reached 80-90% confluence (H1299 cells at 65-75%). Briefly, the cells were washed twice in PBS, 1ml 10% Trypsin/PE solution was added and left until the cells had detached. Media was added and the appropriate number of cells seeded in fresh culture dishes.

2.2.1.3 Nucleotransfection

Amaxa nucleotranfection kits were used according to the manufacturer's instructions. A2780 cells were transfected using kit T, whilst H1299 and PC3 cells were transfected using kit V. An 80% confluent 15cm^2 plate of cells was required per transfection. The cells were washed twice with PBS, detached with 1ml 10% Trypsin/PE solution, resuspended in 10ml media and centrifuged at 1,000rpm for 5 minutes. The media was removed and the cells were washed in 10ml PBS and centrifuged at 1,000rpm for 5 minutes. The cells were resuspended and thoroughly mixed in 100µl solution T/V with added supplements and the appropriate DNA (3µg) or siRNA (5µl of 20mM stock). The suspension was transferred into a cuvette and electroporated on the appropriate setting (A2780: A-023, H1299: X-001, PC3: T-020). 500µl media was quickly added and the cells

were removed gently with a pipette onto the appropriate tissue culture dishes. The cells were left to recover for 24 hours before any experiments were performed.

2.2.1.4 Cell proliferation

To measure cell proliferation, 5,000 cells were seeded into each well of a 12-well plate and counted 24, 48, 72 and 96 hours later. To detach the cells, they were washed twice in PBS and 200µl 10% trypsin/PE solution was added for precisely 5 minutes. To inhibit the trypsin, 200µl media was added. 200µl of cell suspension was added to 19.8ml PBS and the cell number was measured using a Casy cell counter. Each condition was measured in triplicate and the experiment was performed twice.

2.2.1.5 Cell Lysis

After cells had reached 70-90% confluency, the cell culture media was aspirated off and the cells were washed twice on ice with cold PBS. Triton NDLB was supplemented with protease inhibitors (50µgml leupeptin, 50µg/ml aprotinin and 1mM AEBSF) and calpain inhibitors (20µM ALLN and 100µM PD150606). For cell lysis, 300µl was added to each 10cm^2 plate (Tween NDLB was used for immunoprecipitations) and the cells were scraped off the base of the plate. The cell suspension was passed through a 25G needle four times and clarified by centrifugation at 14,000rpm for 10 minutes at 4ºC. The supernatant was carefully removed and either used immediately or stored at -20ºC.

2.2.2 DNA

2.2.2.1 PCR (polymerase chain reaction)

PCR was set up using Platinum PCR SuperMix High fidelity, following manufacturers' instructions. For each reaction, 10ng/µl template plasmid and 5µM of each primer were used (**Table 2.5**). PCR was carried out in a DNA engine Thermal Cycler (Biorad). First, the DNA strands were denatured at 95ºC for 2 minutes. Then the DNA was amplified in 30 cycles of: 95ºC for 45 seconds to denature the DNA, 60ºC for 45 seconds to anneal the primers, and 72ºC for 60 seconds to extend the strand. To ensure all DNA was fully extended, it was

incubated for a final 8 minutes at 72ºC. The DNA product was analysed by agarose gel electrophoresis.

2.2.2.2 Agarose gel electrophoresis and purification

The sizes of amplified or digested DNA products were analysed by gel electrophoresis. First, a 1% (w/v) agarose gel was produced by heating agarose in TAE buffer, supplementing it with 0.2µg/ml ethidium bromide and leaving it to solidify. DNA was mixed with DNA loading dye and loaded into the wells. 1kB ladder was run in adjacent lanes to estimate the size of DNA bands. Electrophoresis was run in a gel container filled with TAE and run at 100V for 1 hour. DNA was visualised using UV translumination. DNA products were cut out of the gel and purified using the QIAquick gel extraction kit following the manufacturer's protocol.

2.2.2.3 Restriction Digestion

DNA digestion with restriction enzymes was carried out according to manufacturer's instructions using the buffers provided with the enzymes. Briefly, 1µg of DNA was digested with two restriction enzymes (1Unit per enzyme) in 20µl at 37ºC for 2 hours. To determine whether the reaction was successful, the DNA products were separated by gel electrophoresis.

2.2.2.4 DNA Ligation

To ligate two DNA fragments together the Quick Ligation Kit was used according to manufacturer's instructions. Briefly, 50ng of vector was mixed with 150ng insert, water, the provided buffer and T4 DNA ligase, and incubated at room temperature for 30 minutes.

2.2.2.5 Transformation of *E.coli*

DH5α or TOP10 competent cells were used for cloning, and BL21(DE3)pLysS cells were used for protein production. The appropriate cells were thawed and mixed with 2µl of the ligation mix or 5ng of DNA on ice. The cells were heat-shocked at 42ºC for 45 seconds and then immediately returned to ice for 2 minutes. The cells were recovered by adding 450µl SOC media and shaking them at 37ºC for one hour. Half the cells were plated onto LB agar containing the appropriate

antibiotic (ampicillin or kanamycin) at 37ºC overnight. To store DNA plasmids, 500µl glycerol was mixed with 500µl transformed bacteria and kept at -80ºC.

2.2.2.6 Plasmid preparation and sequencing

To determine whether any *E.coli* colonies contained the correctly ligated plasmid, the DNA was prepared and purified for sequencing. The colonies were picked and grown in 5ml LB media supplemented with the appropriate antibiotic at 37ºC overnight. The cells were pelleted by centrifugation at 3000rpm for 10 minutes in a Beckman Coulter centrifuge. DNA was prepared using the QIAprep Spin Miniprep kit according to manufacturer's instructions. DNA sequencing was performed on an Applied Biosystems 3130x1 sequencer by the Beatson Molecular Technology services using specifically designed primers (**Table 2.5**). Four primers were required to sequence the full length of EphA2.

For large quantities of DNA, the Beatson Institute central services performed Maxipreps using the QIAprep Spin Maxiprep kit, according to manufacturer's instructions. Before the DNA was used, its concentration was measured using a NanoDrop spectrophotometer.

2.2.3 RNA

2.2.3.1 Extraction of mRNA

RNA was isolated from cells at 70% confluency. The cells were washed twice with cold PBS and drained to remove any residual PBS. Cell lysis was performed by scraping the cells off the plate in RLT buffer mixed with ß-mercaptoethanol, provided by the RNeasy kit. This kit was used according to manufacturer's instructions, including the extra steps to further homogenise lysates using QIAshredder columns and to digest any DNA using the oncolumn DNAse1 digestion. RNA was eluted in sterile water and either used immediately or snap frozen on dry ice.

2.2.3.2 Synthesis of cDNA

cDNA was synthesised from RNA using a DNA engine Thermal Cycler (Biorad) and the ImProm-IITM reverse transcription system kit, according to manufacturer's instructions. Briefly, 1µg RNA was mixed with 0.5µg/ml oligo(dT)s and water,

heated to 70ºC for 5 minutes and then immediately chilled. ImProm-II reverse transcriptase, reaction buffer, 24mM $MgCl_2$, 10mM dNTPs and 40U/µl RNasin was added. To allow annealing the mix was kept at 25ºC and then the cDNA was extended at 42ºC for 1 hour. Once the stands had been synthesised the reaction was heat inactivated at 70ºC for 5 minutes.

2.2.3.3 RT-PCR

Quantitative PCR was performed using the QuantiTect SYBR green PCR kit and a BioRAD DNA engine thermal cycler with a chromo4 engine and Opticon Monitor3 software. Briefly, 10µl SYBR Green mix was mixed with 1µl cDNA (synthesised from 1µg RNA) and 2µl of Quantitect primers (**Table 2.5**). Each condition was performed in triplicate and pipetted into a 96 well plate. The DNA was denatured at 95ºC for 15 minutes. Next, the DNA was amplified in 40 cycles of: 95ºC for 30 seconds to denature the DNA, 60ºC for 30 seconds to anneal the primers and 72ºC for 30 seconds to extend the strand. To ensure all the DNA was fully extended, it was incubated for 5 minutes at 72ºC. A dissociation curve was produced by increasing the temperature from 70ºC to 90ºC in 0.3ºC steps. Opticon Monitor 3 software was used to calculate the changes in gene expression, which was normalised to GAPDH. Each experiment was performed in triplicate.

2.2.4 Protein

2.2.4.1 Protein production and purification

His-RCP and GST-Rab6B were expressed and purified in *E.coli* for use in *in vitro* binding assays. GST-Rab6B was transformed into BL21(DE3)pLysS cells as previously described (**Section 2.2.1.4**). A colony was picked and cultivated in 10ml LB media supplemented with 100µg/µl Ampicillin at 37ºC overnight. This culture was added to 1L LB media supplemented with 100µg/µl Ampicillin. Once the culture reached an optical density of 0.6-0.8 (at 600nm), 0.25mM IPTG was added to induce GST-Rab6B expression. The cells were grown for a further 2 hours. The cells were then centrifuged at 4,000rpm for 30min at 4ºC. The pellet was re-suspended in 20ml PBS pH7.4/0.1% Triton X-100 supplemented with the protease inhibitor cocktail and 1mg/ml lyzosyme. The cells were lysed by

sonication on ice in 8 second cycles until the suspension turned to liquid. Cell debris was removed by centrifugation at 11,000rpm for 30 minutes at 4ºC.

The fusion protein was purified by adding 0.5ml of pre-swollen 50% glutathione (4%) agarose beads to the supernatant and gently mixed for 2 hours at 4ºC. The beads were gently collected by centrifugation at 1,000rpm for 5 minutes at 4ºC and the supernatant was discarded. The beads were resuspended in 20ml PBS 0.1% Triton X-100 and centrifuged at 1,000pm at 4ºC for 5 minutes. This wash step was repeated a further 4 times and then twice with PBS alone. 250µl elution buffer (5mg/ml Glutathione in 50mM Tris, 100mM NaCl, pH8.0) was added and mixed by gently inverting the tube. The slurry was centrifuged at 6,000rpm for 3mins at 4ºC. This elution step was repeated a further two times. The proteins were dialysed in Pierce Dialysis cassettes (10kDA molecular weight cut off) in 5L PBS overnight at 4ºC. To assess the protein concentration Bradford assays were performed (**Section 2.2.4.3**). A similar method was used to generate and purify His-RCP. The proteins were stored at -80ºC.

2.2.4.2 *In vitro* binding assays

First, GST-tagged protein was coupled to agarose beads. Agarose glutathione bead slurry was washed 3 times in PBS (100µl/condition), using centrifugation at 1,000rpm for 3 minutes. They were re-suspended in 1ml PBS 0.15% Tween-20 supplemented with protease (50µgml leupeptin, 50µg/ml aprotinin and 1mM AEBSF) and calpain inhibitors (20µM ALLN and 100µM PD150606) and split into two tubes. 50µg of GST or GST-Rab6B were added to the beads and rotated for 1 hour at 4ºC. To remove excess protein, the beads were washed twice with PBS 0.15% Tween-20 supplemented with protease and calpain inhibitors. The pellets were re-suspended in 0.5ml 37µg His-RCP 0.15% Tween-20 supplemented with protease and calpain inhibitors and rotated for 2 hours at 4ºC. To remove unbound proteins, the suspension was washed four times. All the remaining liquid was removed from the beads. 100µl reducing sample buffer was added and boiled at 100ºC for 5 minutes. The samples (20µl) were immediately analysed by SDS-PAGE or stored at -20ºC. Each *in vitro* binding assay was repeated three times.

2.2.4.3 Bradford assays

Protein concentration was determined using Bradford reagent. Protein standards were used (0.1, 0.2, 0.4, 0.6, 0.8 and 1mg/ml of BSA) to generate a standard curve. Protein samples, standards and the appropriate blank were pipetted in triplicate into a 96 well plate. Bradford reagent was used according to manufacturer's instructions: 200µl was added to each well and incubated at room temperature for 10 minutes. The absorbance was read at 595nm on a Dynatech MR7000 plate reader and protein concentration was determined from the standard curve.

2.2.4.4 SDS-PAGE

To resolve protein samples SDS-PAGE (sodium dodecyl sulphate-polyacrylamide) gels were used. Approximately 30µg protein was reduced in reducing sample buffer at 100ºC for 5 minutes. Molecular weight markers were run in adjacent lanes to the samples. The proteins were resolved on 4-12% denaturing pre-cast gels in MES or MOPs running buffer (depending on protein size) at 120V for 2 hours. These gels were then analysed by Coomassie staining or Western blotting.

2.2.4.5 Coomassie staining

Prior to Coomassie staining, proteins were resolved by SDS-PAGE. The gels were washed three times with distilled water for 5 minutes and then incubated in SimplyBlue SafeStain Coomassie for 30 minutes, rocking at room temperature. To remove background staining, the gel was washed in distilled water until the bands were distinct for analysis.

2.2.4.6 Western blotting

Prior to Western blotting, proteins were resolved by SDS-PAGE. The proteins were transferred from the gel onto PVDF membrane by wet transfer in NuPage blotting buffer at 30V for 90 minutes. The membrane was blocked in 5% milk in TBS-T (or 5% BSA for phospho-antibodies) rocking for 30 minutes at room temperature. Membranes were then incubated in the appropriate antibody in 1% milk in TBS-T (or BSA) (**Table 2.6**) overnight at 4ºC. To remove excess antibody, the membranes were washed in TBS-T three times for 10 minutes. The membranes were incubated in the appropriate HRP-conjugated secondary

antibody for 1 hour at room temperature. To remove excess antibody, the membranes were washed in TBS-T three times for 10 minutes. The membranes were incubated in ECL Western blotting solution for 3 minutes and placed in cassettes. Protein bands were visualised by autoradiography using Fuji Super medical x-ray films in a Kodak X-Omat 488 x-ray processor.

2.2.4.7 Immunoprecipitation

First, the antibody of interest was coupled to magnetic Dynabeads. 30µl Dynabead slurry (per lysate from a 15cm^2 plate) was washed twice in 2 volumes 0.1% BSA in PBS, using a magnetic rack to separate the beads and solution. The beads were resuspended in 2 volumes of 0.1% BSA in PBS with 1.5µg appropriate antibody (per lysate) and rotated at 4ºC for 1 hour. The bead slurry was washed a further two times. Cell lysates were prepared in NDLB-Tween-20 (**Section 2.2.1.5**) and 70µl was kept for analysis. The remaining lysates were added to the beads and rotated for 2 hours at 4ºC. To remove any unbound protein, the bead slurry was washed in 1ml NDLB-Tween-20 four times. All buffer was removed, 100µl 1x reducing sample buffer was added and boiled at 100ºC for 5 minutes to detach and denature the proteins. The proteins were resolved by SDS-PAGE and subjected to Western blotting. Each immunoprecipitation experiment was repeated three times.

2.2.4.8 Proteomic screen

For mass spectrometry analysis high protein concentration is required so five 15cm^2 plates were used per condition. A2780 cells transfected with GFP or GFP-RCP were treated with 1µM Cilengitide or vehicle control for 30 minutes prior to immunoprecipitation (as in **Section 2.2.4.7**). Immunoprecipitated protein was eluted off the beads in 100µl 1%SDS Tris pH6.8 at room temperature for 5 minutes. The eluate was immediately removed and added to 50µl eluate buffer (**Table 2.1.2**). Proteins were resolved on 10% pre-cast polyacrylamide gels and Coomassie stained. The gel was given to the Beatson Institute proteomic facility (David Sumpton and Willie Bienvenut) where the proteins were extracted and analysed by MALDI-TOF mass spectroscopy. The peptides were analysed using Scaffold viewer. This screen was performed with Jim Norman.

2.2.5 Trafficking assays

2.2.5.1 Capture- ELISA

Maxisorp 96 well microtiter plates were incubated with 50µl ELISA coating buffer (**Table 2.1.2**) and the appropriate antibody per well at 4ºC, rocking overnight. Approximately one hour prior to use, the plate was blocked in 5% BSA in PBS-T at 4ºC. The plate was washed with PBS-T twice and any residual liquid was drained off. Cell lysates were added to the plate, which was then incubated at 4ºC rocking overnight. To remove unbound protein, the plate was extensively washed four times with PBS-T. Streptavidin-conjugated HRP was added to 1% BSA in PSB-T (1:1000), 50µl was added to each well and the plate was incubated for 1 hour gently rocking at 4ºC. The plate was extensively washed four times with PBS-T, once with PBS and then drained. 50µl ELISA developing reagent (**Table 2.1.2**) was added to each well and the plate was incubated at room temperature for ~10 minutes. The absorbance of each well was read at 490nm on a plate reader.

2.2.5.2 Internalisation assays

If appropriate, cells were transfected 48 hours prior to this assay so that they were ~70% confluent for the assay. Cell culture media was aspirated off the cells and they were washed twice in cold PBS on ice. The proteins on the cell membrane were labelled with membrane impermeable 5ml 0.13mg/ml sulfo-NHS-SS-Biotin in PBS for 30 minutes at 4ºC. Surplus label was washed from the cells twice in cold PBS on ice. Plates of cells used to measure total protein were kept on ice until cell lysis, whilst the plates used for the blank were kept on ice until MesNa treatment. To allow internalisation, the remaining plates were incubated in DMEM media at 37ºC for the appropriate times. For some experiments, the media was supplemented with 10ng/ml HGF or 0.6mM primaquine. The cells were washed with 5ml PBS and with 5ml biotin reduction buffer on ice (**Table 2.1.2**). To remove the biotin from the membrane proteins, 20mM MesNa in biotin reduction buffer was incubated on the cells for 30 minutes at 4ºC. This reaction was quenched by adding 20mM IAA for a further 10 minutes at 4ºC. The plates were washed and lysed in 100µl 1.5% Triton NDLB as described earlier (**Section 2.4.4.5**). The levels of biotinylated-EphA2, α5-integrin, cMet, EGFR and TfnR were determined by capture-ELISA (**Section 2.2.5.1**).

2.2.6 Protein localisation studies

2.2.6.1 Immunofluorescence

H1299 cells were seeded onto glass coverslips in 6 well plates and left to adhere and grow for 48 hours. The cells were fixed with 4% paraformaldehyde for 15 minutes and permeabilised in 0.2% Triton X-100 in PBS for 5 minutes. The coverslips were immediately washed twice in PBS and then blocked in 1% BSA in PBS for 30 minutes. Primary antibodies were incubated on the coverslips, at the appropriate concentration (**Table 2.6**) in block solution for 2 hours at room temperature. The coverslips were washed three times in PBS for 5 minutes and incubated in the appropriate secondary antibody in 1% BSA PBS for 1 hour at room temperature in the dark. Any remaining antibody was washed from the coverslips in four washes in PBS, each for 5 minutes. The coverslips were mounted onto slides using Vectashield mounting reagent. Cells were visualised by confocal microscopy using an Olympus FV-1000 microscope. Sequential scanning was used to prevent signal bleed through. Controls with no primary antibody were performed for each secondary antibody to ensure that there was no auto-fluorescence.

2.2.6.2 Ephrin stimulation

A2780 cells were transfected with pEGFP-f (farnesylated-GFP) or pEGFP-EphA2 (**Section 2.2.1.3**) and seeded onto glass coverslips in 6 well plates for 24 hours. EphrinA1-Fc was pre-clustered at a ratio of 1µg/ml EphrinA1-Fc/Fc to 10µg/ml IgG in RMPI media at 37ºC for 30 minutes. The media was aspirated from the cells and 500µl clustered EphrinA1-Fc or Fc was added for 30 minutes. The cells were fixed with 4% paraformaldehyde for 15 minutes and mounted onto slides using Vectashield mounting reagent. Cells were visualised by confocal microscopy using an Olympus FV-1000 microscope.

2.2.6.3 Live cell imaging

A2780 or H1299 cells were transfected with 3µg of the appropriate plasmids and seeded onto glass-bottomed plates for live cell imaging. To maximise the signal, cells were visualised 24 hours after transfection on an Olympus FV-1000 microscope. Images or 2 minute movies were taken and cells were treated with

10ng/ml HGF if appropriate. ImageJ software was used to generate images showing co-localised pixels, by first thresholding images using max-entropy and then using the co-localisation highlighter tool. To quantify co-localisation the number of co-localised pixels was measured and normalised to the number of pixels in the red and green channel.

2.2.7 Migration assays

2.2.7.1 Matrigel and Geltrex invasion assays

The inverted invasion assay was first described by Hennigan et al. (1994) and has been adapted for this study (Hennigan et al., 1994). Matrigel was used for the experiments in chapter 3 and Geltrex for the experiments in chapter 4. Both are a gelatinous protein mix secreted from Engelbreth-Holm-Swarm mouse sarcoma cells, which contains many ECM components, including laminin, entactin and collagen. Geltrex/Matrigel was mixed 1:1 with cold PBS, supplemented with 25µg/ml fibronectin and 100µl was put in each transwell. The transwells were incubated at 37ºC for 1 hour to allow the proteins to polymerise. Meanwhile, the appropriate cells were detached, counted and $5x10^5$ cells were prepared in 1ml of media. Transfected cells were left to recover for 18 hours before setting up invasion assays. To adhere the cells to the transwell, 100µl cell suspension was incubated on the base of each transwell at 37ºC for 4 hours. The base of the transwell was washed by sequential dipping in 1ml serum free media and then placed in 1ml serum free media. Serum rich media was supplemented with either 25ng/ml EGF or 10ng/ml HGF and 100µl was carefully placed inside the transwell, which created a chemotactic gradient promoting cell invasion into the plug. These plugs were incubated at 37ºC for 3 days to allow cell invasion. To visualise invasion, the transwells were placed in a fresh 24 well plate and 1ml 4µM calcein-AM (acetomethyl ester) in serum free media was incubated on the transwells for 1 hour at 37ºC. Calcein-AM is a fluorescent dye that is transported into live cells, which was visualised on an Olympus-FV1000 microscope. Optical sections were taken every 10µm/15µm from the base of the transwell in three randomly selected areas of each plug. ImageJ's area calculator plugin was used to quantify the calcein-AM signal from each image. Fold change in invasion was calculated by dividing the signal in images over 30µm or 45µm by the total signal in the strip and normalising it to the non-targeting control. Mean values were

generated from three independent experiments and within each experiment six optical sections were taken from two different transwells per condition.

2.2.7.2 Contact inhibition of locomotion assays

This assay was first described by Astin *et al.* (2010) and has been adapted for this study. First the plates were coated in 150µl Matrigel in 300µl 0.5% Serum RPMI-1640 by pipetting it onto glass-bottomed 6 well plates. To polymerise the Matrigel, the plate was sealed and incubated at room temperature for 1 hour. 2,000 transfected PC3 cells (24 hours before this assay- **Section 2.2.1.3**) were seeded onto each well, and incubated at 37ºC for 24 hours. To starve the cells, they were washed three times with 0.5% Serum media and then incubated in this media for 24 hours. To stimulate migration, 10ng/ml HGF was added and incubated on the cells for a further 12 hours. Cell migration was visualised on a Nikon timelapse microscope. Images were taken every 5 minutes of 8 different regions in each well for 20 hours. Time of cell-cell contact during collision was counted for any collision in which only two cells were involved and both cells were migrating towards each other. The distance and direction each cell migrated 40 minutes before and after the collision was measured using ImageJ software. The average migratory speed and angle was measured for 50 cells from 3 separate experiments, whilst contact time during a collision was measured for every collision that occurred in these experiments.

2.2.7.3 Scattering assays

To analyse the timecourse of HGF induced scattering, 2,000 H1299 cells (Section 2.2.1.3) were seeded onto each well in a 6 well plate. The cells formed small colonies containing 4-8 cells 43 hours after transfection. At this time, 5 pictures were taken on an Olympus CKX41 microscope and 10ng/ml HGF/mock was added to the appropriate wells. 3, 6, 9, 24 and 30 hours later, 5 pictures were taken from each condition. To analyse scattering, the cells in each picture were counted as either ‘scattered’, defined as cells attached to fewer than 2 other cells, or ‘unscattered’, defined as cells attached to 3 or more other cells. For each condition 20 pictures from 4 separate experiments were analysed. For later experiments the same protocol was used, however, pictures were only taken 6

hours after HGF stimulation as it was observed that this is when cells are the most scattered.

2.2.7.4 Time-lapse scattering assays

To analyse H1299 cell migration upon HGF stimulation, 2,000 transfected H1299 cells (**Section 2.2.1.3**) were seeded onto each well in a 6 well plate. Within 43 hours the cells formed small colonies containing 4-8 cells. Cell migration was visualised on a Nikon timelapse microscope. Images were taken every 5 minutes of 8 different regions in each well. After the first round of pictures was taken, 10ng/ml HGF was added to appropriate wells. To track cell migration, ImageJ manual tracking and chemotaxis plugins were used. Every cell that was in a colony of 4-10 cells and did not divide was tracked for 6 hours. The HGF-induced cell speed and distance were calculated by subtracting the untreated value from the HGF treated value and normalising to the non-targeting siRNA control. Averages and SEM of migratory speed, distance, HGF-induced speed and distance were calculated from 3 independent experiments.

2.2.8 Mouse work

2.2.8.1 Genetically modified mice

KPC (Pdx1-Cre, $Kras^{G12D/+}$, $p53^{R172H/+}$) mice have previously been described (Morton et al., 2010). $EphA2^{-/-}$ mice were obtained from the Jackson laboratory, and $RCP^{fl/fl}$ mice were generated by the Beatson transgenic production service. PCR was used to check the genotype of the mice (Transnetyx Inc). Mice were monitored daily and kept in conventional animal facilities. All experiments were performed in compliance with UK Home Office guidelines. Tumourigenesis was assessed by gross pathology and confirmed by histology. This work was carried out by Bryan Miller and Joan Grindlay and the Beatson Institute mouse house facilities.

2.2.8.2 Immunohistochemistry

Histological staining was performed by Joan Grindlay and Colin Nixon (Beatson Institute Histology services). Briefly, tissue sections that had been formalin fixed and embedded in paraffin, were deparaffinised, rehydrated in xylene and passed

through a graded ethanol series (twice 100%, once 70%). Endogenous peroxidase activity was prevented using 3% hydrogen peroxide/methanol for 5 minutes and antigens were retrieved in heated citrate buffer (pH6). The sections were washed in TBS-T and then blocked in 5% serum at room temperature for 1 hour. RCP was stained by incubation of the sections in an antibody that recognises mouse-RCP for 1 hour at room temperature. The sections were washed in TBS-T and incubated with Dako EnVision rabbit secondary for 45 minutes at room temperature. Tissue sections were washed in TBS-T, stained with DAB colour reagent for 1 minute at room temperatures and counterstained with Gills Haematoxylin. Immunohistochemical staining on sections of PDACs were visualised using a Zeiss Acioskop 50 microscope.

2.2.8.3 Generating cell lines

Primary mouse cell lines were derived from PDACs harvested from KPC (Pdx1-Cre, $Kras^{G12D/+}$, $p53^{R172H/+}$) WT, KPC EphA2$^{-/-}$ and KPC $RCP^{fl/fl}$ mice. Tumour samples were chopped up into small pieces and incubated in DMEM media until cell lines were established. The cell lines were authenticated by morphology, Western blotting and growth curve analysis.

2.2.9 Statistics

Statistical analysis was performed on all relevant experiments. To compare two data sets, Student's T-tests (if data were normally distributed) or Mann-Whitney tests (if data were not normally distributed) were used, whilst to compare multiple data sets, two-way ANOVA tests were used. p-values are indicated on graphs and the statistical test that was used is written in the figure legends.

3 The RCP interactome

3.1 Introduction

3.1.1 RCP is amplified in some cancers and has a role in metastasis

RCP is overexpressed in some breast (Zhang et al., 2009), head and neck (Dai et al., 2012), colon and lung cancers (Mills et al., 2009). The gene for RCP is located on the 8p11-12 chromosomal locus, which has been found amplified in 10-25% of breast cancers (Zhang et al., 2009) and in non-small cell lung carcinoma (NSCLC) (Balsara et al., 1997). Studies in human breast cancer and head and neck cancer demonstrate that RCP over-expression decreases survival and increases metastatic progression (Zhang et al., 2009). Indeed, it has been shown that implanting breast cancer cells (MDA-MB-231) expressing shRNAs to suppress RCP expression into mammary fat pads of NOD-SCID mice, reduces tumour growth and metastasis to the lungs. Furthermore, several cell culture based studies have shown that RCP is required for efficient invasion into 3D microenvironments (Caswell et al., 2008; Muller et al., 2009). Understanding the function of RCP may help us understand metastatic progression and determine whether it could be a potential drug target.

3.1.2 RCP regulates integrin and growth factor receptor trafficking

In a human ovarian carcinoma cell line (A2780) α5ß1-integrin promotes tumour cell invasion while αvß3-integrin restrains it (Caswell et al., 2008). Two compounds inhibit αvß3-integrin: osteopontin, a secreted ligand for αvß3-integrin (Rangaswami et al., 2006), and Cilengitide, a cyclic RGD peptide (cRGDfV) that mimics the RGD receptor binding motif found in integrin ligands (Dechantsreiter et al., 1999). Inhibition of αvß3-integrin promotes association of RCP with α5ß1-integrin, and drives RCP-dependent recycling of α5ß1-integrin to the plasma membrane (Caswell et al., 2008). This causes rapid and random cell migration in 2D and an increase in 3D cell invasion into a collagen rich microenvironment. Unexpectedly, α5ß1-integrin recycling does not influence the strength of its interaction with its extracellular ligand fibronectin. Instead, RCP recruits α5ß1-integrin and EGFR into a complex. This integrin associates with the C-terminus of RCP while EGFR associates with a region found in its N-terminus. The formation of this complex results in the two receptors returning to the

plasma membrane with similar kinetics and in an RCP-dependent fashion (Caswell et al., 2008). RCP is not required for transferrin receptor trafficking (Caswell et al., 2008), which suggests RCP is not involved in all recycling in the cell but only that of specific cargo. RCP contains a C2 domain that associates with phosphatidic acid, which is synthesised by diacylglycerol kinase (DGKα) (Rainero et al., 2012). This kinase is required for RCP-positive vesicles, containing α5ß1-integrin and EGFR, to be tethered to the plasma membrane at the tip of invasive pseudopods, and for efficient cell invasion. Indeed, a constitutively active mutant of DGKα is sufficient to drive RCP-dependent invasion in the absence of αvß3 inhibition (Rainero et al., 2012) (**Figure 3.1**).

Further work has addressed the downstream mechanism through which RCP-dependent recycling may increase pro-migratory signalling and the invasiveness of cancer cells. Morello et at. (2011) have shown that silencing ß1-integrin expression in NSCLC A549 cells dampens EGFR activation, but increases the amount of EGFR at the plasma membrane. Overexpressing RCP in these ß1-integrin depleted cells recovers this reduction in EGFR signalling (Morello et al., 2011), although the authors did not study the effect of overexpression of RCP on EGFR trafficking. These observations differ slightly from the study by Caswell et al. (2008) but this may be due to differences in the two cell lines. In breast cancer cells it has been shown that RCP overexpression increases H-Ras activation, which increases downstream MAPK signalling. Furthermore, RCP directly associates with this proto-oncogene (Zhang et al., 2009). Perhaps in cells expressing H-Ras this is another downstream mechanism by which RCP may increase cancer cell invasion.

Recent work has identified a novel Akt substrate, RacGAP1, which acts downstream of RCP-driven α5ß1/EGFR recycling (Jacquemet et al., 2013). Activated RacGAP1 associates with IQGAP1 in the tips of the invasive pseudopod where it locally inhibits Rac1 activity, preventing Rac1's inhibition of RhoA (**Figure 3.1**). This results in an increase in RhoA activity at the front of the cell, which is required for RCP driven invasion into a 3D matrix (Jacquemet et al., 2013), thus demonstrating that recycling can promote the activity of proteins involved in the dynamics of the actin cytoskeleton required for cell migration.

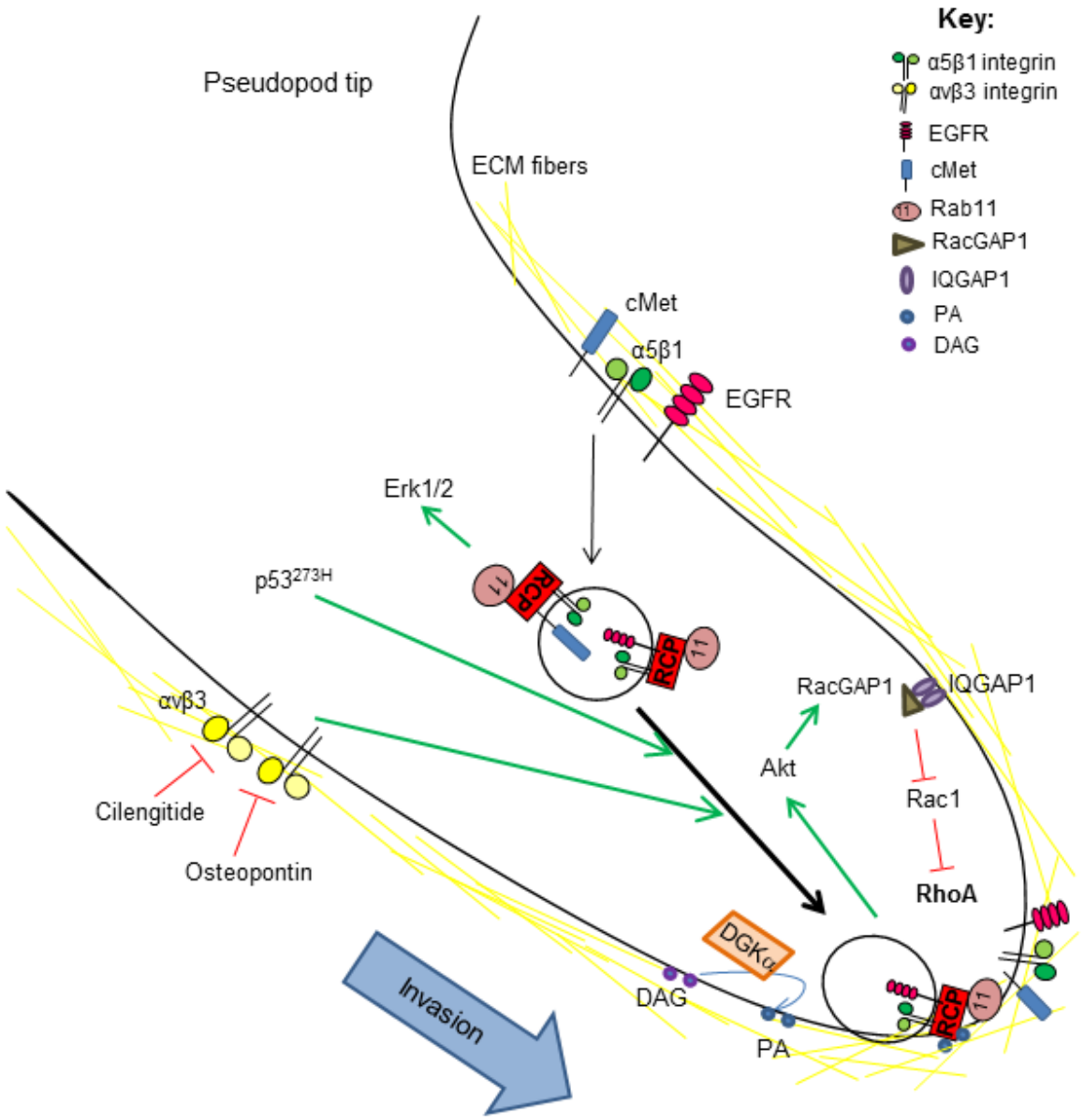

Figure 3-1 RCP-dependent integrin and RTK trafficking in the invasive pseudopod
Inhibition of αvβ3-integrin or expression of the gain-of-function mutation of p53 (273H) promotes the association of RCP with α5β1-integrin/EGFR/cMet and increases the recycling of RCP-positive vesicles in the tip of the pseudopod. DGK phosphorylates DAG into PA that tethers RCP positive vesicles at the tip of the pseudopod and localises downstream signalling to Akt/Erk in the tip of the pseudopod. Akt phosphorylates RacGAP1, which is recruited to IQGAP1 into the pseudopod tip and leads to the inhibition of Rac1. Rac1's inhibition on RhoA is damped, resulting in increased RhoA activity, which drives the extension of the pseudopod and cell invasion. Green arrows represent the activation of a pathway, red inhibitory arrows represent the inhibition of a pathway and a black arrow shows the route of trafficking.

3.1.3 RCP is required for mutant-p53 driven cell invasion

The tumour suppressor protein p53 acts as a transcription factor to slow cell growth or induce cell death in response to oncogenic stress. p53 is frequently mutated in human cancers (Vogelstein et al., 2000), often in the DNA binding

domain of the protein. Recent work has demonstrated that some of these mutations result in p53 gaining functions (Olive et al., 2004; Tepper et al., 2005). In particular it has been shown in cell lines and mouse models that expression of two transcriptionally inactive mutants of p53 ($p53^{175H}$ or $p53^{273H}$) drives cell migration, invasion and metastasis (Adorno et al., 2009; Morton et al., 2010; Muller et al., 2009). RCP has an important role in mutant-p53 driven invasion in 3D. Indeed, Muller et al. (2009) showed that in several cell lines, including H1299 cells (a NSCLC line), expression of $p53^{175H}$ or $p53^{273H}$ enhances RCP/α5β1-integrin/EGFR association and increases RCP-dependent α5β1-integrin and EGFR recycling, thus activating EGFR signalling. Mutant p53 also has a role in RCP-dependent trafficking of other RTKs. Indeed, RCP associates with the hepatocellular growth factor (HGF) receptor cMet (Muller et al., 2013). Expression of $p53^{273H}$ in H1299 cells enhances cMet signalling and recycling in an RCP dependent fashion. Mutant-p53 expression has been shown to increase RCP-dependent invasion towards a gradient of EGFR or HGF but not PDGFβ or IGF1 (Muller et al., 2013), demonstrating some specificity.

In summary, RCP is required for the enhanced cMet, EGFR and α5β1-integrin recycling and signalling, which are responsible for mutant-p53 ($p53^{175H}$ or $p53^{273H}$) driven invasion (**Figure 3.1**). Since p53 is frequently mutated in many human cancers (Vogelstein et al., 2000), a drug that inhibits the gain of function activities of mutant-p53 would be a good therapeutic target. More work is required to further understand the role of RCP in cancer in order to investigate its potential as a drug target.

3.1.4 Aims

In this chapter I aim to identify novel RCP-associated proteins by performing a non-biased proteomic screen. Any interesting hits will be confirmed using co-immunoprecipitation approaches and the site of the association will be investigated. Imaging techniques, such as immunofluorescence and the use of fluorescently tagged proteins, will be used to determine whether the identified hits co-localise with RCP. Finally, the role of these proteins in cancer cell invasion will be investigated.

3.2 Results

3.2.1 Identification of novel RCP associated proteins

3.2.1.1 Development of the proteomic approach

To further understand the role of RCP in cancer cell migration I sought to identify novel RCP-interacting proteins using a proteomic approach. To do this, RCP was immunoprecipitated from cancer cell lysates and mass spectrometry was used to identify any co-immunoprecipitated proteins. As most functional studies of RCP have been performed in ovarian carcinoma A2780 cells, these cells were chosen for this screen. I was unable to find an antibody capable of efficiently immunoprecipitating endogenous RCP, so I choose to use an overexpression plasmid in which RCP was N-terminally tagged to GFP (**Figure 3.2A**), as this can be efficiently immunoprecipitated with an anti-GFP antibody. A2780 cells were transfected with GFP-RCP and visualised by live cell microscopy. GFP-RCP was localised in a peri-nuclear compartment and small vesicles in the cytoplasm (**Figure 3.2B**). This localisation concurs with that of previous studies using an anti-RCP antibody, which showed that endogenous RCP co-localises with Rab11 in the PNRC (Peden et al., 2004).

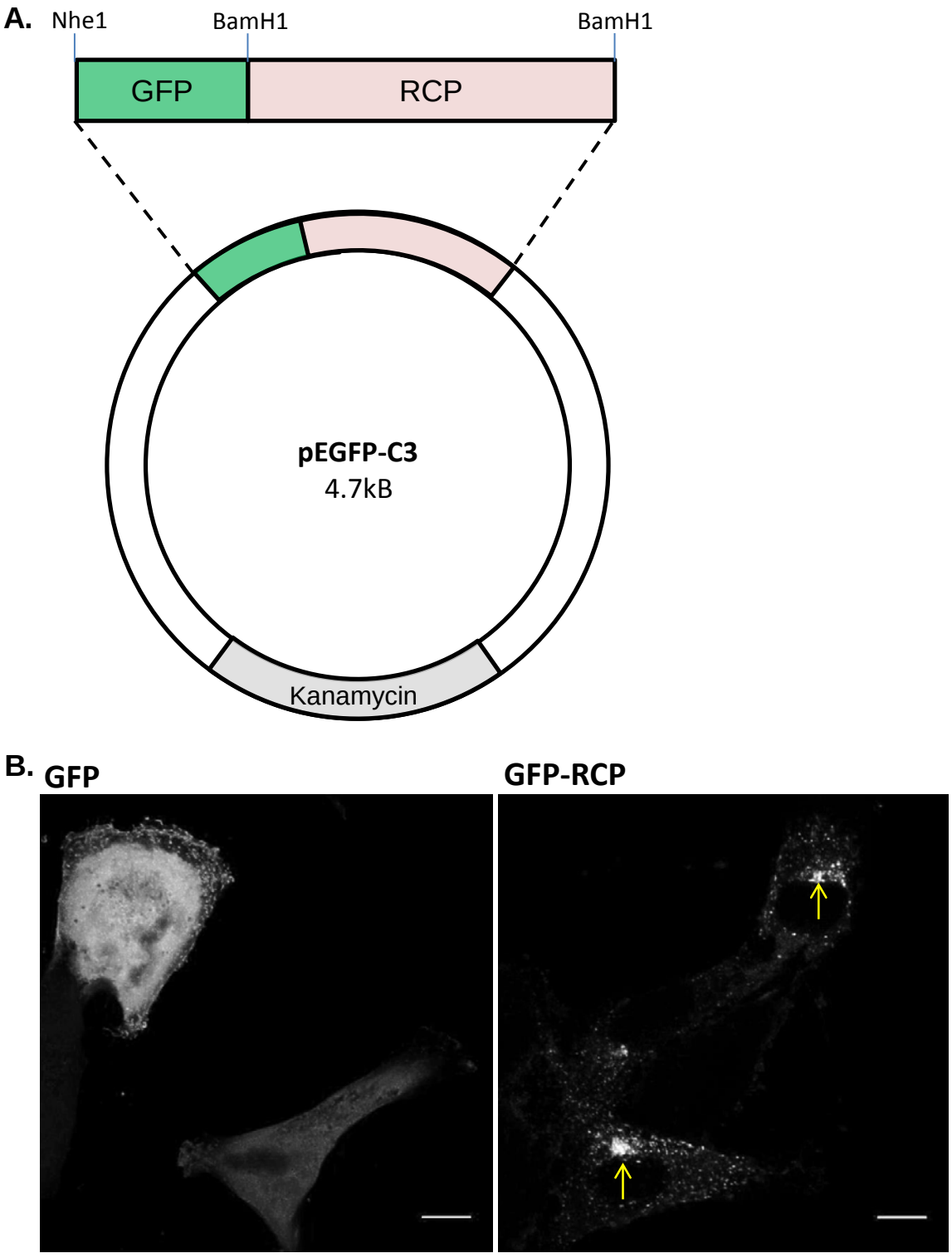

Figure 3-2 Schematic representation and cellular localisation of GFP-RCP
A. Vector map of GFP-RCP construct. B. A2780 cells were transfected with GFP or GFP-RCP and visualised by live cell microscopy. Yellow arrows indicate the PNRC. Scale bar is 10μm.

RCP has been previously shown to associate with Rab11 and Rab4, but not Rab5 (Caswell et al., 2008). I sought to ensure that these associations were detectable using this construct. GFP or GFP-RCP were transfected into A2780 cells and GFP was immunopreciptated with an anti-GFP antibody. Immunoprecipitates were analysed by SDS-PAGE and immunoblotting using antibodies recognising GFP, Rab11, Rab4 and Rab5 (**Figure 3.3**). Rab11 co-immunoprecipitated very efficiently and specifically with GFP-RCP. As expected Rab5 was absent from GFP-RCP immunoprecipitation indicating the specificity of the RCP-Rab11 interaction. Surprisingly, Rab4 was not present in the GFP-RCP co-immunoprecipitation. The association between Rab4 and RCP was demonstrated by yeast-2-hybrid (Lindsay et al., 2002), but only found weakly associated using *in vitro* binding assays (Peden et al., 2004), so perhaps this interaction is not found *in vivo*.

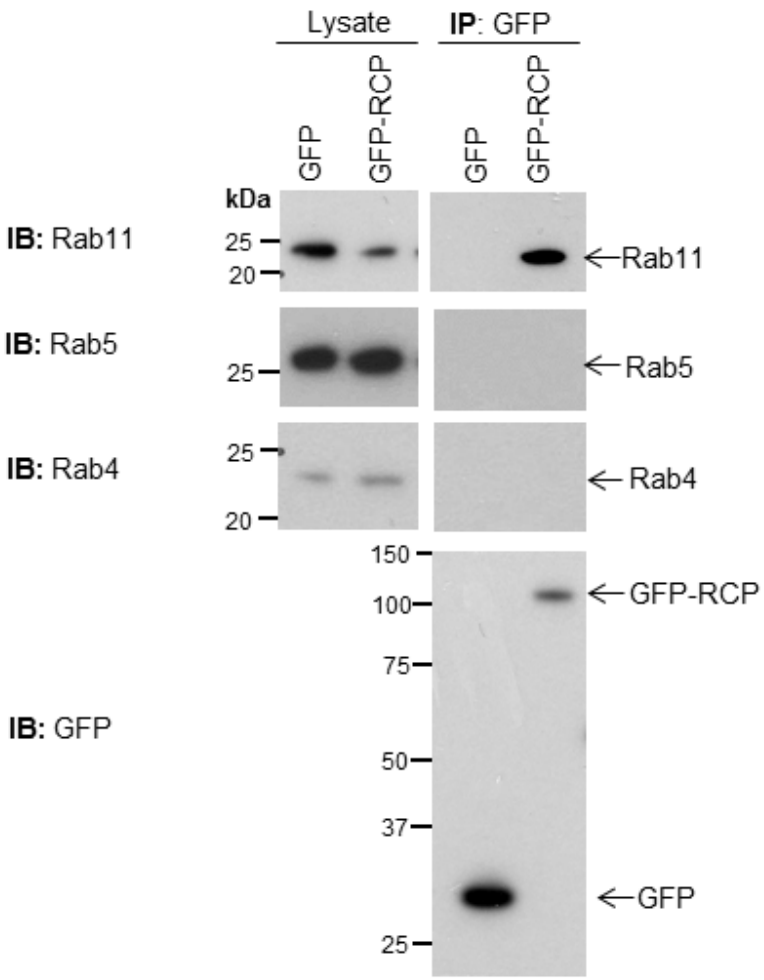

Figure 3-3 GFP-RCP associates with Rab11, but not Rab4 or Rab5
A2780 cells were transfected with GFP or GFP-RCP. GFP was immunoprecipitated from the lysates with an anti-GFP antibody 48 hours after transfection. Immunoprecipitates were analysed by SDS-PAGE. GFP, Rab11, Rab5 and Rab4 were detected by immunoblotting.

The association of EGFR and α5β1-integrin with RCP is known to be enhanced upon engagement of αvβ3-integrin with its soluble ligand osteopontin, or Cilengitide (Caswell et al., 2008; Dechantsreiter et al., 1999). To corroborate this finding, GFP-RCP was expressed and immunoprecipitated from A2780 cells treated with Cilengitide, osteopontin or vehicle control for 30 minutes. Indeed, GFP-RCP was found associated with both α5-integrin and EGFR and this association was enhanced upon osteopontin and Cilengitide treatment (F**igure 3.4**).

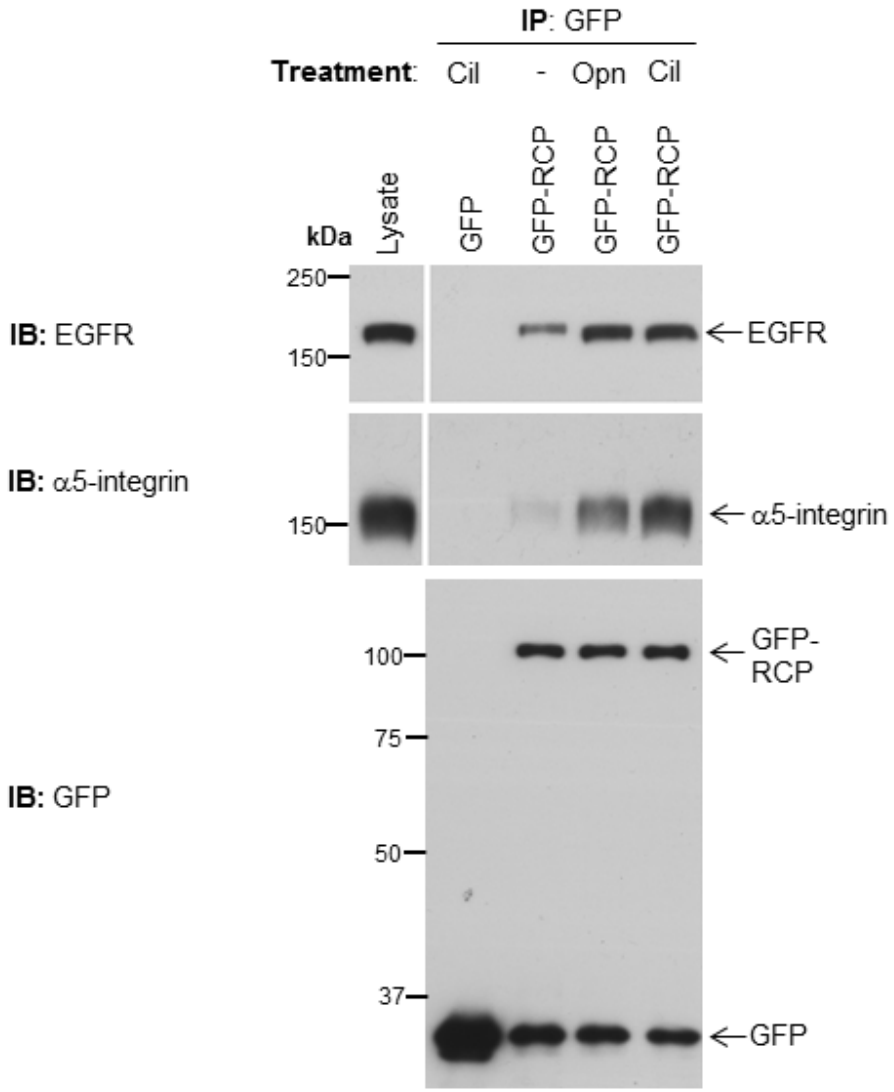

Figure 3-4 GFP-RCP associates with α5-integrin and EGFR
A2780 cells were transfected with GFP or GFP-RCP and treated with 1μM Cilengitide, 0.5μg/ml Osteopontin or vehicle control for 30 minutes before cell lysis. GFP was immunoprecipitated from the lysates with an anti-GFP antibody. Immunoprecipitates were analysed by SDS-PAGE. GFP, α5-integrin and EGFR were detected by immunoblotting. This was performed by Pat Caswell.

3.2.1.2 RCP interactome

Having confirmed the effectiveness and specificity of the GFP-RCP immunoprecipitation, I immunoprecipitated GFP-RCP (using GFP as a control) from A2780 cells under various conditions that might be expected to alter the RCP interactome (such as Cilengitide treatment or overexpressing Rab25). MALDI-TOF mass spectrometry was used to identify the co-immunoprecipitated proteins. Coomassie blue staining of SDS-PAGE gels of the immunoprecipitations revealed a number of proteins to be associated with both the GFP-RCP and GFP immunoprecipitates and these were deemed to be non-specific (**Figure 3.5**). Nevertheless, the GFP-RCP immunoprecipitates contained a number of proteins that were not detectable in the GFP immunoprecipitates and these are likely to be proteins that specifically associated with RCP. Amongst these a band corresponding to GFP-RCP itself was clearly visible. To identify these specifically associated proteins the SDS-PAGE gels were cut into strips and the protein was extracted from the gel and digested with trypsin. The resulting peptides were identified using MALDI-TOF mass spectrometry and analysed using Scaffold software. Proteins that were not significantly different between GFP-RCP and GFP immunoprecipitates (the non-specific contaminant proteins) were excluded. Under these stringent conditions I identified a small list of proteins that were found to be significantly more abundant in the GFP-RCP than the GFP immunprecipitates.

No consistent differences were observed in the RCP interactome between the control and Cilengitide treated A2780 cells nor between the control or Rab25 expressing cells. Therefore, I have pooled the data from all the conditions and will consider them together (**Table 3.1**). Several known RCP-associated proteins were detected, for example, ß1-integrin, EGFR and Rab11B. Most interestingly, novel associated RCP proteins were also found. Many of the proteins identified have roles in trafficking or could be potential RCP-cargoes, whilst others have diverse roles, such as proteins with various enzymatic activities and heat shock proteins. Since I am interested in cancer cell migration and trafficking, novel RCP associations with Rab14, Rab6 and EphA2 were confirmed and investigated.

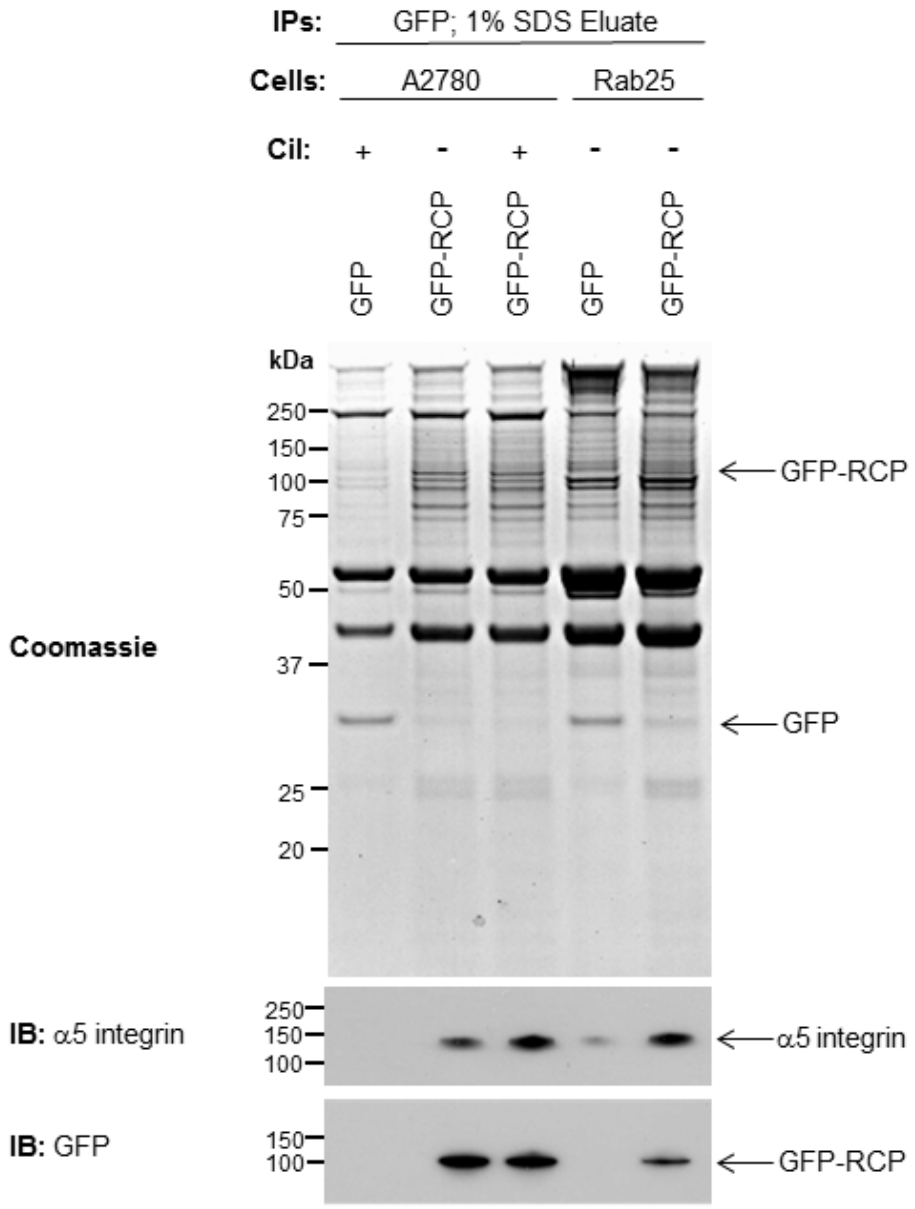

Figure 3-5 RCP interactome in Coomassie stained gels
A2780 and A2780-Rab25 cells were transfected with GFP or GFP-RCP and treated with 1μM Cilengitide or vehicle control for 30 minutes. The cells were lysed and GFP was immunoprecipitated with an anti-GFP antibody. The lysates and immunoprecipitates were separated by SDS-PAGE and Coomassie stained. The immunoprecipitated samples were separated by SDS-PAGE, and GFP-RCP and α5-integrin were detected by immunoblotting.

Protein	Accession Number	IP:GFP		IP:GFP-RCP	
		Number of Peptides (unique)	Percentage covered (%)	Number of Peptides (unique)	Percentage covered (%)
Ubiquitin	P62988	-	-	4 (3)	50
Rab11B	Q15907	-	-	53 (8)	40
Rab25	P57735	1 (1)	5	51 (7)	36
Heat shock cognate 71kDa	P11142	1 (1)	3	43 (16)	32
Rab6A	**P20340**	**-**	**-**	**18 (5)**	**25**
α-actinin 4	O43707	-	-	32 (16)	23
RCP	Q6WKZ4	-	-	60 (17)	16
Clathrin heavy chain 1	Q00610	-	-	27 (15)	13
FIP5	Q9BXF6	-	-	11 (5)	13
Rab14	**P61106**	**-**	**-**	**6 (2)**	**13**
5'-nucleotidase	P21589	1 (1)	2	9 (5)	13
Myoferlin	Q9NZM1	-	-	34 (20)	12
Aminopeptidase N	P15144	-	-	21 (9)	12
Ephrin type-A receptor 2	**P29317**	**-**	**-**	**18 (9)**	**12**
Peroxisomal multifunctional enzyme type 2	P51659	-	-	11 (5)	10
Desmoglein 2	Q14126	-	-	8 (6)	10
Myeloid-associated differentiation marker	Q96S97	-	-	8 (2)	10
Heat shock 70 kDa protein 1	P08107	-	-	3 (3)	10
Integrin-β1	P05556	1 (1)	1	17 (5)	9
EGFR	P00533	-	-	17 (7)	8
Neurabin 2	Q96SB3	-	-	7 (6)	8
4F2 cell-surface antigen heavy chain	P08195	-	-	3 (3)	8
Leucyl-cystinyl aminopeptidase	Q9UIQ6	-	-	6 (6)	7
Discoidin, CUB and LCCL domain-containing protein 2	Q96PD2	1 (1)	2	4 (4)	7
Integrin αv	P06756	-	-	8 (5)	6
Podocalyxin-like protein 1	O00592	4 (1)	3	21 (2)	5
Integrin α2	P17301	-	-	6 (4)	4
Myosin-Id	O94832	-	-	4 (4)	4
Tyrosine-protein kinase receptor ufo	P30530	-	-	3 (3)	4
Myosin-Ie	Q12965	-	-	3 (3)	3
Cation-independent mannose-6-phosphate receptor	P11717	-	-	4 (4)	2
Filamin-A	P21333	-	-	6 (4)	2

Table 3-1 RCP interactome in A2780 cells
Proteins identified by MALDI-TOF mass spectrometry that are significantly more abundant in GFP-RCP than GFP immunoprecipitates. Proteins identified in mock treated, Cilengitde treated and Rab25 overexpressing cells were pooled as no significant differences between the conditions were observed. The number of peptides identified by mass spectrometry and the percentage of protein coverage by these peptides are indicated. The mass spectrometry was performed by W. Bienvenut and D. Sumpton.

3.2.2 Rab14 associates with RCP

3.2.2.1 The role of Rab14 in trafficking and cell migration

Rab14 is closely related to Rab2 and Rab4 based on sequence homology, and localises to both the Golgi apparatus and the early endosomes (Junutula et al., 2004). Rab14 has been shown to regulate the trafficking between these organelles as the GTP-locked form ($Rab14^{Q70L}$) localises with early endosome associated vesicles, whilst the GDP-locked form ($Rab14^{S25N}$) localises with the Golgi apparatus (Junutula et al., 2004). Yamamoto et al. (2010) were the first to identify a Rab14 effector, RUFYI, and depletion of either Rab14 or RUFYI was shown to prevent efficient transferrin recycling. This work was corroborated by live cell imaging, which demonstrated that the transferrin receptor is trafficked through a Rab14 compartment distinct from the Rab5 and Rab11 compartments (Linford et al., 2012). This more recent work suggests that Rab14 is involved in receptor recycling as well as Golgi to early endosome trafficking.

Rab14 trafficking has been shown to have several important functions. It has a role in the apical targeting of proteins in polarised epithelial cells (Kitt et al., 2008). In MDCK cells, Rab14 co-localises with the junctional protein Claudin 2, and atypical-PKC, in both an intracellular vesicular compartment and at the plasma membrane (Lu et al., 2015). Indeed, atypical-PKC and Rab14 associate and regulate Claudin-2 trafficking from the recycling endosome back to the plasma membrane (Lu et al., 2015; Lu et al., 2014). Furthermore it has been demonstrated that Rab14 is required for efficient incorporation of the envelope glycoprotein complex in the HIV lifecycle (Qi et al., 2013), and has a role in the fusion of phagosomes and lysosomes in *Dictyostelium* phagocytosis (Harris and Cardelli, 2002). Interestingly, it has been shown that suppression of Rab14 expression reduces the speed of A549 lung epithelial cells migrating on plastic in a wound healing assay (Linford et al., 2012). Reducing Rab14 expression levels causes an increase in N-Cadherins at cell-cell junctions, preventing the cells migrating away from each other. Linford et al. (2012) found that this is because Rab14 is required for efficient trafficking of ADAM10, which sheds N-Cadherins from the cell-cell contacts allowing cells to migrate into the wound (Linford et al., 2012).

3.2.2.2 Rab14 associates and co-localises with RCP

Since Rab14 has previously been shown to have an important role in regulating recycling (Yamamoto et al., 2010), and is required for efficient A579 cell migration (Linford et al., 2012), I sought to confirm its association with RCP. A2780 and A2780-Rab25 cells were transfected with GFP or GFP-RCP and treated with Cilengitide (or mock) for 30 minutes. GFP/GFP-RCP was immunoprecipitated from the cell lysates and proteins separated by SDS-PAGE, and Rab14 and GFP were detected by immunoblotting. Endogenous Rab14 was found associated with GFP-RCP but not GFP alone in both mock and Cilengitide-treated A2780 cells, as well as in Rab25 overexpressing cells (**Figure 3.6A**). In parallel, A2780 cells were transfected with GFP-Rab14 and co-immunoprecipitations were performed as previously described. Endogenous RCP was found associated with GFP-Rab14 (**Figure 3.6B**). The Rab11-Fip family of proteins are divided into two classes: Class 1 (RCP, Fip2 and Rip11) have a role in receptor trafficking (Caswell et al., 2008; Prekeris et al., 2000; Schwenk et al., 2007), and class 2 (Fip3 and Fip4) are involved in cytokinesis (Fielding et al., 2005; Simon et al., 2008). My collaborators have analysed the association further and found that Rab14 associated with all Class1-Fips but not Class2-Fips in a GTP-dependent manner in yeast-2 hybrid studies (Kelly et al., 2010).

To determine whether Rab14 and RCP co-localise, GFP-RCP and mCherry-Rab14 were co-transfected into H1299 cells and seeded onto glass-bottomed plates. Confocal microscopy was used to visualise the cells, and showed that there is some co-localisation of Rab14 and RCP in the perinuclear region (**Figure 3.6C**). Furthermore, co-immunofluorescence studies demonstrated that Rab14 co-localises with RCP, Fip2 and Rip11 (Kelly et al., 2010). Taken together these data show that Rab14 associates and colocalises with all the Class1-Fips.

3.2.2.3 Rab14 associates with the C-terminal region of RCP containing the RBD

To determine whether Rab14 associated with a specific RCP protein domain, the association between RCP and Rab14 was further analysed using several GFP-tagged RCP truncations in co-immunoprecipitation studies (**Figure 3.7A**). Rab14 associated with the C-terminal fragment of RCP, containing the coiled-coiled domain and the Rab Binding Domain (RBD) (**Figure 3.7B**). Interestingly, when

GFP-RCP is mutated in the RBD (I621E), a substitution that is known to prevent Rab11 binding, Rab14 was no longer found associated with GFP-RCP (**Figure 3.7B**). Therefore, I propose that Rab11 and Rab14 both interact with RCP's RBD, or that Rab14 can only associate with RCP only once it is already associated with Rab11. I have looked in detail at the role of Rab14 in cell migration in chapter 4 (**Section 4.2.3**).

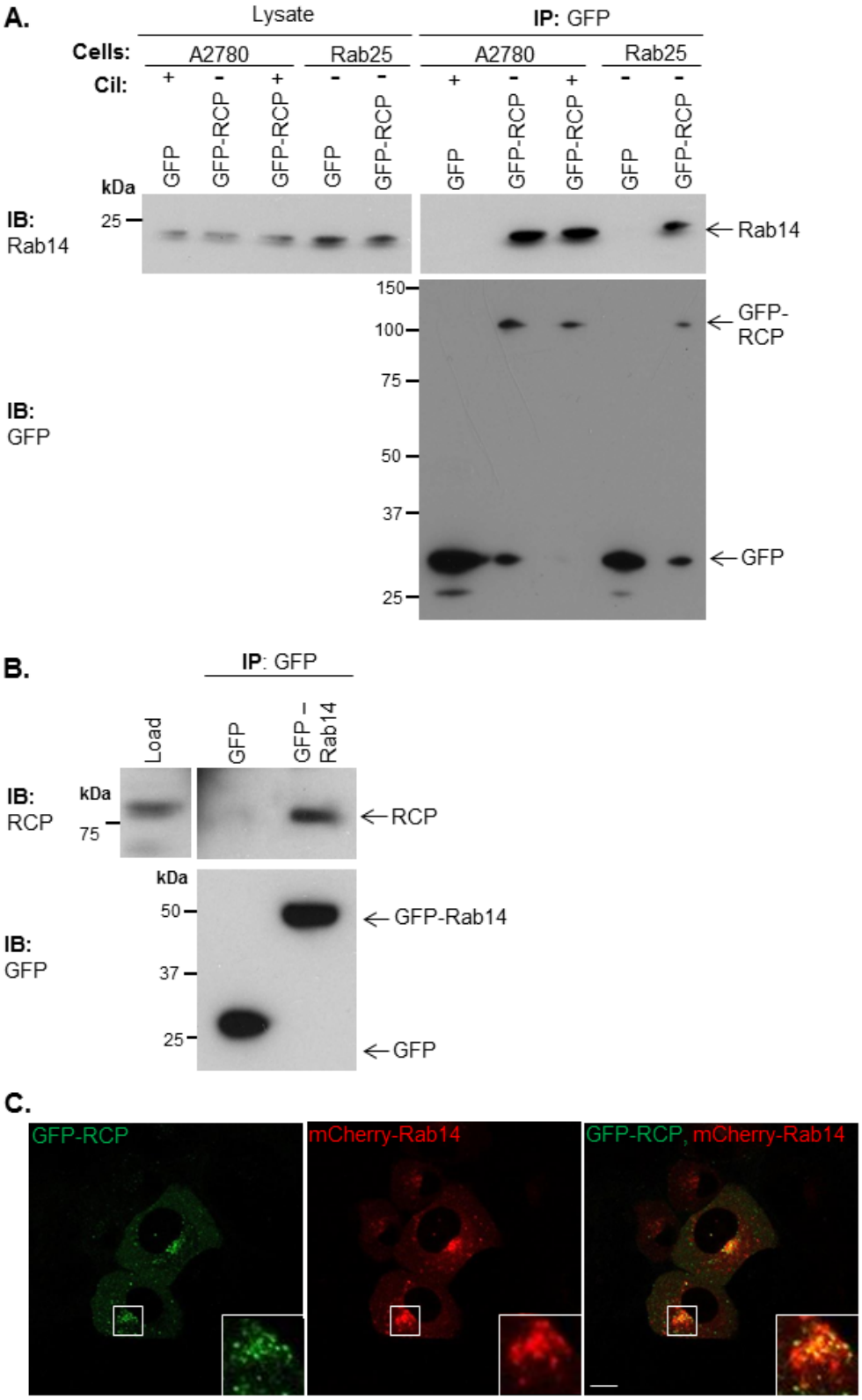

Figure 3-6 Rab14 associates and partially co-localises with RCP
A. A2780 and A2780-Rab25 cells were transfected with GFP or GFP-RCP for 48 hours. The cells were treated with 1μM Cilengitide or vehicle control for 30 minutes and GFP was immunoprecipitated from the cell lysates with an anti-GFP antibody. The immunoprecipitates were analysed by SDS-PAGE, and Rab14 and GFP were detected by immunoblotting. B. GFP or GFP-Rab14 were transfected in A2780 cells for 48 hours. GFP was immunoprecipitated using an anti-GFP antibody and the proteins were separated by SDS-PAGE. RCP and GFP were detected by immunoblotting. C. H1299 cells were transfected with GFP-RCP and mCherry-Rab14 and seeded onto glass-bottomed plates. The cells were visualised and representative images are shown. The scale bar represents 10μm.

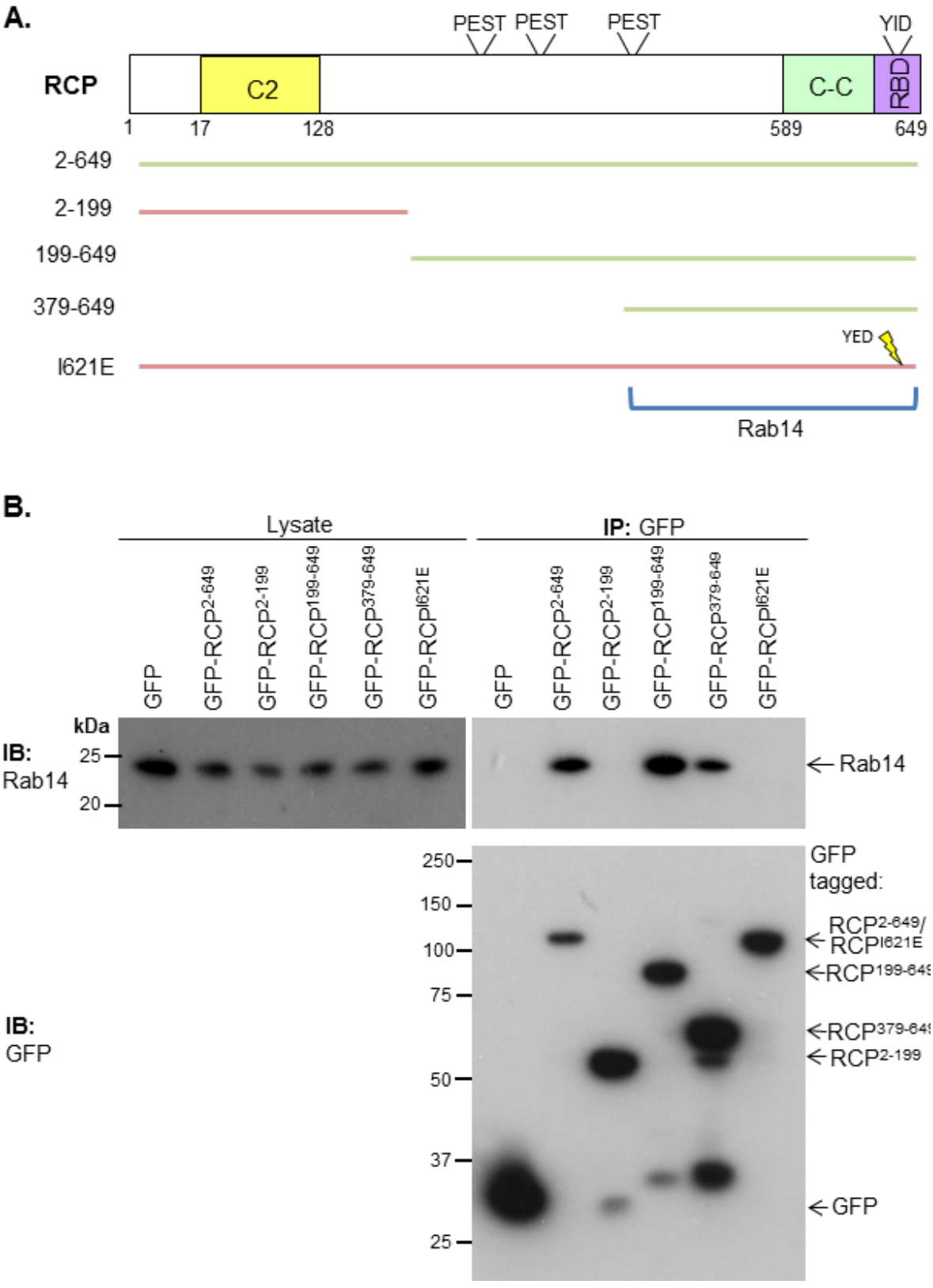

Figure 3-7 Rab14 associates with the C-terminal region of RCP
A. Schematic representation of RCP truncates and a point mutant, which abolishes the RCP-Rab11 interaction. Green fragments were found associated with Rab14, whilst red fragments were not found associated with Rab14. B. A2780 cells were transfected with GFP, GFP-RCP$^{2-649}$, GFP-RCP$^{2-199}$, GFP-RCP$^{199-649}$, GFP-RCP$^{379-649}$ or GFP-RCP^{I621E}. GFP was immunoprecipitated 48 hours after transfection with an anti-GFP antibody. Immunoprecipitates were analysed by SDS-PAGE, and GFP and Rab14 were detected by immunoblotting.

3.2.3 Rab6 associates with RCP

3.2.3.1 The role of Rab6 in retrograde trafficking and cytokinesis

There are three Rab6 isoforms: Rab6A, Rab6A' and Rab6B. Rab6A and Rab6A' only differ by three amino acids in the GTP binding domain and are generated by alternative splicing of homologous exons within the gene (**Figure 3.9A**) (Echard et al., 2000). Rab6B is less well characterised and is encoded by a second gene, which displays 91% homology to Rab6A/A' protein (**Figure 3.8**). Rab6A and Rab6A' are ubiquitously expressed, whilst Rab6B is preferentially expressed in the brain (Opdam et al., 2000).

The Rab6 subfamily were originally described as Golgi-associated GTPases involved in regulating retrograde transport (Goud et al., 1990). Rab6 has been shown to have a role in several diseases for which the retrograde trafficking pathway is important, for example, in Herpes (Johns et al., 2014), HIV (Brass et al., 2008) and Alzheimer's disease (Elfrink et al., 2012). Overexpression of dominant positive (Q72L) and negative (T27N) Rab6A and Rab6A' mutants showed that Rab6A' regulates trafficking from endosomes to the trans-Golgi network (TGN), whilst Rab6A regulates Golgi to ER trafficking (Mallard et al., 2002; White et al., 1999). In another study Rab6A and Rab6A' isoforms were specifically targeted by siRNA. This revealed that Rab6 is largely dispensable in Shiga toxin retrograde trafficking events, whilst suppressing Rab6A' expression disrupted this trafficking (Del Nery et al., 2006). The consensus of these studies is that Rab6 has a role in retrograde transport, but the exact order and involvement of the different isoforms is disputed.

As well as retrograde trafficking, Rab6 has been shown to be involved in exocytosis. Indeed, Rab6A co-localises with the microtubule motor protein Kinesin-1 on exocytic vesicles (Grigoriev et al., 2007). Rab6A is thought to have a role in vesicular docking and fusion in both Hela cells and in C.elegans oocyte-embryo transition (Grigoriev et al., 2011; Kimura and Kimura, 2012). It is unclear how and why Rab6 is involved in anterograde and retrograde trafficking. Interestingly, more recent studies have shown a role for Rab6A trafficking in the immune system. Expression of a Rab6A dominant-negative mutant, or depletion of its expression, inhibits TNF secretion in macrophages (Micaroni et al., 2013).

Rab6 has been shown to have an important role in three more functions: cytokinesis and maintaining Golgi homeostasis. Silencing Rab6 expression increases the number and size of TGN cisternae (Storrie et al., 2012), perhaps due to the accumulation of vesicles that can no longer bud from the TGN. Many Rab6 effector proteins have been identified, and several of these proteins have been shown to have a role with Rab6 in cytokinesis. For example, Rabkinesin-6 is a kinesin like interacting protein involved in transport along the cytoskeleton during cytokinesis (Echard et al., 1998), and GAPCenA is a Rab6 GAP that is associated with the centrosome, co-ordinating microtubule and Golgi dynamics (Cuif et al., 1999).

3.2.3.2 A2780 cells express all isoforms of Rab6

Many Rab6 peptides were identified in the GFP-RCP immunoprecipitates in A2780 and A2780-Rab25 cells. The peptide sequences were analysed to determine whether the Rab6 association with RCP might be isoform-specific. However, the peptides identified from the GFP-RCP co-immunoprecipitation were a mix of Rab6A/A' isoform-specific and non-specific peptides (**Figure 3.8**). To determine whether one specific Rab6 isoform associates with RCP, I first sought to determine whether all three isoforms were expressed in A2780 cells. Briefly, mRNA was extracted from A2780 and A2780-Rab25 cells and synthesised into cDNA. Rab6A/A' and Rab6B specific primers were used to amplify Rab6A/A' and Rab6B from the cDNA by PCR. The DNA products were run in a 1% agarose gel. Both cell types expressed both Rab6A/A' and Rab6B isoforms (**Figure 3.9B**). It is possible to distinguish between the Rab6A and Rab6A' isoforms, as the Rab6A' alternatively spliced exon contains a unique *Pst1* site (**Figure 3.9A**) (Echard et al., 2000). Therefore, the amplified Rab6A/A' gene transcript was digested with *Pst1* and the DNA products were run in a 1% agarose gel indicating that A2780 and A2780-Rab25 cells express all three Rab6 isoforms (**Figure 3.9C**).

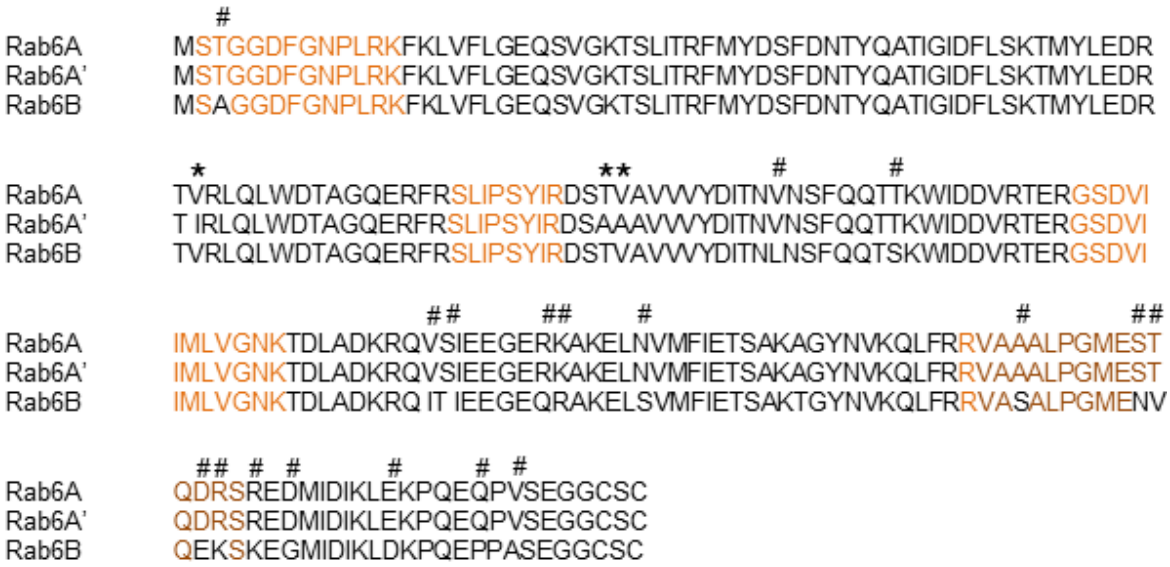

Figure 3-8 Rab6 peptides identified by mass spectroscopy in the RCP interactome
The Rab6 family of proteins were aligned using BLAST. Differences in the isoforms are shown between Rab6A and Rab6A' (*), and between RabA/A' and Rab6B (#). Coloured text indicates the peptides identified by mass spectrometry that were found associated with GFP-RCP (orange represents peptides identified and brown represents overlapping peptides).

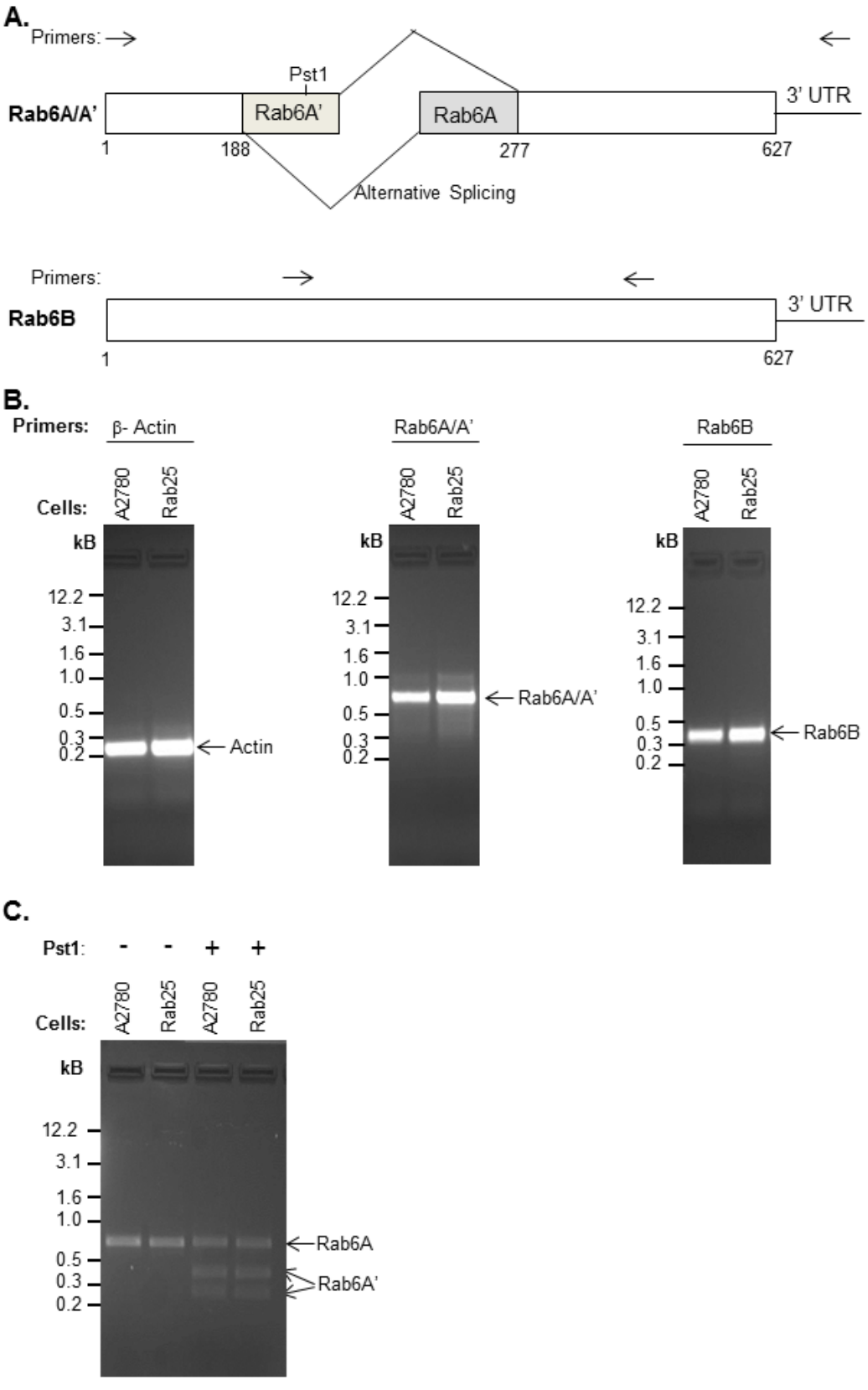

Figure 3-9 Rab6 family expression in A2780 and A2780-Rab25 cells
A. Rab6A and Rab6A′ are generated by splicing alternative exons whereas Rab6B is encoded by a separate gene. Both isoforms were amplified by Rab6A/A′ specific primers but could be distinguished by a unique *Pst1* site in the Rab6A′ specific exon. B. mRNA was extracted from A2780 and A2780–Rab25 cells and synthesised into cDNA. Isoform-specific primers were used in PCR to amplify Rab6A/A′ (675bp), Rab6B (383bp) and β-actin (235bp, control) from the template cDNA. DNA products were run in a 1% agarose gel. C. Rab6A/A′ PCR product (B.) was purified and digested with *Pst1*. Undigested Rab6A is 675bp whilst digested Rab6A′ is 264bp and 411bp.

3.2.3.3 Rab6A and Rab6B associate with RCP

Endogenous Rab6A was found to efficiently co-immunoprecipitate with GFP-RCP in both A2780 and A2780-Rab25 cells (**Figure 3.10**). To further confirm this association, and determine whether the RCP association is specific for the Rab6A isoform, plasmids were cloned in which Rab6A and Rab6B were N-terminally tagged to GFP (**Figure 3.11A**). These plasmids were transfected into A2780 cells and GFP was immunoprecipitated with an anti-GFP antibody. GFP-Rab6A and GFP-Rab6B were well-expressed in these cells, and immunoblot analysis using an anti-GFP antibody detected bands at the appropriate sizes (**Figure 3.11B**). Endogenous RCP was found to co-immunoprecipitate with both GFP-Rab6A and GFP-Rab6B. These data confirm that there is an association between RCP and both Rab6A and Rab6B.

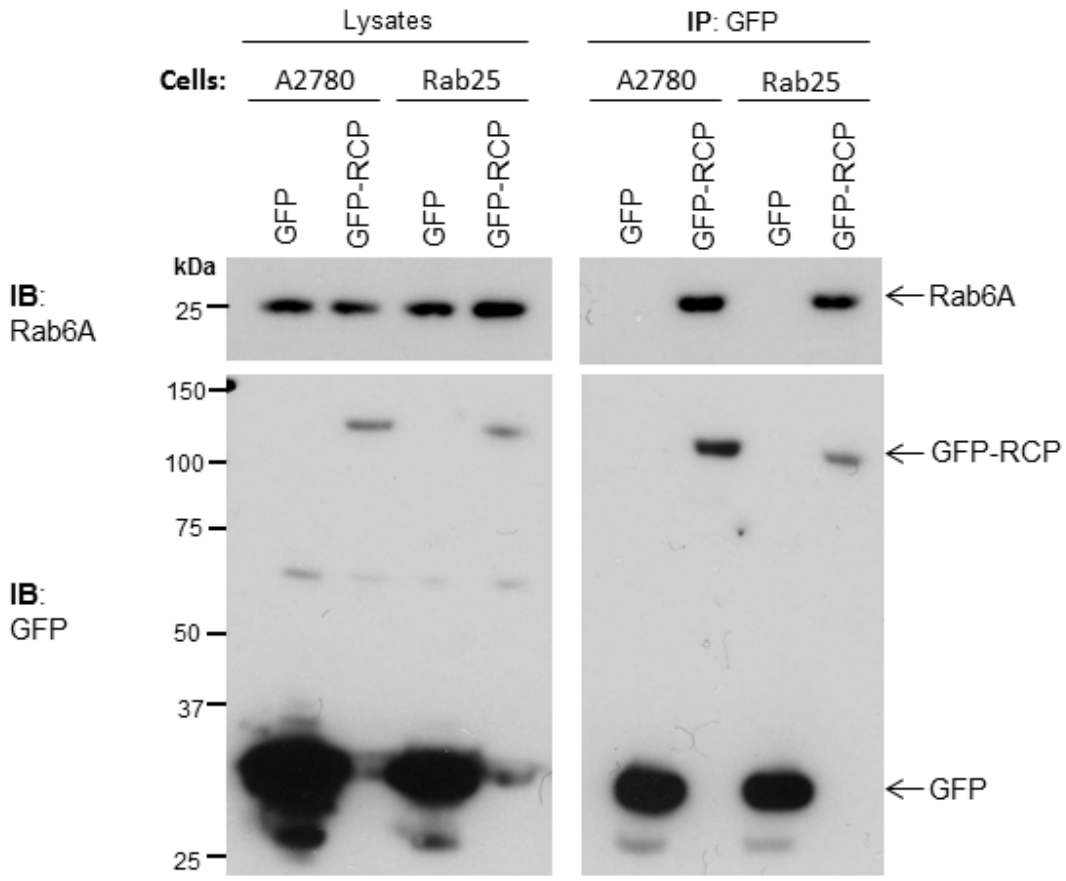

Figure 3-10 GFP-RCP associates with endogenous Rab6A
A2780 and A2780-Rab25 cells were transfected with GFP or GFP-RCP. GFP was immunoprecipitated from the cell lysates 48 hours after transfection with an anti-GFP antibody and the immunoprecipitates were analysed by SDS-PAGE. Rab6A and GFP were detected by immunoblotting.

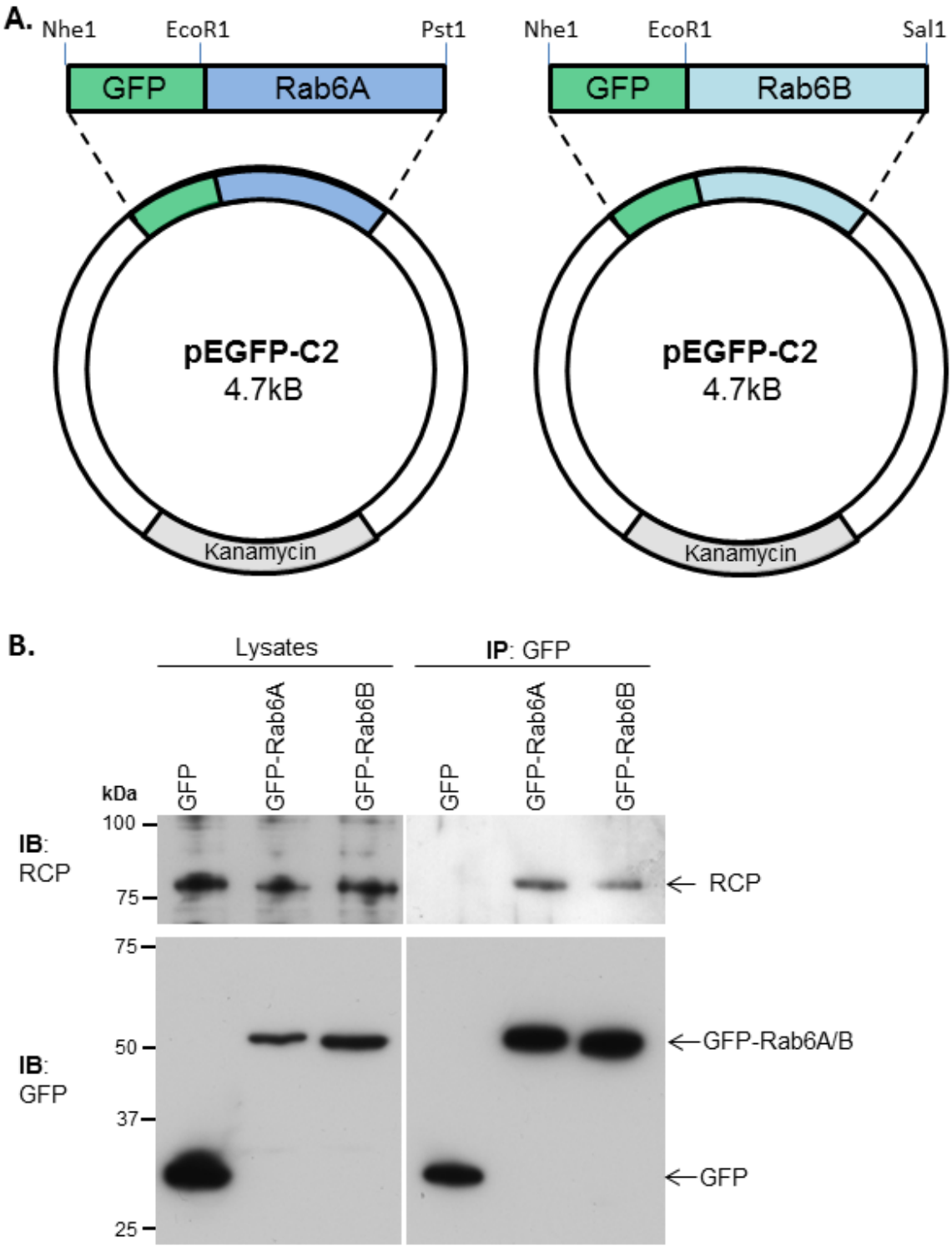

Figure 3-11 GFP-Rab6A and GFP-Rab6B associate with endogenous RCP
A. Vector maps of the GFP-Rab6A and GFP-Rab6B constructs. B. A2780 cells were transfected with GFP-Rab6A or GFP-Rab6B. GFP was immunoprecipitated and the proteins were analysed by SDS-PAGE. RCP and GFP were detected by immunoblotting.

3.2.3.4 Rab6B directly interacts with RCP

Co-immunoprecipitation assays show whether there is an association between two proteins, but do not indicate whether this association is a direct interaction or an indirect association. In order to ascertain whether Rab6 and RCP interact directly, *in vitro* binding assays were performed. First a GST-Rab6B fusion construct was cloned (**Figure 3.12A**). His-RCP and GST-Rab6B were expressed in *E.coli* and the proteins were purified. These recombinant proteins were then used in GST pull-down assays. Briefly, His-RCP was incubated with GST/GST-Rab6B bound Gluthathione beads. The beads were thoroughly washed and then boiled in sample buffer. The proteins were separated by SDS-PAGE and analysed by immunoblotting. His-RCP was associated with GST-Rab6B but not GST alone, which indicates that these proteins are capable of forming a direct interaction with one another (**Figure 3.12B**).

3.2.3.5 Rab6 associates with the central region of RCP

Since the interaction between RCP and Rab6B was found to be potentially direct, I sought to identify which RCP domain interacts with Rab6. This showed that Rab6A associates with the central region of RCP, $RCP^{199-379}$ by co-immunoprecipitation (**Figure 3.13A/B**). Little is known about this region of RCP, except the presence of PEST sequences, which can target RCP for calpain cleavage (Marie et al., 2005). In comparison, Rab11 and Rab14 interact with the C-terminal fragment of RCP, $RCP^{379-649}$, which contains the Rab binding domain (RBD). Mutating a key residue in this domain, I621E, reduced the association between Rab11 and RCP (Lindsay and McCaffrey, 2004) (**Figure 3.13A**). Although Rab6 and Rab11 associate with different RCP truncations, Rab6 was not found associated with RCP^{I621E}, suggesting that the Rab11-RCP interaction is required before Rab6 can interact with RCP.

3.2.3.6 GFP-Rab6 and mCherry-RCP do not co-localise

Live cell microscopy was used to visualise RCP and Rab6 and to determine whether they are localised in the same sub-cellular compartment. mCherry-tagged RCP and GFP-tagged Rab6A or Rab6B (as well as mCherry and GFP controls) were transfected into A2780 cells and visualised by confocal microscopy. Both RCP and Rab6 were found to be localised to a peri-nuclear

compartment (**Figure 3.14**). However, although the RCP and Rab6 compartments were found very close together, under closer examination no co-localisation was detected (**Figure 3.14**).

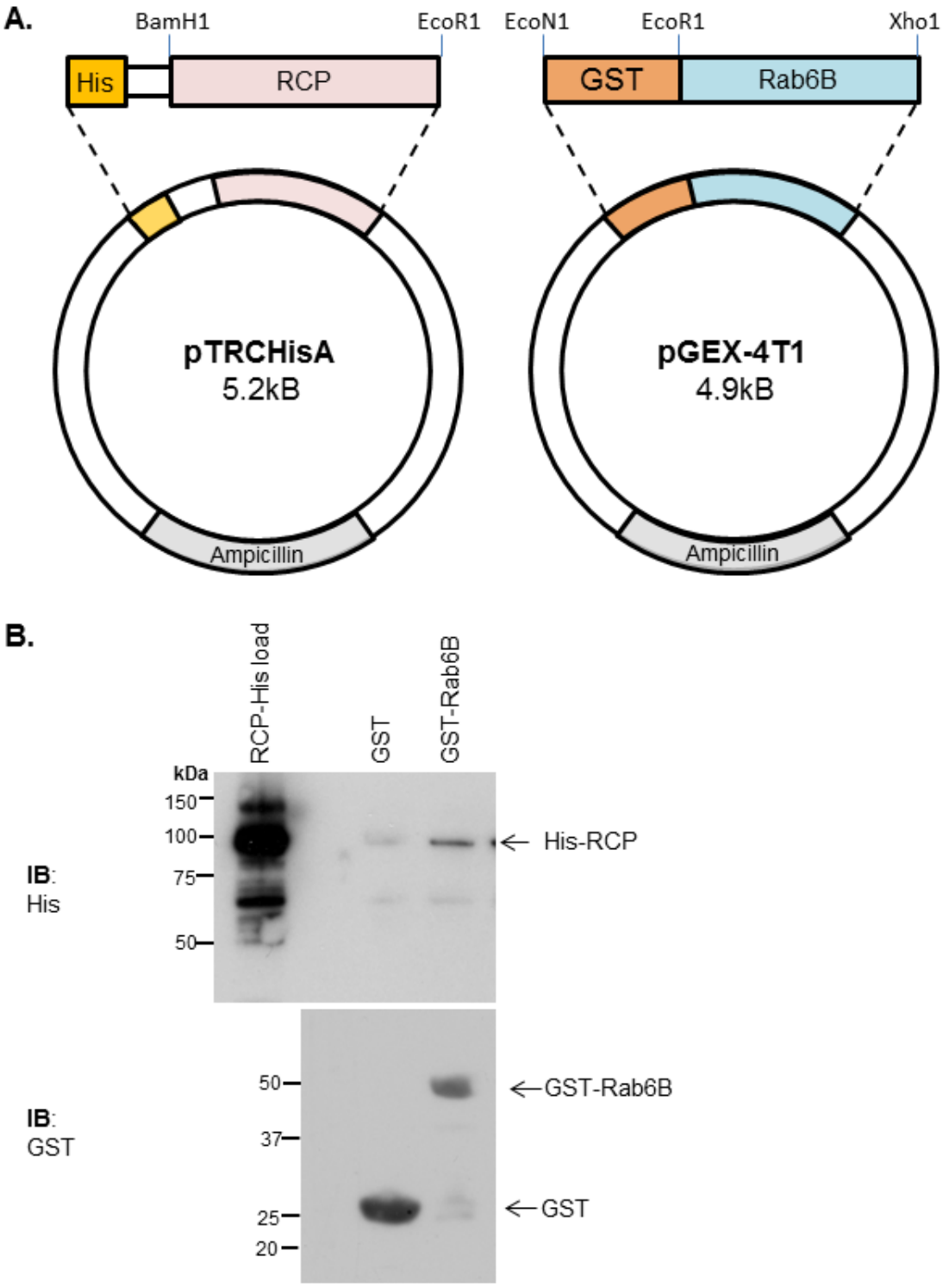

Figure 3-12 RCP directly associates with Rab6B
A. Vector maps of the GST-Rab6B and His-RCP constructs. B. Purified recombinant GST-Rab6B or GST were immobilised onto Glutathione agarose beads. The beads were washed and incubated for 2 hours at 4ºC with purified recombinant His-RCP. The beads were washed thoroughly and the associated protein eluted. Eluates were separated by SDS-PAGE. His and GST were detected by immunoblotting.

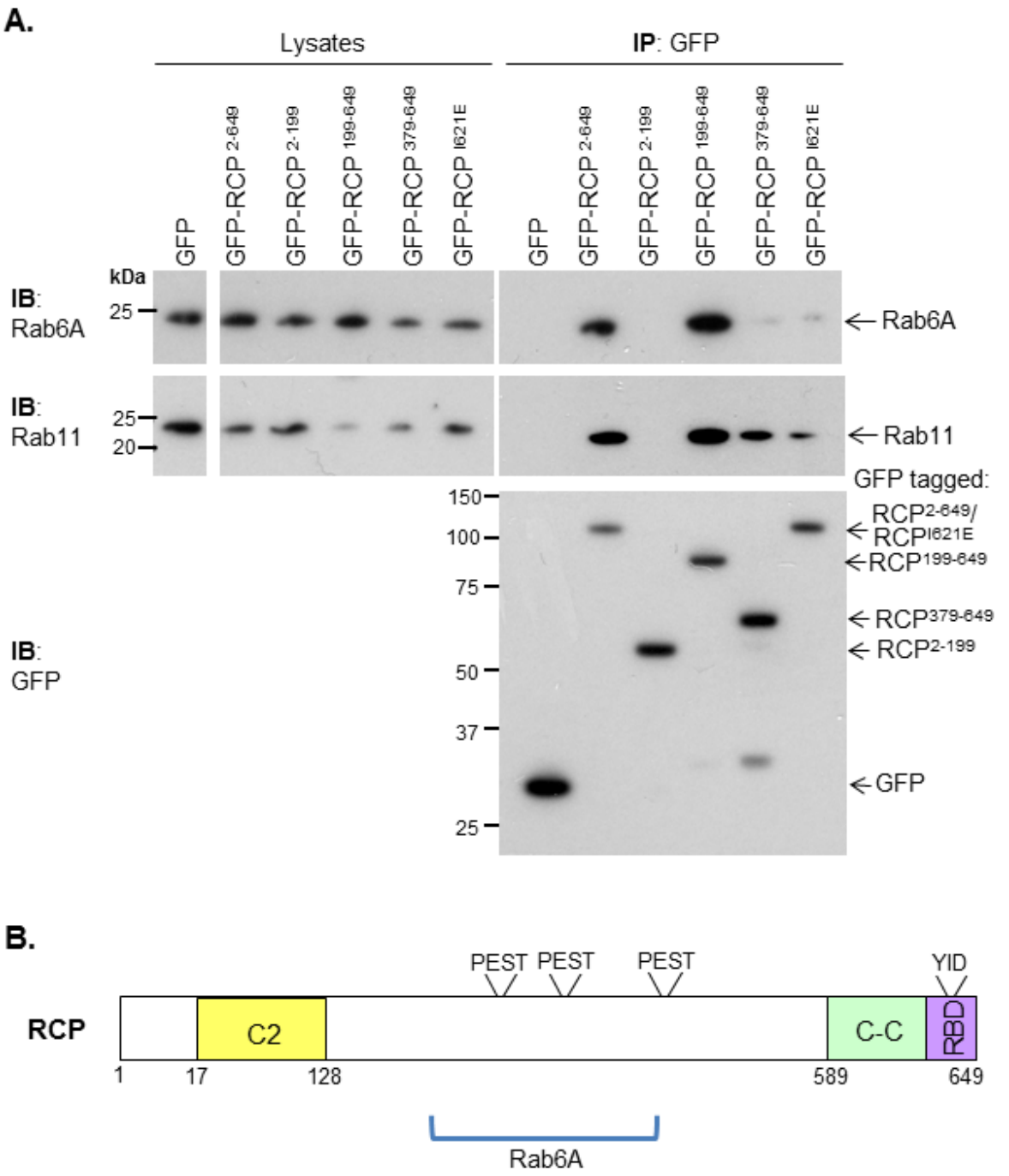

Figure 3-13 Rab6A associates with the central region of RCP
A. A2780 cells were transfected with GFP, GFP-RCP$^{2-649}$, GFP-RCP$^{2-199}$, GFP-RCP$^{199-649}$, GFP-RCP$^{379-649}$ or GFP-RCP^{I621E}. GFP was immunoprecipitated 48 hours after transfection with an anti-GFP antibody. Immunoprecipitates were analysed by SDS-PAGE, and GFP, Rab6A and Rab11 were detected by immunoblotting. B. Schematic representation of RCP with a blue line showing the region in which Rab6A associated with RCP.

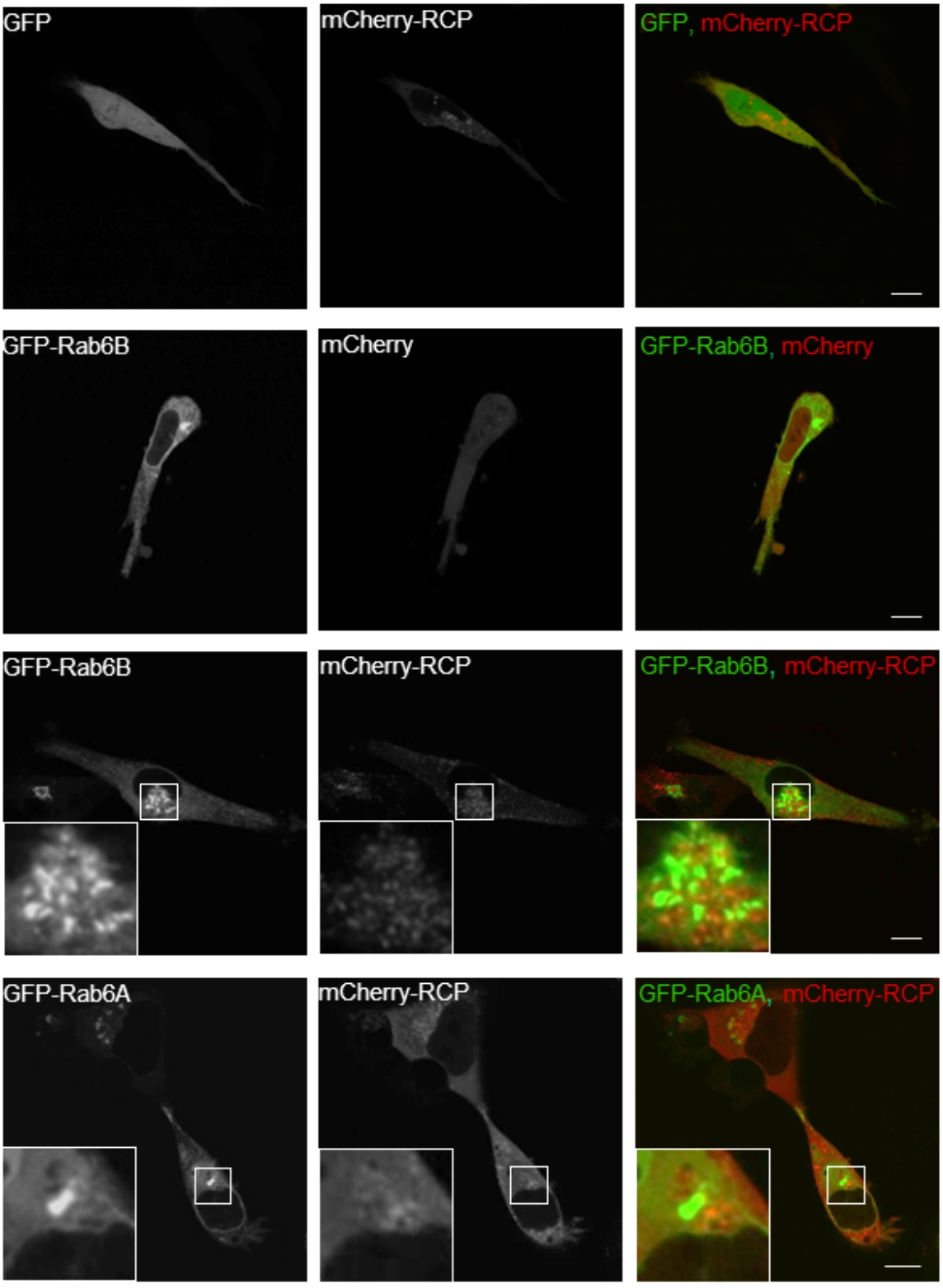

Figure 3-14 GFP-Rab6A/Rab6B and mCherry-RCP do not co-localise
A2780 cells were transfected with the following plasmids: GFP and mCherry-RCP, GFP-Rab6B and mCherry, GFP-Rab6B and mCherry-RCP, and GFP-Rab6A and mCherry-RCP. The cells were directly seeded onto glass-bottomed dishes and visualised by live confocal microscopy 24 hours after transfection. Representative images are shown with a scale bar of 10μm.

Taken together these data show that RCP associates with both Rab6A and Rab6B and this association is potentially direct. Rab6 associates with the central region of RCP and is only found associated with RCP if the Rab11 binding site (I621) is maintained. Overexpressed GFP-Rab6A/B and mCherrry-RCP localise in neighbouring but non-overlapping compartments in A2780 cells.

3.2.3.7 Depleting Rab6A and Rab6B expression increases A2780-Rab25 but not A2780 cell invasion

The role of Rab6 in cell migration and invasion has not been previously investigated. I sought to determine whether Rab6 has an involvement in A2780 cell invasion. First Rab6A/A' expression was transiently suppressed using Rab6A-specific siRNA SMARTpool and the Rab6A/A' knockdown was assessed by Western blotting (**Figure 3.16A**). To determine whether the knockdown was isoform-specific, mRNA was extracted from the Rab6A/A' knockdown cells and used to synthesise cDNA. cDNA was used as a template in PCR using Rab6A/A' and Rab6B specific primers and run in 1% agarose gels (**Figure 3.16B**). Taken together this showed that Rab6A/A' (but not Rab6B) expression is reduced by transfection of siRNA targeting Rab6A, thus confirming the isoform-specificity of the siRNA strategy. A2780 cells treated with Rab6A/A'-targeting or non-targeting siRNA were seeded onto the bottom of transwells and allowed to migrate through a fibronectin enriched Matrigel plug towards an EGF serum gradient (**Figure 3.15**). This analysis revealed that the suppression of Rab6A expression had no effect on A2780 cell invasion (**Figure 3.16C/D**).

A2780 cells are not particularly invasive, so I sought to determine whether Rab6 is required for invasion in a more invasive cell line, A2780-Rab25 cells (Caswell et al., 2007). A2780-Rab25 cells were transfected with Rab6A, Rab6B and non-targeting siRNA and lysed after 48 hours. Immunoblotting analysis using an anti-Rab6A antibody demonstrated that Rab6A protein expression was suppressed (**Figure 3.17A**). The same anti-Rab6A antibody detected a weak suppression of Rab6A expression upon Rab6B-targeting siRNA transfection (**Figure 3.17B**), suggesting that the Rab6B-targeting siRNA treatment had an effect on Rab6A expression levels or that the antibody is not very specific. To ensure the specificity of the Rab6B siRNA, PCR was performed. Reduction in Rab6B but not Rab6A mRNA was observed in Rab6B-targeting siRNA transfected cells, which

demonstrated that the Rab6B-targeting siRNA was isoform-specific (**Figure 3.17C**). A2780-Rab25 cells treated with Rab6A- or Rab6B-targeting siRNA were seeded onto inverse invasion assays. Intriguingly, suppression of either Rab6A or Rab6B expression significantly increased the invasiveness of A2780-Rab25 cells (**Figure 3.18**). I did not persue this association further due to time limitations and instead persued the functional relevance of the association between EphA2, Rab14 and RCP.

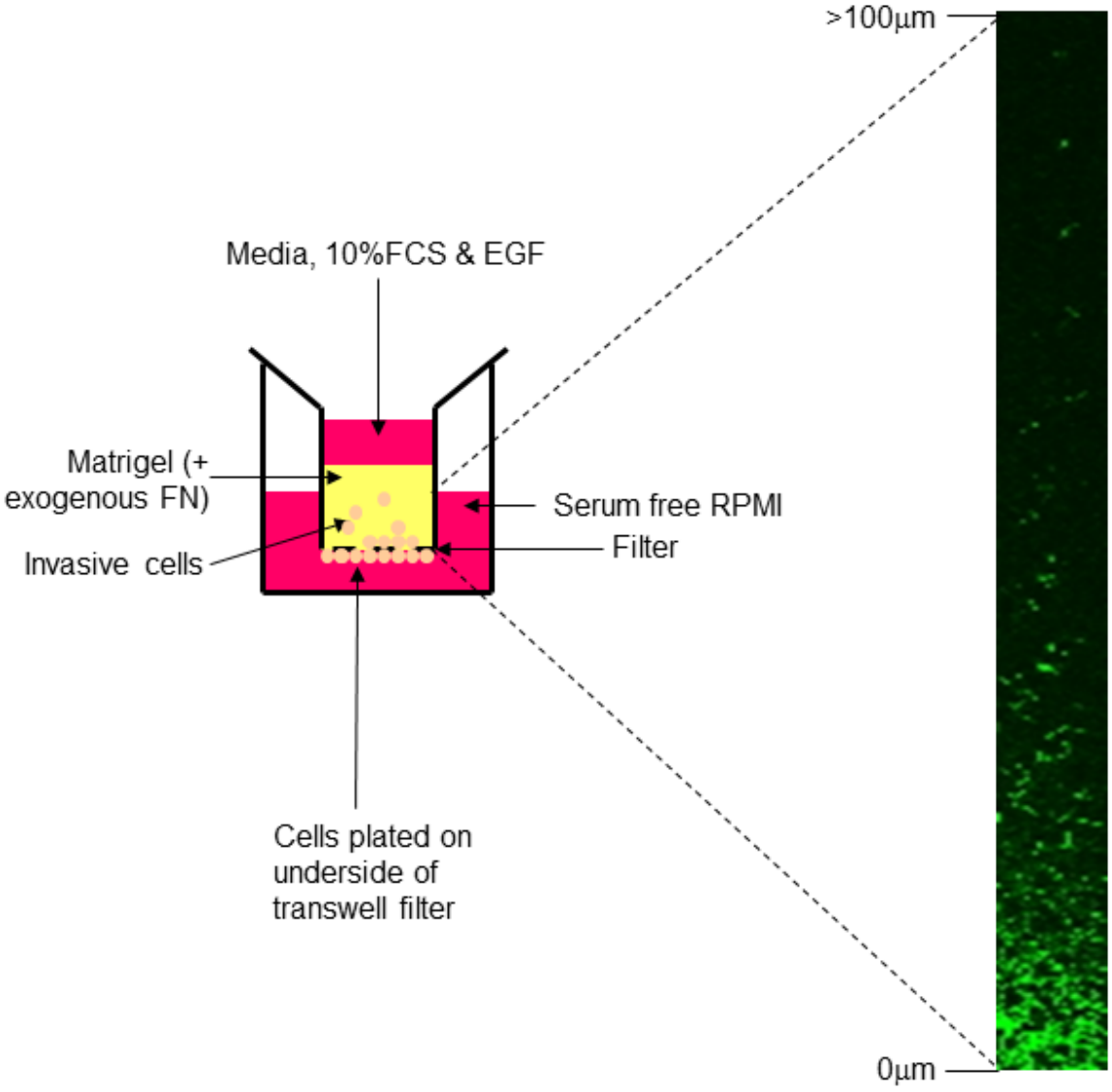

Figure 3-15 Schematic representation of the invasion assay
The cells migrated through the filter and invaded into the Matrigel up an EGF and serum gradient. Sample confocal optical sections of calcein-AM stained invading cells are shown.

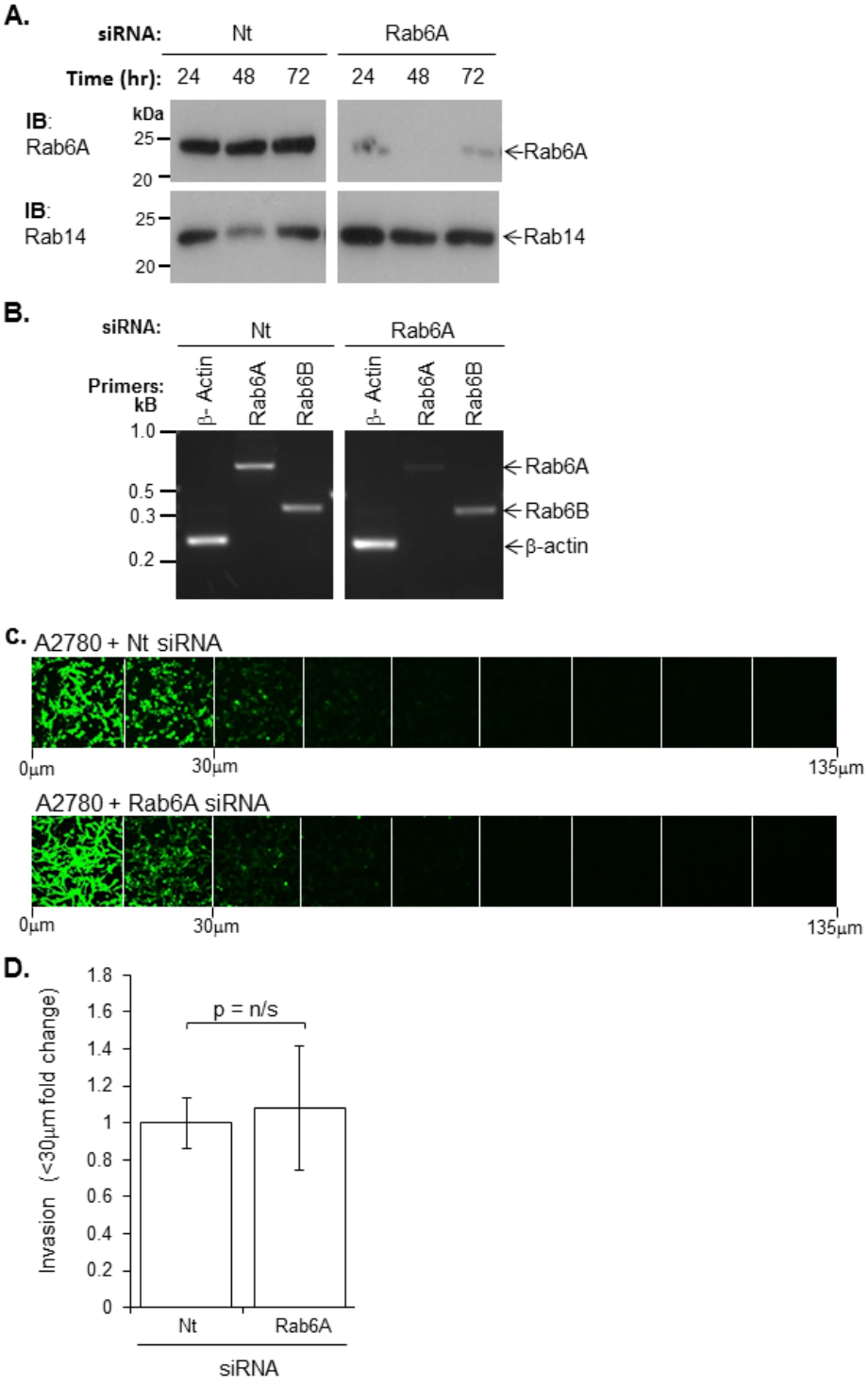

Figure 3-16 Suppression of Rab6A/A' has no effect on A2780 cell invasion
A2780 cells were transfected with non-targeting (Nt) or Rab6A/A'-targeting siRNA. A. The cells were lysed 24, 48, and 72 hours after transfection, and the proteins were extracted and separated by SDS-PAGE. Rab6A and Rab14 (loading control) were detected by immunoblotting. The samples were run and transferred on the same gel and blot. B. mRNA was extracted from the transfected A2780 cells 48 hours after transfection and synthesised into cDNA. Isoform-specific primers were used in PCR to amplify Rab6A/A′ (675bp), Rab6B (383bp) and β-actin (235bp, control) from the template cDNA. DNA products were run in the same 1% agarose gel. C. Nt or Rab6A/A' siRNA treated cells were plated on the underside of transwell plugs containing Matrigel enriched with 25μg/ml fibronectin. The cells migrated towards EGF supplemented serum rich media for 72 hours, and were stained with calcein-AM to visualise invasion by confocal microscopy. Optical sections were taken every 15μm and consecutive images were assembled from left to right. D. Quantification of cells invading beyond 30μm relative to A2780 cells transfected with Nt siRNA. The graph shows the averages and SEM of twelve regions of cell invasion in four transwell plugs from two separate experiments (n/s: not statistically significant).

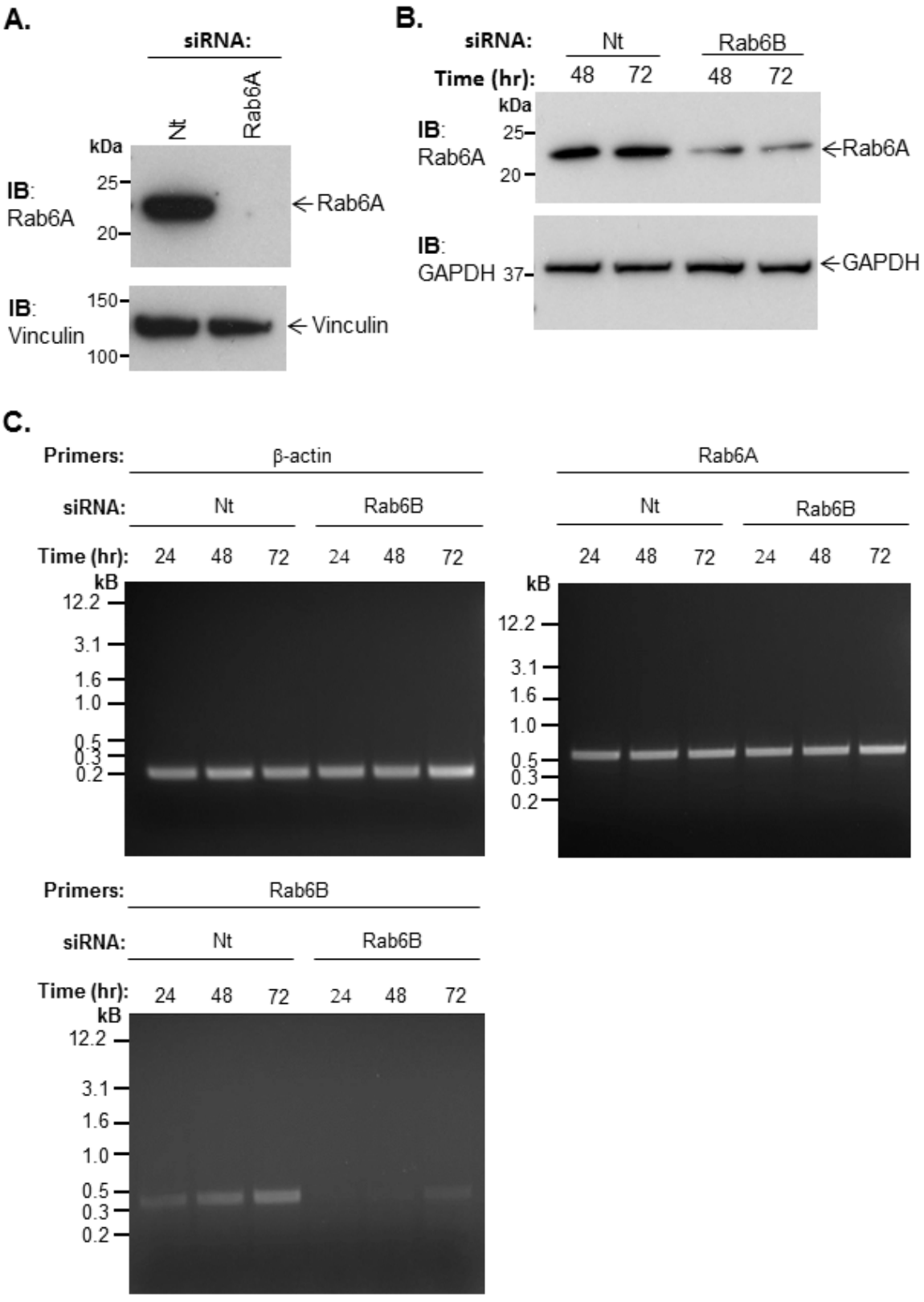

Figure 3-17 Suppression of Rab6A/A' and Rab6B expression in A2780-Rab25 cells
A2780-Rab25 cells were transfected with Rab6A/A'-, Rab6B- or non-targeting (Nt) siRNA. A. Rab6A/A' and Nt siRNA transfected cells were lysed 48 hours after transfection and Rab6A and Vinculin were detected by immunoblotting. B. Rab6B and Nt siRNA transfected cells were lysed 48 and 72 hours after transfection and Rab6A and GAPDH were detected by immunoblotting. C. mRNA was extracted from the Rab6B and Nt siRNA transfected A2780 cells, 24, 48 and 72 hours after transfection and synthesised into cDNA. Isoform-specific primers were used in PCR to amplify Rab6A/A′ (675bp), Rab6B (383bp) and β-actin (235bp, control) from the template cDNA. DNA products were run in a 1% agarose gel.

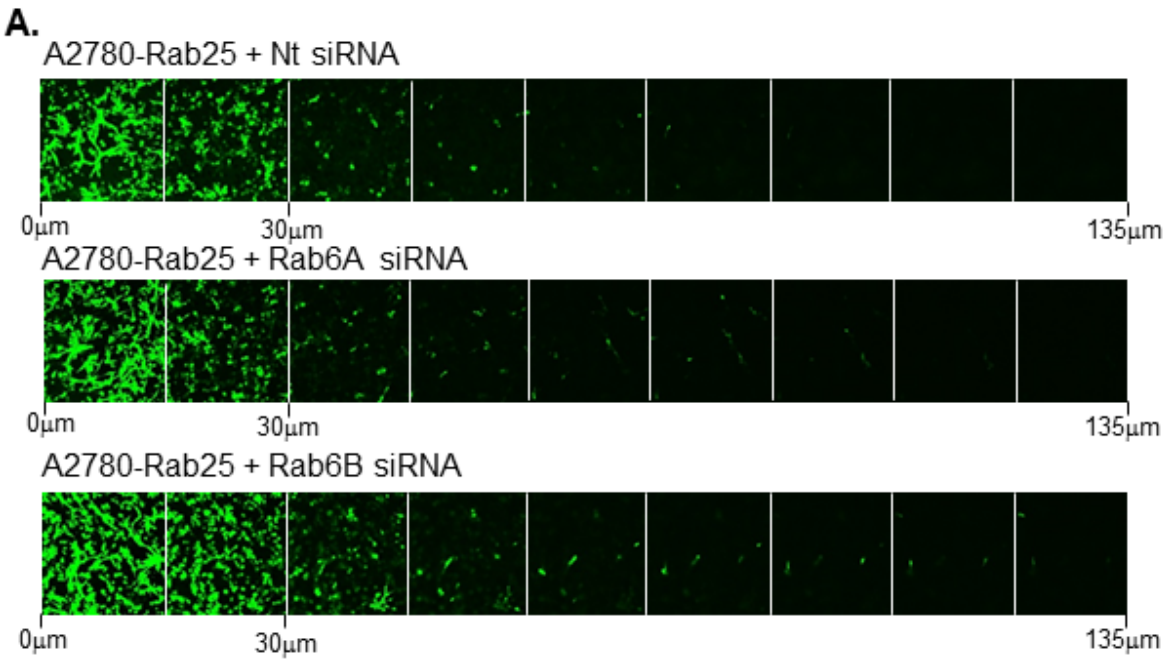

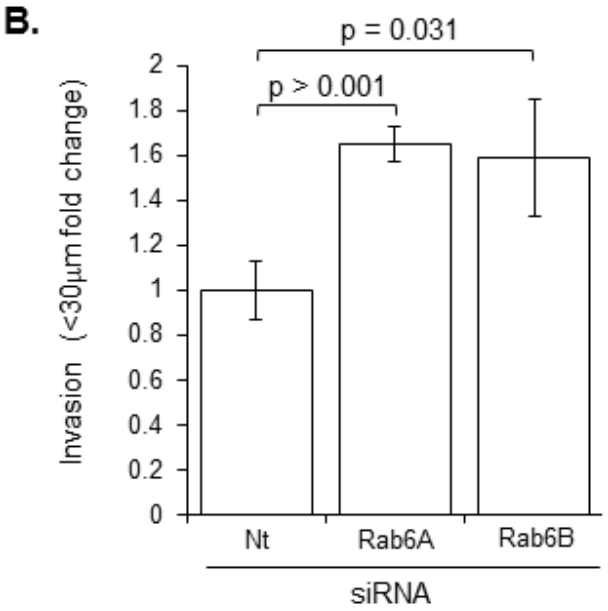

Figure 3-18 Suppression of Rab6A/A' or Rab6B increases the invasiveness of A2780-Rab25 cells

A2780-Rab25 cells were transfected with Rab6A-, Rab6B- or non-targeting (Nt) siRNA SMARTpools and were plated on the underside of transwell plugs containing Matrigel enriched with 25µg/ml fibronectin. The cells migrated towards EGF-supplemented serum rich media for 72 hours, and were stained with calcein-AM to visualise invasion by confocal microscopy. A. Optical sections were taken every 15µm and consecutive images were assembled from left to right. B. Quantification of cells invading beyond 30µm relative to A2780-Rab25 cells transfected with Nt siRNA. The graph shows the averages and SEM of 24 regions of cell invasion in 8 transwell plugs from four separate experiments for Nt and Rab6A/A' siRNA transfection, and 6 regions of cell invasion in 2 transwell plugs for Rab6B siRNA transfection.

3.2.4 EphA2 associates with RCP

3.2.4.1 Ephs have a complex role in cancer and little is known about their trafficking

The roles of Ephs and Ephrins in human cancers are thoroughly documented, but their roles in tumour etiology, progression and metastasis are complex and there are many discrepancies between different studies (Pasquale, 2010). They can act as both tumour suppressors and oncogenes, and have diverse roles in metastasis and cell migration, as previously discussed **(Section 1.2.6.3)**. Some recent work has shown that EphA2 is internalised then either degraded or recycled back to the membrane **(Section 1.3.5)** (Boissier et al., 2013). However, no work has determined the role of EphA2 recycling or identified any proteins involved in EphA2 recycling. I identified EphA2 as a novel RCP-associated protein in my proteomic screen (Table 3.1). Since EphA2 has an interesting role in migration and little is known about its recycling, it would be interesting to confirm its association with RCP and investigate whether RCP has a role in known EphA2 functions.

3.2.4.2 EphA2 is the only EphA expressed in A2780 cells

All but one of the ten unique EphA2-derived peptides identified in the proteomic screen were found in the C-terminal cytoplasmic region of the protein (**Figure 3.19**). Since only one of the fourteen Eph proteins was identified in the screen, I sought to determine whether EphA2 is the only Eph expressed in A2780. RNA was extracted from the A2780 cells and subjected to microarray analysis on a HG U-133 Plus 2.0 chip (performed by M. Dozynkiewicz). I analysed these data to determine which Eph receptors and ligands were expressed and found that EphA2 was the only EphA with mRNA present in A2780 cells, but two EphBs were also expressed: EphB1 and EphB2 (**Table 3.2**). Three Ephrins were also identified.

A.

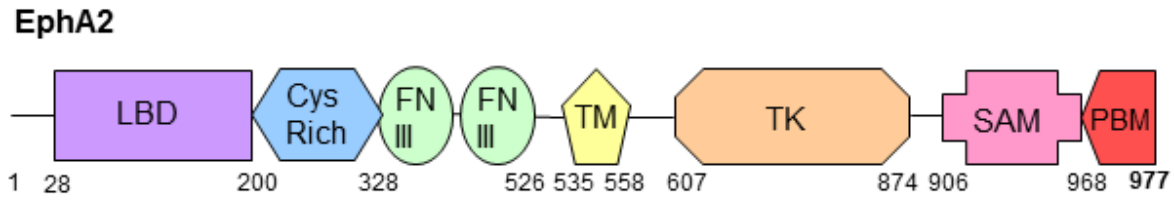

B.

MELQAARACFALLWGCALAAAAAAQGKEVVLLDFAAAGGELGWLTHPYGKGWDLM
QNIMNDMPIYMYSVCNVMSGDQDNWLRTNWVYRGEAERIFIELKFTVRDCNSFPGG
ASSCKETFNLYYAESDLDYGTNFQKRLFTKIDTIAPDEITVSSDFEARHVKLNVEERSV
GPLTRKGFYLAFQDIGACVALLSVRVYYKKCPELLQGLAHFPETIAGSDAPSLATVAG
TCVDHAVVPPGGEEPRMHCAVDGEWLVPIGQCLCQAGYEKVEDACQACSPGFFKF
EASESPCLECPEHTLPSPEGATSCECEEGFFRAPQDPASMPCTRPPSAPHYLTAVG
MGAKVELRWTPPQDSGGREDIVYSVTCEQCWPESGECGPCEASVRYSEPPHGLTR
TSVTVSDLEPHMNYTFTVEARNGVSGLVTSRSFRTASVSINQTEPPKVRLEGRSTTS
LSVSWSIPPPQQSRVWKYEVTYRKKGDSNSYNVRRTEGFSVTLDDLAPDTTYLVQV
QALTQEGQGAGSKVHEFQTLSPEGSGNLAVIGGVAVGVVLLLVLAGVGFFIHRRRKN
QRARQSPEDVYFSKSEQLKPLKTYVDPHTYEDPNQAVLKFTTEIHPSCVTRQKVIGA
GEFGEVYKGMLKTSSGKKEVPVAIKTLKAGYTEKQRVDFLGEAGIMGQFSHHNIIRLE
GVISKYKPMMIITEYMENGALDKFLREKDGEFSVLQLVGMLRGIAAGMKYLANMNYV
HRDLAARNILVNSNLVCKVSDFGLSRVLEDDPEATYTTSGGKIPIRWTAPEAISYRKF
TSASDVWSFGIVMWEVMTYGERPYWELSNHEVMKAINDGFRLPTPMDCPSAIYQL
MMQCWQQERARRPKFADIVSILDKLIRAPDSLKTLADFDPRVSIRLPSTSGSEGVPF
RTVSEWLESIKMQQYTEHFMAAGYTAIEKVVQMTNDDIKRIGVRLPGHQKRIAYSLL
GLKDQVNTVGIPI

Figure 3-19 Ten unique EphA2 peptides were identified in the proteomic screen
A. Schematic representation of EphA2 with colours highlighting each protein domain and motif. B. EphA2 protein sequence with colours corresponding to A. The bold and underlined regions highlight peptides that were identified by mass spectrometry in the GFP-RCP but not GFP immunoprecipitates. (LBD: ligand binding domain, Cys Rich: cysteine rich region, FNIII: fibronectin type 3 repeats, TM: transmembrane domain, TK: tyrosine kinase domain, SAM: sterile α motif, PBM: PDZ binding motif)

	Human Cell lines		
Gene	**A2780**	**H1299**	**PC3**
EphA1			
EphA2	+	+	+
EphA3			
EphA4			+
EphA5			
EphA6			
EphA7			
EphA8			
EphA10			
EphB1	+		
EphB2	+	+	+
EphB3			+
EphB4		+	+
EphB6			+
EphrinA1		+	+
EphrinA2			
EphrinA3			+
EphrinA4	+	+	+
EphrinA5	+		+
EphrinB1			+
EphrinB2	+	+	+
EphrinB3		+	+

Table 3-2 Expression profile of Eph Receptors and Ephrins in A2780, H1299 and PC3 cells
RNA was extracted from A2780 and H1299 cells and subjected to microarray analysis on the HG U-133 Plus 2.0 chip and Illumina HT12 microarray, respectively (performed by M. Dozynkiewicz and P. Muller). At least one probe was present in the arrays for each gene of interest. The expression profile of Eph receptors and Ephrins in PC3 cells was taken from Astin et al. (2010). Eph receptor and Ephrin genes found to be expressed in each cell type are indicated (+).

3.2.4.3 EphA2 associates with RCP

EphA2 co-immunoprecipitated with GFP-RCP in both control and Rab25-overexpressing A2780 cells (**Figure 3.20A/B**). To further confirm this association in cells that had not been transfected, endogenous EphA2 was immunoprecipitated from cell lysates of a number of different cell types. RCP was found to efficiently co-immunoprecipitate with EphA2 in A2780, PC3 and H1299 cells (but not with a control –RG16) (**Figure 3.20C-E**).

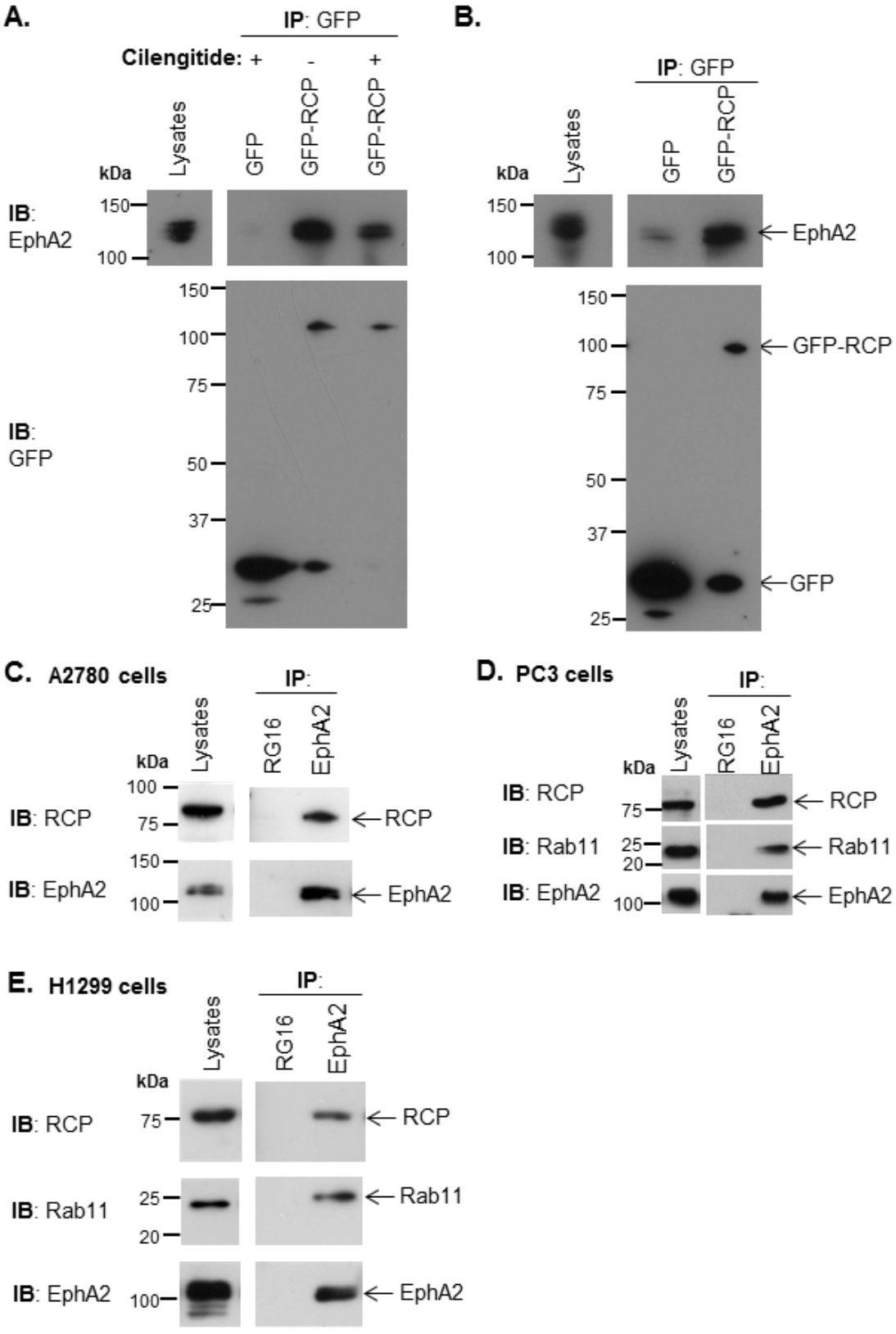

Figure 3-20 EphA2 associates with RCP
A/B. A2780 (A.) or A2780-Rab25 (B.) cells were transfected with GFP or GFP-RCP for 48 hours. A2780 cells were treated with 1μM Cilengitide or mock for 30 minutes. The cells were lysed and GFP was immunoprecipitated from the cell lysates with an anti-GFP antibody. The immunoprecipitates were analysed by SDS-PAGE, and EphA2 and GFP were detected by immunoblotting. C-E. A2780 (C.), PC3 (D.) or H1299 (E.) cells were lysed and endogenous EphA2 was immunoprecipitated using an anti-EphA2 or RG16 (control) antibody. The immunoprecipitates were separated by SDS-PAGE, and EphA2, RCP and Rab11 were detected by immunoblotting.

3.2.4.4 The internal pool of EphA2 co-localises with RCP and Rab11

EphA2 has previously been reported to be localised in a peri-nuclear compartment in HT-29 colon carcinoma cells (Orsulic and Kemler, 2000). Therefore, immunofluorescence was used to determine whether EphA2 is found at the peri-nuclear recycling compartment (PNRC) in which RCP localises. Anti-RCP or anti-Rab11 antibodies were used in combination with an anti-EphA2 antibody on fixed H1299 cells. Confocal microscopy was used to visualise the localisation of these proteins. EphA2 was found localised at cell-cell junctions and in membrane ruffles (**Figure 3.21**). A fraction of EphA2 was found in an intracellular pool that co-localised with both RCP and Rab11 in the PNRC (**Figure 3.21**).

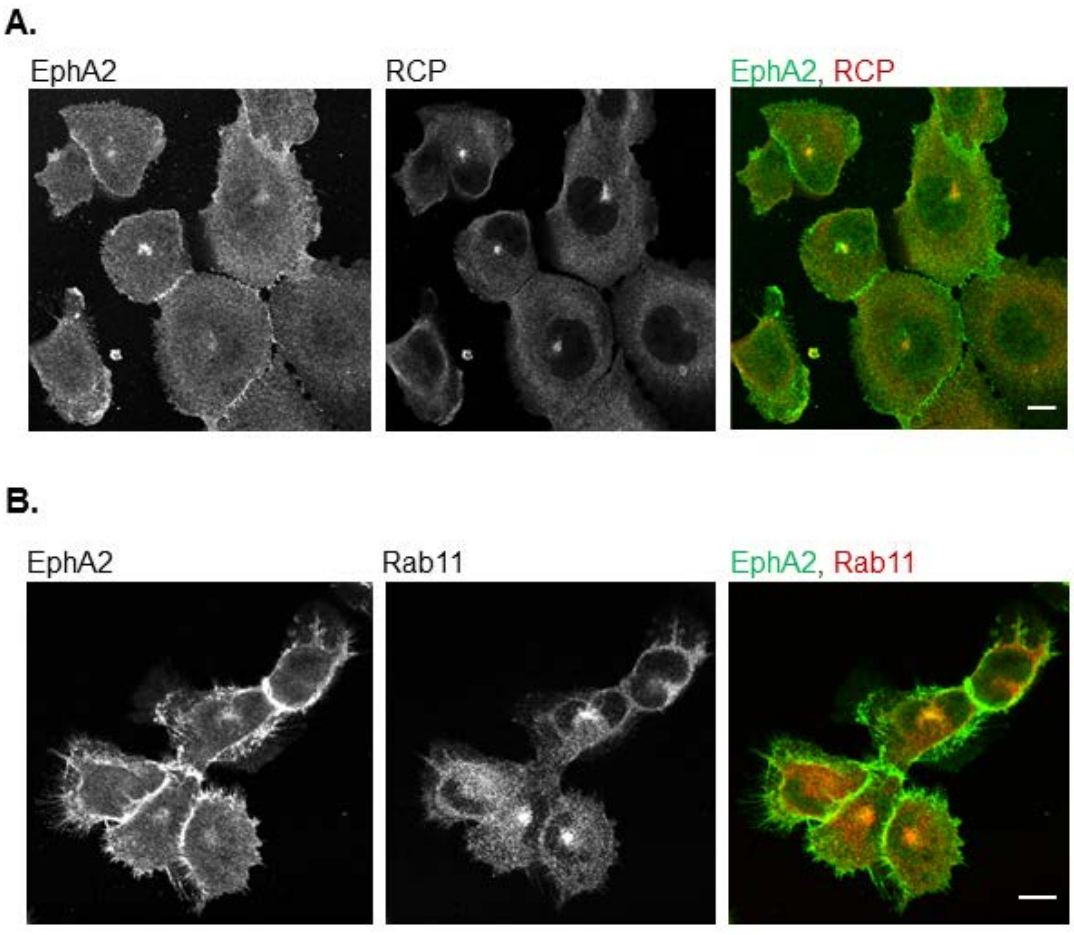

Figure 3-21 The internal pool of EphA2 co-localises with RCP and Rab11
H1299 cells were seeded onto coverslips and fixed with 4% paraformaldehyde (PFA). The cell membranes were permeabilised with 0.2% Triton-X100 for 5 minutes and blocked in 5% BSA for 30 minutes. Immunostaining was performed with mouse-anti-EphA2 and chicken-anti-RCP/rabbit-anti-Rab11, and Cy2-anti-mouse and Cy-3-anti-chicken/rabbit antibodies for 1 hour. Coverslips were thoroughly washed with PBS and mounted with Vectashield mounting media. Cells were viewed by confocal microscopy and representative images are shown.

3.2.4.5 EphA2 associates with all Rab11-Fips

The five members of the Rab11-Fip family of proteins are divided into two classes: Class 1 (RCP, Fip2 and Rip11) are involved in trafficking various receptors (Caswell et al., 2008; Prekeris et al., 2000; Schwenk et al., 2007), whereas class 2 (Fip3 and Fip4) have a role in cytokinesis (Fielding et al., 2005; Simon et al., 2008) (**Figure 3.22A**). To determine which of these Rab11-Fips were able to associate with EphA2, I expressed GFP-fused proteins of each of the Rab11-Fips in A2780 cells. EphA2 was found to associate with all of the GFP tagged Rab11-Fips (**Figure 3.22B**), thus demonstrating that the association is not specific for RCP.

3.2.4.6 EphA2 associates with the C-terminal region of RCP

The association between RCP and EphA2 was further investigated by expressing GFP-tagged truncations of RCP in A2780 cells. EphA2 associated with the C-terminal portion of RCP, which contains the coiled-coiled domain and RBD, but not the N-terminal portion (**Figure 3.23**). Interestingly, EphA2 associated with the same C-terminal portion of RCP that has previously been shown to bind to α5β1-integrin (Caswell et al., 2008). EphA2 was not found associated with the Rab11-binding deficient mutant of RCP (I621E) (**Figure 3.23**), indicating the likelihood that RCP must be recruited to membranes by association with Rab11 in order to be capable of recruiting EphA2.

3.2.4.7 α5β1-integrin does not act as a molecular bridge between EphA2 and RCP

Previous studies have reported an association between α5β1-integrin and EphA2 (Makarov et al., 2013; Prévost et al., 2005). Therefore, I hypothesised that α5β1-integrin could act as a molecular bridge holding EphA2 and RCP together into a co-immunoprecipitable complex. To test this, EphA2 was immunoprecipitated from cells in which α5-integrin levels were suppressed using siRNA. RCP co-immunoprecipitated with EphA2 in the presence and absence of α5-integrin (**Figure 3.24**), which suggests that α5β1-integrin is not acting as a molecular bridge between EphA2 and RCP.

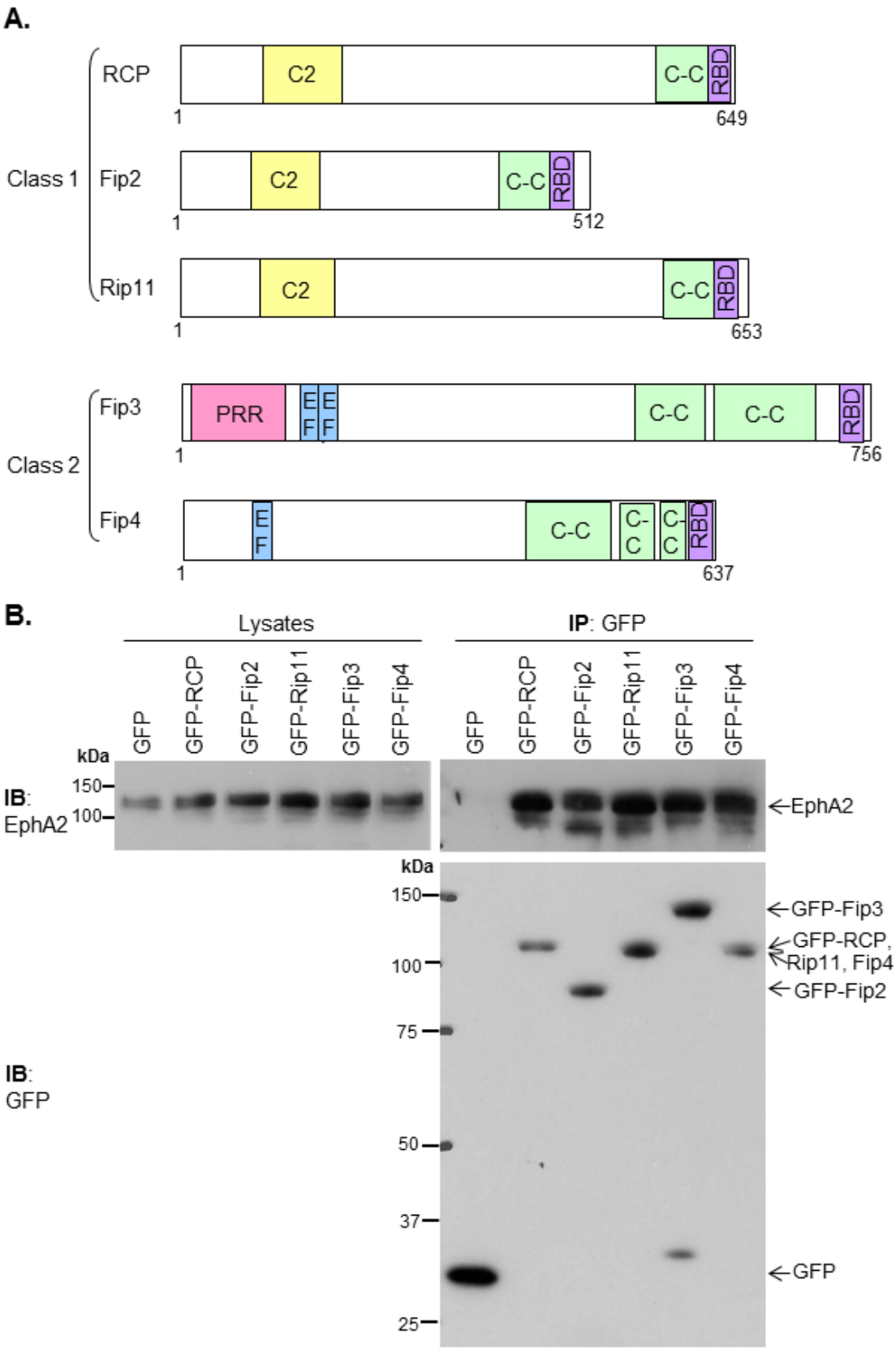

Figure 3-22 EphA2 associates with all Rab11-FIPs
A. Schematic representation of the class 1 and class 2 Rab11-Fips. B. A2780 cells were transfected with GFP, GFP-RCP, GFP-Fip2, GFP-Rip11, GFP-Fip3 or GFP-Fip4. GFP was immunoprecipitated 48 hours after transfection with an anti-GFP antibody. Immunoprecipitates were analysed by SDS-PAGE, and GFP and EphA2 were detected by immunoblotting. (C2: membrane targeting domain, CC: coiled-coiled region, RBD: Rab binding domain, PRR: Proline rich region, EF: EF hand motif).

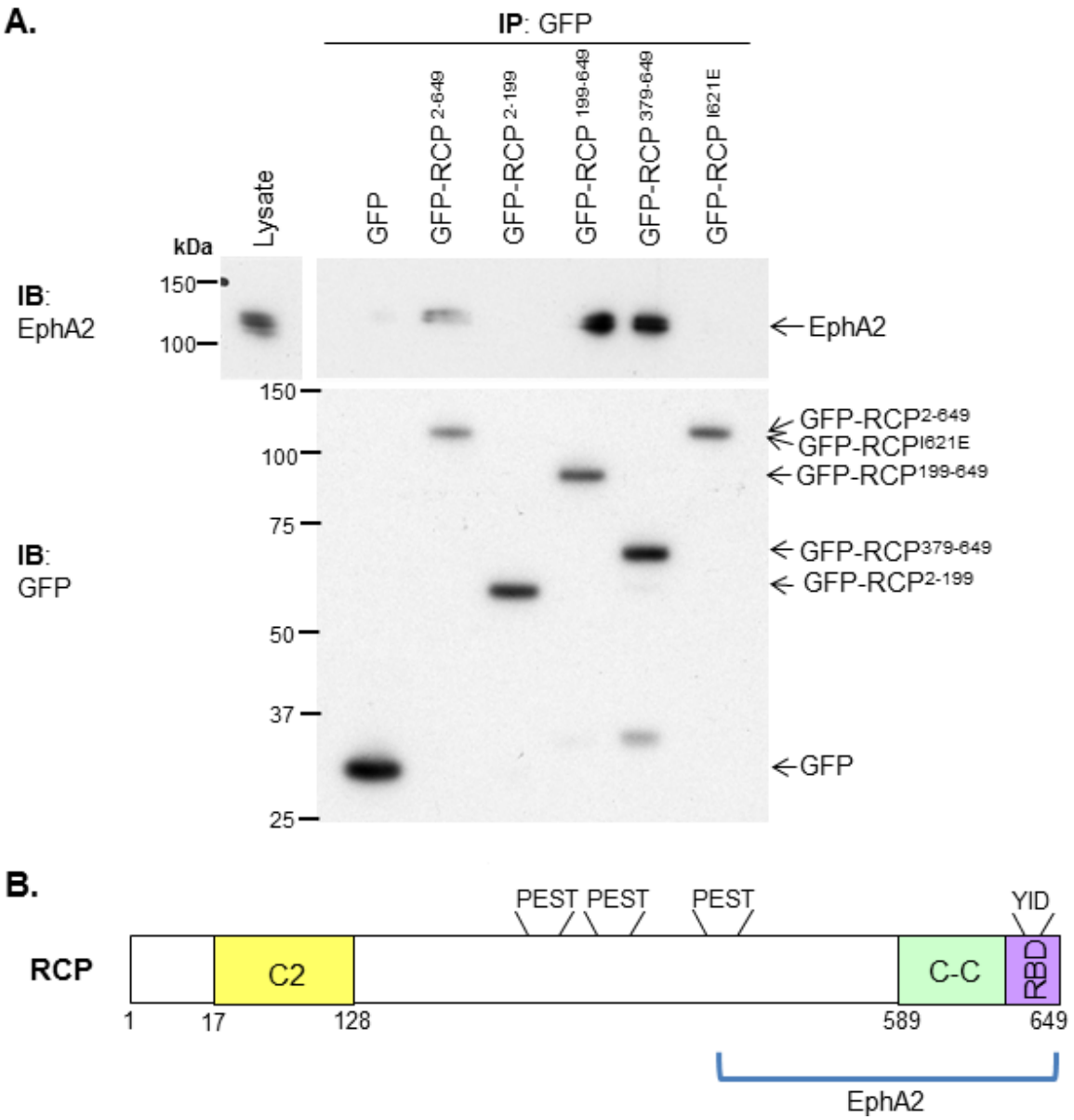

Figure 3-23 EphA2 associates with the C-terminal region of RCP
A. A2780 cells were transfected with GFP, GFP-RCP$^{2-649}$, GFP-RCP$^{2-199}$, GFP-RCP$^{199-649}$, GFP-RCP$^{379-649}$ or GFP-RCP^{I621E}. GFP was immunoprecipitated 48 hours after transfection with an anti-GFP antibody. Immunoprecipitates were analysed by SDS-PAGE, and GFP and EphA2 were detected by immunoblotting. B. Schematic representation of RCP with the location of the EphA2 association marked.

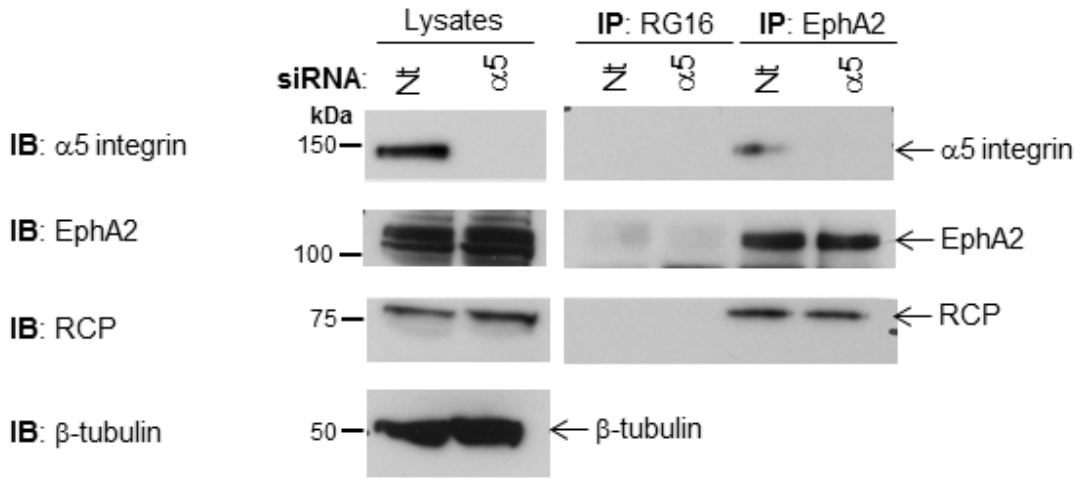

Figure 3-24 Suppression of α5-integrin levels has no effect on the association between EphA2 and RCP
A2780 cells were transfected with non-targeting (Nt) or α5-integrin-targeting siRNA. The cells were lysed 48 hours after transfection and EphA2 was immunoprecipitated from the lysates with an anti-EphA2 or an RG16 control antibody was used. The immunoprecipitates were analysed by SDS-PAGE, and EphA2, α5-integrin, β-tubulin and RCP were detected by immunoblotting.

3.2.4.8 Generation of a GFP-tagged EphA2 and validation of its functionality

A GFP-EphA2 construct was cloned to determine whether it would associate with His-RCP, and as a tool for further work on EphA2. In addition, we tested whether it was functionally active by seeing whether it responded to EphrinA1. The EphA2 gene was amplified with primers, digested with restriction enzymes and ligated into the pEGFP-N1 plasmid (**Figure 3.25A**). The plasmid was transfected into A2780 cells, the cells were lysed and EphA2, GFP and ß-tubulin were detected by immunoblotting. A band was observed at ~150kDa in the GFP and EphA2 blots, which is the predicted size of GFP-EphA2 (**Figure 3.25B**). This shows that GFP-EphA2 is well expressed by A2780 cells. Next, I sought to determine whether GFP-EphA2 is capable of associating with RCP. A2780 cells were co-transfected with His-RCP and GFP-EphA2/GFP. The cells were lysed and GFP was immunoprecipitated from the lysates. The immunoprecipitates were analysed by SDS-PAGE and Western blotting. Indeed, His-RCP was found co-immunoprecipitated with GFP-EphA2 but not GFP, thus demonstrating that GFP-EphA2 can associate with His-RCP (**Figure 3.25C**).

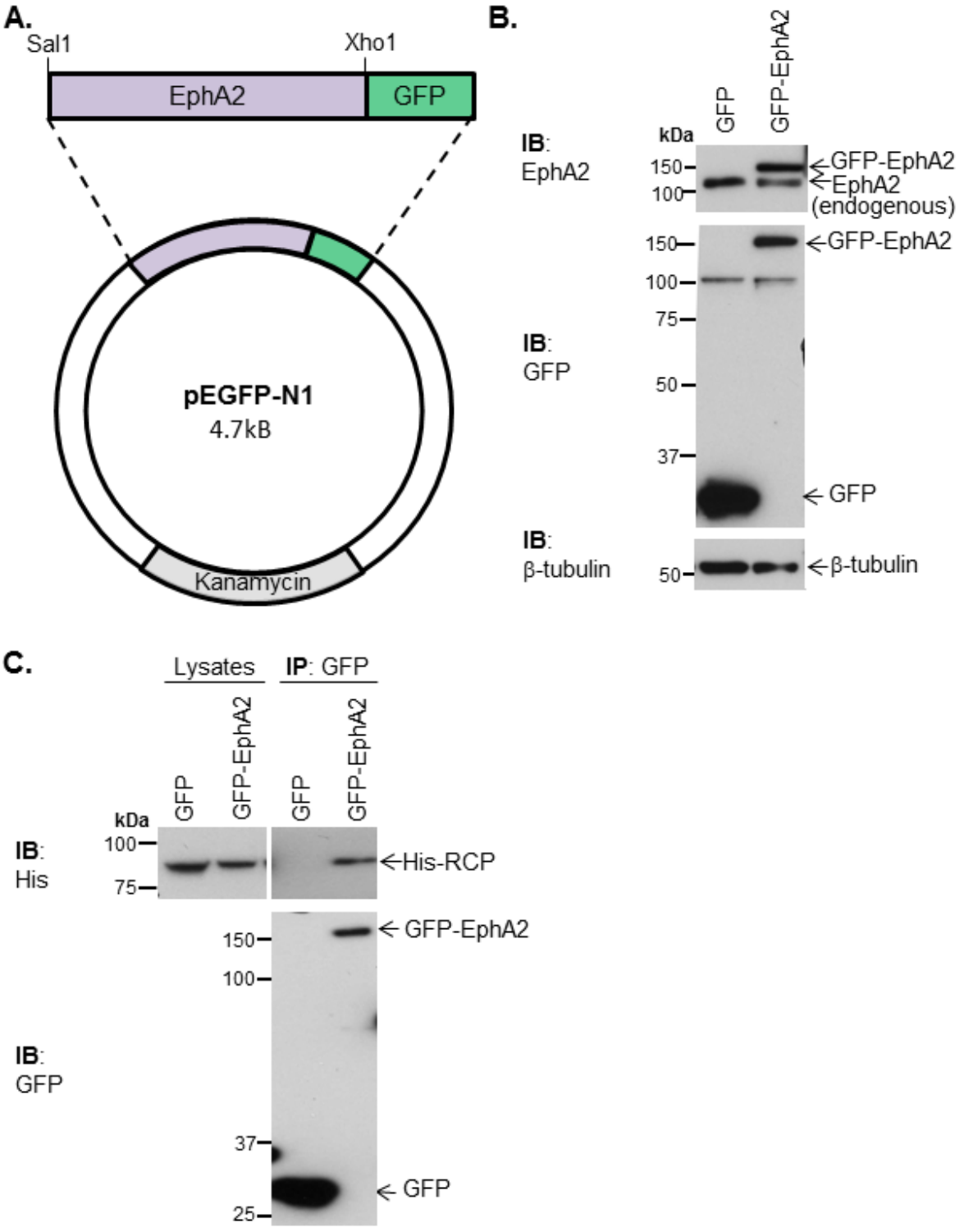

Figure 3-25 GFP-EphA2 associates with His-RCP
A. Vector map of the GFP-EphA2 construct. B. H1299 cells were transfected with GFP or GFP-EphA2. The cells were lysed 24 hours after transfection and the lysates were analysed by SDS-PAGE. EphA2, β-tubulin and GFP were detected by immunoblotting. C. A2780 cells were transfected with GFP/GFP-EphA2 and His-RCP. The cells were lysed 48 hours after transfection and GFP was immunoprecipitated using an anti-GFP antibody. The immunoprecipitates were separated by SDS-PAGE, and EphA2 and His were detected by immunoblotting.

It has previously been shown that addition of EphrinA1-soluble ligand binds to EphA2 and leads to its internalisation (Astin et al., 2010). To determine whether GFP-EphA2 is functional in this regard, EphrinA1 was added to GFP-EphA2-expressing cells and the localisation of the fluorescent reporter was visualised, whilst farnesylated-GFP expressing cells (GFP-f) were used as a control. GFP-f localises to the plasma membrane but would not be expected to bind to EphrinA1. GFP-EphA2 was localised to the plasma membrane and small positive vesicles were observed in the cells (**Figure 3.26**). The cells were then treated with EphrinA1-Fc coupled to IgG (to cluster the Eph ligands), or Fc coupled to IgG as a control. Addition of EphrinA1-Fc/IgG drove extensive internalisation of GFP-EphA2 into small cytoplasmic vesicles, whereas Fc/IgG was ineffective in this regard (**Figure 3.26**). Moreover, distribution of GFP-f was not affected by addition of clustered EphrinA1-Fc. These data indicate that the GFP-EphA2 fusion protein is functionally active, and is capable of associating with and being activated by its cognate ligand, EphrinA1.

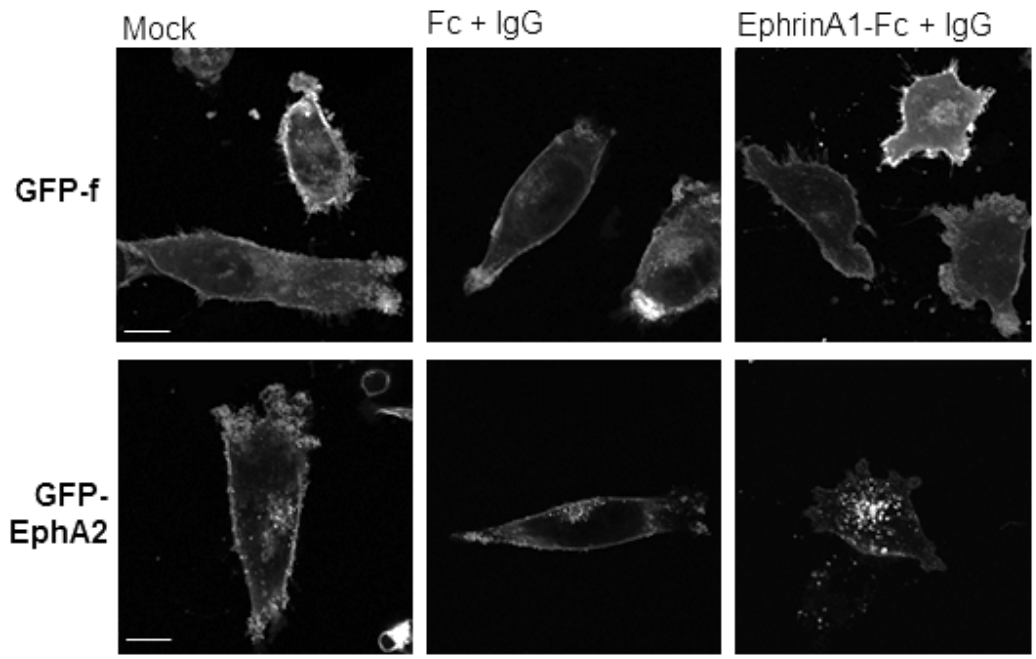

Figure 3-26 GFP-EphA2 internalises upon EphrinA1 treatment
A2780 cells were transfected with GFP-f or GFP-EphA2 and seeded onto glass coverslips. The cells were starved and then left untreated or treated with 1µg/ml EphrinA1-Fc or 1µg/ml Fc and 10µg/ml IgG for 30 minutes. The coverslips were fixed in 4% PFA and mounted onto slides. The cells were visualised by confocal microscopy and representative cells are shown with a scale bar of 10µm.

3.3 Discussion

3.3.1 RCP interactome

Although there have been several recent publications on RCP, this was the first non-biased proteomic screening approach to identify novel RCP associated proteins. Since this screen was performed, a similar screen has been performed in the Norman lab comparing the RCP interactome with and without $p53^{273H}$ expression in H1299 cells (Muller et al., 2013). Many of the same associations were found in both screens, including Rab6, Rab14 and EphA2. Rather few proteins were identified since my criteria for hits were set high and any proteins which were also found significantly associated with GFP were excluded. This suggests that the hits may not be an exhaustive list of associated proteins, especially of proteins with peptides that are notoriously hard to detect by MALDI-TOF mass spectrometry. However, many of the known RCP associated proteins were identified, which validated this approach, and many of the novel proteins identified are interesting and worth pursuing.

Several plasma membrane proteins were identified, which could be novel RCP cargo proteins. Two isoforms of integrin, α2 and αv, associated with RCP, suggesting that RCP may have a role in regulating the trafficking of other integrins as well as α5β1 (**Table 3.1**). Interestingly, two proteins were identified that are found in cell-cell adhesions: EphA2 is an RTK that has been found to have a role in cancer (Pasquale, 2010), whilst desmoglein 2 is a cadherin-type membrane protein that is a component of the desmosome (Saito et al., 2012). Less is known about the other two membrane proteins identified: Podocalyxin-like protein 1 is a transmembrane glycoprotein in the sialomucin family that is expressed in colorectal cancer (Larsson et al., 2013), and Tyrosine-protein kinase receptor Ufo is a member of the TAM RTK family (Lemke, 2013).

Many proteins with known roles in trafficking were identified as RCP-associated proteins (**Table 3.1**). Fip5 is another family member of the Rab11-Fips and was found associated with RCP. Further work would be required to determine whether different members of the Rab11-Fips can associate and function together. RCP was also found associated with two more members of the Rab-GTPase family: Rab14, which is localised in the Golgi apparatus and early

endosomes (Junutula et al., 2004), and Rab6A, which is found the trans-Golgi network and involved in retrograde transport (Martinez et al., 1994). In addition, several proteins were identified that have diverse roles in vesicular trafficking including: clathrin heavy chain, that coats and stabilises vesicles; myoferlin, a protein required for vesicle fusion (Bernatchez et al., 2009); myosin and filamin, proteins involved in transporting vesicles (DePina and Langford, 1999; Sheen, 2014); and α-actinin-4, a protein required for required for transferrin receptor recycling (Yan et al., 2005). It would be interesting to confirm that these proteins associate with RCP and are involved in the trafficking of RCP-positive vesicles.

Some proteins were found associated with RCP that have functions independent of trafficking and cell migration, such as ubiquitin, heat shock proteins, a protein involved in fatty acid dehydroxylation, and several enzymes that have various activities including peptidases and nucleotidases (**Table 3.1**). These associations may allude to novel RCP functions, but they would have to be confirmed before further investigation. Since I am interested in cancer cell migration and trafficking, this thesis contains work in which the associations between RCP and Rab14, Rab6 and EphA2 were investigated.

3.3.2 The Rab14-RCP association

Rab14 has previously been shown to regulate TfnR (Yamamoto et al., 2010) and ADAM10 trafficking, and has a role in cell migration (Linford et al., 2012), so it is an interesting hit in the proteome screen to follow up. The association between RCP and Rab14 is confirmable by co-immunoprecipitation experiments using GFP-RCP or GFP-Rab14. Furthermore, live microscopy revealed that GFP-RCP and mCherry-Rab14 co-localise in the PNRC. This work was published alongside yeast-2-hybrid and far-Western data demonstrating that Rab14 directly associates all the Class-1 Rab11-Fips, and co-localisation studies demonstrating that Rab14 and RCP are found in the same sub-cellular compartment (Kelly et al., 2010). However, a contrary study demonstrated that Rab14 associated with RCP but not Fip2 or Rip11 using the same in vitro methods, and that Rab14 associates with RCP on a site adjacent to the RBD, rather than with the RBD as I had initially hypothesised. It is unclear why these conflicting findings have been reported. Further work is required to clarify these findings. Indeed, Qi et al.

(2013) mapped the Rab14-RCP interaction and found two key residues required for this association: Serine-580 and Serine-582. Mutating these residues ($RCP^{S580N/S582L}$) prevented Rab14 but not Rab11 co-localisation with RCP (Qi et al., 2013). In my study, both RCP truncations ($RCP^{199-649}$ and $RCP^{379-649}$) that were found to be capable of associating with Rab14 contain both the RBD and Serine-580/Serine-582, thus preventing us from distinguishing the precise site of interaction. Mutating RCP's RBD abolishes association with either Rab14 or Rab11. I have also shown that RCP^{I621E} is unable to associate with EphA2 or Rab6; previous work demonstrates it is also unable to associate with EGFR or α5ß1-integrin, and is found dispersed in the cytoplasm (Caswell et al., 2008). It is likely that this mutation prevents RCP's recruitment to the membrane, so it cannot associate with any of its partners.

Linford et al. (2012) identified Rab14 as a strong hit in a non-biased scratch-assay screen in A549 cells. All Rab-GTPases were targeted with siRNA to determine which were involved in cell migration. Suppression of Rab14 expression inhibited cell migration, thus preventing the scratch wound from closing (Linford et al., 2012). The role of Rab14 in RCP-dependent trafficking and cell migration will be further studied in Chapter 4.

3.3.3 The Rab6-RCP association

I have identified Rab6 as a novel RCP-associated protein. Two Rab6 isoforms, Rab6A and Rab6B, associate with RCP; the latter directly interacts *in vitro*. Since Rab6A and Rab6A' differ by only 3 amino acids it is likely that both isoforms associate with RCP. Despite this, GFP-Rab6A and GFP-Rab6B do not co-localise with mCherry-RCP in A2780 cells. I sought to look at the localisation of endogenous Rab6 by immunofluorescence, however no signal was seen with several anti-Rab6 antibodies. Perhaps under certain conditions these proteins co-localise, for example if cells are migrating or are in a different microenvironment. Further work would be required to investigate this.

Rab6 has been shown to have a role in regulating retrograde trafficking (White et al., 1999). R6IP1 (Rab6 interacting protein 1) acts as a Rab6 effector and also associates with Rab11A, where it is proposed to regulate retrograde transport between Rab11-positive recycling endosomes and Rab6-positive Golgi apparatus.

FLIM-FRET analysis revealed that overexpression of R6IP1 promotes an interaction between Rab11a and Rab6 (Miserey-Lenkei et al., 2007). Perhaps RCP may have a similar function in promoting interactions with multiple Rab-GTPases in order to regulate trafficking between distinct membrane compartments. Rab6 and Rab11 are found to associate with distinct sites on RCP, so RCP may associate with both these GTPases to co-ordinate trafficking to precise compartments. Indeed, RCP has also been shown to have a role in retrograde transport. The trafficking of Shiga toxin from the recycling endosomes to the TGN is disrupted by the suppression of RCP or Rab11 expression (Jing et al., 2010). Jing et al. proposed that RCP binds Golgin-97, and that this association is required for both vesicle tethering and fusion between the vesicle and the TGN. Taken together, RCP, Rab6 and Rab11 have all been shown to be involved in retrograde transport. Further investigation would be required to determine if the RCP-Rab6 association is important for retrograde trafficking.

Surprisingly, suppression of Rab6A or Rab6B expression increases cell invasion in Rab25-overexpressing A2780 cells. Perhaps depletion of all Rab6 isoforms would have a bigger effect on A2780-Rab25 cell invasion. As Rab25 is found associated with RCP, one hypothesis is that inhibiting Rab6 expression could free RCP and promote its association with Rab25, thus promoting α5β1-integrin and EGFR trafficking in the tip of the pseudopod and driving cell invasion. Further work is required to test this hypothesis and to determine whether Rab6 has a role in known RCP functions.

3.3.4 The EphA2-RCP association

I have identified a novel association between EphA2 and RCP using a non-biased proteomic approach, and I have confirmed this in three different carcinoma cell lines. A previous study demonstrated that EphA2 is found in a peri-nuclear compartment (Orsulic and Kemler, 2000). Since EphA2 associates with RCP, I sought to determine whether EphA2 localises in the peri-nuclear recycling compartment. Indeed, EphA2 is co-localised with RCP in this compartment. Rab11, which associates with RCP, has previously been shown to co-localise with EphA2 upon Ephrin stimulation (Boissier et al., 2013). I found that the intracellular pool of EphA2 co-localises with Rab11 in the recycling compartment, and that Rab11 co-immunoprecipitates with EphA2. This is the

first Rab protein and effector that have been found to associate with EphA2. In order to determine whether there is a direct physical contact between EphA2, RCP and Rab11, *in vitro* protein binding assays would have to be performed. Unfortunately, EphA2 is large and has kinase activity, which prevents efficient expression in *E.coli*. Therefore it is difficult to purify, so these experiments could not be performed.

α5- and ß3-integrin associate much more efficiently with RCP than they do with Fip2 or Rip11 (Caswell et al., 2008). In contrast, EphA2 is found in a co-immunoprecipitable complex with all the Rab11-Fip family members. Perhaps this means there are some functional redundancies between the Rab11-Fips. α5-integrin associates with the C-terminal region of RCP containing the Rab binding domain and coiled-coiled domain ($RCP^{379-649}$). Interestingly, EphA2 is co-immunoprecipitable with the C-terminal, but not the N-terminal portion of RCP. Two previous studies have detected an association between α5ß1-integrin and EphA2 (Makarov et al., 2013; Prévost et al., 2005). Therefore, we hypothesised that EphA2 could be co-immunoprecipitable with RCP indirectly via α5-integrin. Indeed, endogenous α5-integrin associates with endogenous EphA2 in A2780 cells. Interestingly, RCP is still co-immunoprecipitable with EphA2 in cells depleted of α5-integrin, demonstrating that EphA2 associates with RCP independently from α5-integrin.

I have chosen to pursue the role played by RCP in the trafficking and functions of EphA2. In the following chapter I describe results indicating that RCP is involved in EphA2 trafficking, and that this influences EphA2's ability to mediate CIL and cell-cell repulsion during cell scattering.

4 The role of RCP in EphA2 trafficking and EphA2-dependent cell-cell repulsion

4.1 Introduction

4.1.1 The role of Ephs and Ephrins in contact inhibition of locomotion

Contact inhibition of locomotion (CIL) is thought to play an important role in cancer metastasis (**Section 1.1.3**). Malignant cell migration is unimpeded when cancer cells contact non-cancerous cells, demonstrating a failure to undergo heterotypic CIL (Abercrombie and Turner, 1978). Nevertheless, cancer cells undergo normal homotypic CIL with other cancer cells, perhaps facilitating local cancer cell dispersion (Paddock and Dunn, 1986). It has been known for some time that Ephs and Ephrins have an important role in regulating CIL during development (Krull et al., 1997; Smith et al., 1997). More recently, a study using a prostate cancer cell line (PC3 cells) was the first to identify a role for Ephs and Ephrins in CIL in cancer (Astin et al., 2010). EphAs (EphA2 and EphA4), and not EphBs, are required for CIL between PC3 cells (Astin et al., 2010). Indeed, PC3 cells undergo normal homotypic CIL, and this is opposed by knocking down all the EphAs expressed (EphA2 and EphA4), suggesting that the type-A receptors are required for CIL with neighbouring cancer cells (Astin et al., 2010).

Ephs activate downstream Rho GTPases, which are also required for contact inhibition. In PC3 cells, EphA2/EphA4 activation via interaction with EphrinAs increases RhoA activity during homotypic collisions, while association of EphrinB2 with EphB3/EphB4 increases Cdc42 activity (Astin et al., 2010). In these cells EphA signals to RhoA via Vav2, which acts as a Rho GEF and is required for efficient CIL (Batson et al., 2014). Inhibition of Rho-ROCK signalling stabilises microtubules at the contact site and prevents formation of new lamellipodia, inhibiting CIL (Kadir et al., 2011). In glioma cells (U87MG), expression of EphrinB1 disrupts heterotypic CIL with glial cells via a mechanism involving the regulation of Tiam1, which contributes to the activation of Rac1 (Tanaka et al., 2012). Tanaka et al. propose that the disruption of heterotypic CIL promotes invasion of glioblastoma in the brain of nude mice.

4.1.2 EphA2 and RCP in cell scattering

Hepatocyte growth factor (HGF), also known as scatter factor, stimulates scattering of cell colonies via activation of its receptor cMet and downstream signalling to Akt, MAPK and FAK (Nakamura et al., 2011). Misregulation of HGF-cMet signalling is common in cancer via upregulation of components in the pathway or activating mutations in cMet, so many drugs have been designed to target this pathway (Graveel et al., 2013). Considering EphA2's role in CIL, I hypothesised that this RTK may be required for HGF-induced scattering. EphAs have been reported to have a role in several HGF-dependent functions. For example, HGF drives mammary branching morphogenesis *in vivo* and in Matrigel, and this is prevented in mammary epithelial cells derived from EphA2$^{-/-}$ mice (Vaught et al., 2009). Furthermore, addition of soluble EphrinA1 to MDCK cells antagonises HGF-induced epithelial branching morphogenesis and prevents HGF-induced scattering of MDCK1 cells. To date no studies have investigated the role of EphA2 is HGF-driven cancer cell scattering.

RCP has been shown to be required in cell scattering. Mutant-p53 drives scattering in H1299 cells and this is opposed by RCP knockdown (Muller et al., 2013). Mutant-p53 increases invasion towards an HGF gradient in an RCP and cMet dependent fashion by enhancing RCP dependent cMet signalling and trafficking. Indeed, cMet is found in a co-immunoprecipitable complex with RCP (Muller et al., 2013). The role of RCP in HGF-induced scattering has not been examined, nor has the role of EphA2 in mutant-p53 or HGF induced scattering in cancer cells.

4.1.3 Pancreatic mouse models

Pancreatic cancer is an aggressive malignancy that is normally diagnosed in its later stages. Unfortunately, only ~5% of patients survive for more than 5 years after diagnosis. Pancreatic ductal adenocarcinoma (PDAC) accounts for over 85% of human pancreatic cancer cases (Warshaw and Fernández-del Castillo, 1992). The exact progenitor cell of PDAC is unidentified but it has been postulated to be a ductal epithelial cell (Stanger and Dor, 2006). Pancreatic intraepithelial neoplasms (PanINs) are microscopic lesions that contain columnar cells and are thought to be the main precursors to PDAC. Examination of human PanINs shows

that *KRAS* mutations, *p16INK4* loss and *TP53* mutations and loss are commonly found (Hruban et al., 2000).

There has been substantial effort to genetically manipulate mice to generate pancreatic cancer models for studying disease and for testing potential treatments. Since mice that express constitutively active Kras ($Kras^{G12D}$, a common mutation found in human invasive PDACs) succumb to lung cancer before PanINs develop (Johnson et al., 2001), conditional organ-specific models have been generated. In one such model, the mice have one allele of mutant Kras (G12D) and one allele of mutant-p53 (R172H), a common combination of mutations found in the human disease (Hruban et al., 2000). This model uses Cre-Lox technology in which the mutant proteins are only expressed upon the recombination of two lox sites that removes a stop codon located in between the gene and promoter. Recombination of the lox sites occurs in the presence of Cre-recombinase. Expression of Cre-recombinase is regulated by the pancreas-specific promoter, Pdx1, so $Kras^{G12D}$ and $p53R^{172H}$ are specifically expressed in the pancreas. In this model PanINs are found, which progress to metastatic PDAC. The burden of the disease is observed in the animals within 10 weeks (Hingorani et al., 2005). The pathology of PDACs from these mice and the site of metastases recapitulate the human disease.

4.1.4 The role of EphA2 in pancreatic cancer

A large scale clinical study was recently performed to characterise the genetic changes in tumours from patients with PDAC (Biankin et al., 2012). Most interestingly, frequent and diverse somatic mutations were identified in genes involved in axon guidance and development, including genes involved in Slit, Semaphorin and Eph signalling (Biankin et al., 2012). It has previously been shown that EphA2 is expressed in 95% of human pancreatic cancers, and is highly expressed in lymph node metastases but less so in liver metastases, demonstrating some metastatic organ specificity (Mudali et al., 2006). Indeed, high EphA2 expression is associated with poor patient outcome (Van den Broeck et al., 2012). Furthermore, reducing EphA2 levels in pancreatic cancer cells decreases cell invasion *in vitro* and reduces tumour growth and metastasis in nude mice implanted subcutaneously with pancreatic cells (Duxbury et al., 2004). Recent work shows that EphA4 is expressed in pancreatic cancer cell

lines, and suppression of its expression also reduces cell motility and invasion via upregulating E-cadherin expression and downregulation of MMP2 activity (Liu et al., 2014). In summary, EphA2 is highly expressed in aggressive human pancreatic cancer and has been shown to have a role in cancer cell invasion *in vitro.*

4.1.5 Aims

In this chapter I aim to identify whether RCP has a role in EphA2 function in the implementation of processes such as CIL and cell-cell repulsion. As RCP is a known regulator of RTK recycling, the role of RCP in EphA2 trafficking will be investigated. Since several Rab GTPases were identified as RCP associated proteins, I will test whether these are required for CIL, cell-cell repulsion and EphA2 trafficking. To determine whether EphA2 and RCP are important for cell migration and metastasis *in vivo*, EphA2$^{-/-}$ and RCP$^{fl/fl}$ mice will be crossed into the KPC (Kras^{G12D}, p53R^{172H} and Cre1-Pdx1) model of PDAC. Also, the *in vitro* invasiveness of cells derived from tumours removed from these animals will be investigated to determine the degree of cell autonomy in EphA2's control of cell-cell repulsion and invasion.

4.2 Results

4.2.1 RCP, but not Fip2, Fip3 or α5-integrin, is required for efficient contact inhibition of locomotion

The two EphA receptors, EphA2 and EphA4, are required for efficient homotypic contact inhibition of locomotion (CIL) in PC3 cells (Astin et al., 2010). As EphA2 associates with RCP, I wanted to determine whether RCP is important for contact inhibition phenomena in the assay established by Astin et al. (2010) to quantify CIL in PC3 cells. These cells were seeded sparsely onto 6 well Matrigel-coated glass-bottomed plates, serum starved for 24 hours, and treated with HGF to activate cell migration. Cell movement was recorded using time-lapse microscopy over a period of 24 hours. Under these conditions, PC3 cells migrated

on Matrigel and numerous examples of CIL could be observed when the migrating cells collided with one another. A typical example of PC3 cells undergoing CIL is shown in **Figure 4.1B**. Two PC3 cells migrated towards one another (green arrows). At the point of cell-cell contact (0 min) the cells stopped migrating for several minutes. Following this, the two cells migrated away from each other in a direction that was different from the one in which they approached one another (red arrow). Quantification of a large number of collisions indicate that the average cell-cell contact time during the collision was ~39 minutes (+/-5 min) (**Figure 4.2B**), and the average vectoral difference between the direction of cell migration before and after the collision was 91º (+/- 6º) (**Figure 4.1C**).

Since I have shown that EphA2 associates with all the Rab11-Fip family members, I wanted to determine whether suppression of RCP and other Rab11-Fips influences CIL in PC3 cells. PC3 cells expressed RCP, Fip2 and Fip3 at levels that were detectable by Western blotting and these could be selectively reduced by siRNA (**Figure 4.2A, 4.3A**). siRNA of RCP or Fip3 had no effect on migration speed of non-colliding cells, whilst Fip2 knockdown significantly reduced the speed of cell migration (**Figure 4.2C, 4.3E**). Interestingly, knockdown of RCP (using either a SMARTpool or 2 individual oligo sequences) significantly increased the time that colliding cells remained in contact prior to migrating away from one another (**Figure 4.2B, 4.3D**), whilst siRNA of Fip2 or Fip3 were ineffective in this regard (**Figure 4.3D**). Moreover, siRNA of RCP increased the difference between the direction of cell migration before and after the collision (**Figure 4.3B/C**) indicating the decreased tendency of RCP knockdown cells to change direction following collisions.

Given the role that RCP plays in α5β1-integrin trafficking, I sought to determine whether this integrin contributes to CIL. However, knockdown of α5-integrin did not increase the cell-cell contact time during collisions (**Figure 4.4**), demonstrating that this integrin does not influence contact inhibition nor the reacquisition of cell migration following collisions.

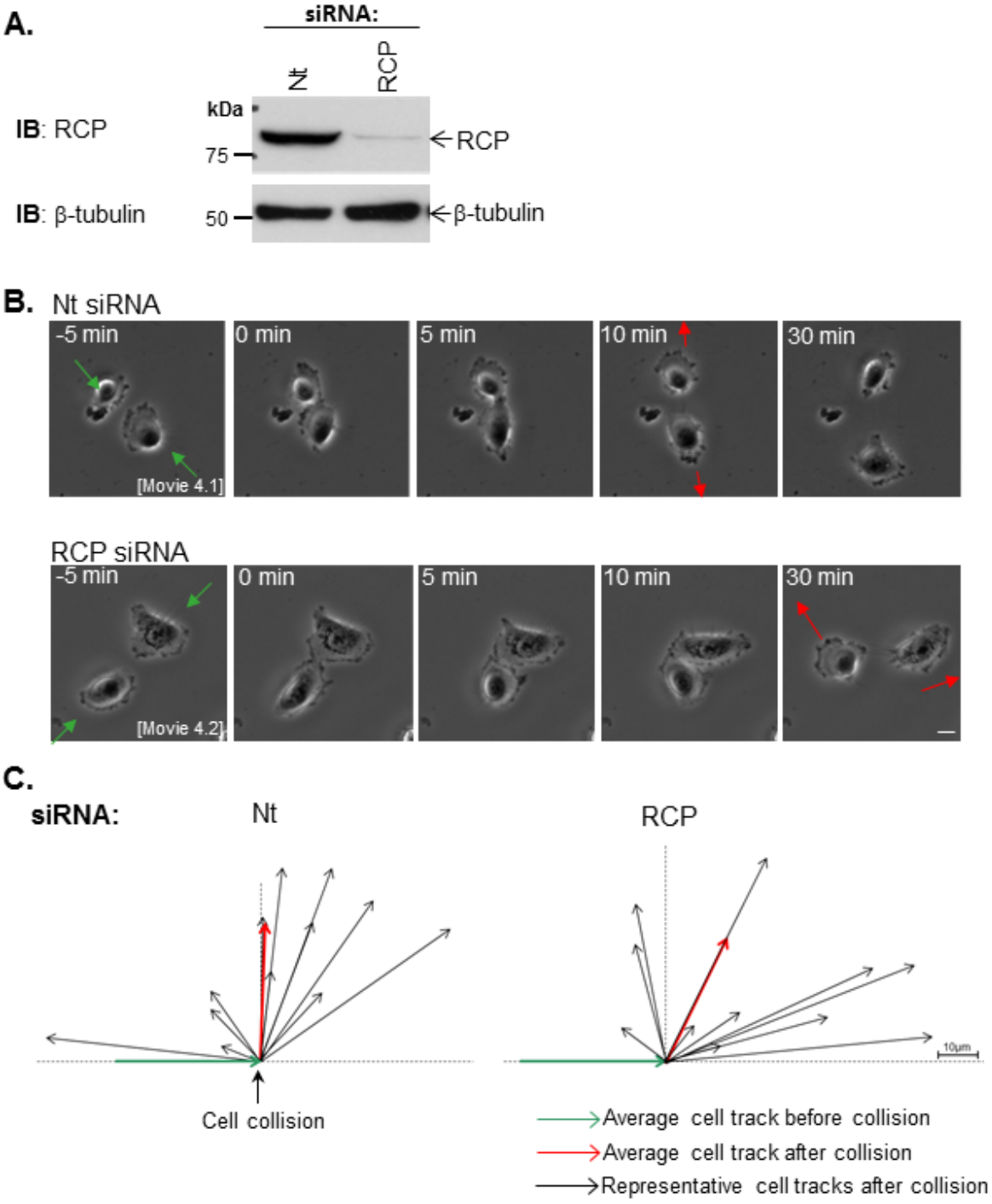

Figure 4-1 Suppression of RCP expression prevents efficient contact inhibition of locomotion

A. PC3 cells were transfected with a SMARTpool of siRNA targeting RCP or non-targeting siRNA. Proteins were extracted 72 hours after transfection. RCP and β-tubulin were detected by Western blotting. B. Transfected cells were sparsely seeded onto Matrigel-coated glass plates. The cells were serum-starved for 24 hours and then treated with 10ng/ml HGF for 12-14 hours. Time-lapse microscopy was used to record cell migration. Representative collisions are shown. The scale bar is 10μm. C. Lines represent the vectorial tracks of cell migration 40 minutes before and after cell-cell collisions. The green line is the average distance travelled before the cells collide, the black lines are representative tracks of the distance and angle of cell migration after the collision and the red line shows the average distance and angle of cell migration after the collision. Over 50 collisions were tracked per condition.

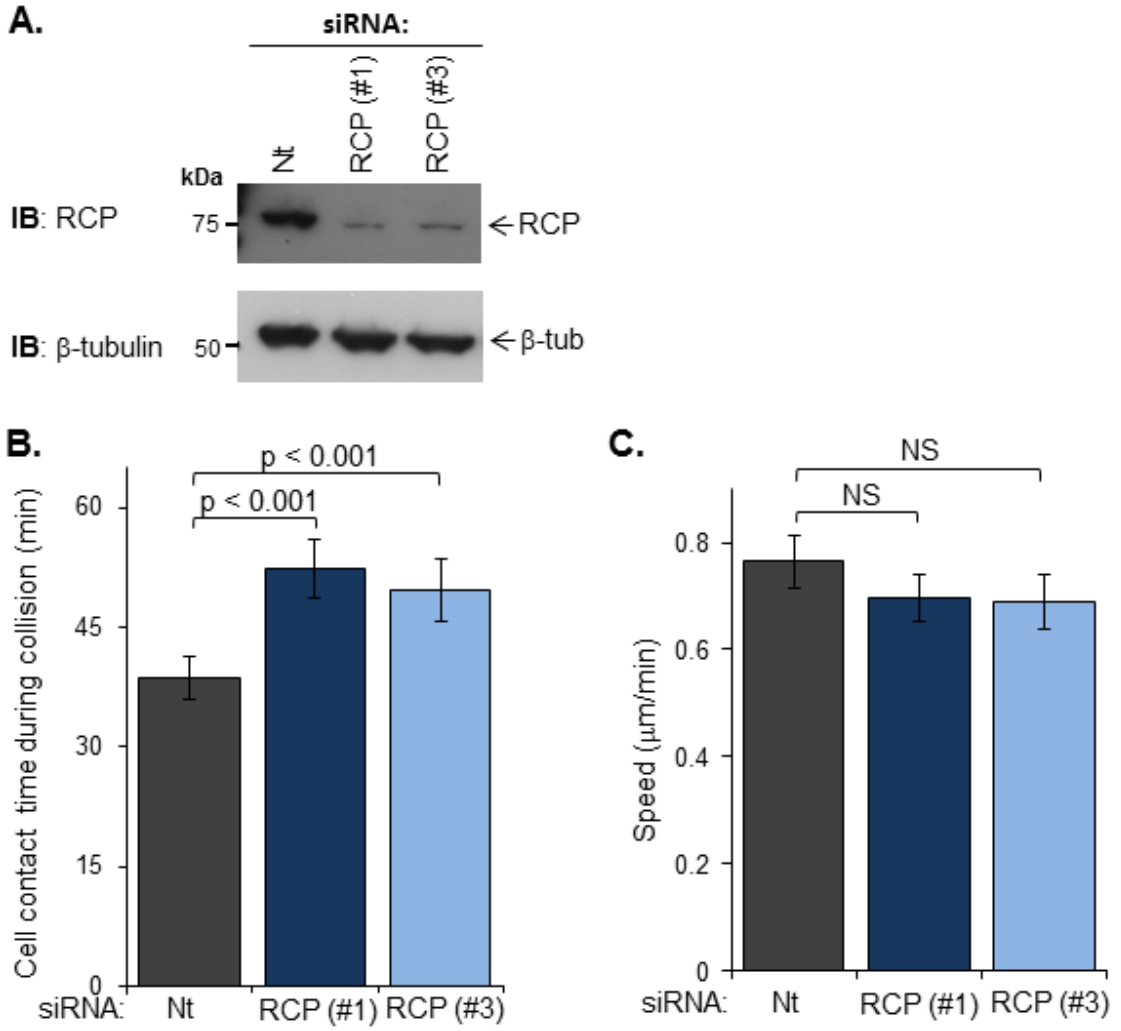

Figure 4-2 Suppression of RCP, with two different targeted siRNAs, prevents efficient contact inhibition of locomotion

A. PC3 cells were transfected with two different siRNA oligos targeting RCP or non-targeting siRNA. Proteins were extracted 72 hours after transfection. RCP and β-tubulin were detected by Western blotting. B/C. Transfected cells were sparsely seeded onto Matrigel-coated glass plates. The cells were serum starved for 24 hours and then treated with 10ng/ml HGF for 12-14 hours. Time-lapse microscopy was used to record cell migration. Time of contact during the collision (B) and speed of cell migration (C) are represented graphically. Over 50 collisions were tracked per condition in 3 separate experiments. Mann-Whitney statistical tests were performed and p-values are shown.

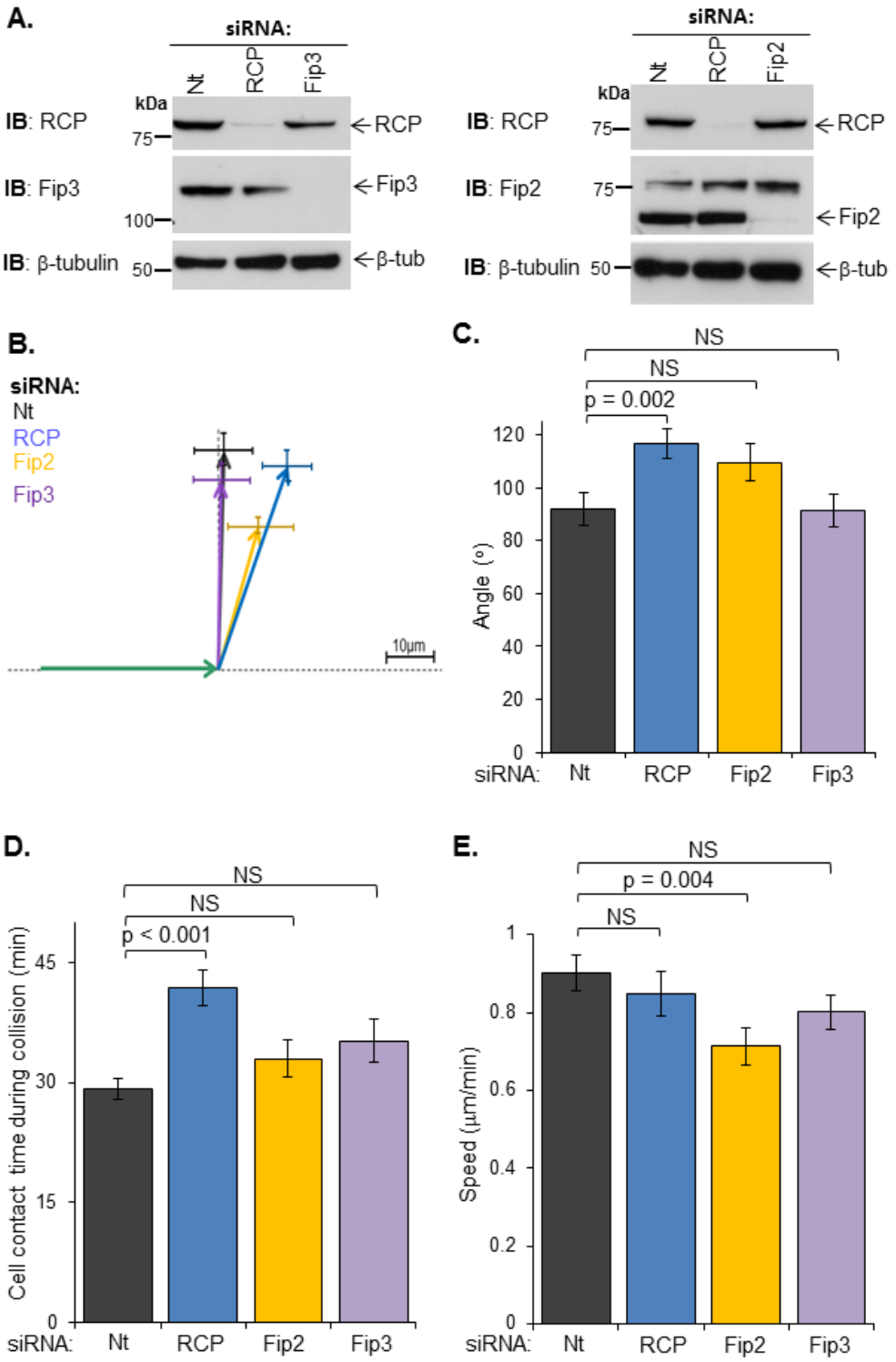

Figure 4-3 Fip2 and Fip3 are not required for efficient contact inhibition of locomotion
A. PC3 cells were transfected with a SMARTpool of siRNA targeting RCP, Fip2 or Fip3, or a non-targeting siRNA. Proteins were extracted 72 hours after transfection. RCP, Fip2, Fip3 and β-tubulin were detected by Western blotting. B-E. Transfected cells were sparsely seeded onto Matrigel coated glass plates. The cells were serum starved for 24 hours and treated with 10ng/ml HGF for 12-14 hours. Time-lapse microscopy was used to record cell migration. B. Average vectorial tracks of cell migration 40 minutes before and after cell-cell collisions. The green line is the average distance travelled before the cells collide, the black (Nt), blue (RCP), yellow (Fip2) and purple (Fip3) lines show the average distance and angle of cell migration after the collision. The angle of migration after the collision (C), time of cell-cell contact during the collision (D) and speed of cell migration (E) are represented graphically. Over 50 collisions were tracked per condition in 3 separate experiments. Mann-Whitney statistical tests were performed and p-values are shown.

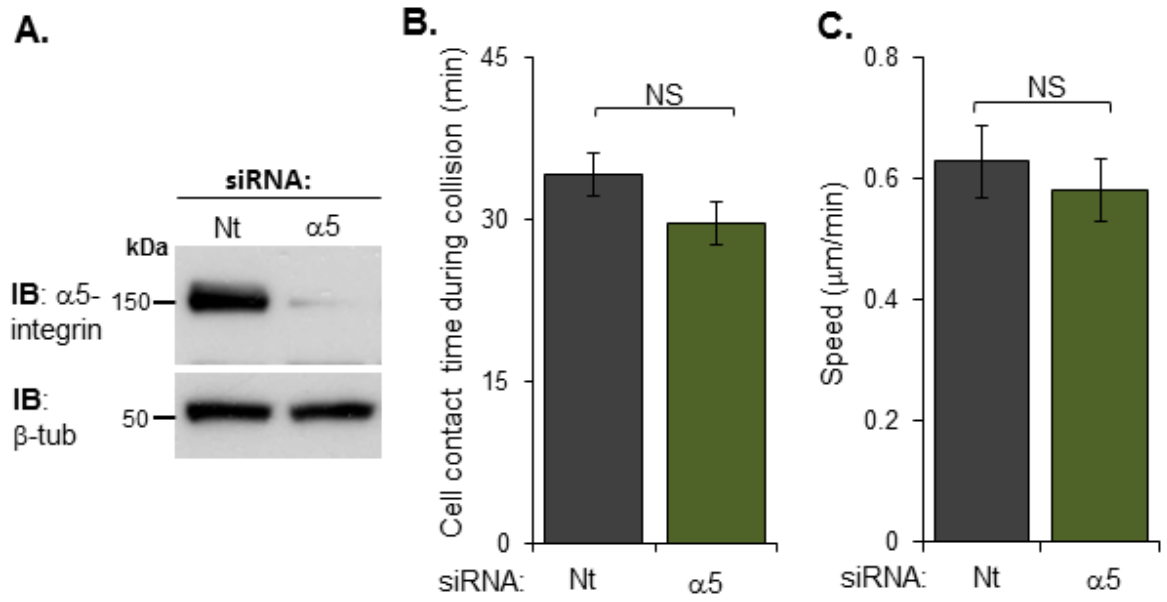

Figure 4-4 α5-integrin is not required for efficient contact inhibition of locomotion
A. PC3 cells were transfected with α5-integrin-targeting or non-targeting siRNA. Proteins were extracted 72 hours after transfection. α5-integrin and β-tubulin were detected by Western blotting. B-C. Transfected cells were sparsely seeded onto Matrigel-coated glass plates. The cells were serum starved for 24 hours and then treated with 10ng/ml HGF for 12-14 hours. Time-lapse microscopy was used to record cell migration. Time of contact during the cell-cell collision (B) and the speed of cell migration (C) are represented graphically. Over 50 collisions were tracked per condition in 3 separate experiments. Mann-Whitney statistical tests were performed and p-values are shown.

4.2.2 EphA2 and RCP are required for HGF induced cell scattering

As cell-cell repulsion is likely to contribute to cancer cell dissemination, I tested the requirement for EphA2 and RCP in cell scattering. H1299 cells were used for this as they grow in tight colonies that scatter in response to HGF (**Figure 4.5**). Unlike PC3 cells, EphA2 is the only EphA expressed by H1299 cells (**Table 3.2**). Addition of HGF drove a rapid increase in scattering of H1299 cells, as determined by scoring the number of cells that contacted 2 or fewer cells (scattered cells) as a proportion of the total number of cells (**Figure 4.6B**). Scattering was scored for untreated and HGF-treated cells (**Figure 4.7B/4.8B/4.9B**) and HGF-induced scattering was analysed by quantifying the difference between the scattering of HGF and untreated cells and normalising to the control (Nt siRNA treated cells) (**Figure 4.7C/4.8C/4.9C**). These different quantification methods focus on HGF-independent or –depedent events. Both methods are shown as focus on HGF-dependent phenotypes alone may mask phenotypic differences from knockdown alone. The ability of HGF to promote scattering was partially (but significantly) opposed by siRNA of RCP (**Figure**

4.6D, 4.8) and ablated by knockdown of EphA2 (**Figure 4.6C, 4.7**) using either an siRNA SMARTpool or 2 different siRNA oligos to target either protein. Conversely siRNA of Fip2 or Fip3 was ineffective in this regard (**Figure 4.9**).

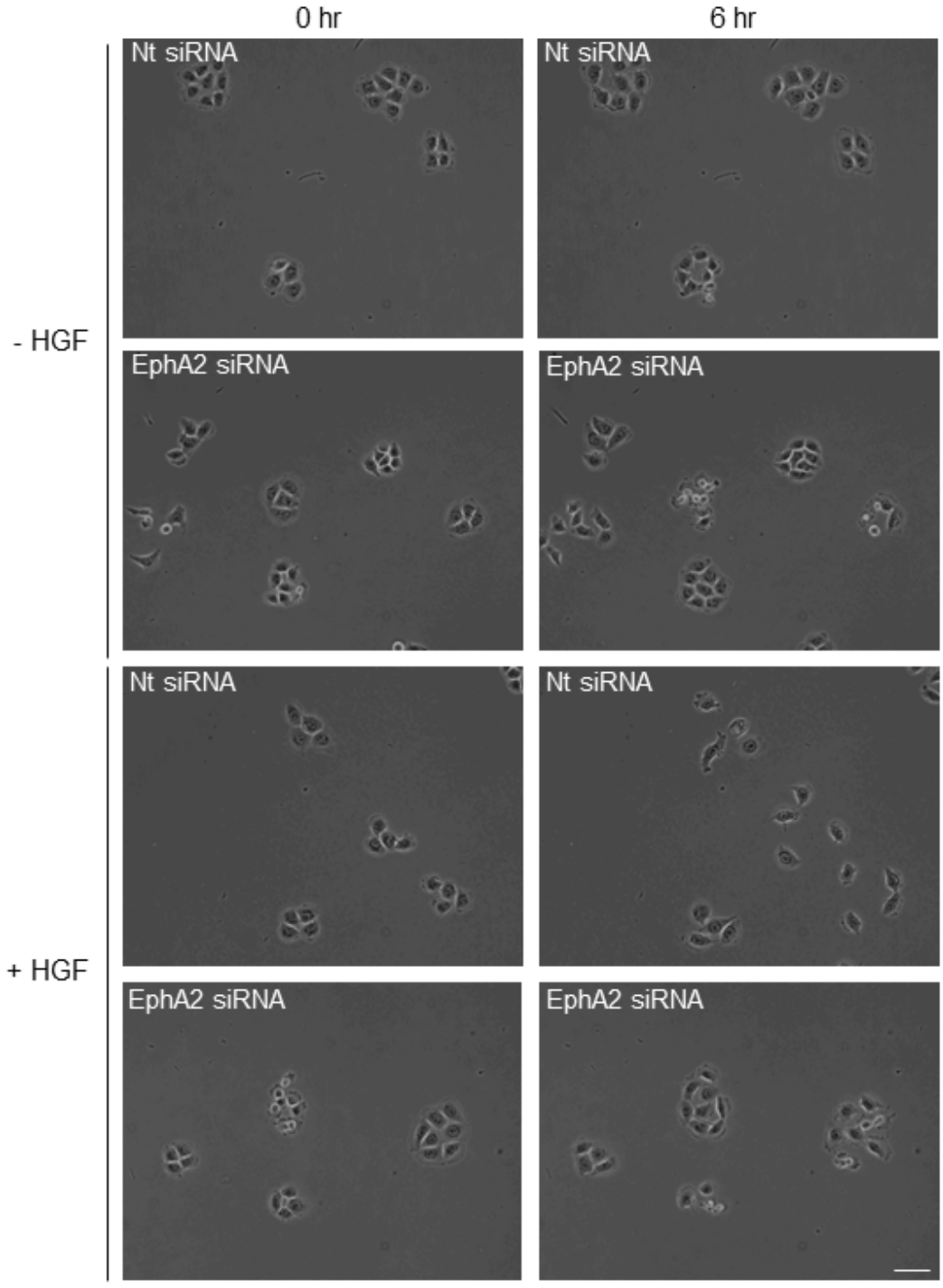

Figure 4-5 Suppression of EphA2 expression prevents HGF-induced cell scatter
H1299 cells were transfected with EphA2- or non-targeting siRNA and seeded sparsely. 10ng/ml HGF was added to the appropriate wells 48 hours after transfection. Representative pictures were taken at 0 and 6 hours.

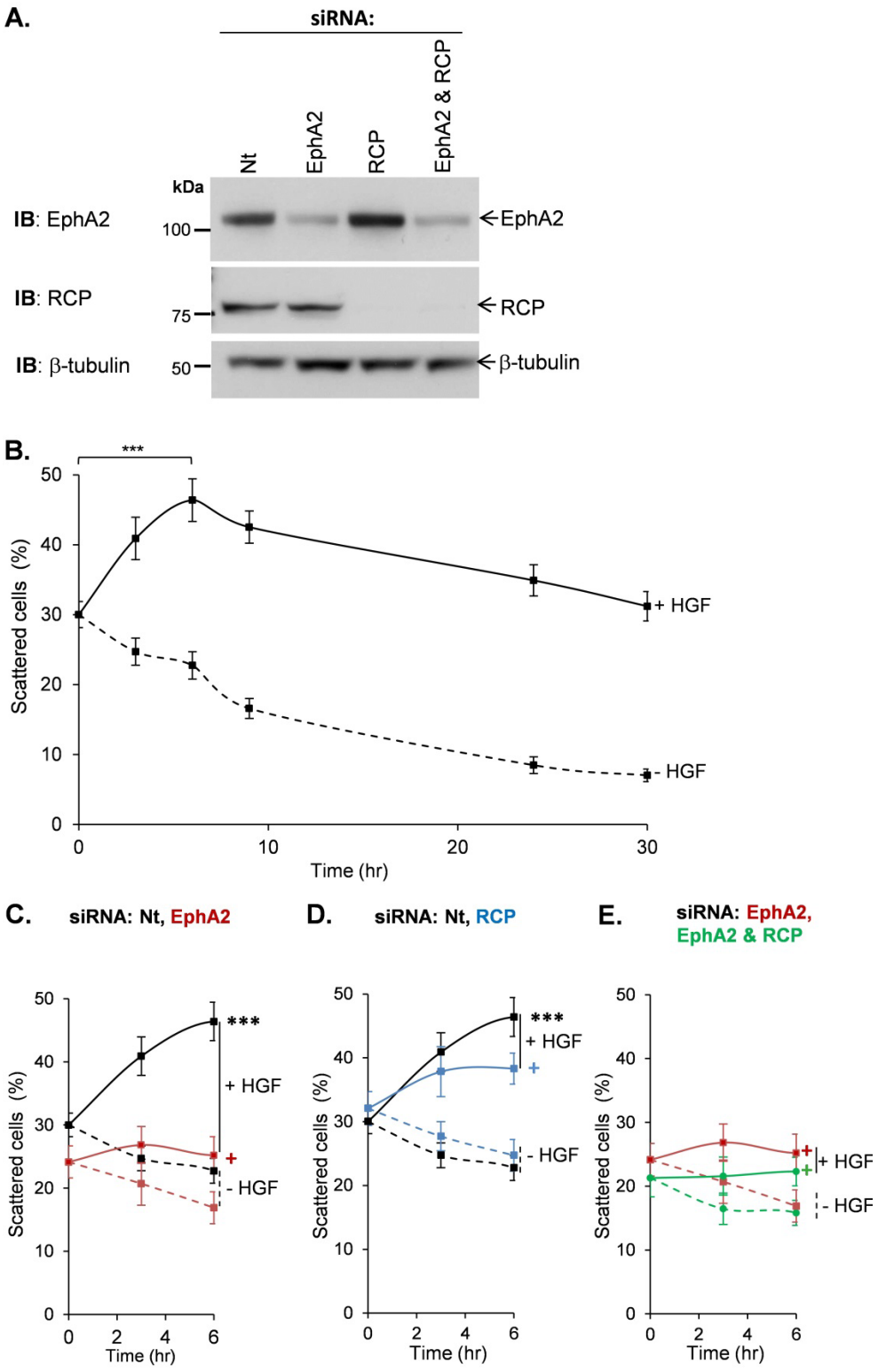

Figure 4-6 HGF-induced cell scatter is reduced by depletion of EphA2 or RCP expression
A. H1299 cells were transfected with non-targeting, EphA2- (oligo #4), RCP- (SMARTpool) or EphA2- & RCP-targeting siRNA and seeded sparsely. Proteins were extracted 48 hours after transfection. EphA2, RCP and β-tubulin were detected by Western blotting. B-E. 43 hours after transfection, 10ng/ml HGF/mock was added to the cells and at the appropriate times representative pictures of the cells were taken. The cells in each picture were counted as either 'scattered' (cells attached to less than 2 other cells) or 'in colonies' (cells attached to 3 or more other cells). The average percentage of scattered cells is plotted at each time point for cells transfected with non-targeting control (B) and for the first 6 hours for cell transfected with EphA2 (C), RCP (D) or EphA2 & RCP (E) siRNA. 20 pictures from 4 separate experiments were analysed. Statistical analysis was performed using a Mann-Whitney test comparing the scattering from the 0 and 6 hour time point (***:p <0.001, +:not significant)

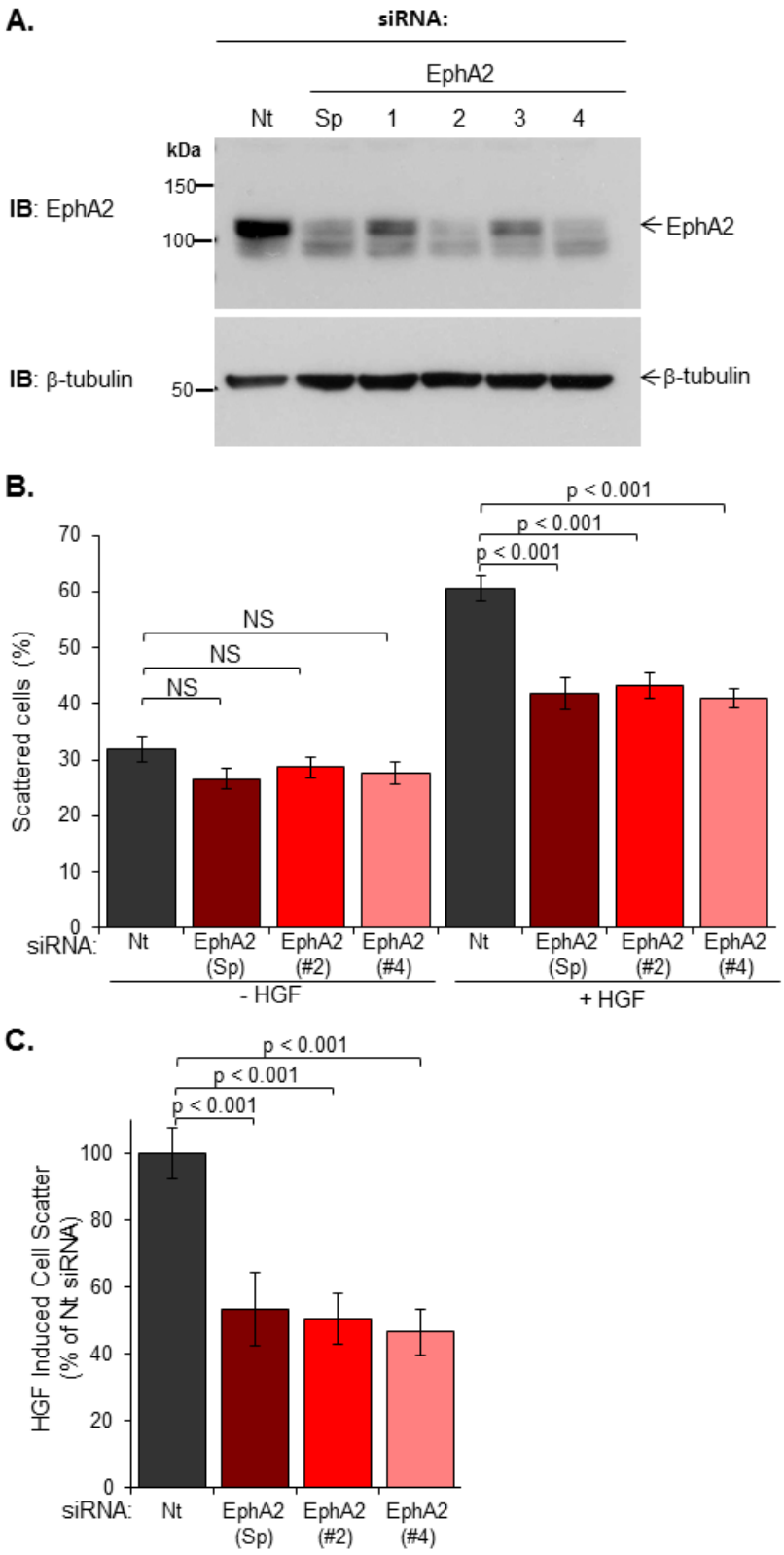

Figure 4-7 Suppression of EphA2 expression levels prevents HGF-induced cell scatter
A. H1299 cells were transfected with non-targeting siRNA, two different single siRNAs or a SMARTpool targeting EphA2, and seeded sparsely. Proteins were extracted 48 hours after transfection. EphA2 and β-tubulin were detected by Western blotting. B/C. 10ng/ml HGF/mock was added to each well 43 hours after transfection. After 6 hours of HGF treatment, representative pictures were taken from each condition. B. The percentage of scattered cells is plotted. C. HGF-induced cell scatter was calculated by subtracting the untreated value from the HGF treated value for each condition, and normalising to the non-targeting control. 15 pictures from 3 separate experiments were analysed. Statistical analysis was performed using a Mann-Whitney test and p values are shown.

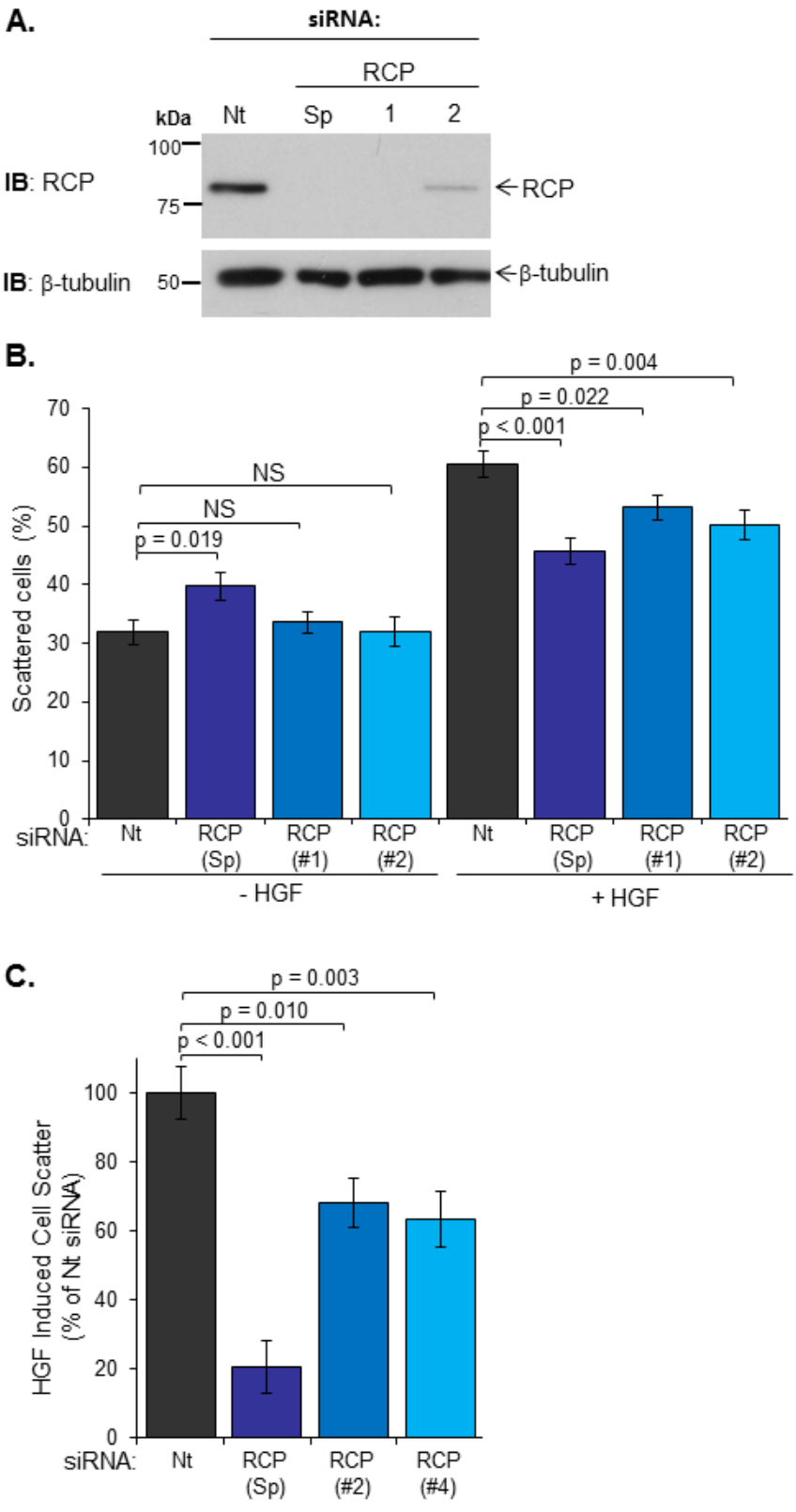

Figure 4-8 Suppression of RCP expression levels prevents HGF-induced cell scatter
A. H1299 cells were transfected with non-targeting siRNA, two different single siRNAs or a SMARTpool targeting RCP, and seeded sparsely. Proteins were extracted 48 hours after transfection. RCP and β-tubulin were detected by Western blotting. B/C. 10ng/ml HGF/mock was added to each well 43 hours after transfection. After 6 hours of HGF treatment, representative pictures were taken from each condition. B. The average percentage of scattered cells is plotted. C. HGF-induced cell scatter was calculated by subtracting the untreated value from the HGF treated value for each condition, and normalising to the non-targeting control. 15 pictures from 3 separate experiments were analysed. Statistical analysis was performed using a Mann-Whitney test and p-values are shown.

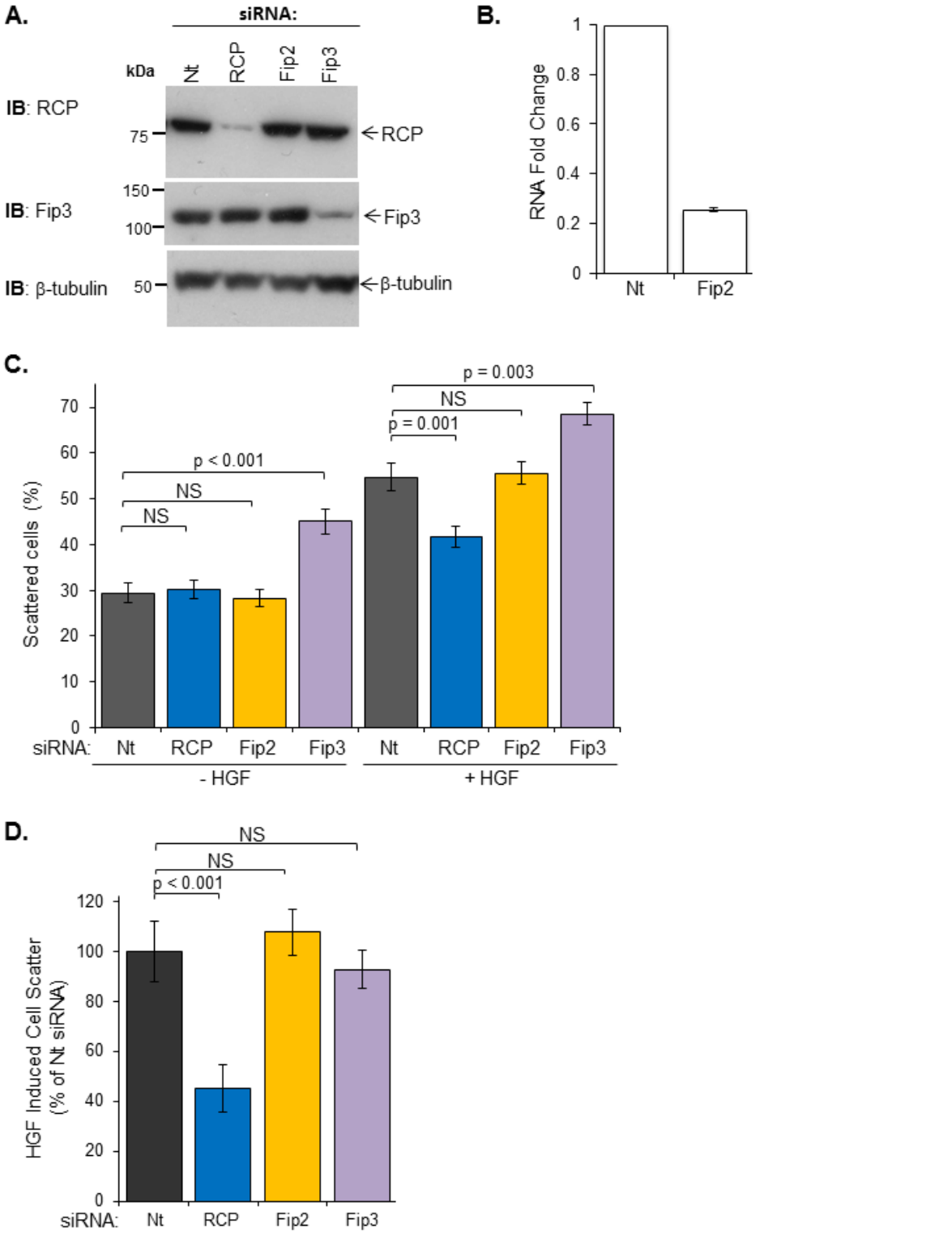

Figure 4-9 Suppression of Fip2 and Fip3 expression levels has no effect on HGF-induced cell scatter

H1299 cells were transfected with RCP (SMARTpool), Fip2 (SMARTpool), Fip3 (SMARTpool) or non-targeting siRNA and seeded sparsely. Proteins and mRNA were extracted 48 hours after transfection. A. RCP, Fip3 and β-tubulin were detected by Western blotting. B. mRNA was copied into cDNA. Quantitative-PCR was performed with Fip2 and GAPDH primers. The fold change of Fip2 cDNA was normalised to GAPDH, and is represented graphically. B/C. 10ng/ml HGF/mock was added to each well 43 hours after transfection. After 6 hours of HGF treatment, representative pictures were taken. B. The percentage of scattered cells is plotted. C. HGF-induced cell scatter was calculated by subtracting the untreated value from the HGF treated value for each condition, and normalising to the non-targeting control. 15 pictures from 3 separate experiments were analysed. Statistical analysis was performed using a Mann-Whitney test and p-values are shown.

The approach used to quantify scattering (described in the previous paragraph) suffers from the drawback that it does not discriminate between RCP or EphA2 contributing to dissemination of cell colonies, and these proteins affecting re-formation of colonies following a successful scatter reaction. Therefore, I performed time-lapse microscopy to obtain a detailed picture of the influence of RCP and EphA2 on colony dissemination. H1299 cells were allowed to form into groups of ~4/8 cells per colony. They were treated with HGF and the resulting scattering of the colonies was followed by time-lapse microscopy and cell tracking. Examination of the movies displayed in **Figure 4.10** and the track-plots derived from movies such as these **(Figure 4.11A)** indicated that HGF drove rapid scattering of cells from their colonies, and that cells moved up to 100µm from their start point within 6 hours of HGF addition.

Suppression of cellular levels of either EphA2 or RCP (each with two siRNA sequences) strongly suppressed the ability of HGF to stimulate cell scattering as measured by this time-lapse/cell tracking approach **(Figures 4.10-4.13)**. Indeed, following knockdown of EphA2 or RCP, cells were able to respond to HGF by ruffling and extending flat lamellae, but were incapable of losing contact with their neighbours to move away from their start positions **(Figures 4.10, 4.12)**. Furthermore, and consistent with the 'colony scoring' approach previously described, siRNA of Fip2 or α5-integrin did not suppress HGF-driven scattering in H1299 cells **(Figure 4.14)**. Taken together these data support a role for EphA2 in cell-cell repulsion and scattering, and indicate that RCP may be required for EphA2 functions.

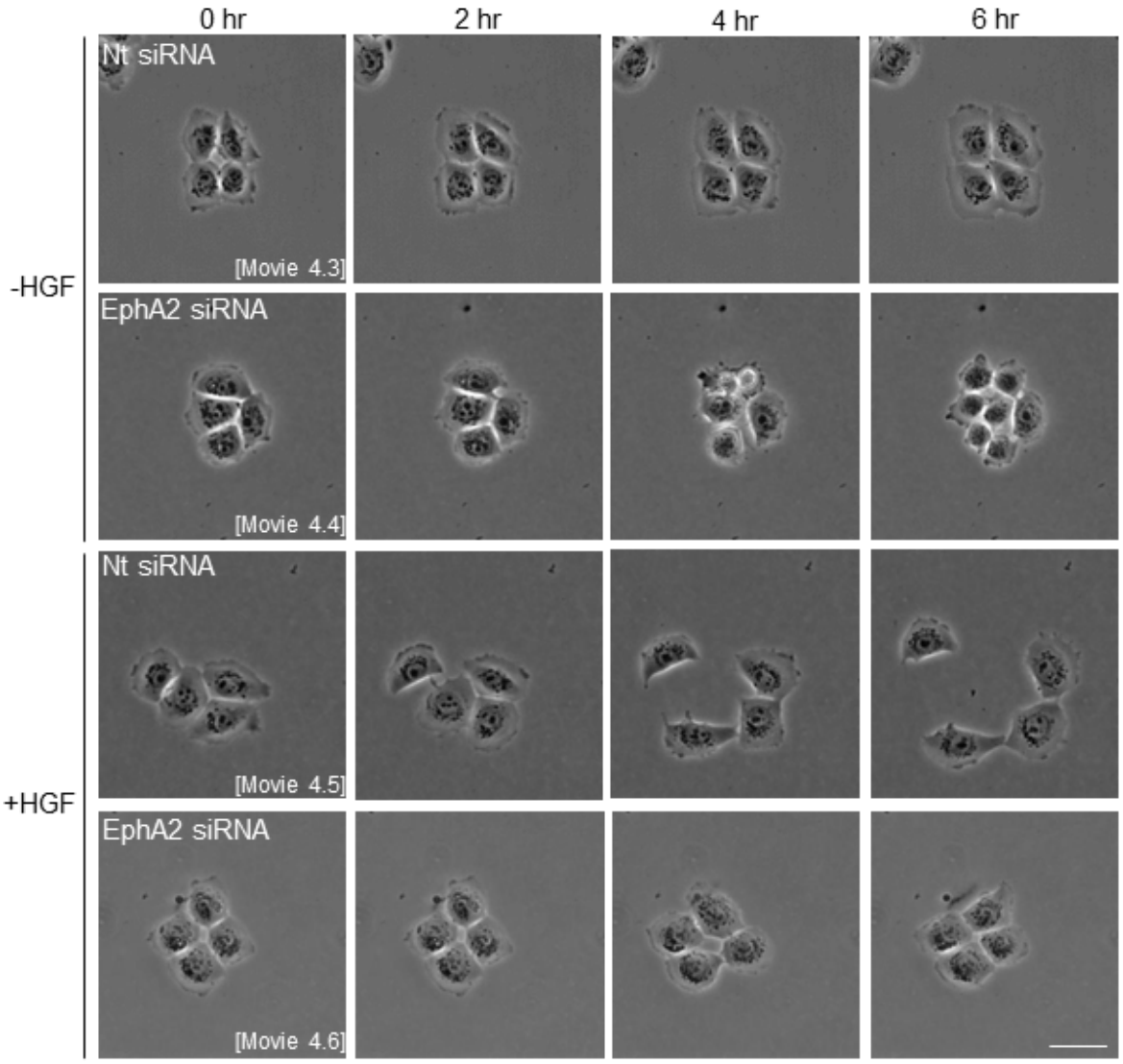

Figure 4-10 HGF-driven cell scattering is inhibited by depletion of EphA2 expression
H1299 cells were transfected with EphA2- or non-targeting siRNA and seeded sparsely. The cells were recorded by time-lapse microscopy 43 hours after transfection when 10ng/ml HGF/mock was added to the appropriate wells. Representative pictures and movies are shown for the first 6 hours. Scale bar is 50µm.

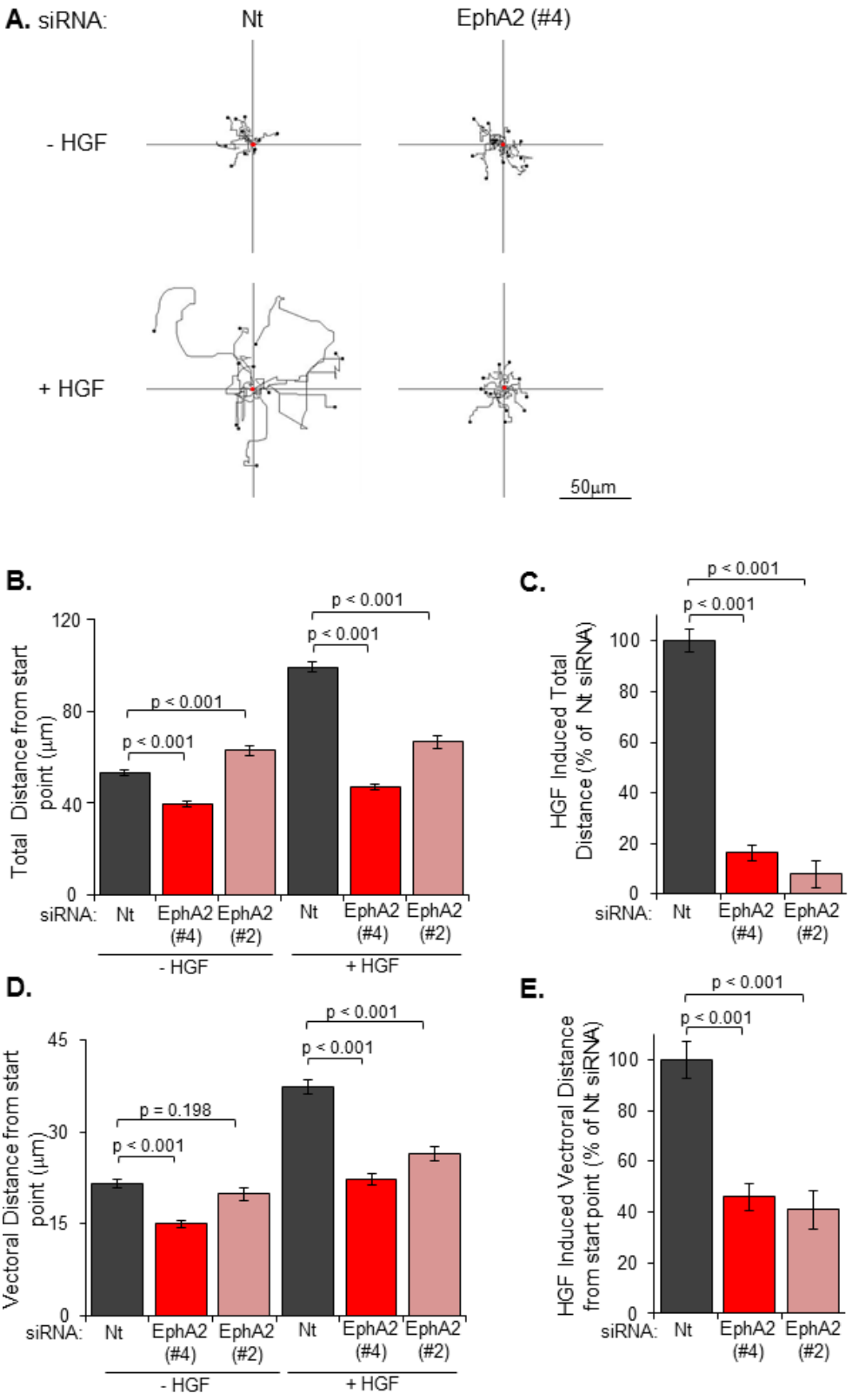

Figure 4-11 Depletion of EphA2 expression reduces the speed and distance of cell migration upon HGF addition

H1299 cells were transfected with two different EphA2 targeting siRNA oligos or non-targeting siRNA and seeded sparsely. The cells were recorded by time-lapse microscopy 43 hours after transfection when 10ng/ml HGF/mock was added to the appropriate wells. A. Representative tracks of cell migration for the first 6 hours. The total distance (B), HGF-induced distance (C), vectorial distance (D) and HGF-induced vectorial distance (E) are represented graphically. The HGF-induced cell speed and distance were calculated by subtracting the untreated value from the HGF treated value for each condition, and normalising to the non-targeting control. Cells were tracked from 8 different regions on the plate in 3 separate experiments. Statistical analysis was performed using a Mann-Whitney test and p-values are shown.

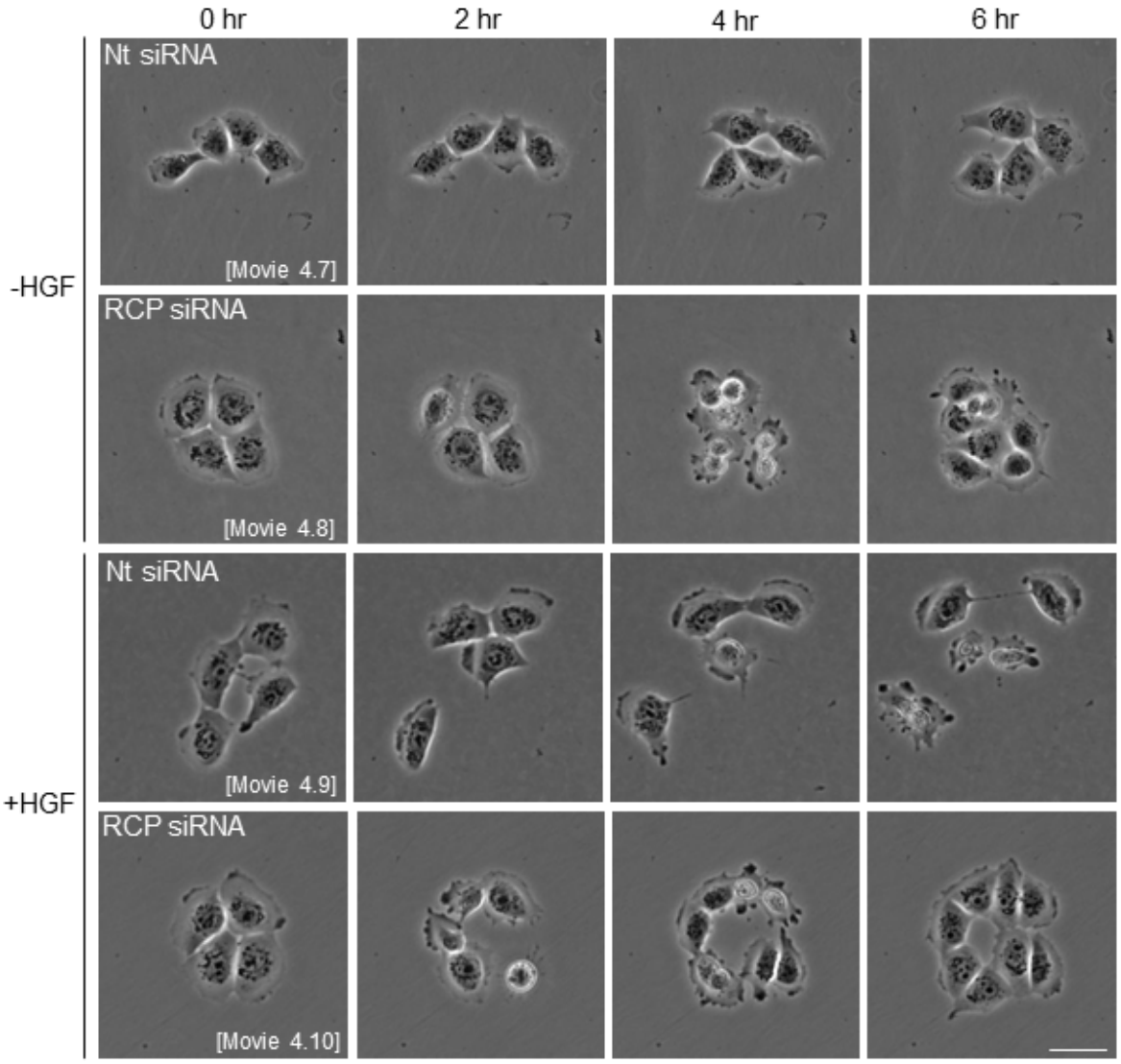

Figure 4-12 HGF-driven cell scattering is inhibited by depletion of RCP expression
H1299 cells were transfected with RCP- or non-targeting siRNA and seeded sparsely. The cells were recorded by time-lapse microscopy 43 hours after transfection when 10ng/ml HGF was added to the appropriate wells. Representative pictures and movies are shown for the first 6 hours. Scale bar is 50µm.

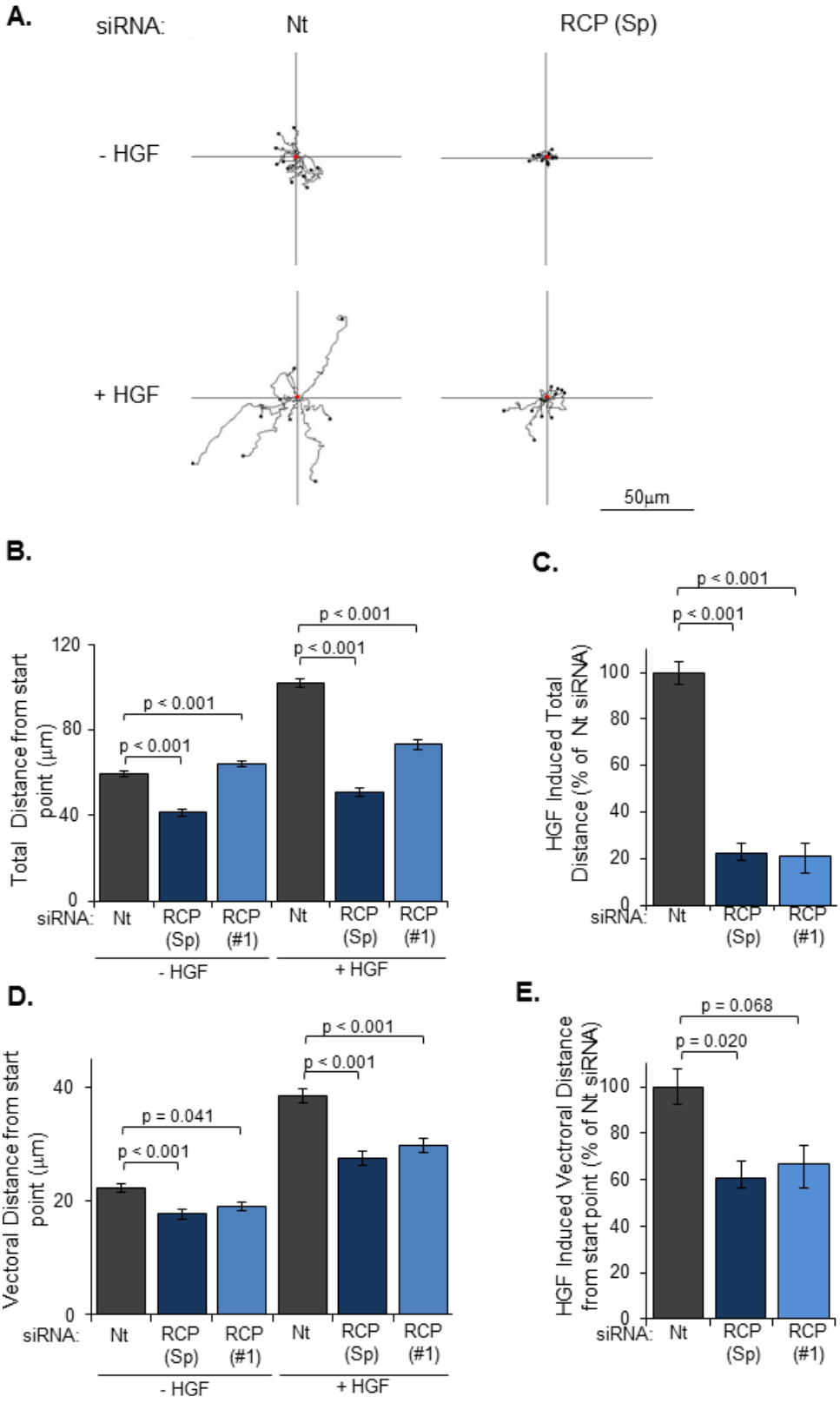

Figure 4-13 Depletion of RCP expression reduces the speed and distance of cell migration upon HGF addition

H1299 cells were transfected with a single or SMARTpool set of four siRNA RCP-targeting oligos or non-targeting siRNA and seeded sparsely. The cells were recorded by time-lapse microscopy 43 hours after transfection when 10ng/ml HGF was added to the appropriate wells. A. Representative tracks of cell migration for the first 6 hours are shown. The total distance (B), HGF-induced total distance (C), vectorial distance (D) and HGF-induced vectorial distance (E) are represented graphically. The HGF-induced cell speed and distance were calculated by subtracting the untreated value from the HGF treated value for each condition, and normalising to the non-targeting control. Cells were tracked in 8 different regions on the plate in 3 separate experiments. Statistical analysis was performed using a Mann-Whitney test and p-values are shown.

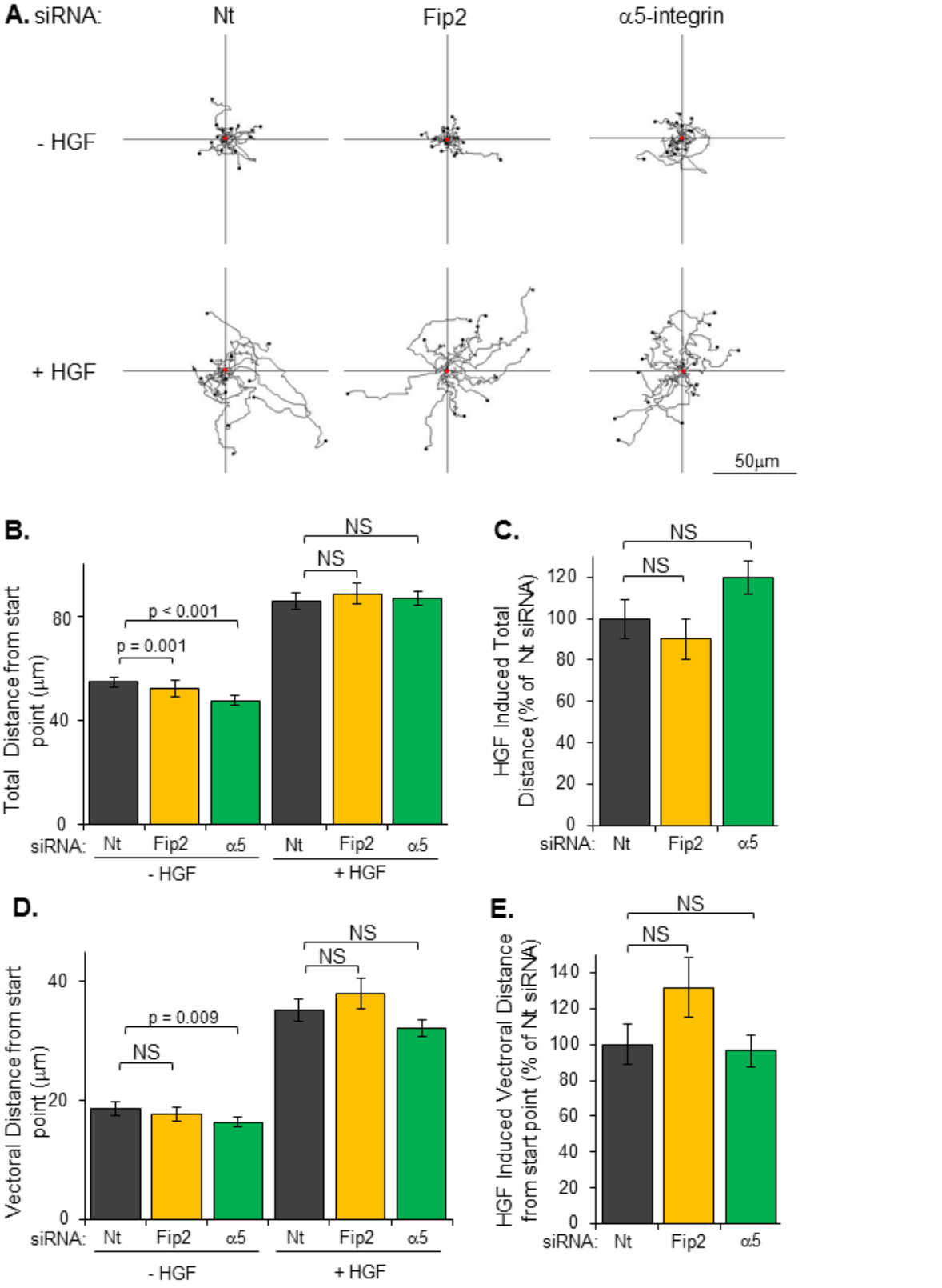

Figure 4-14 Suppression of Fip2 and α5-integrin expression has no effect on the speed and distance of cell migration upon HGF addition

H1299 cells were transfected with α5-integrin, Fip2 or non-targeting (Nt) siRNA and seeded sparsely. The cells were recorded by time-lapse microscopy 43 hours after transfection when 10ng/ml HGF was added to the appropriate wells. A. Representative tracks of cell migration for the first 6 hours. The total distance (B), HGF-induced total distance (C), vectorial distance (D) and HGF-induced vectorial distance (E) are represented graphically. The HGF-induced cell speed and distance were calculated by subtracting the untreated value from the HGF treated value for each condition, and normalising to the non-targeting control. Cells were tracked from 8 different regions on the plate in 3 separate experiments. Statistical analysis was performed using a Mann-Whitney test and p-values are shown.

4.2.3 Rab14, but not Rab6A/B or Rab11A/B, is required for HGF induced cell scattering and contact inhibition of locomotion

Rab6, Rab11 and Rab14 were identified as RCP associated proteins (**Sections 3.2.2.2 & 3.2.3.3**), therefore, I sought to determine if any of these Rab GTPases were required for cell-cell repulsion. H1299 cells expressed Rab6A/B, Rab11A/B and Rab14 at levels that were detected by Western blotting and the levels of each of these could be selectively reduced by siRNA (**Figure 4.15A**). Throughout the rest of this chapter, I refer to these double knockdowns as their gene name alone (ie. Rab11 is Rab11A/B double knockdown). Interestingly Rab11A/B or Fip3 knockdown (**Figure 4.9, Figure 4.15B**) increased HGF-independent scattering suggesting they may possibly act together to supress scattering. As assessed by scoring scattered cells **(Figure 4.15)** or using time-lapse microscopy analysed by cell tracking **(Figure 4.16)**, siRNA of Rab14 significantly reduced HGF-induced scattering of H1299 cells, whilst knockdown of either Rab11A/B or Rab6A/B was completely ineffective in this regard. Consistent with this, Rab14 (but not Rab11A/B) was found to suppress cell-cell repulsion in PC3 cells. Indeed, whilst siRNA of Rab11A/B or Rab14 had no effect on the ability of non-colliding PC3 cells to migrate **(Figure 4.17E)**, knockdown of Rab14 significantly increased the time that colliding cells remained immobile prior to resuming migration and moving away from one another **(Figure 4.17D)**. siRNA of Rab11A/B, on the other hand, did not influence this index. It is important to note, however, that unlike RCP, Rab14 did not seem to influence the direction of cell migration following a collision **(Figure 4.17B/C)**.

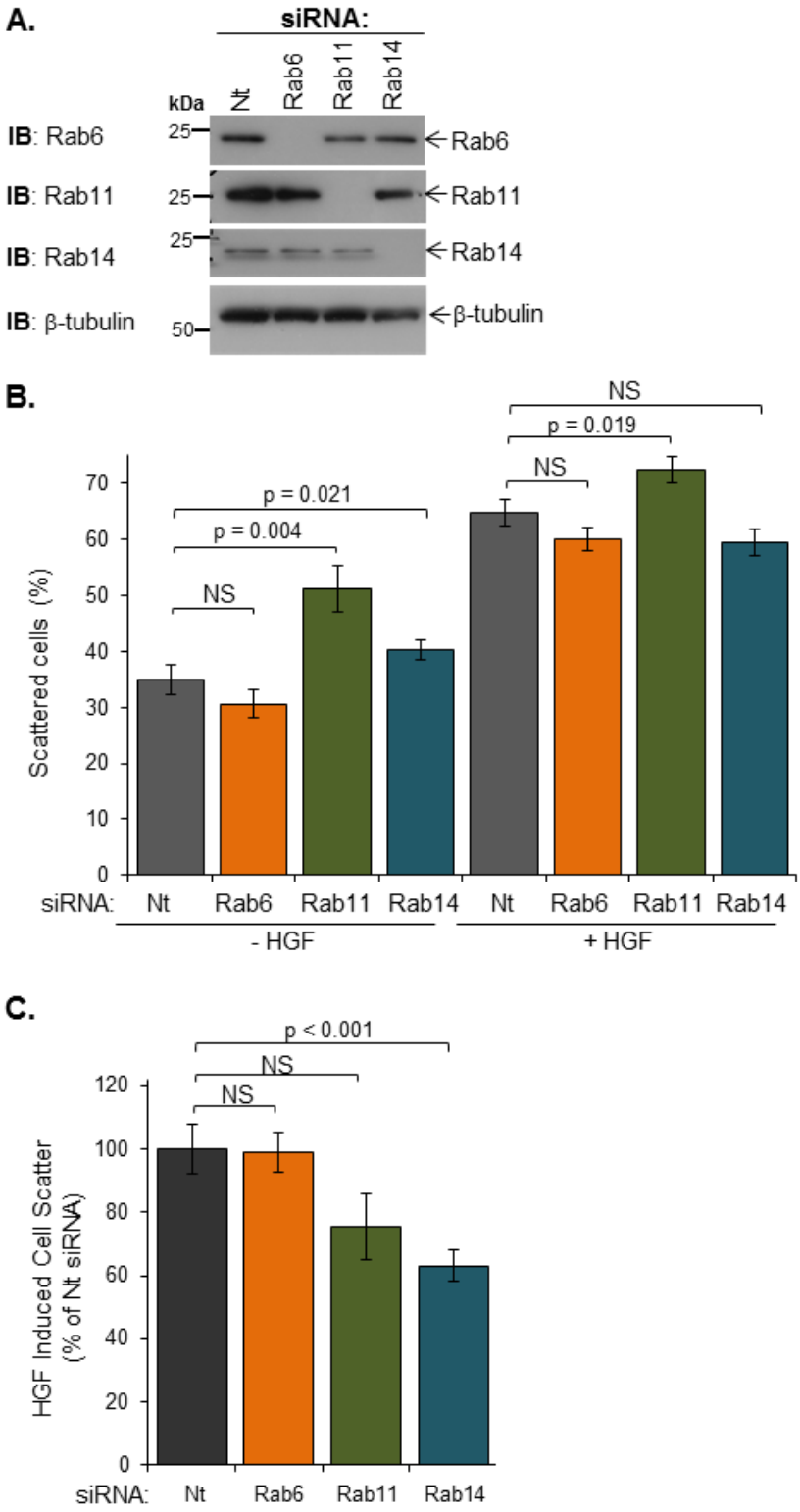

Figure 4-15 Suppression of Rab14 expression, but not Rab6A/B or Rab11A/B expression, inhibits HGF-induced cell scatter

H1299 cells were transfected with Rab6A/B (SMARTpool), Rab11A/B (SMARTpool), Rab14 (SMARTpool) or non-targeting (Nt) siRNA and seeded sparsely. A. Proteins were extracted 48 hours after transfection. Rab6A/B, Rab11A/B, Rab14 and β-tubulin were detected by Western blotting. B/C. 10ng/ml HGF/mock was added to each well 43 hours after transfection. After 6 hours of HGF treatment, representative pictures were taken. B. The average percentage of scattered cells is plotted. C. The HGF-induced cell scatter was calculated by subtracting the untreated value from the HGF treated value for each condition, and normalising to the non-targeting control. 15 pictures from 3 separate experiments were analysed. Statistical analysis was performed using a Mann-Whitney test and p-values are shown. Rab11 and Rab6 in the figure refer to the double knockdown conditions.

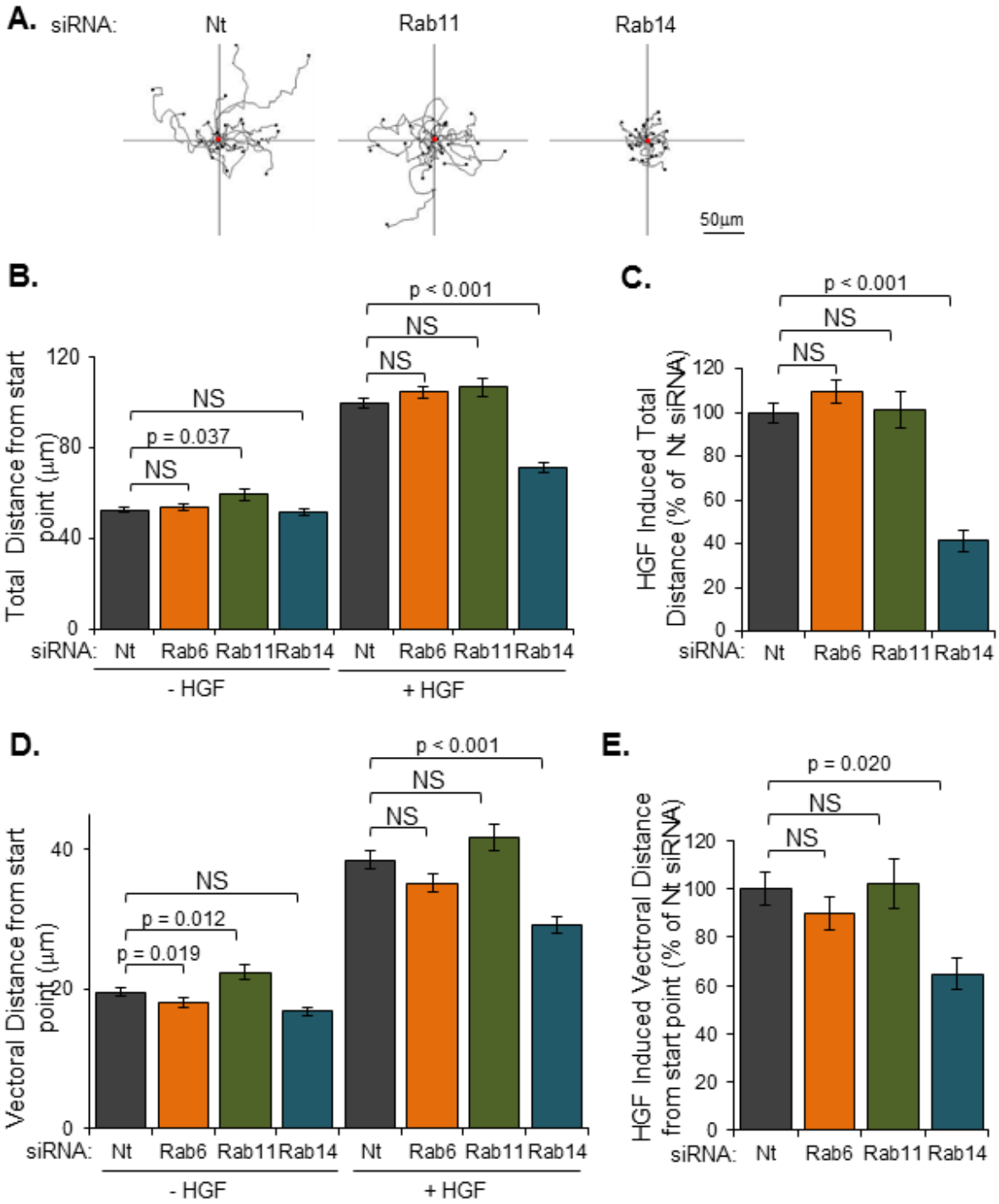

Figure 4-16 Suppression of Rab14 expression, but not Rab6 or Rab11 expression, reduces the speed and distance of cell migration upon HGF addition
H1299 cells were transfected with Rab6A/B, Rab11A/B and Rab14 or non-targeting (Nt) siRNA and seeded sparsely. The cells were recorded by time-lapse microscopy 43 hours after transfection when 10ng/ml HGF/mock was added to the appropriate wells. A. Representative tracks of cell migration are shown with HGF treatment for the first 6 hours. The total distance (B), HGF-induced total distance (C), vectorial distance (D) and HGF-induced vectorial distance (E) are represented graphically. The HGF-induced cell speed and distance were calculated by subtracting the untreated value from the HGF treated value for each condition, and normalising to the non-targeting control. Cells were tracked from 8 different regions on the plate in 3 separate experiments. Statistical analysis was performed using a Mann-Whitney test and p-values are shown.

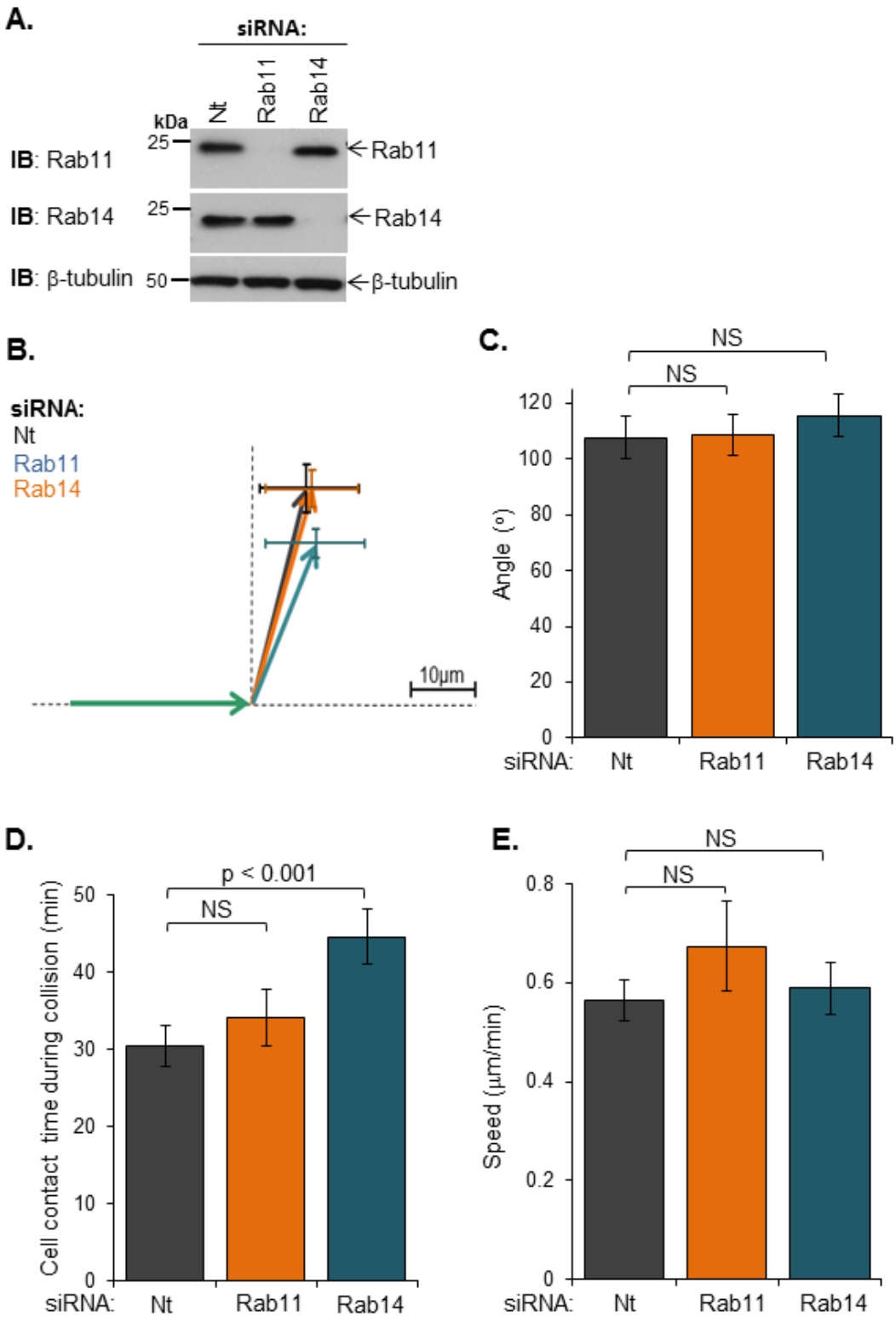

Figure 4-17 Depletion of Rab14 expression increases cell-cell contact time during contact inhibition of locomotion

A. PC3 cells were transfected with Rab11A/B, Rab14 or non-targeting (Nt) siRNA. Proteins were extracted 72 hours after transfection. Rab11A/B, Rab14 and β-tubulin were detected by Western blotting. B-E. Transfected cells were sparsely seeded onto Matrigel-coated glass plates. The cells were serum-starved for 24 hours and then treated with 10ng/ml HGF for 12-14 hours. Time-lapse microscopy was used to record cell migration. B. Representative vectorial tracks of cell migration 40 minutes before and after cell-cell collisions. The green line shows the average distance travelled before the cells collide, the black (Nt), orange (Rab11) and blue (Rab14) lines show the average distance and angle of cell migration after the collision. The angle of migration after the collision (C), time of cell-cell contact during the collision (D) and speed of cell migration (E) are represented graphically. Over 50 collisions were tracked per condition in 3 separate experiments. Mann-Whitney statistical tests were performed and p-values are shown.

4.2.4 Depletion of Rab14 or RCP does not increase N-cadherin expression

A previous report indicated that Rab14 promotes disruption of cell-cell junctions by driving recycling of the disintegrin metalloprotease, ADAM10, to cleave N-cadherin at the plasma membrane (Linford et al., 2012). Thus, a consequence of Rab14 action is that it may lead to shedding of N-cadherin from the cell surface. Accordingly the authors reported that Rab14 knockdown cells had increased levels of N-cadherin (Linford et al., 2012). As it was possible that Rab14/ADAM10-mediated cleavage of N-cadherin might contribute to HGF-induced scattering of H1299 cells, I investigated the influence of Rab14 knockdown on N-cadherin levels in these cells. However, in H1299 cells siRNA of Rab14 or RCP did not lead to increased N-Cadherin levels (**Figure 4.18**), indicating that this is unlikely to be a mechanism by which either Rab14 or RCP influence cell scattering in these cells.

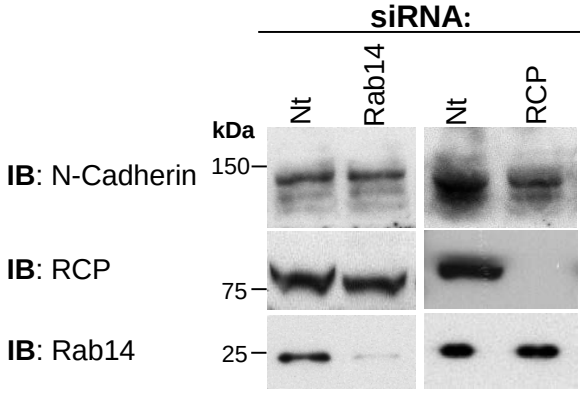

Figure 4-18 Depletion of Rab14 or RCP expression does not increase N-cadherin expression
H1299 cells were transfected with Rab14, RCP or non-targeting (Nt) control siRNA. Proteins were extracted 48 hours after transfection. The proteins were separated by SDS-PAGE and analysed by immunoblotting using antibodies that recognise N-cadherin, RCP and Rab14.

4.2.5 HGF increases RCP-dependent EphA2 trafficking

4.2.5.1 Development of an EphA2 trafficking assay

As RCP and Rab14 have a known role in receptor recycling, I sought to determine whether they are required for EphA2 trafficking and whether HGF treatment alters EphA2 trafficking. EphA2 trafficking has not been well studied, so a biotin-labelling based approach was established (Caswell et al., 2008; White et al., 2007). This approach had to be validated and optimised to detect EphA2. First, I tested whether EphA2 was efficiently labelled with sulfo-NHS-SS-biotin at the cell surface and whether this could be detected by immunoprecipitation. H1299 cells were labelled with sulfo-NHS-SS-biotin, which forms covalent bonds with the free amino groups in proteins. As it is membrane impermeant, only extracellular proteins and ectodomains were labelled. Moreover, sulfo-NHS-SS-biotin has a disulphide bond in a linker between the biotin and NHS moieties, which can be cleaved by the treatment of cells with the membrane-impermeant reducing agent, MesNa, thus removing the label from receptors that remain at the cell surface. The cells were thoroughly washed to remove any remaining label, thus preventing free sulfo-NHS-SS-biotin from binding to proteins when the cells were then lysed in a Triton-x100 lysis buffer. Anti-EphA2 was conjugated to magnetic beads, which were added to the cell lysates to immunoprecipitate EphA2. The immunoprecipitates were analysed by SDS-PAGE and Western blotting. EphA2 was efficiently immunoprecipitated by the EphA2 antibody, but not by a control IgG (RG16) (**Figure 4.19A**). Exposing the blots to HRP-conjugated streptavidin, which associates with biotin, revealed a predominant band of biotinylated protein corresponding to the size of EphA2 (~120kDa) in the EphA2 immunoprecipitate. This indicates that EphA2 may be efficiently labelled at the cell surface using sulfo-NHS-SS-biotin.

A capture-ELISA was developed to accurately quantify biotinylated EphA2. In this, anti-EphA2 was used as a capture antibody and biotinylated receptor was detected using HRP-conjugated streptavidin followed by colorimetric reaction with ortho-phenylenediamine and hydrogen peroxide substrate **(Figure 4.19B)**. I first established the specificity and antibody coating-concentration for the capture-ELISA, and then proceeded to confirm that the assay responded linearly to increasing concentrations of biotinylated EphA2 in the lysate **(Figure 4.19C)**.

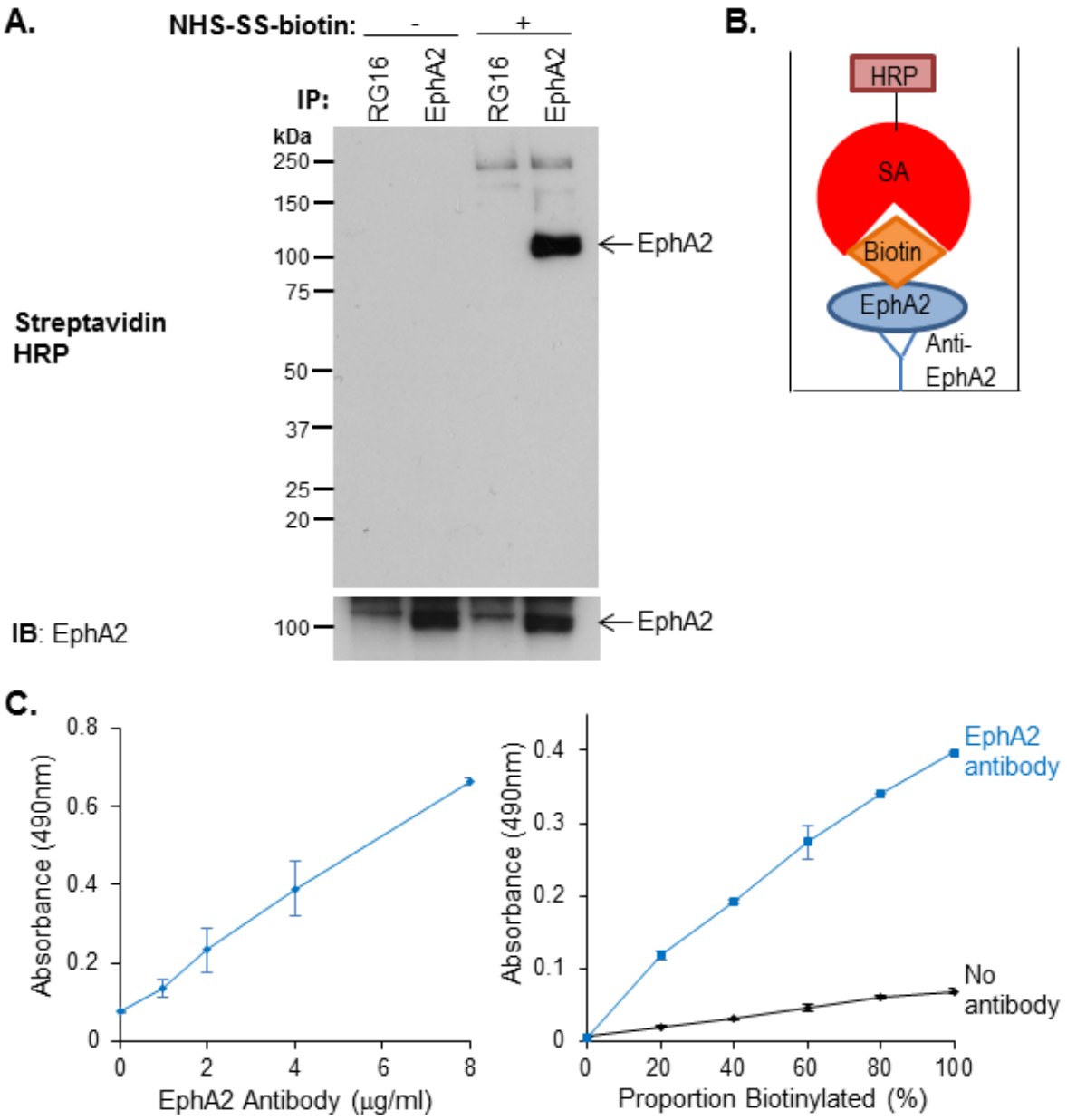

Figure 4-19 Validation of the EphA2 trafficking assay in H1299 cells
H1299 cells were surface labelled with 0.13mg/ml sulfo-NHS-SS-biotin (or mock) for 30 minutes at 4ºC. The cells were thoroughly washed with PBS and lysed. A. Immunoprecipitations were performed on these lysates with an anti-EphA2 or RG16 (negative control) antibody. Immunoprecipitates were analysed by SDS-PAGE. EphA2 was detected by immunoblotting and biotin was detected using HRP-conjugated streptavidin. B. Schematic representation of the capture-ELISA detection method. (SA: streptavidin, HRP: horseradish peroxidase) C. Biotinylated-EphA2 was detected from the cell lysates by capture-ELISA using microtiter wells coated with increasing concentrations of anti-EphA2 monoclonal antibody. D. Labelled and unlabelled cell lysates were prepared and mixed at the appropriate ratios. Biotinylated-EphA2 was detected by capture-ELISA.

4.2.5.2 EphA2 trafficking

Having developed a capture-ELISA to quantify biotinylated EphA2, I then proceeded to measure the rate of the receptor's internalisation. To do this, H1229 cells were surface-labelled with sulfo-NHS-SS-biotin at 4ºC, warmed to 37ºC for various times to allow internalisation, then treated with MesNa at 4ºC to remove any biotin from receptors remaining at the cell surface. Biotinylated EphA2 remaining in the cells was then determined using capture-ELISA. This indicated that ~30% of surface EphA2 was internalised by H1299 cells in 22.5 minutes **(Figure 4.20B)**.

Most receptors are in continuous flux between the plasma membrane and internal compartments **(Figure 4.20A)**, rendering it difficult to obtain 'pure' measurements of internalisation that are uncontaminated by the rapid return of receptor to the plasma membrane. To determine whether EphA2 is a 'cycling' receptor, I measured the rate of apparent EphA2 internalisation in presence of the receptor recycling inhibitor, primaquine. Addition of primaquine caused a very marked increase (>10 fold) in the internalisation rate of EphA2 **(Figure 4.20B)**. From this, I concluded that EphA2 is internalised and recycled very quickly-thus the measure of apparent EphA2 internalisation observed in the absence of primaquine represents components of both internalisation and recycling.

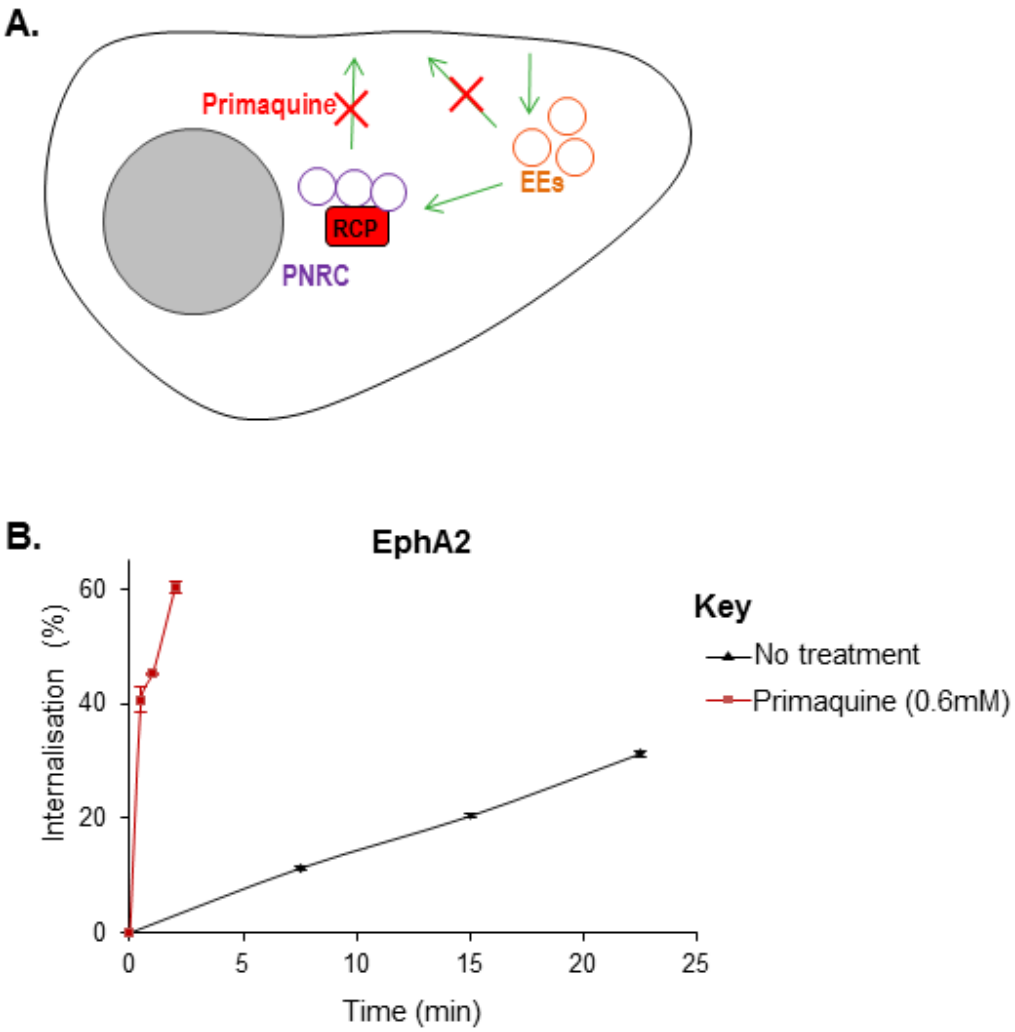

Figure 4-20 EphA2 trafficking kinetics in H1299 cells upon HGF addition
A. Schematic diagram showing possible EphA2 trafficking routes and the action site of primaquine. B. H1299 cells were surface labelled with 0.13mg/ml sulfo-NHS-SS-biotin for 30 minutes at 4ºC. Internalisation of cell surface protein was allowed for the indicated time points in DMEM media with 0.6mM primaquine/mock and 10ng/ml HGF at 37ºC. Biotin was removed from proteins on the plasma membrane by incubating the cells with 20mM MesNa for 30 minutes at 4ºC. This reaction was quenched by the addition of 20mM IAA for a further 10 minutes. Biotinylated-EphA2 was detected by capture-ELISA using microtiter wells coated with an EphA2 targeted antibody. Internalized proteins are plotted as a proportion of the total labelled protein at the indicated time points.

4.2.5.3 HGF increases RCP-dependent EphA2 trafficking

HGF drove a significant increase (~1.5 fold) in the apparent internalisation of EphA2, and knockdown of RCP did not affect EphA2 internalisation in the absence of HGF **(Figure 4.21)**. However, the HGF-induced increase in apparent EphA2 internalisation was completely opposed by knockdown of RCP. To determine the specificity of RCP's influence over EphA2 trafficking, I measured the internalisation of two other RTK's (cMet and EGFR) and TfnR as a control. As expected, HGF drove internalisation of its receptor, cMET **(Figure 4.21)**. However, cMet trafficking and that of EGFR and TfnR was not altered by RCP knockdown, indicating that RCP's influence over HGF-driven EphA2 trafficking has some specificity.

To determine whether RCP influences EphA2 internalisation per se, I performed these assays in the presence of primaquine. siRNA of RCP had no effect on the internalisation of EphA2 when receptor recycling was blocked **(Figure 4.22)**. Taken together, these data indicate that HGF influences the intracellular trafficking of EphA2 so as to slow or delay its return to the plasma membrane, and RCP is required for this to occur.

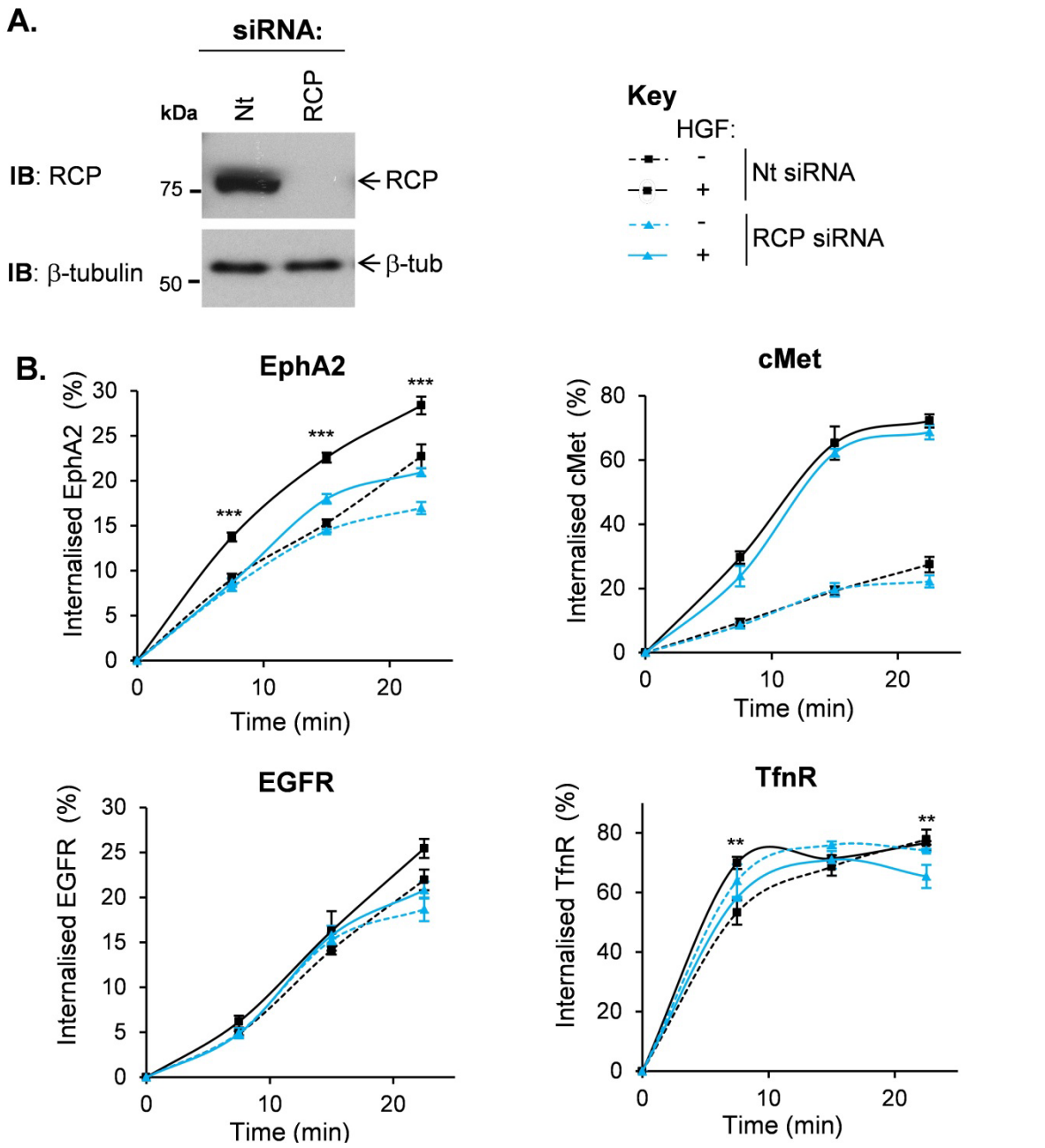

Figure 4-21 HGF increases EphA2 trafficking in an RCP-dependent fashion
A. H1299 cells were transfected with RCP- or non-targeting (Nt) control siRNA. Proteins were extracted 48 hours after transfection, and RCP and β-tubulin were detected by Western blotting. B. Transfected H1299 cells were surface labelled with 0.13mg/ml sulfo-NHS-SS-biotin for 30 minutes at 4ºC. Internalisation of cell surface protein was allowed for the indicated time points in DMEM media with 10ng/ml HGF/mock stimulation at 37ºC. Biotin was removed from proteins on the plasma membrane by incubating the cells in 20mM MesNa for 30 minutes at 4ºC. This reaction was quenched by the addition of 20mM IAA for a further 10 minutes. Biotinylated-EphA2, -cMet, -EGFR, and -TfnR were detected by capture-ELISA using microtiter wells coated with the appropriate targeted monoclonal antibodies. Internalized proteins are plotted as a proportion of the total labelled protein at the indicated time points. The graphs show the averages and SEM of 8 replicates of 4 separate experiments. Two way Anova statistical tests were performed and any significant difference between Nt and RCP siRNA transfected HGF treated cells is indicated on the graph (* : $p<0.05$, **: $p<0.01$, ***: $p<0.001$).

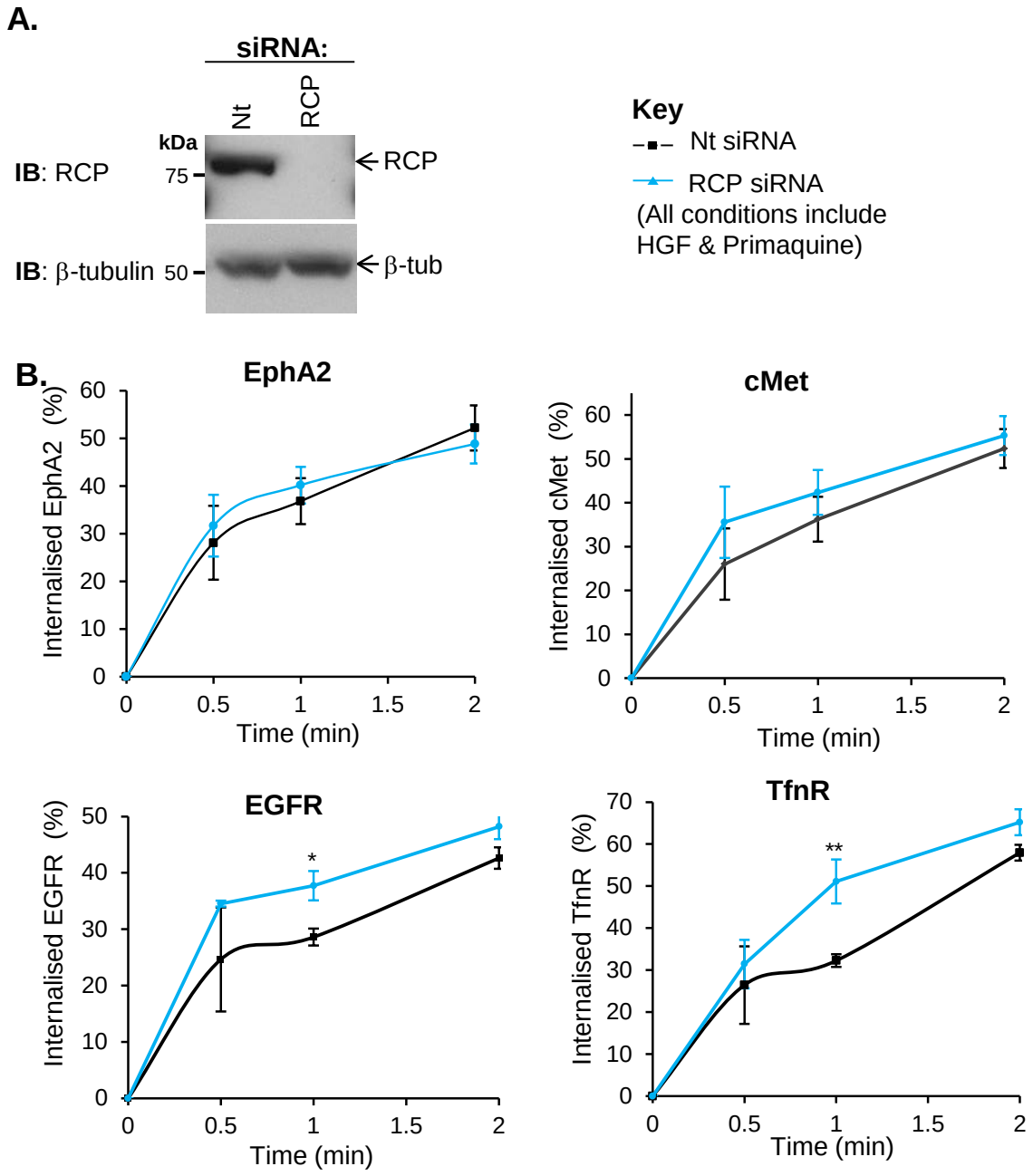

Figure 4-22 RCP is not required for EphA2 internalisation upon HGF treatment
A. H1299 cells were transfected with RCP targeting SMARTpool or non-targeting (Nt) control siRNA. Proteins were extracted 48 hours after transfection, and RCP and β-tubulin were detected by Western blotting. B. Transfected H1299 cells were surface labelled with 0.13mg/ml sulfo-NHS-SS-biotin for 30 minutes at 4ºC. Internalisation of cell surface protein was allowed for the indicated time points in DMEM media with 0.6mM primaquine and 10ng/ml HGF at 37ºC. Biotin was removed from proteins on the plasma membrane by incubating the cells in 20mM MesNa for 30 minutes at 4ºC. This reaction was quenched by the addition of 20mM IAA for a further 10 minutes. Biotinylated-EphA2, -cMet, -EGFR, and -TfnR were detected by capture-ELISA using microtiter wells coated with the appropriate targeted monoclonal antibodies. Internalized proteins are plotted as a proportion of the total labelled protein at the indicated time points.

4.2.5.4 HGF does not influence EphA2 degradation

EphA2 has been reported to be substrate for MT1-MMP resulting in its shedding from the cell surface (Sugiyama et al., 2013). Furthermore, EphA2 is known to be subject to lysosomal degradation following ligation with its Ephrin ligands (Wang et al., 2002). As it is probable that either shedding or lysosomal degradation of EphA2 could influence the values obtained from surface biotinylation/capture-ELISA assays, I determined whether HGF or RCP affected EphA2 degradation over the time course of the internalisation assays that I had performed. Clearly there was no detectable reduction in EphA2 levels following addition of HGF and this was unaffected by RCP knockdown **(Figure 4.23)**. Furthermore, EphA2 ran at its predicted molecular weight, and I was unable to detect the presence of any proteolytic fragments of the receptor (such as those that would result from MT1-MMP cleavage) in the presence or absence of HGF.

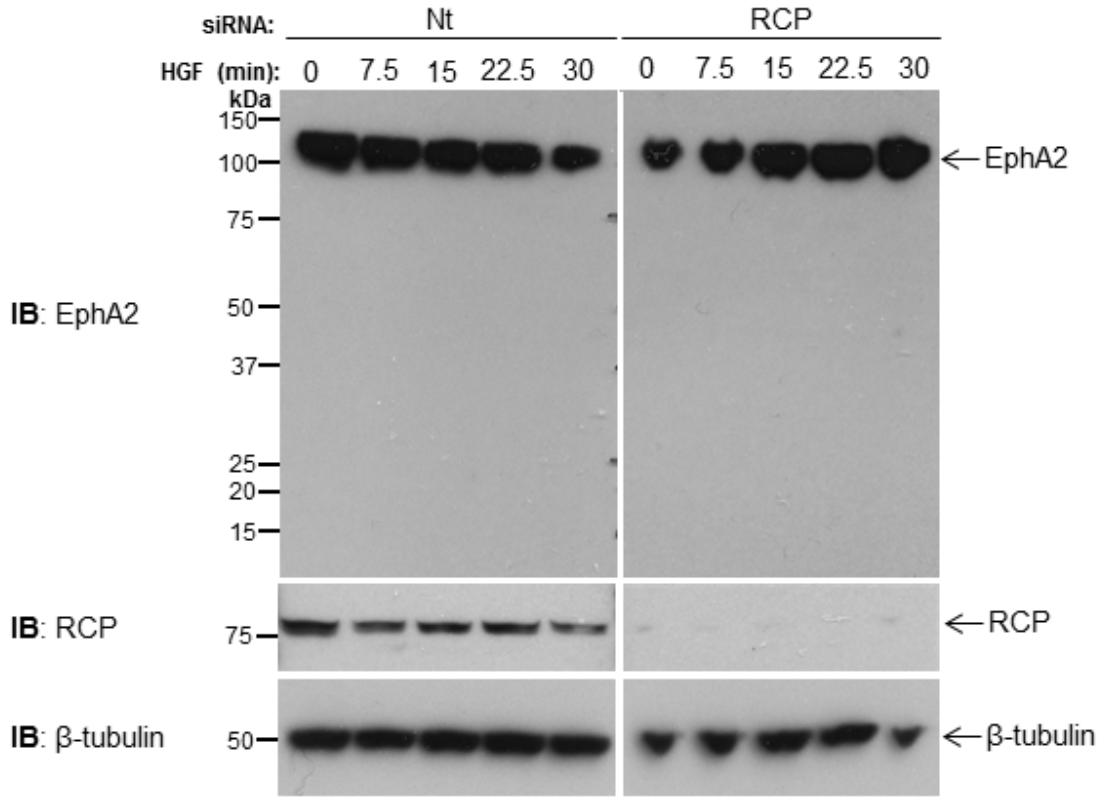

Figure 4-23 Neither HGF treatment nor suppression of RCP expression alters EphA2 degradation
H1299 cells were transfected with RCP- or non-targeting (Nt) control siRNA and treated with 10ng/ml HGF for the appropriate times. Proteins were extracted 48 hours after transfection and separated by SDS-PAGE. EphA2, RCP and β-tubulin were detected by immunoblotting.

4.2.6 HGF drives sorting of EphA2 to an RCP-positive compartment

The internalisation assays (described previously) indicated that HGF alters intracellular trafficking of EphA2 in an RCP-dependent fashion. Therefore, I used a fluorescence live cell imaging approach to directly visualise EphA2 trafficking. H1299 cells were co-transfected with GFP-EphA2 and mCherry-RCP, seeded onto glass-bottomed plates and viewed by confocal microscopy. GFP-EphA2 was present at the plasma membrane and in a set of intracellular vesicles that were in constant motion **(Figure 4.24A/B & movie 4.11)**. mCherry-RCP was seen to localise, as expected, to a vesicular compartment that was concentrated in the peri-nuclear region. Reviewing stills for these movies indicated that there was little co-localisation between GFP-EphA2 and mCherry-RCP **(Figure 4.24B)**. Following addition of HGF, GFP-EphA2 was seen to relocate to RCP-positive structures, such that the two proteins were then seen to move around together **(Figure 4.24A)**, and quantitative analysis indicated that increased co-localisation of EphA2 and RCP was statistically significant across a number of experiments **(Figure 4.24C)**. Taken together with the results from the internalisation assays in the previous sections, these data indicate that HGF diverts EphA2 from a rapid recycling pathway into one that is slower and includes passage through an RCP-positive compartment.

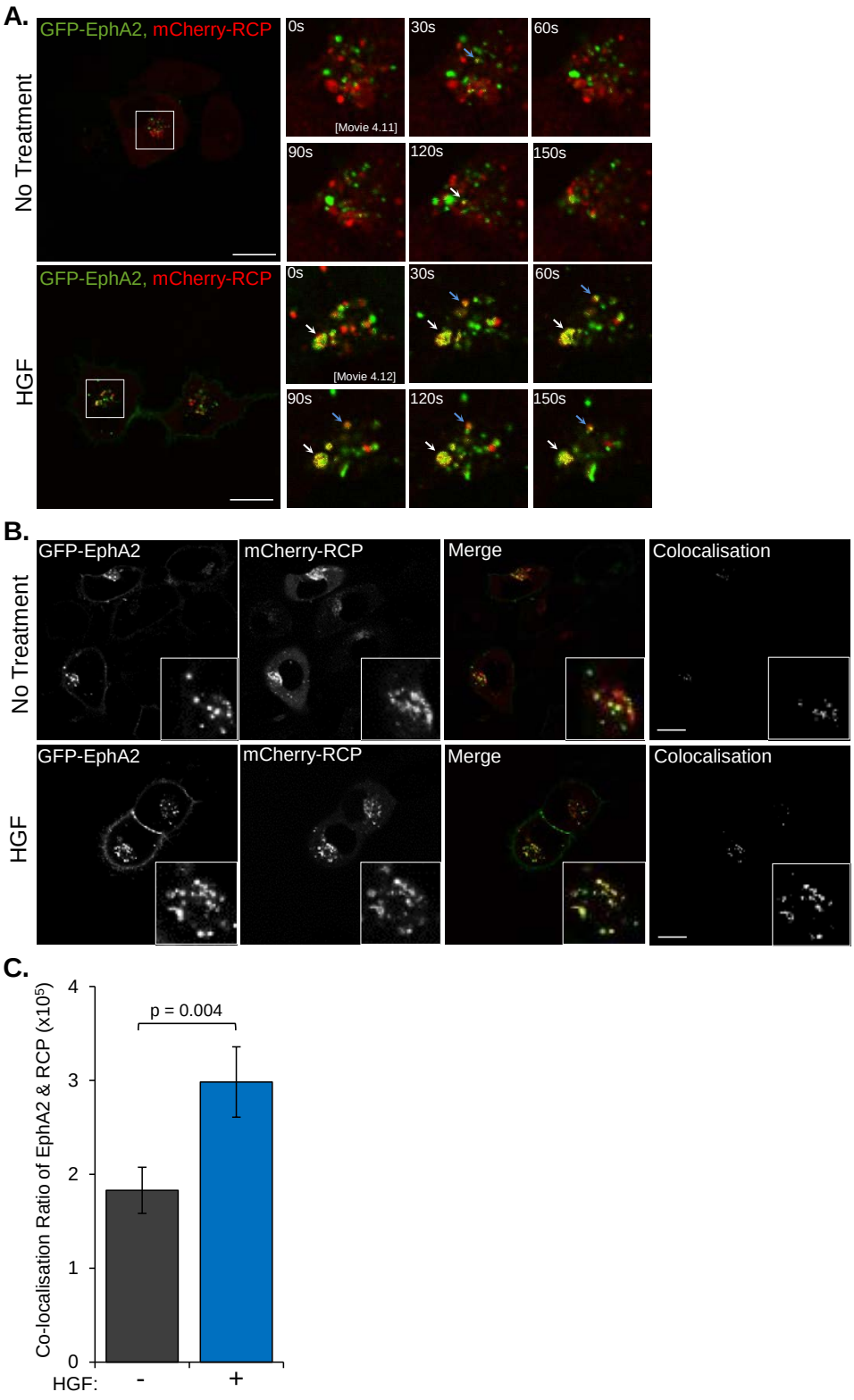

Figure 4-24 HGF increases the co-localisation between GFP-EphA2 and mCherry-RCP in vesicles

H1299 cells were co-transfected with GFP-EphA2 and mCherry-RCP and seeded onto glass-bottomed dishes. 24 hours after transfection, 10ng/ml HGF/mock was added to the plates. Short time-lapse recordings were taken of the cells by confocal microscopy. A. Representative merged images during the time-lapse are shown. B. Representative images of GFP-EphA2, mCherry-RCP, merged GFP-EphA2 & mCherry-RCP and co-localised regions are shown. C. ImageJ software was used to quantify co-localised pixels relative to the GFP-EphA2 and mCherry-RCP pixels in individual cells. The average co-localisation is represented graphically. The co-localisation of approximately 60 cells from 3 separate experiments was measured. Mann-Whitney statistical tests were performed and the p-value is indicated.

4.2.7 HGF induces EphA2 trafficking through a Rab14-positive compartment

I have previously shown that Rab14 associates with RCP (**Section 3.2.2**). Moreover, my observation that Rab14, but not Rab11, is required for HGF-induced cell scattering and CIL led me to investigate the role of this GTPase in EphA2 trafficking. siRNA of Rab14 completely opposed the ability of HGF to drive the apparent internalisation of EphA2 **(Figure 4.25)**, suggesting that this GTPase is required for HGF to delay EphA2 recycling. Consistent with this, I found that HGF may be able to divert trafficking of EphA2 to Rab14-positive endosomes. In the absence of HGF, EphA2 vesicles are relatively motile and do not often come into contact with Rab14, which is localised primarily in the perinuclear region, as is RCP **(Figure 4.26B & movie 4.13)**. Following addition of HGF, EphA2 began to co-localise with Rab14 and structures that contain both proteins were seen to move together **(Figure 4.26A & movie 4.13)**. A quantitative analysis of a number of movies indicated that HGF induced a statistically significant increase in co-localisation between EphA2 and Rab14 **(Figure 4.26C)**. Taken together these data indicate that EphA2 is internalised and recycled in H1299 cells. Addition of HGF delays EphA2 recycling whilst the receptor is diverted to RCP- and Rab14-positive vesicles, and this requires the presence of both RCP and Rab14.

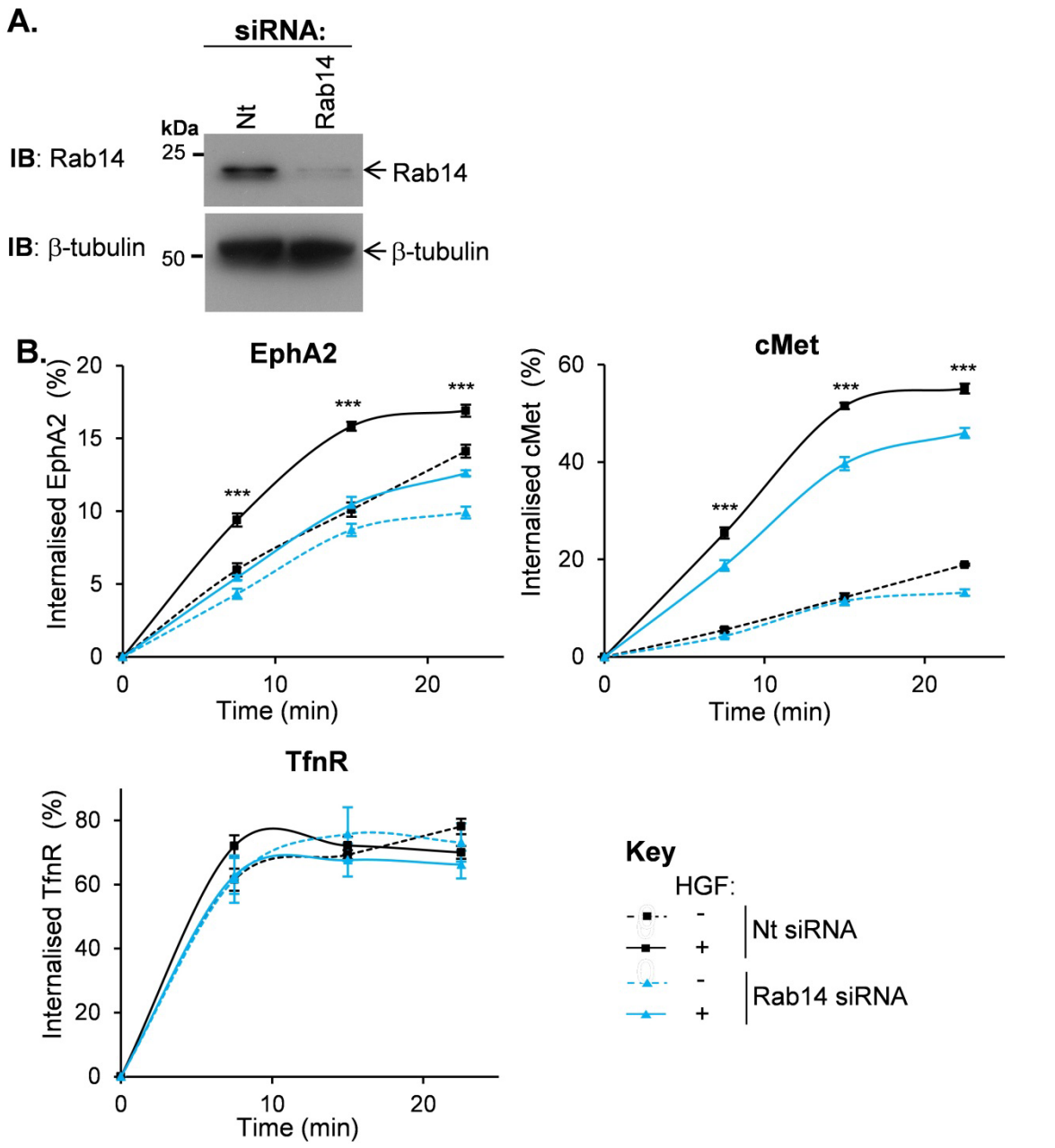

Figure 4-25 HGF increases EphA2 trafficking in a Rab14-dependent fashion
A. H1299 cells were transfected with Rab14 or non-targeting (Nt) control siRNA. Proteins were extracted 48 hours after transfection, and Rab14 and β-tubulin were detected by Western blotting. B. Transfected H1299 cells were surface labelled with 0.13mg/ml sulfo-NHS-SS-biotin for 30 minutes at 4ºC. Internalisation of cell surface protein was allowed for the indicated time points in DMEM media with 10ng/ml HGF/mock stimulation at 37ºC. Biotin was removed from proteins on the plasma membrane by incubating the cells in 20mM MesNa for 30 minutes at 4ºC. This reaction was quenched by the addition of 20mM IAA for a further 10 minutes. Biotinylated-EphA2, -cMet, and -TfnR were detected by capture-ELISA using microtiter wells coated with the appropriate targeted monoclonal antibodies. Internalized proteins are plotted as a proportion of the total labelled protein at the indicated time points. The graphs show the averages and SEM of 6 replicates of 3 separate experiments. Two way Anova statistical tests were performed between Nt and Rab14 siRNA transfected HGF treated cells and any significant difference is indicated on the graph (*: $p<0.05$, **: $p<0.01$, ***: $p<0.001$).

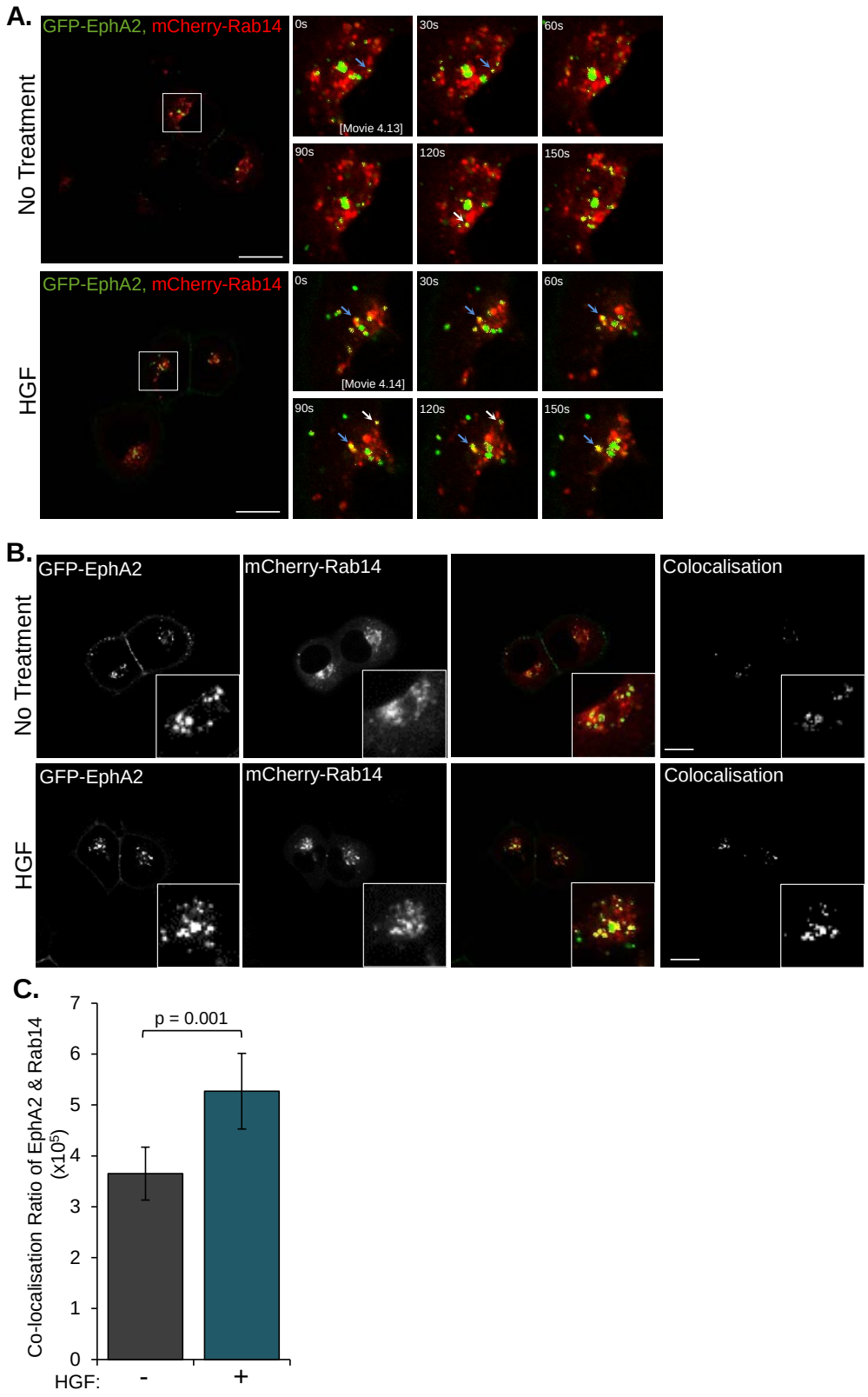

Figure 4-26 HGF increases the co-localisation between GFP-EphA2 and mCherry-Rab14 in vesicles

H1299 cells were co-transfected with GFP-EphA2 and mCherry-Rab14 and seeded onto glass-bottomed dishes. 24 hours after transfection, 10ng/ml HGF/mock was added to the plates. Short time-lapse recordings were taken of the cells by confocal microscopy. A. Representative merged images during the time-lapse are shown. B. Representative images of GFP-EphA2, mCherry-Rab14, merged GFP-EphA2 & mCherry-Rab14 and co-localised regions are shown. C. ImageJ software was used to quantify co-localised pixels relative to the GFP-EphA2 and mCherry-Rab14 pixels in individual cells. The average co-localisation is represented graphically. The co-localisation of approximately 60 cells from 3 separate experiments was measured. Mann-Whitney statistical tests were performed and the p-value is indicated.

4.2.8 RCP is phosphorylated at Serine^{435}

Prior to my arrival in the lab, a mass spectrometry phospho-mapping approach was used to identify residues in RCP that might function as phospho-acceptors. To do this, GFP-RCP was expressed in A2780 cells and then immunoprecipitated using an anti-GFP antibody coupled to magnetic beads. The resulting immunoprecipitated material was trypsinised and analysed by MALDI-TOF mass spectrometry. Peptides that were potentially phosphorylated were identified, and the most abundant of these were ^{430}ESRRSS(HPO$_3$)LLSLMTGK^{443} and ^{523}RPPISS(HPO$_3$)PRAPQTRA^{537}.

A phospho-specific antibody was then raised by injecting rabbits with a synthetic peptide corresponding to RCP$^{427\text{-}439(pSer\text{-}435)}$ (^{427}KKPESRRSS(HPO$_3$)LLSL^{439}). The resulting anti-serum was affinity purified using the RCP$^{427\text{-}439(pSer\text{-}435)}$ peptide and then pre-cleared with the non-phosphorylated version of the same sequence to remove antibodies that were not phospho-specific. To assess this antibody and to determine whether RCP is phosphorylated on Serine^{435} in cells, GFP-RCP was expressed in A2780 cells, GFP was immunoprecipitated and the product was probed with the anti-pSer^{435}-RCP antibody by immunoblotting. This antibody recognised a single band corresponding to phosphorylated GFP-RCP, but did not recognise a mutant of RCP in which the phosphor-acceptor Serine^{435} had been substituted with Alanine **(Figure 4.27A)**. Furthermore, addition of the broad-spectrum Serine/Threonine kinase inhibitor, Staurosporine, for 1 hour led to a substantial reduction in the signal detected by anti-pSer^{435}-RCP **(Figure 4.27B)** indicating that RCP phosphorylation is potentially regulated in these cells.

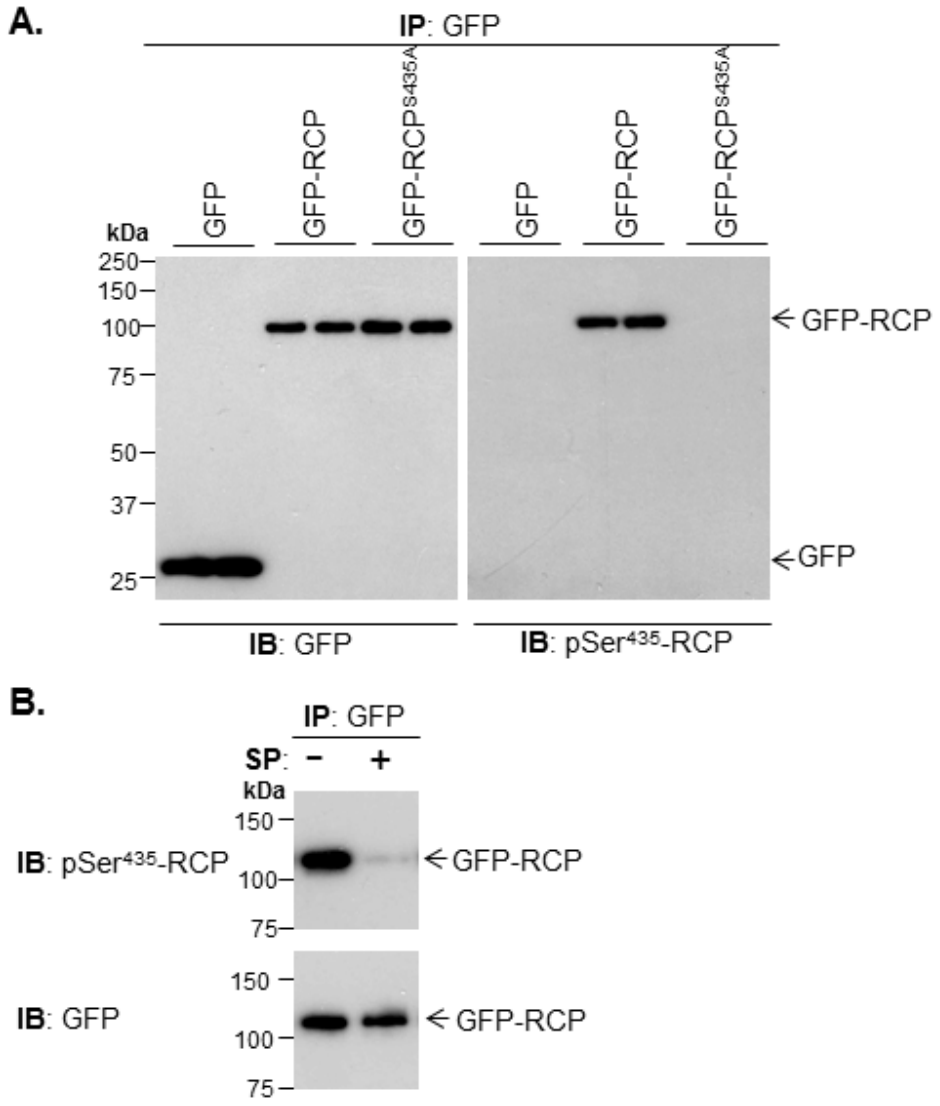

Figure 4-27 RCP is phosphorylated on Serine[435] and this phosphorylation is blocked by Staurosporine treatment

A. A2780 cells were transfected with GFP, GFP-RCP or GFP-RCP^{S435A}. The cells were lysed and GFP was immunoprecipitated with an anti-GFP antibody. The immunoprecipitates were analysed by SDS-PAGE, and Western blotting with antibodies that recognise GFP and pSer435-RCP. Each condition was performed in duplicate. B. A2780 cells were transfected with GFP-RCP. The cells were treated with 10ng/ml Staurosporine (SP) for 1 hour, lysed, and GFP was immunoprecipitated with an anti-GFP antibody. The immunoprecipitates were analysed by SDS-PAGE and Western blotting with antibodies that recognise GFP and pSer435-RCP. This work was performed by Andrew Campbell.

4.2.9 HGF drives RCP phosphorylation and enhances the association between EphA2, RCP and Rab14

Using the approaches discussed in the previous section, I found that RCP was phosphorylated on Serine^{435} in H1299 cells, and this was increased by the addition of HGF **(Figure 4.28A)**. Although the degree of HGF-induced RCP phosphorylation varied between experiments, densitometric analysis of Western blots of 4 independent experiments indicated that HGF addition for 1 minute drove a ~4 fold increase in RCP phosphorylation **(Figure 4.28B)**. Consistently, endogenous pSer^{435}-RCP was found to be co-immunoprecipitated with endogenous EphA2 and this was also enhanced following HGF addition **(Figure 4.29)**.

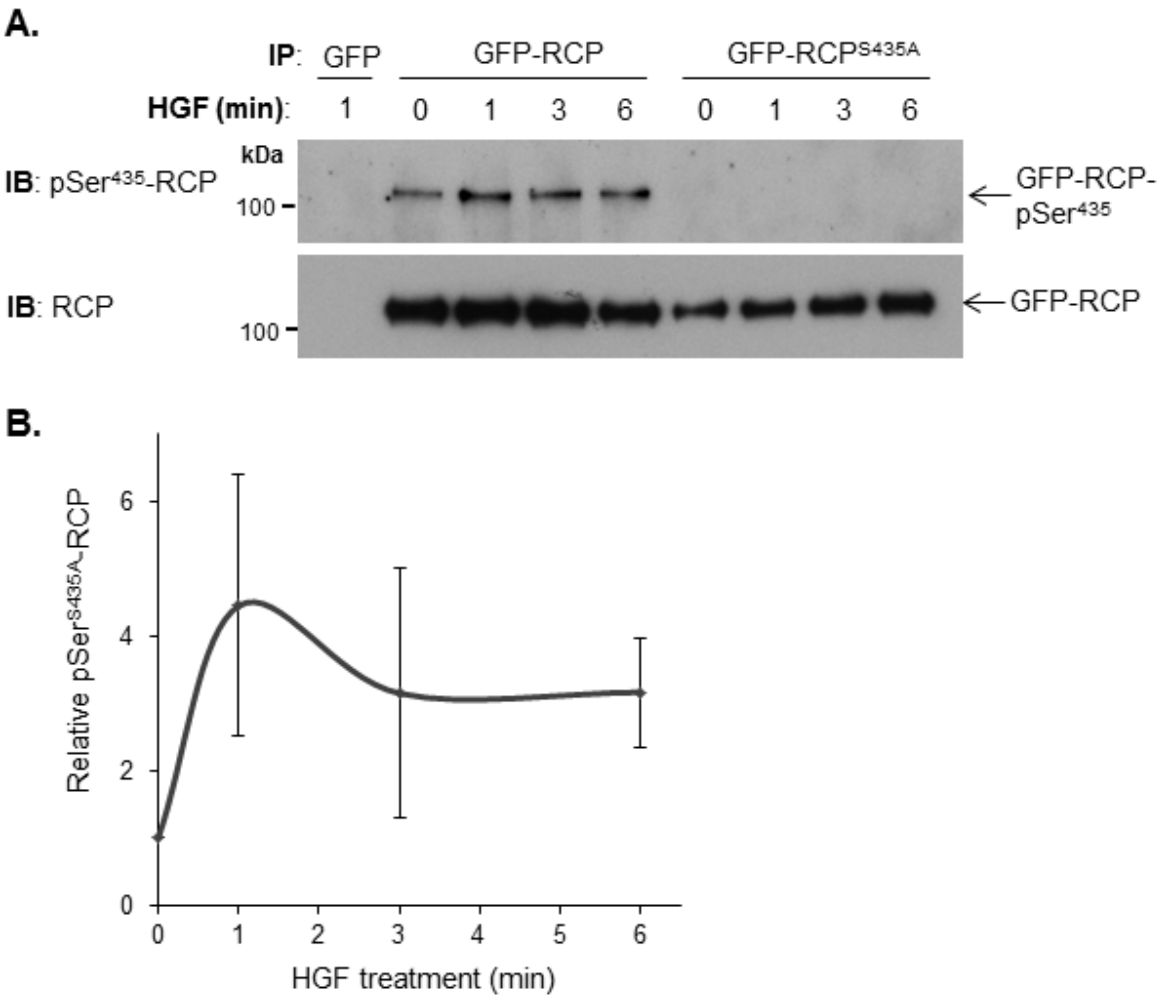

Figure 4-28 RCP is phosphorylated upon HGF treatment
H1299 cells were transfected with GFP, GFP-RCP or GFP-RCP^{S435A}. The cells were treated with 10ng/ml HGF for the indicated times, 48 hours after transfection. The cells were lysed and GFP was immunoprecipitated with an anti-GFP antibody. A. The immunoprecipitates were analysed by SDS-PAGE and Western blotting with antibodies that recognise RCP and pSer435-RCP. B. ImageJ software was used to quantify the amounts of pSer435-RCP relative to RCP in 4 separate experiments. The mean and SEM are represented graphically.

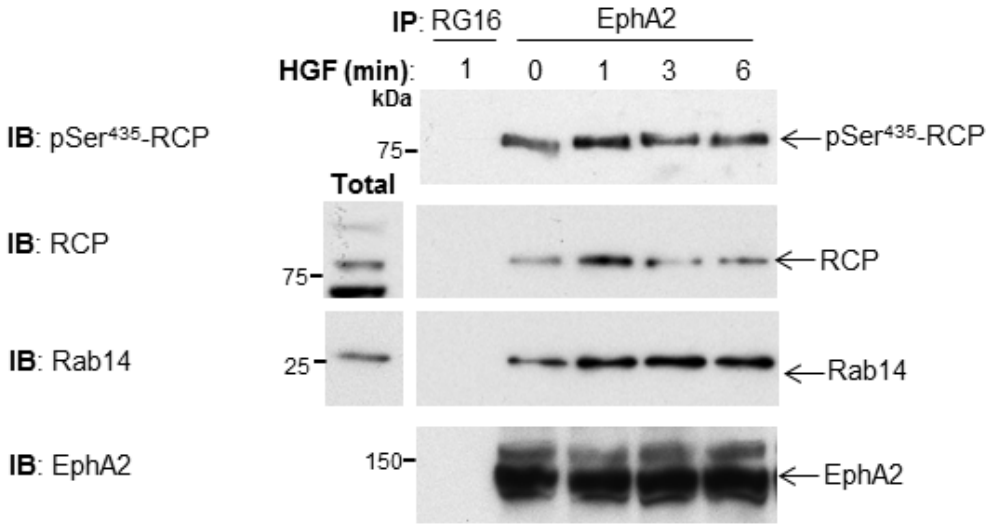

Figure 4-29 The association between endogenous EphA2, RCP and Rab14 is enhanced by HGF treatment
H1299 cells were treated with HGF for the indicated times. Endogenous EphA2 was immunoprecipitated with an anti-EphA2 antibody and RG16 was used as a non-specific control. The immunoprecipitates were analysed by SDS-PAGE and immunoblotting with antibodies that recognise RCP, pSer435-RCP, EphA2 and Rab14.

Analysis of fluorescent-protein dynamics in living cells **(Section 4.2.6)** indicated that HGF treatment drives sorting of EphA2 to an RCP/Rab14 positive compartment. To determine whether this was also reflected in altered physical association between the proteins, co-immunoprecipitation analysis was performed. As before, EphA2 and Rab14 specifically immunoprecipitated with GFP-RCP, and the co-immunoprecipitation of both of these proteins was significantly enhanced following HGF addition **(Figure 4.30A)**. As for RCP phosphorylation this varied somewhat between experiments, but densitometric analysis of three independent experiments indicated that HGF enhanced EphA2 (6-fold) and Rab14 (3-fold) co-immunoprecipitation with RCP **(Figure 4.30B)**. Moreover, although Rab11 associated with RCP under basal conditions, this association was not enhanced (and in some experiments reduced) by HGF addition **(Figure 4.30A)**. EphA2 and Rab14 were found to weakly co-immunoprecipitate with mutant RCP that lacks the phospho-acceptor site, GFP-RCP^{S435A}. However, addition of HGF was unable to enhance the association of EphA2 and Rab14 with GFP-RCP^{S435A} **(Figure 4.30A)**. Taken together these data indicate that an HGF-activated kinase is responsible for phosphorylation of RCP at Serine^{435}, and that this is necessary for effective recruitment of one of its receptor cargo, EphA2, and an important regulatory GTPase, Rab14, to an RCP-containing complex.

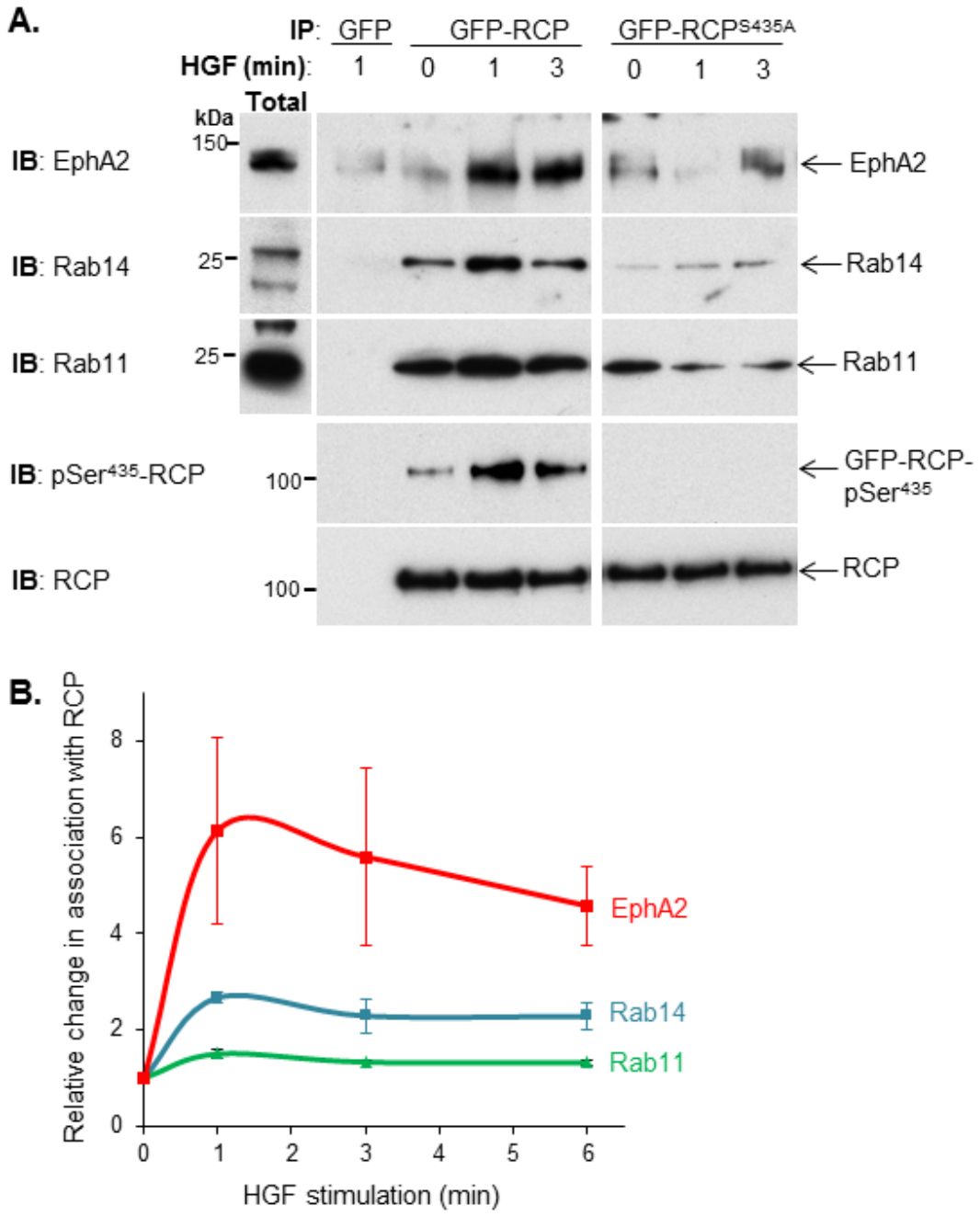

Figure 4-30 HGF enhances the association of RCP with Rab14 and EphA2
H1299 cells were transfected with GFP, GFP-RCP or GFP-RCP^{S435A}. The cells were treated with 10ng/ml HGF for the indicated times, 48 hours after transfection. The cells were lysed and GFP was immunoprecipitated with an anti-GFP antibody. A. The immunoprecipitates were analysed by SDS-PAGE and Western blotting with antibodies that recognise RCP, pSer435-RCP, EphA2, Rab11 and Rab14. B. ImageJ software was used to quantify the amounts of EphA2, Rab11 and Rab14 relative to RCP in 4 separate experiments for Rab11 and Rab14, and 2 separate experiments for EphA2. The mean and SEM are represented graphically.

4.2.10 Phosphorylation of RCP at Serine^{435} is required for EphA2 trafficking and cell scattering

My observation that phosphorylation of RCP at Serine^{435} is required for its association with two proteins that are key to cell scattering prompted me to test whether RCP phosphorylation contributes to EphA2 trafficking and function. In H1299 cells that expressed GFP-RCP, HGF drove a significant increase in the apparent internalisation rate of EphA2 **(Figure 4.31)**, indicating that overexpression of RCP does not have a detectable influence on the ability of HGF to delay EphA2 recycling. However, expression of GFP-RCP^{S435A} completely opposed the ability of HGF to increase EphA2 trafficking **(Figure 4.31)**.

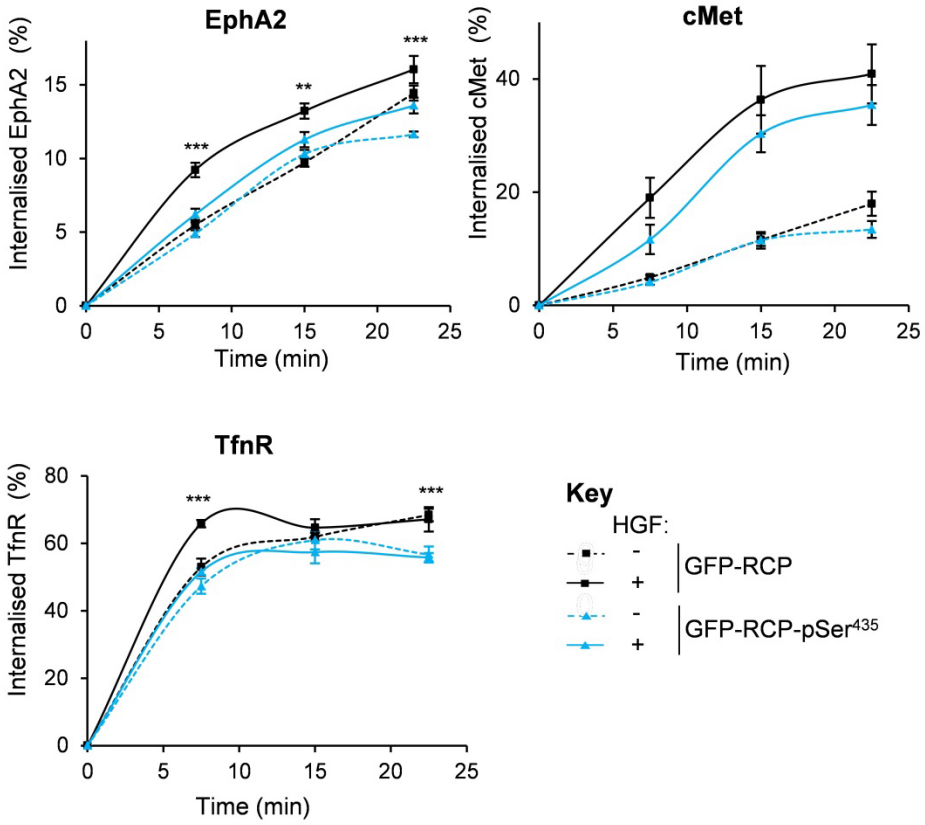

Figure 4-31 Expression of an unphosphorylatable mutant of RCP, GFP-RCP^{S435A}, reduces HGF-driven EphA2 trafficking
H1299 cells were transfected with GFP-RCP and GFP-RCP^{S435A}. Transfected H1299 cells were surface labelled with 0.13mg/ml sulfo-NHS-SS-biotin for 30 minutes at 4ºC. Internalisation of cell surface protein was allowed for the indicated time points in DMEM media with 10ng/ml HGF/mock stimulation at 37ºC. Biotin was removed from proteins on the plasma membrane by incubating the cells in 20mM MesNa for 30 minutes at 4ºC. This reaction was quenched by the addition of 20mM IAA for a further 10 minutes. Biotinylated-EphA2, cMet, and TfnR were detected by capture-ELISA using microtiter wells coated with the appropriate targeted monoclonal antibodies. Internalized proteins are plotted as a proportion of the total labelled protein at the indicated time points. The graphs show the averages and SEM of 6 replicates of 3 separate experiments. Two way Anova statistical tests were performed and any significant difference, between GFP-RCP and GFP-RCPS435A transfected and HGF stimulated cells, is indicated on the graph (*:p<0.05, **:p<0.01, ***:p<0.001).

Next I sought to determine whether phosphorylation of RCP at Serine^{435} influenced EphA2-dependent scattering. Despite indications that expression of GFP-RCP in H1299 cells drove a small but significant increase in HGF-independent cell scattering, GFP-RCP-expressing cells scattered efficiently in response to HGF addition **(Figures 4.32B, 4.33A/B/D)**. However, expression of GFP-RCP^{S435A} inhibited the ability of HGF to drive cell scattering and this was significant when quantified by the colony-scoring **(Figures 4.32)** and cell tracking approaches **(Figure 4.33)**. Taken together, these data indicate that HGF drives phosphorylation of RCP at Serine^{435} to promote EphA2 trafficking, which, in turn, contributes to the ability of cells to move away from one another as they scatter.

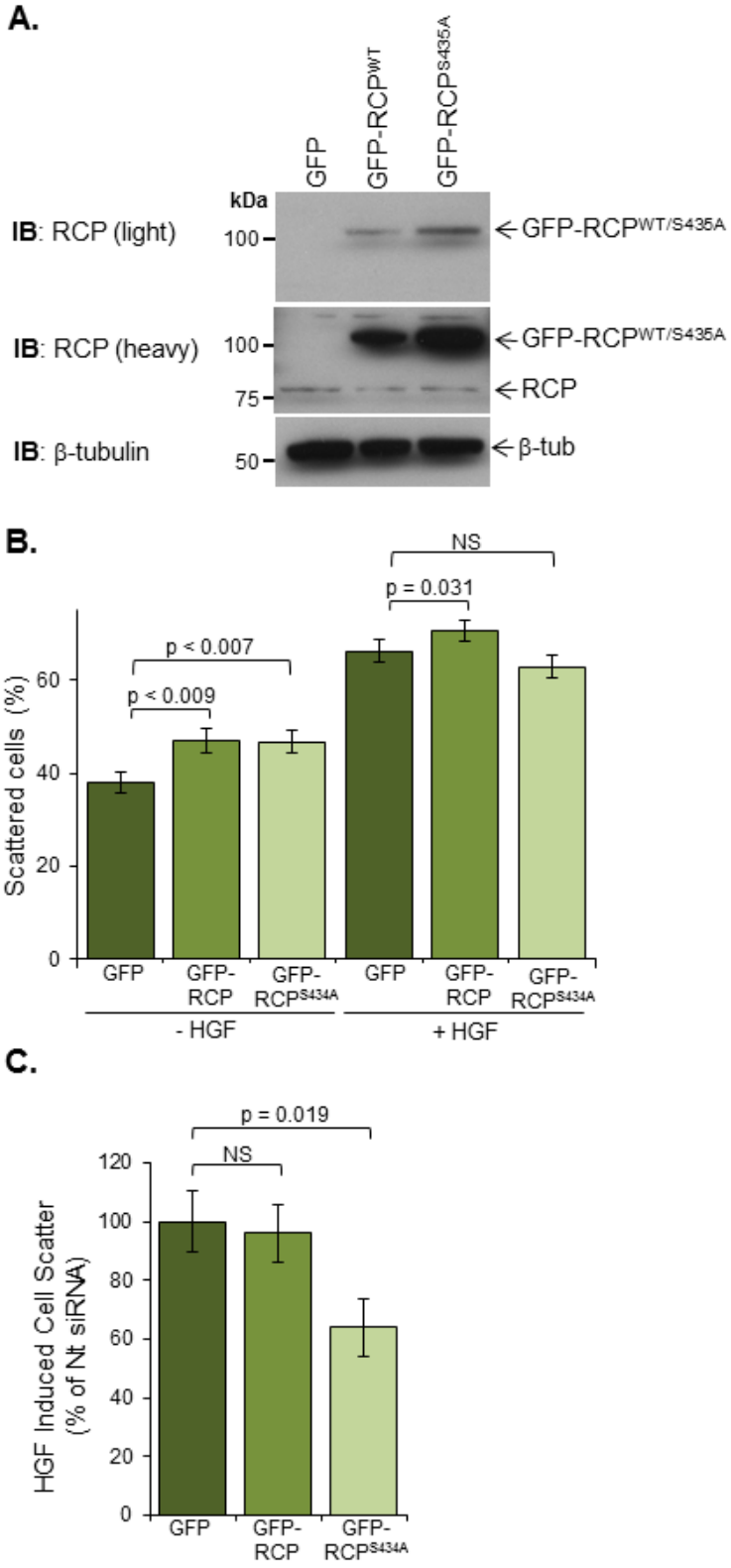

Figure 4-32 Expression of an unphosphorylatable mutant of RCP, GFP-RCP^{S435A}, reduces HGF-driven cell scattering

H1299 cells were transfected with GFP, GFP-RCP and GFP-RCP^{S435A} and seeded sparsely. A. Proteins were extracted 48 hours after transfection. GFP, RCP and β-tubulin were detected by Western blotting. B/C. 10ng/ml HGF/mock was added to the cells, 43 hours after transfection. After 6 hours of HGF addition, representative pictures were taken from each condition. B. The percentage of scattered cells is represented graphically. C. HGF-induced cell scatter was calculated by subtracting the untreated value from the HGF treated value for each condition, and normalising to the GFP control. 15 pictures from 3 separate experiments were analysed. Statistical analysis was performed using a Mann-Whitney test and p-values are shown.

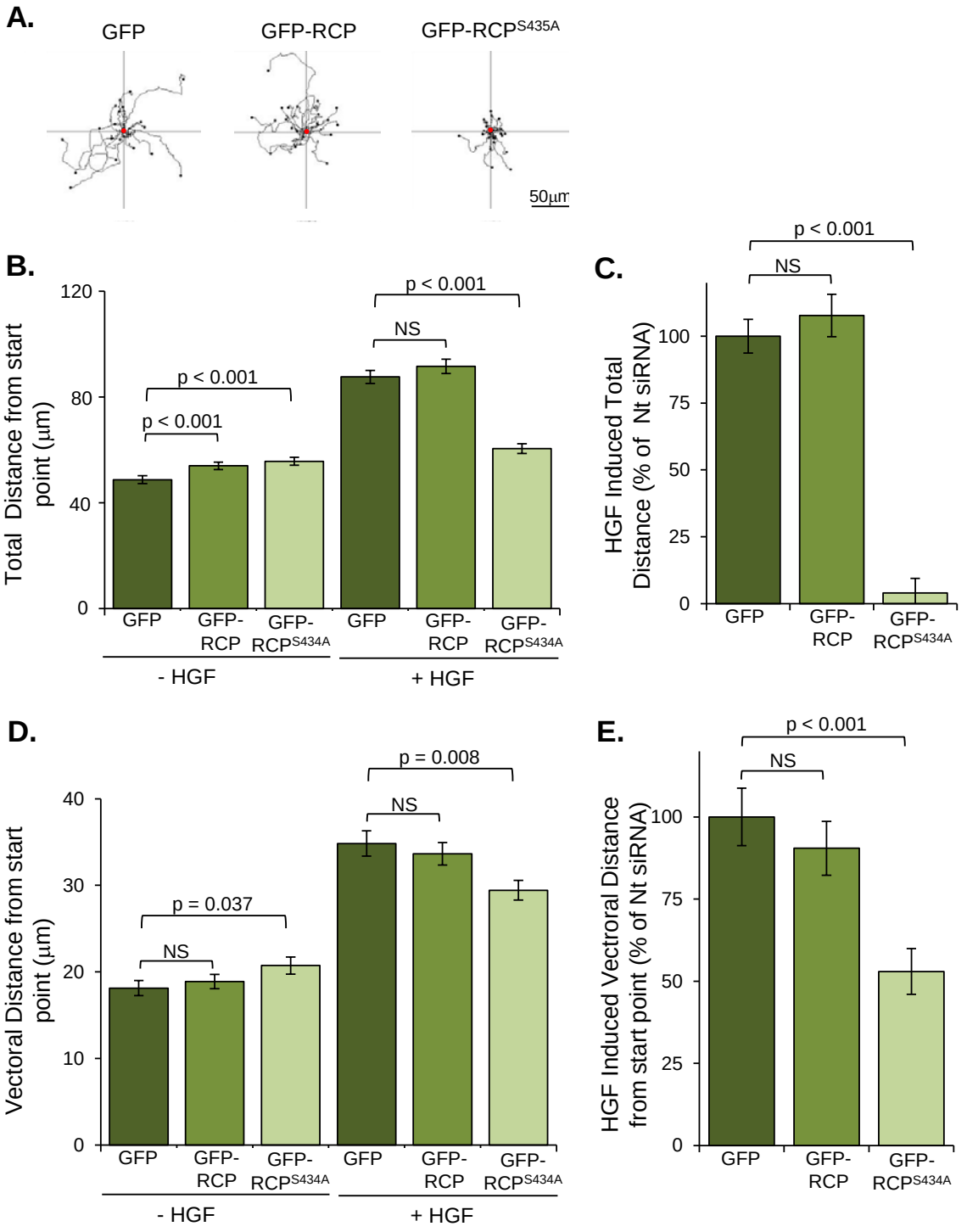

Figure 4-33 Expression of an unphosphorylatable mutant of RCP, GFP-RCPS435A, reduces the speed and distance of cell migration upon HGF addition
H1299 cells were transfected with GFP, GFP-RCP and GFP-RCPS435A and seeded sparsely. The cells were recorded by time-lapse microscopy, 43 hours after transfection when 10ng/ml HGF/mock was added. A. Representative tracks of cell migration are shown with HGF addition for the first 6 hours. The total distance (B), HGF-induced total distance (C), vectorial distance (D) and HGF-induced vectorial distance (E) are represented graphically. The HGF-induced cell speed and distance were calculated by subtracting the untreated value from the HGF treated value for each condition, and normalising to the GFP control. Cells were tracked from 8 different regions on the plate from 3 separate experiments. Statistical analysis was performed using a Mann-Whitney test and p-values are shown.

4.2.11 Knockout of EphA2 or RCP reduces liver metastasis in a mouse model of PDAC.

Having identified a clear role for EphA2 and its RCP-dependent trafficking in cell-cell repulsion and cell scattering, I sought to determine whether this RTK contributes to invasion and metastasis. To do this, an autochthonous model of metastatic PDAC was chosen (described in **Section 4.1.3)**. The *EPHA2* gene, which is located on chromosome 1p36, has previously been disrupted in mice, and these animals were obtained from the Jackson Laboratory (Brantley-Sieders et al., 2004). EphA2$^{-/-}$ mice are viable and have no overt developmental abnormalities. The morphology of the pancreas was found to be unaffected by disruption of the *EPHA2* gene. Therefore, EphA2$^{-/-}$ mice were crossed into the KPC (Pdx1-Cre, Kras$^{G12D/+}$, p53$^{R172H/+}$) PDAC model by my collaborator Bryan Miller **(Figure 4.34A)**. Disruption of the *EPHA2* gene did not oppose initiation or growth of primary PDAC in the KPC mice. In fact, PDAC formation was increased in EphA2$^{-/-}$ mice, and this was reflected in decreased survival of the knockout animals **(Figure 4.34B/C)**, as it is the growth of the primary tumour and the resulting gastrointestinal complications, rather than the incidence of metastasis, that dictate survival in the KPC model of PDAC. We then investigated the incidence of liver metastasis in KPC EphA2$^{+/+}$, KPC EphA2$^{+/-}$ and KPC EphA2$^{-/-}$ animals by examination of the liver and staining sections of this tissue with H&E. In these experiments liver metastases were observed in 33% of control tumour-bearing animals (KPC EphA2$^{+/+}$) and this was unaffected by loss of one allele of EphA2 (KPC EphA2$^{+/-}$) indicating that this RTK exhibits haplosufficieny in the context of PDAC metastasis **(Figures 4.34D)**. Moreover, KPC EphA2$^{-/-}$ mice had reduced incidence of liver metastasis indicating a possible role for this RTK in the dissemination of PDAC *in vivo.*

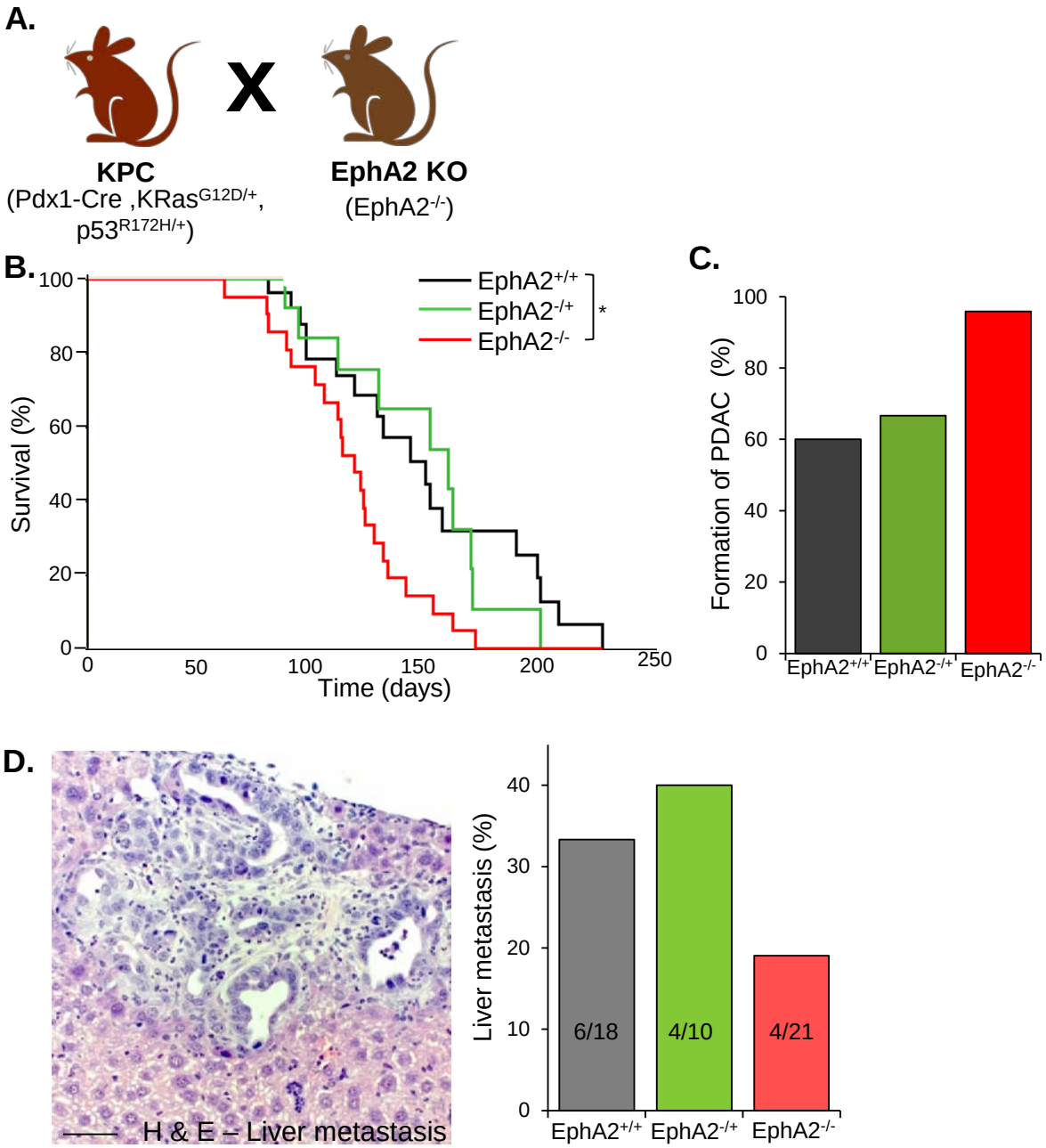

Figure 4-34 KPC EphA2$^{-/-}$ mice have reduced survival, increased formation of PDAC and decreased liver metastasis

A. KPC (Pdx1-Cre, Kas$^{G12D/+}$, p53$^{R172H/+}$) mice were crossed with EphA2$^{-/-}$ mice. B. The survival of KPC EphA2$^{+/+}$ mice, KPC EphA2$^{-/+}$ mice and KPC EphA2$^{-/-}$ mice was represented by a Kaplan-Meier curve. Statistical analysis was performed using log-rank tests (*:p=0.03). Mice that succumbed but did not develop PDAC were excluded. C. The percentage of mice that developed PDAC is represented graphically. D. Representative image of a liver metastasis stained with hematoxylin and eosin (H&E). The number of mice that had detectable liver metastasis is plotted as a percentage. Scale bar is 50µm. This work was performed by Bryan Miller.

Given that I have established a role for RCP in EphA2 trafficking and function, I wished to determine whether this Rab effector contributes to metastasis of PDAC. First, I sought to determine whether RCP was expressed in pancreatic tissue, pancreatic intraepithelial neoplasms (PanINs) and PDACs. Slices of normal mouse pancreas, KPC PanINs and KPC PDACs were stained by immunohistochemistry with an antibody that recognises mouse RCP. In PanINs the expression of RCP appeared to be localised to the apical region of neoplasms that displayed some glandular structure, but was also present as a diffuse staining in the more dysplastic PanINs (**Figure 4.35B)**. In PDAC, RCP expression was markedly elevated and RCP-positive structures were distributed throughout the cells of the tumours **Figure 4.35D**. To ensure the specificity of the RCP staining in PanINs, a pre-absorption control is displayed in **Figure 4.35C** demonstrating the specificity of the staining.

Next, an inducible RCP KO mouse was generated that contains a Neomycin cassette flanked by Lox sites following exon 2 of RCP in the mouse genome by the Beatson Transgenic Services (**Figure 4.36A).** Recombination of the Lox sites induces a frameshift mutation resulting in the transcription of a non-functional translation product. To determine whether RCP expression is diminished in the presence of Cre- recombinase, mouse embryonic fibroblasts (MEFs) were extracted and Western blot analysis demonstrated that RCP levels were suppressed in cells treated with Adeno-Cre (**Figure 4.36B**). $RCP^{fl/fl}$ mice are viable and had no obvious developmental abnormalities, so they were crossed into the KPC (Pdx1-Cre, $Kras^{G12D/+}$, $p53^{R172H/+}$) PDAC model **(Figure 4.36C)**. Immunohistochemistry staining of tumour tissue from these mice demonstrated that RCP expression was efficiently depleted in PDAC from these mice (**Figure 4.35D**). Most interestingly, KPC $RCP^{fl/fl}$ and KPC $RCP^{fl/+}$ mice had fewer metastases in the liver (**Figure 4.36E**), however no difference in survival was detected (**Figure 4.36D**).

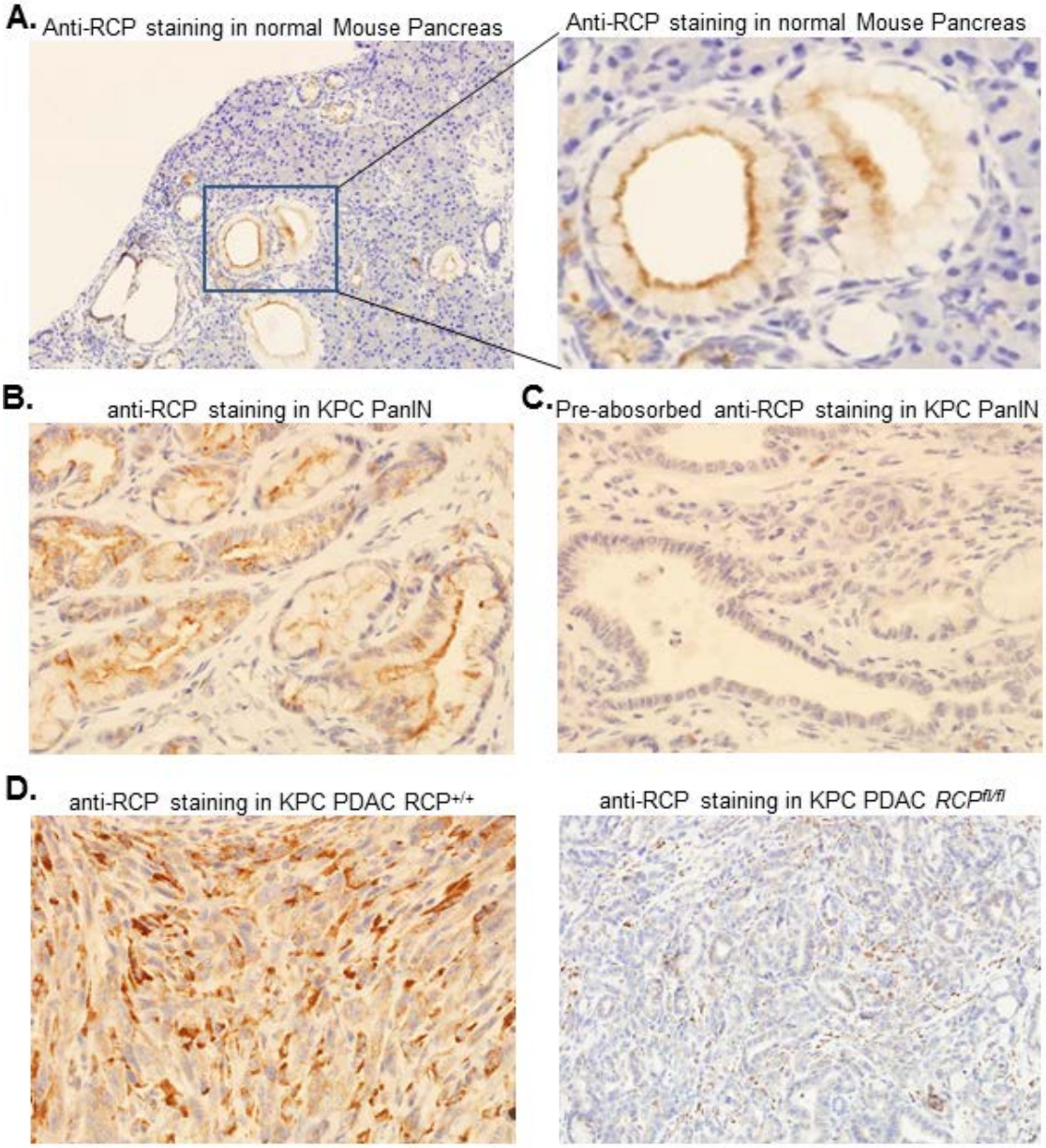

Figure 4-35 RCP is highly expressed in KPC PanINs and PDAC
A/B. Immunohistochemistry images using anti-RCP antibody on tissue sections of normal mouse pancreas (A) and PanINs from KPC mice (B). C. Tissue sections of PanINs from KPC mice were stained with anti-RCP antibody that was pre-absorbed with GST-RCP. D. Immunohistochemistry images of KPC $RCP^{+/+}$ and KPC $RCP^{fl/fl}$ PDAC stained with anti-RCP antibody. This work was performed by Joan Grindlay.

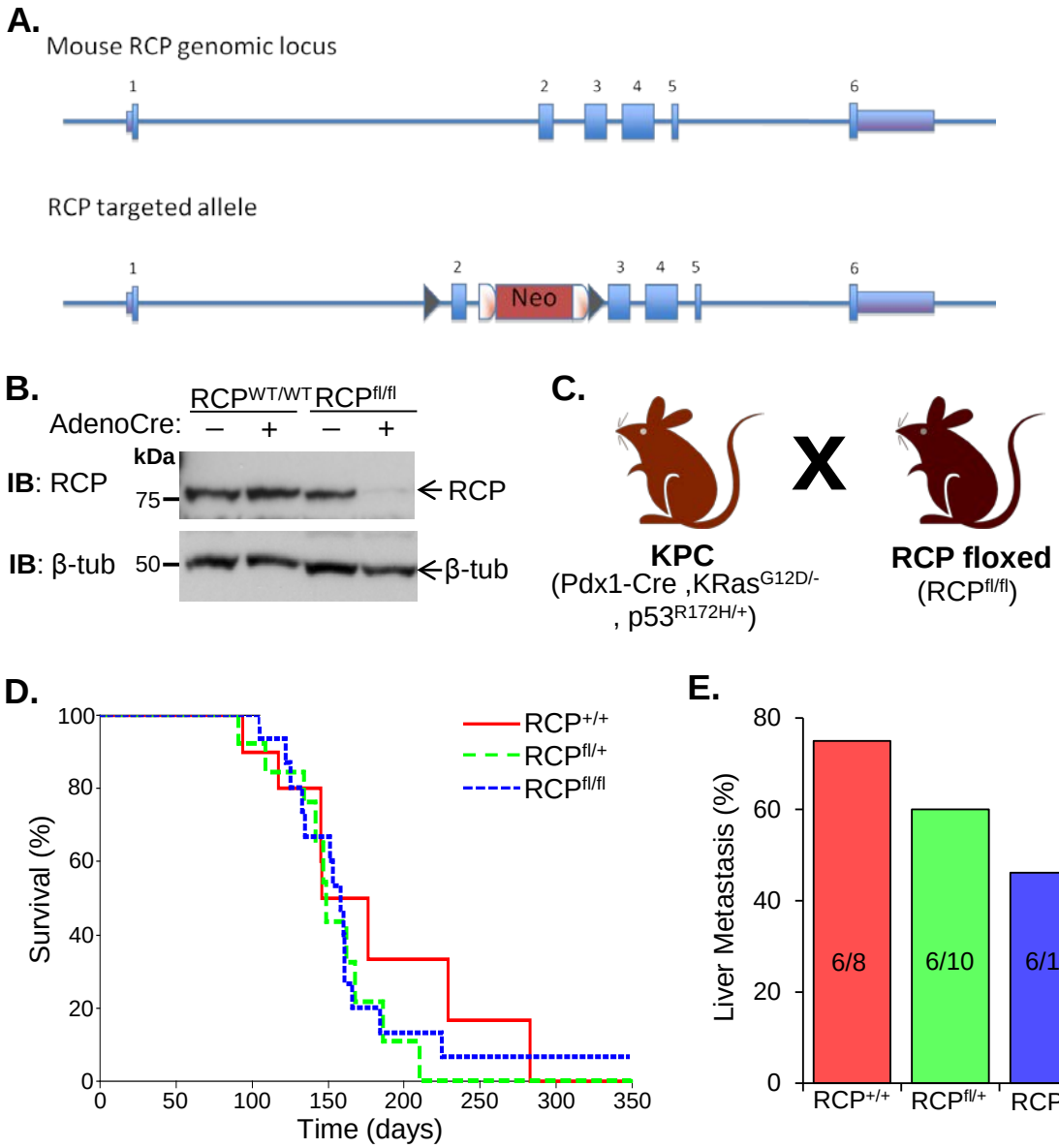

Figure 4-36 KPC RCP$^{fl/fl}$ mice have reduced liver metastasis
A. Schematic representation of the strategy for the generation of RCP$^{fl/fl}$ mice. B. Mouse embryonic fibroblasts (MEFs) were taken from the RCP$^{+/+}$ and RCP$^{fl/fl}$ mice and treated with Adeno-Cre. The cells were lysed and subjected to SDS-PAGE and immunoblot analysis using anti-mouse-RCP and anti-β-tubulin antibodies. C. KPC (Pdx1-Cre, Kas$^{G12D/+}$, p53$^{R172H/+}$) mice were crossed with RCP$^{fl/fl}$ mice. D. The survival of KPC RCP$^{-/-}$, KPC RCP$^{fl/+}$ and KPC RCP$^{fl/fl}$ mice was plotted in a Kaplan-Meier curve. Statistical analysis was performed using log-rank tests and no significant differences were found. Mice that succumbed but did not develop pancreatic cancer were excluded. E. The number of mice that had detectable liver metastasis is plotted as a percentage of total mice. This work was performed by Joan Grindlay.

4.2.12 Knockout of EphA2 and RCP oppose KPC PDAC cell invasion *in vitro*

To determine whether the reduced metastasis in EphA2$^{-/-}$ and RCP$^{fl/fl}$ animals is due to cell autonomous effects on PDAC cell invasion, I derived cell lines from several pancreatic tumours. Primary PDACs from KPC WT, KPC EphA2$^{-/-}$ and KPC RCP$^{fl/fl}$ mice were examined and placed in culture for several weeks until the tumour cells continued to grow. The resulting cell lines expressed Cre-recombinase (as determined by RT-PCR), confirming that their cells of origin were from the pancreas and not from a tumour-associated stromal lineage. Moreover, Western blotting confirmed the knockout of RCP and EphA2 in these PDAC cell lines (**Figure 4.37A**), and interestingly there were indications that RCP-depleted cells had reduced levels of EphA2, perhaps indicating a requirement for RCP dependent trafficking in the maintenance of cellular levels of EphA2. RCP and EphA2 knockout KPC-PDAC cell lines proliferated at rates that were similar to the KPC WT controls, indicating that EphA2 and its trafficking does not influence cell growth (**Figure 4.37B**).

I then proceeded to investigate the migratory and invasive properties of these PDAC lines. Cells derived from KPC WT PDAC tumours were found to grow as loose colonies in which cells did not appear to form stable junctions. It was normally possible to see substantial spaces between cells within the same loose colonies and many migratory cells at the colonies' edges. By contrast, cells from RCP and EphA2 knockout tumours grew in closely-knit colonies with a defined edge and there was very little indication that these cells were able to migrate away from the colonies (**Figure 4.37C**). Next, I sought to determine whether cell lines derived from EphA2 and RCP knockout tumours had altered ability to invade into Matrigel towards an HGF gradient. The two cell lines derived from KPC WT tumours invaded efficiently into Matrigel as previously shown by Timpson et al. (2011) (**Figure 4.38**). By contrast, cell lines from KPC EphA2$^{-/-}$ and KPC RCP$^{fl/fl}$ tumours had severely reduced capability to invade into Matrigel (**Figure 4.38**). These data indicate that expression of both EphA2 and RCP is necessary for PDAC cells to assume a scattered and invasive phenotype, consistent with the role that I had described for RCP-mediated EphA2 trafficking in cell scattering.

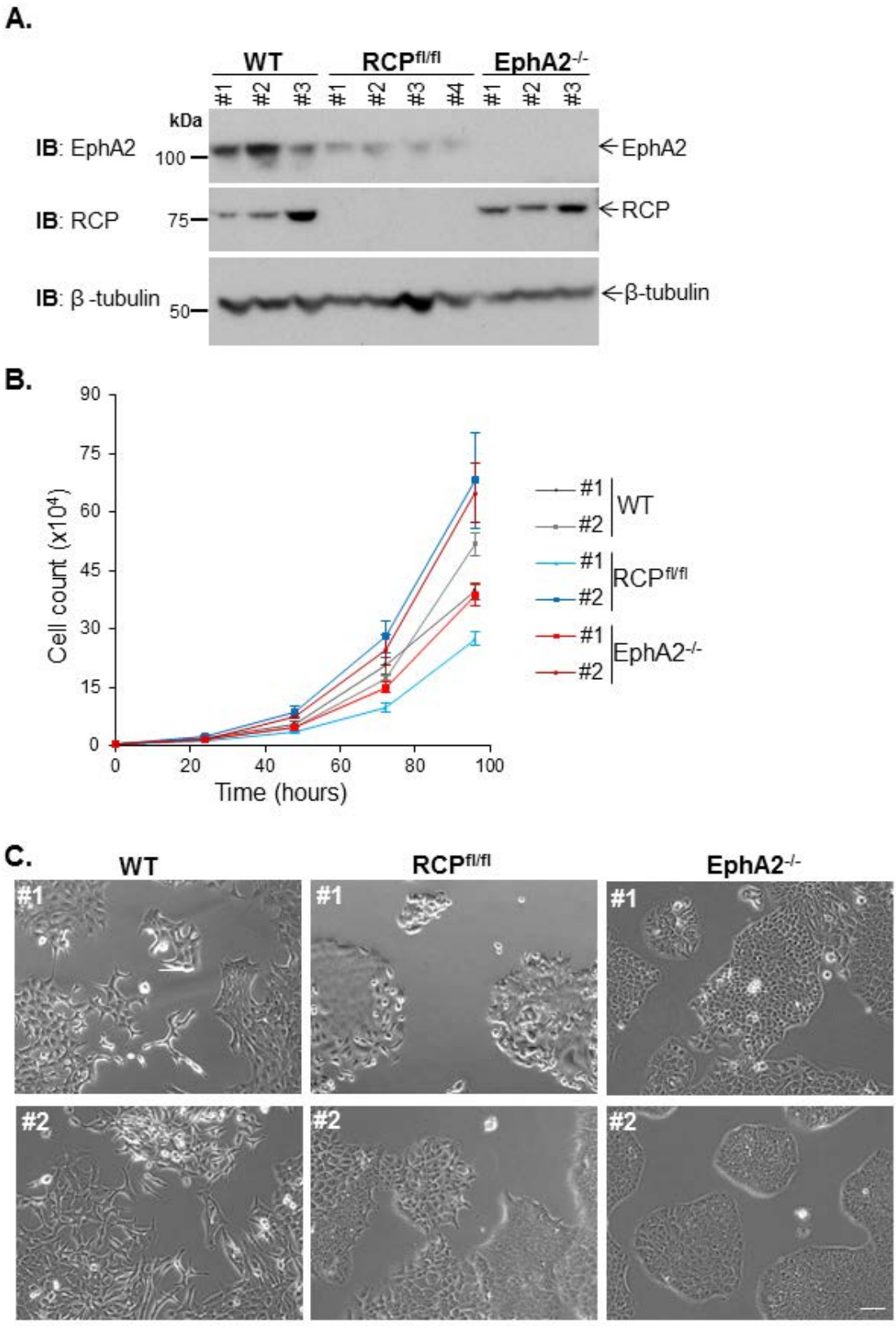

Figure 4-37 Cells derived from KPC EphA2$^{-/-}$ and KPC RCP$^{fl/fl}$ PDAC have a less scattered phenotype

Cells lines were derived from KPC WT, KPC EphA2$^{-/-}$ and KPC RCP$^{fl/fl}$ PDAC. A. The cells were lysed and the proteins subjected to SDS-PAGE and Western blotting analysis using anti-mouse-RCP, anti-EphA2 and anti-β-tubulin antibodies. B. These cells were seeded onto plates and counted using a Casy cell counter at the appropriate times. Cell number is represented graphically. The graphs show the averages and SEM of 6 replicates of 2 separate experiments. C. Representative images of the cells with a scale bar of 100µm.

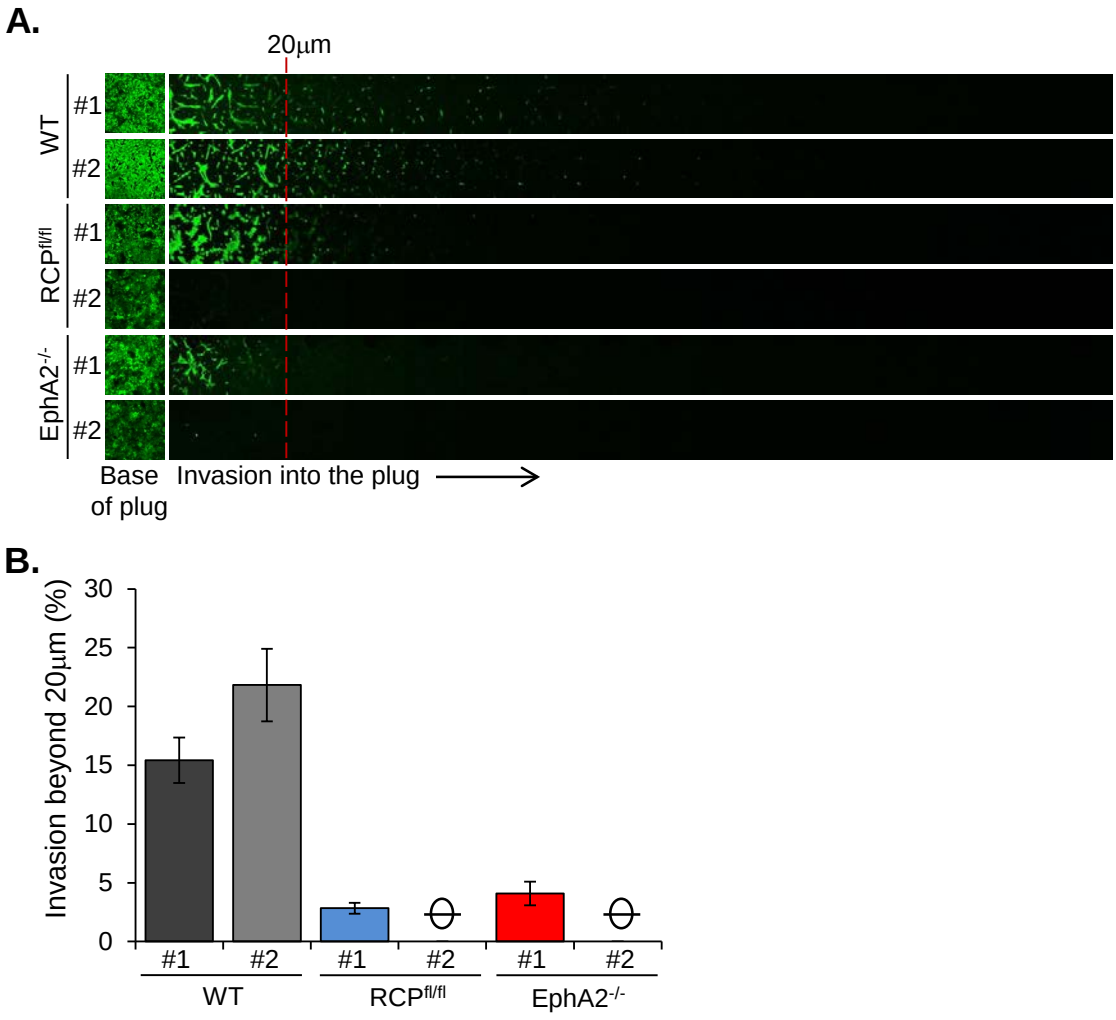

Figure 4-38 Cells derived from KPC EphA2$^{-/-}$ and KPC RCP$^{fl/fl}$ PDAC are less invasive than those derived from KPC WT PDAC

Cells lines were derived from KPC WT, KPC EphA2$^{-/-}$ and KPC RCP$^{fl/fl}$ PDAC. These cells were plated onto the underside of transwells containing Geltrex plugs enriched with 25µg/ml fibronectin. Cells migrated up towards HGF-supplemented serum-rich media for 72 hours. Cells were stained with Calcein-AM and visualised by confocal microscopy. A. Optical sections were taken every 10µm and consecutive images were assembled from left to right. B. The average cell invasion beyond 20µm was quantified. The graph shows the averages and SEM of 18 regions in six transwell plugs from three separate experiments.

4.3 Discussion

Having identified and confirmed an association between endogenous EphA2 and RCP (**Section 3.2.4**), I sought to find the functional significance of this interaction. Indeed, I have demonstrated that RCP has a role in the trafficking of EphA2 between the plasma membrane and a Rab14-positive internal compartment. Using a transgenic mouse model of PDAC we have shown that both EphA2 and RCP contribute to liver metastasis. Since *in vitro* cell invasion is reduced in PDAC cells derived from EphA2 or RCP knockout mice, these effects are anticipated to be cell autonomous. It is possible that the effects on metastasis and cell invasion are influenced by the requirement of EphA2 and RCP for CIL and cell scattering, which has been demonstrated in human cancer cell lines. Furthermore, the roles of EphA2, RCP and Rab14 in CIL and cell scattering maybe specific, as expression of other RCP-associated Rab GTPases and Rab11-Fips are not required for these phenomena. From the data shown in this chapter, I postulate that HGF treatment activates a kinase responsible for phosphorylating RCP on Serine^{435}. RCP phosphorylation recruits EphA2 and Rab14 into a co-immunoprecipitable complex in a vesicular compartment, slowing the return of EphA2 back to the plasma membrane and promoting cell-cell repulsion. I speculate that this HGF-dependent change in EphA2 trafficking may alter downstream signalling of this receptor which drives cell-cell repulsion events (**Section 5.2.2**).

4.3.1 Contact inhibition of locomotion

CIL was originally defined by Abercrombie as 'the stopping of the continued locomotion of a cell in the direction which has produced a collision with another cell' (Abercrombie, 1979). This definition has been subsequently elaborated to describe not just contact inhibition, but also includes the formation of new lamellipodia and subsequent cell migration (Mayor and Carmona-Fontaine, 2010). For interpreting and quantifying my results, however, I have not found the more recent description of CIL useful. Also, I have found some technical problems with the contact acceleration index, Cx, which some previous studies have used to analyse CIL. This index uses several parameters, including the vectorial distance a cell moves 40 minutes before and after a collision, and the angle of change in direction upon a collision. I observed that PC3 cells migrate

with low persistence, so the vectorial distance does not reflect the total path length of cell migration. Furthermore, the angle is influenced not only by the collision, but also by random changes in the direction of cell migration in the 40 minute periods. Therefore, I simplified my analysis by measuring the time that the cells remain in contact before migrating away from the collision site. Knockdown of RCP or Rab14 increased the time cells remained in contact before migrating away from one another. This indicates that RCP and Rab14 do not affect contact inhibition per se, but are required for cell-cell repulsion after two cells have collided. As I have shown that EphA2, RCP and Rab14 are also required for HGF-driven scattering, this suggests that these proteins may have an important role in tumour dissemination.

4.3.2 Proteolytic cleavage

Rab14 delivers ADAM10 to the plasma membrane where the protease cleaves N-cadherin, thereby promoting cell junction disassembly and cell migration (Linford et al., 2012). In H1299 cells, N-cadherin levels are not altered by the suppression of Rab14 expression, suggesting that this mechanism does not account for the defects in scattering of H1299 cells depleted of Rab14 expression. EphA2 is cleaved by MMP-MT1 internalisation of membrane-bound EphA2 to activate Src and RhoA, thereby promoting single cell migration (Sugiyama et al., 2013). These studies led me to hypothesise that Rab14 may deliver a protease to the plasma membrane to cleave EphA2 and trigger this RTK's internalisation, thereby activating downstream signalling proteins and cell-cell repulsion. However, upon further investigation, no cleaved EphA2 products were observed after siRNA of RCP or HGF treatment, nor were any reductions in full-length EphA2 protein detected. Furthermore, only full-length EphA2 was detected in a co-immunoprecipitable complex with GFP-RCP, and no cleaved EphA2 products were detected in the trafficking assay by Western blotting. As there is no evidence that EphA2 was cleaved in these cells, and I found that full-length EphA2 associated with both RCP and Rab14, I propose an alternative mechanism for the involvement of EphA2, RCP and Rab14 is HGF-driven cell scattering.

4.3.3 Diversion of EphA2 trafficking

In H1299 cells, EphA2 is in rapid flux between the plasma membrane and internal compartments. I postulate that HGF treatment diverts EphA2 from a rapid recycling route into a slower pathway that proceeds via an RCP/Rab14-positive compartment (**Figure 4.39**). This hypothesis is supported by my experimental data showing that HGF increases the size of the EphA2 internal pool in an RCP- and Rab14-dependent fashion. Further investigation revealed that this change is not due to increased internalisation, but a delay in EphA2 recycling back to the plasma membrane. Moreover, I have shown that the addition of HGF increases EphA2 co-localisation with RCP and Rab14 in stable vesicular structures. It has recently been proposed that Rab14 has a role in recycling ADAM10 and transferrin from (Rab4- and Rab5-positive) early endosomes back to the plasma membrane (Linford et al., 2012). Consistent with this work, I have found that Rab14 is required for EphA2 recycling, suggesting that EphA2 is another cargo for the Rab14 recycling pathway.

In this work EphA2 trafficking was analysed using a biotin-labelling based approach. The main drawback of this assay is that it gives only an indirect snapshot readout of EphA2 recycling. To confirm that HGF alters EphA2 trafficking in an RCP-dependent fashion, further experiments should be performed, for example 17ºC temperature blocks or photoactivatable approaches could be used. At 17ºC receptors are accumulated in endosomes as a number of recycling pathways are inhibited whilst endocytosis proceeds (Song et al., 1994). When cells are returned to 37ºC recycling of these receptors can be measured. Alternatively, it would be interesting to study EphA2 recycling by photo-activating paGFP-EphA2 in vesicles and using time-lapse microscopy to visualise its trafficking back to the plasma membrane (Caswell et al., 2007). Futhermore, this approach could be used to visualise how HGF alters EphA2 recycling.

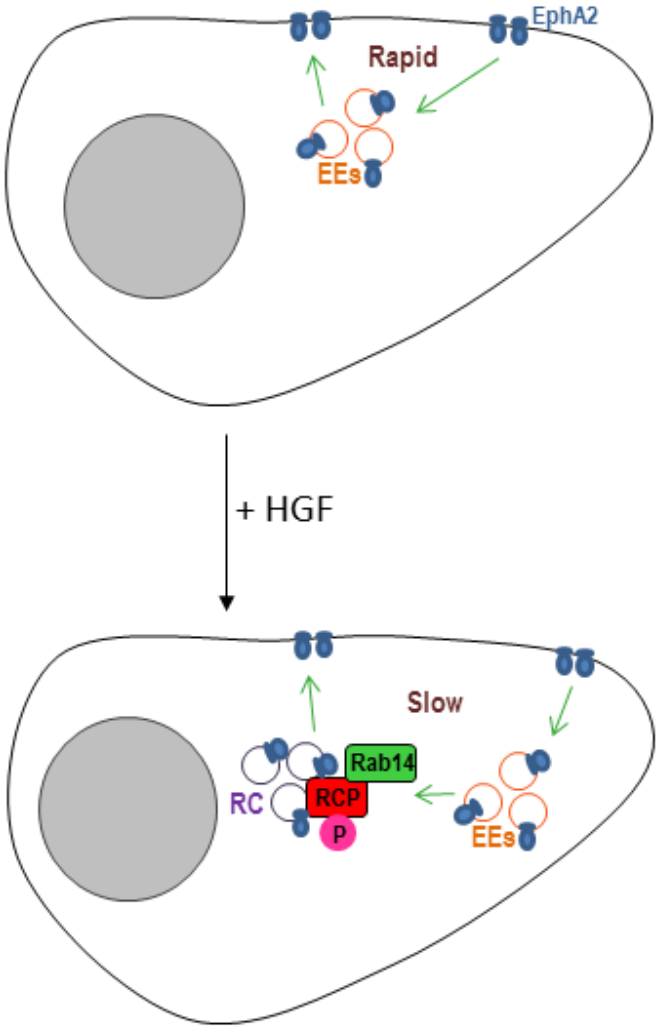

Figure 4-39 Working model of EphA2 trafficking
In untreated cells EphA2 is in rapid flux between the plasma membrane and an internal compartment. HGF addition diverts EphA2 into an RCP- and Rab14-rich compartment, and delays EphA2 recycling to the plasma membrane (EE: early endosomes, RC: recycling compartment).

4.3.4 RCP phosphorylation

Rab14 and Rab11 have recently been proposed to associate with RCP at distinct neighbouring sites (Qi et al., 2013). Indeed, mutating RCP on Serine^{580} and Serine^{582} disrupts Rab14 association, but has little effect on Rab11 binding (Qi et al., 2013). Several other Rab effector proteins have been shown to have several binding domains for different GTPases, for example, Fip3 associates with both Arf6 and Rab11 (Fielding et al., 2005) and Rabaptin5 associates with both Rab4 and Rab5 (Christoforides et al., 2012). Most interestingly, in migrating cells PKD phosphorylates Rabaptin5 at Serine^{407} favouring Rab4 association over Rab5

(Christoforides et al., 2012). Consistent with this, I have shown that phosphorylation of RCP on Serine^{435} enhances RCP's association with Rab14, but has little effect on Rab11 binding. Thus it is probable that phosphorylation of Rab effectors may alter the trafficking routes of cargo by influencing the Rab GTPase they associate with. Phosphorylation of RCP could either provide a phosphor-specific site for Rab14, or alter intramolecular interactions to remodel the structure of the protein to expose a Rab14-binding site. X-ray crystallography would be required to determine the exact nature of the association and how phosphorylation affects it. I postulate that phosphorylation of RCP is key in altering Rab GTPase association and thereby regulating the trafficking of EphA2 during cell-cell repulsion. Further work is required to determine how altering EphA2 trafficking contributes to cell-cell repulsion (**Section 5.2**). RCP and EphA2 are required for both PDAC metastasis in a mouse model and scattering/CIL *in vitro,* suggesting that cell-cell repulsion may have an important role in cancer dissemination *in vivo.* Further work is required to examine the role of cell-cell repulsion in PDAC metastasis (**Section 5.4**).

5 Summary and Future Directions

5.1 Summary

The role of EphA2 in tumourigenesis and metastasis has been investigated previously by ablating EphA2 expression in several transgenic mouse models. For example, EphA2 deficiency impairs tumourigenesis and reduces metastasis in a ErbB2-overexpressing breast cancer model (Brantley-Sieders et al., 2008), and reduces the number and size of tumours in the $APC^{Min/+}$ colorectal model (Bogan et al., 2009). Since EphA2 is often upregulated in human PDAC (Mudali et al., 2006), we crossed $EphA2^{-/-}$ mice into a transgenic mouse model of PDAC. In contrast to the breast and colon models, EphA2 does not reduce the formation of primary tumours (in fact it increases tumour formation), but does reduce liver metastasis. As I have shown that EphA2 associates with RCP, and that it is recycled through an RCP-positive compartment during cell scattering, we investigated RCP's role in PDAC tumourigenesis and metastasis. Like EphA2, ablation of RCP expression in the PDAC model reduces liver metastasis, but has no effect on primary tumour formation. Since EphA2 and RCP are required for cell-cell repulsion, I propose that this phenomenon may be involved in PDAC tumour dissemination *in vivo*. Rab14 is also required for cell-cell repulsion, however other RCP-associated Rab GTPases are not. Interestingly, HGF addition increases RCP phosphorylation on $Serine^{435}$, and enhances the association and co-localisation of EphA2, RCP and Rab14. This phosphorylation is required for cell scattering, so the kinase responsible for it is likely to have a role in cell-cell repulsion events. In summary, I propose that HGF addition activates a kinase that phosphorylates RCP, thereby diverting internalised EphA2 into an RCP/Rab14-positive compartment, thus stimulating cell-cell repulsion (**Figure 5.1**).

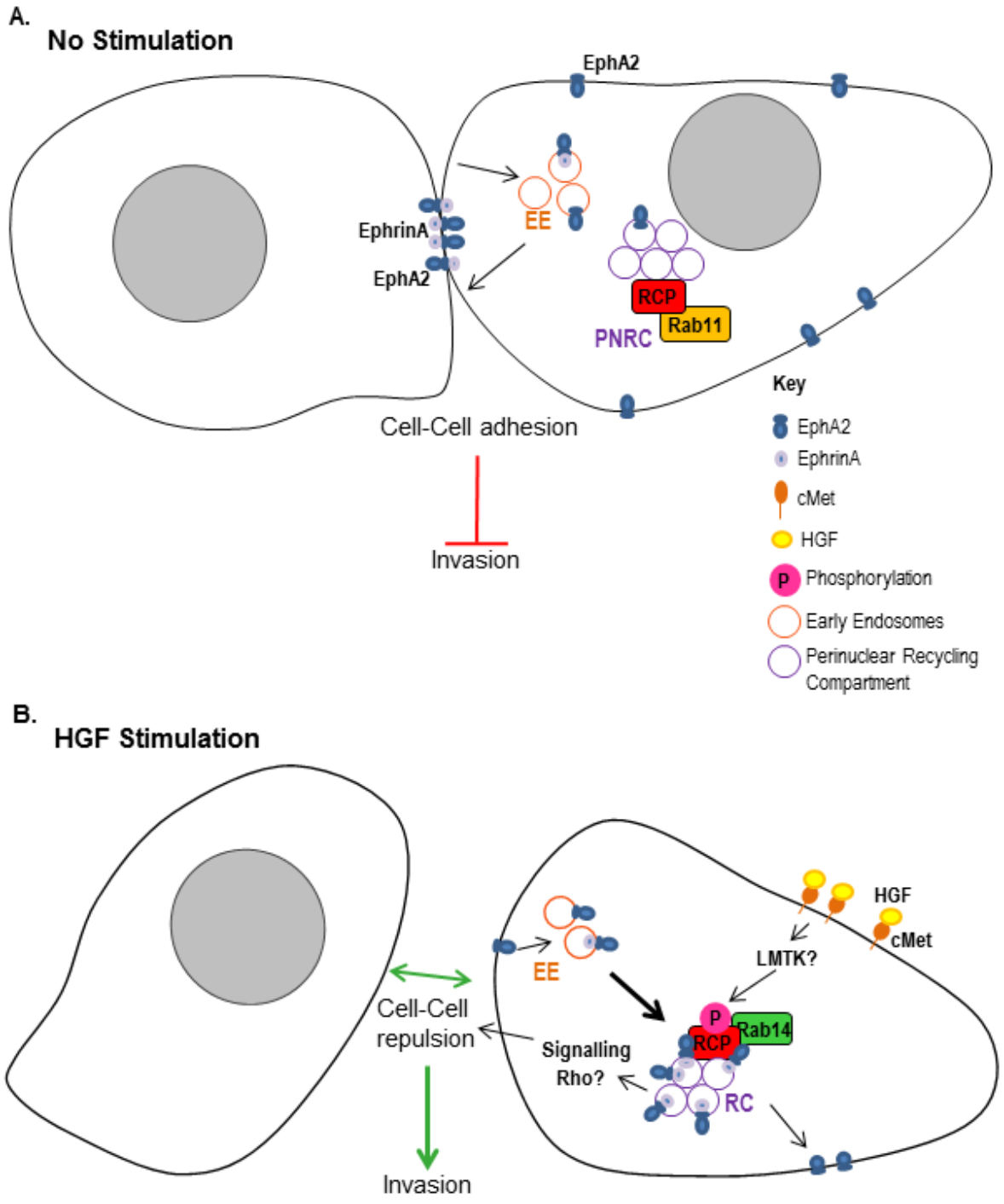

Figure 5-1 Working model of EphA2 trafficking during HGF driven cell-cell repulsion
A. EphA2 is in constant flux between the plasma membrane and an internal compartment. These cells remain attached and invade poorly. B. HGF increases RCP phosphorylation by LMTK3, which recruits Rab14 into a recycling compartment. EphA2 is internalised into this compartment, which stimulates cell-cell repulsion and results in a more invasive phenotype.

5.2 Future Directions

5.2.1 Which kinases phosphorylate RCP?

Two kinases were found associated with RCP in proteomic screens (Peter van den Berge & Patricia Muller, unpublished): CK2, a pleiotropic, ubiquitous and constitutively active kinase often overexpressed in tumours (Piazza et al., 2012); and LMTK2, a transmembrane kinase that colocalises with Rab11 in endosomes (Takano et al., 2012). The Serine/Threonine Lemur Tyrosine Kinase (LMTK) family has three members: LMTK1/AATK1, LMTK2/BREK and LMTK3. In human breast cancer, high LMTK3 expression correlates with poor disease-free survival and predicts patients' responses to endocrine therapy (Giamas et al., 2011). Furthermore, Giamas et al. (2011) showed that suppressing LMTK3 expression reduces tumour growth in an orthotypic mouse model. Interestingly, LMTK3 has a role in NMDA trafficking (Inoue et al., 2014), while LMTK2 has a role in CFTR trafficking (Luz et al., 2014).

Wang and Brautigan (2006) identified several peptides that LMTK2 phosphorylates, including a sequence contained in CFTR (Wang and Brautigan, 2006). Most interestingly, this sequence is very similar to RCP's phosphorylation site (**Figure 5.2**), suggesting it is a good candidate as an RCP kinase. Therefore, I performed some preliminary experiments using siRNA to suppress levels of LMTKs in H1299 cells, to investigate whether these kinases influence phosphorylation of RCP on Serine^{435}. As I have been unable to obtain antibodies recognising LMTKs, I used RT-PCR to confirm suppressed expression of the kinases in H1299 cells (not shown). Knockdown of LMTK3 prevented HGF-induced phosphorylation of RCP; however siRNA of LMTK2 (not shown) and LMTK1 had little effect (**Figure 5.3A**). Consistent with this, co-immunoprecipitation of EphA2, Rab14 and RCP is reduced in cells treated with LMTK3 siRNA (**Figure 5.3**). These data indicate that LMTK3 is activated downstream of HGF and is in itself responsible for RCP phosphorylation on Serine^{435}. Furthermore, preliminary work in the lab has shown that LMTK3 is required for HGF-dependent EphA2 trafficking, RCP-EphA2 co-localisation and cell-cell repulsion events (not shown).

LMTK consensus	RRX**S**ΦΦPD
CFTR$^{734-741}$	RRL**S**LVPD
RCP$^{432-439}$	RRS**S**LLSL

Figure 5-2 Sequence alignment of LMTK's consensus phosphorylation site with potential candidate sequences in CFTR and RCP.
Single amino acid code is used in which X represents any amino acid and Φ represents a hydrophobic amino acid.

LMTK3 has a role in cancer progression of ERα^{+} but not ERα^{-} breast cancer, and is thought to phosphorylate ERα, which prevents the receptor from proteasomal degradation (Giamas et al., 2011). Recently it has been shown that LMTK3 regulates α5β1-integrin expression *in vitro,* and in human breast cancer tumours the expression levels of these proteins positively correlate (Xu et al., 2014). Interestingly, RCP and its phosphorylation are also required for α5β1-integrin trafficking (not shown), which confirms that LMTKs may have a role in regulating α5β1-integrins.

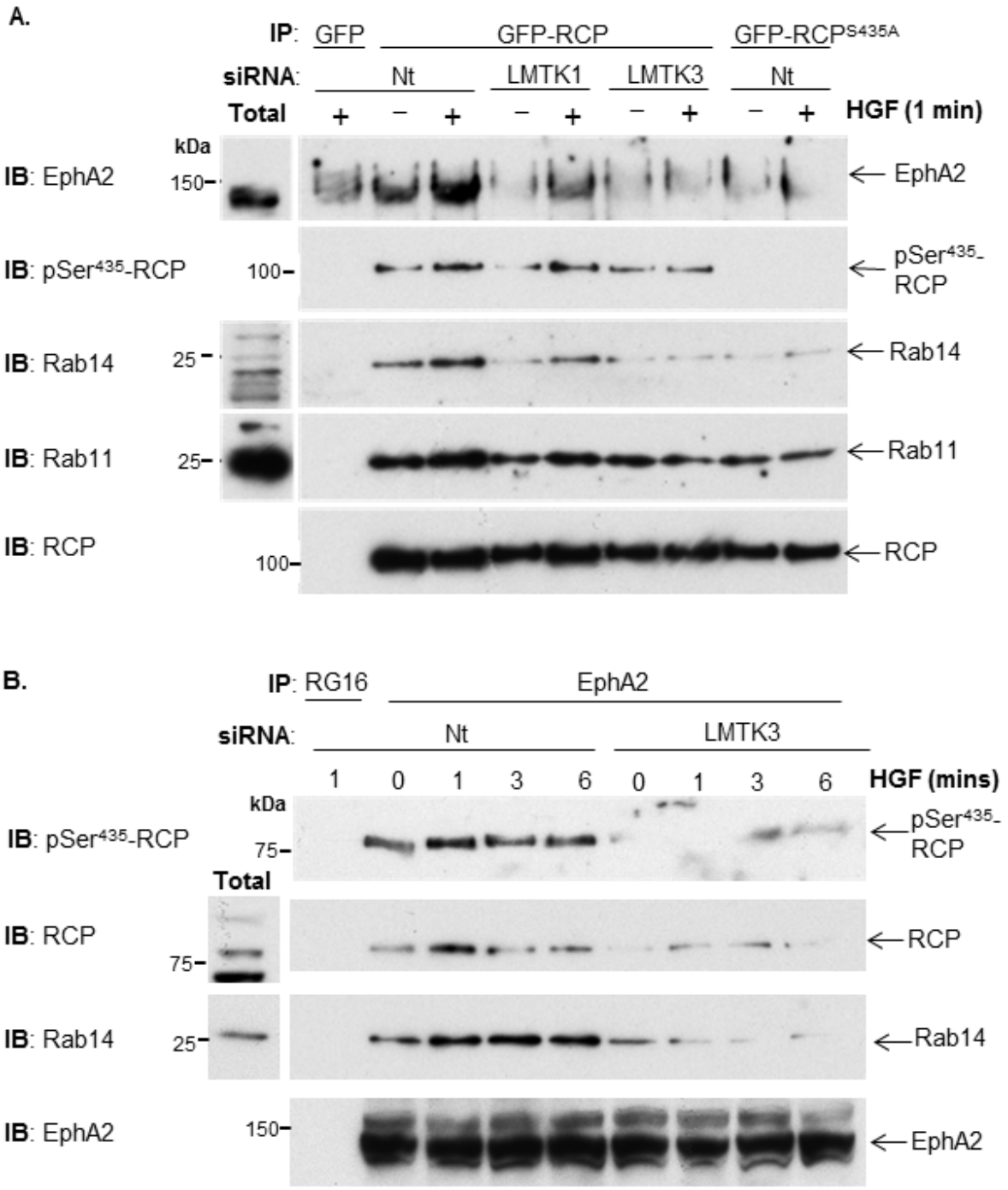

Figure 5-3 Suppression of LMTK3 expression, but not LMTK1, prevents RCP phosphorylation and the association between EphA2, RCP and Rab14
A. H1299 cells were co-transfected with GFP, GFP-RCP or GFP-RCPS435A and LMTK1, LMTK3 or non-targeting siRNA and stimulated with 10ng/ml HGF for the indicated times. The cells were lysed and GFP was immunoprecipitated with an anti-GFP antibody. The immunoprecipitates were analysed by SDS-PAGE and Western blotting with antibodies that recognise RCP, pSer435-RCP, EphA2, Rab11 and Rab14. B. H1299 cells were transfected with LMTK3 or non-targeting siRNA and stimulated with 10ng/ml HGF for the indicated times. The cells were lysed and endogenous EphA2 was immunoprecipitated with an anti-EphA2 antibody. The immunoprecipitates were analysed by SDS-PAGE and Western blotting with antibodies that recognise RCP, pSer435-RCP, EphA2 and Rab14.

5.2.2 Are Rho GTPases activated downstream of EphA2/RCP trafficking?

RhoA is activated during cell-cell repulsion to regulate the actomyosin cytoskeleton, thereby promoting cell-cell junction protein disassembly and cell migration (Carmona-Fontaine et al., 2008). Several studies have shown that Rho-GTPases are activated downstream of EphA signalling during cell-cell repulsion events in axon guidance and CIL (Astin et al., 2010; Wahl et al., 2000). I hypothesise that during HGF-induced scattering, EphA2 activates Rho GTPases, but there is an apparent paradox as HGF decreases the levels of EphA2 on the plasma membrane (where one might expect RhoA to be activated to promote cell-cell repulsion). However, there is increasing evidence that trafficking regulates and spatially restricts Rho GTPase activity. For example, RhoA is activated by ENDO180 (a pro-migratory receptor for collagen) on endosomes at the rear of the cell, promoting detachment from the ECM (Sturge et al., 2006). Also, Tiam1 (a Rac1 GEF) localises on endosomes where it locally activates and triggers Rac1 recycling to dorsal ruffles (Palamidessi et al., 2008). Most interestingly, a novel Akt substrate, RacGAP1, is activated downstream of RCP-driven α5β1-integrin/EGFR recycling (Jacquemet et al., 2013). Once activated, RacGAP1 is recruited to IQGAP1 at the tip of the pseudopod, where it locally inhibits Rac1 and stimulates a spike in RhoA activity, thus driving cancer cell invasion into a 3D matrix (Jacquemet et al., 2013). Moreover, it has been shown that EphA2 trafficking is required for Rac1 activation. EphA2 is internalised into endosomes where it associates with and activates Tiam1 to switch on Rac1 (Boissier et al., 2013). I postulate that HGF diverts EphA2 trafficking into an RCP/Rab14-positive compartment. It remains unclear how trafficking into a Rab14 vs Rab11 compartment affects the fate of EphA2. One hypothesis is that altering EphA2's trafficking pathway may alter its downstream signalling, such as Rho GTPases, and thereby promoting cell-cell repulsion (**Figure 5.1**). Althernatively altered trafficking kinetics may alter downstream signalling. To test this, the spatial and temporal activity of Rho GTPases could be analysed using FRET reporter probes following HGF treatment.

5.2.3 How could mutant-p53 modulate HGF driven EphA2 trafficking?

Muller et al. (2013) showed that mutant-p53 increases RCP-dependent α5ß1-integrin and cMet recycling, thereby increasing the cells' sensitivity to HGF-induced phosphorylation of key tyrosine residues in the catalytic domain of cMet (**Figure 5.4**). In this thesis, I have shown that HGF addition increases RCP phosphorylation on Serine^{435} by LMTK3, diverting EphA2 trafficking into an RCP/Rab14-positive compartment, and thus driving cell scattering (**Figure 5.4**). Taken together, I postulate that RCP has two different roles in scattering: it is involved first in setting the sensitivity of cMet to HGF, and second in controlling EphA2 trafficking. Since the concentration of HGF is much lower in tumours than in scattering assays, both of RCP's roles in scattering are likely to have an important role in cancer dissemination.

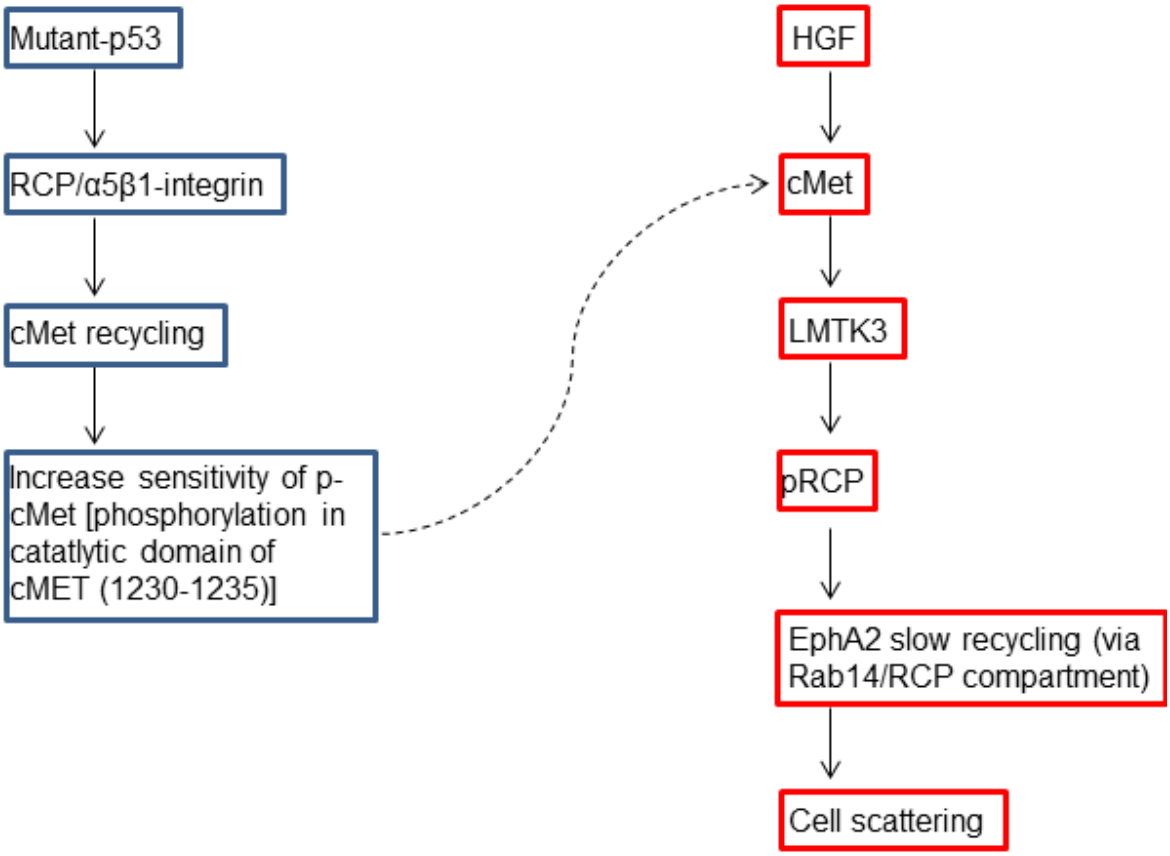

Figure 5-4 Schematic summary of mutant-p53's proposed role in HGF-induced scattering
Mutant-p53 increases α5β1-integrin and cMet recycling in an RCP-dependent fashion, thereby increasing the cells' sensitivity to HGF-induced phosphorylation of key tyrosine residues in the catalytic domain of cMet. HGF drives LMTK3 phosphorylation of RCP on Serine435, altering the EphA2 trafficking route into an RCP/Rab14 compartment, thus driving cell scattering.

5.2.4 What is the role of cell-cell repulsion in PDAC metastasis?

EphA2 and RCP contribute similarly to liver metastasis in the PDAC mouse model. These proteins could be required for several different steps during metastasis, such as cancer cell dissemination from the primary tumour, invasion through the basement membrane, survival in the circulation or at the secondary site, or establishment and growth of metastases. As I have shown that EphA2 and RCP are required for *in vitro* cell-cell repulsion and invasion, I would postulate that these proteins are likely to contribute to cancer cell dissemination and/or invasion. Histological analysis of the invasive front of metastasising human PDAC suggests that these cancer cells invade collectively with only a few isolated cancer cells being observed (Bronsert et al., 2014). However, it is difficult to gain a full understanding of dynamic cell migration and invasion using tissue samples from single time points. Furthermore, it has been shown using intravital imaging that the acquisition of a single cell migratory mode is reversible *in vivo (Giampieri et al., 2009)*. My data show using single cell systems (not just clonal cell lines but also tumour-derived mixed population of cells), that metastasis correlates with cell-cell repulsion. The pathway required for HGF-induced scattering involves LMTK3 phosphorylating RCP and recruiting EphA2 and Rab14 into an internal compartment. I postulate that this pathway is activated at certain times *in vivo,* promoting tumour dissemination in a reversible fashion. Further studies are required to investigate the contributions of this mechanism to metastasis. To determine the distribution of EphA2, Rab14, RCP and $pSer^{435}$-RCP in the invasive front of tumours, human PDAC microarrays will be stained with the appropriate antibodies. Genetic studies using LMTK3 and Rab14 knock-out and RCP^{S435A} knockin mice will be used to investigate the importance of RCP phosphorylation in tumourigenesis and metastasis. This will determine whether LMTK3 would be a good novel target for cancer therapeutics.

Appendix

Sequence of EphA2 cloned into pEGFP-N1

C C C G A A T T C A C A T G G A G C T C C A G G C A G C C C G C G C C T G C T T C G C C C T G C T G T G G G G C T G T G
C G C T G G C C G C G G C C G C G G C G G C G C A G G G C A A G G A A G T G G T A C T G C T G G A C T T T G C T G C A
G C T G G A G G G G A G C T C G G C T G G C T C A C A C A C C C G T A T G G C A A A G G G T G G G A C C T G A T G C A
G A A C A T C A T G A A T G A C A T G C C G A T C T A C A T G T A C T C C G T G T G C A A C G T G A T G T C T G G C G A
C C A G G A C A A C T G G C T C C G C A C C A A C T G G G T G T A C C G A G G A G A G G C T G A G C G T A T C T T C A
T T G A G C T C A A G T T T A C T G T A C G T G A C T G C A A C A G C T T C C C T G G T G G C G C C A G C T C C T G C A
A G G A G A C T T T C A A C C T C T A C T A T G C C G A G T C G G A C C T G G A C T A C G G C A C C A A C T T C C A G A
A G C G C C T G T T C A C C A A G A T T G A C A C C A T T G C G C C C G A T G A G A T C A C C G T C A G C A G C G A C T
T C G A G G C A C G C C A C G T G A A G C T G A A C G T G G A G G A G C G C T C C G T G G G G C C G C T C A C C C G C
A A A G G C T T C T A C C T G G C C T T C C A G G A T A T C G G T G C C T G T G T G G C G C T G C T C T C C G T C C G T
G T C T A C T A C A A G A A G T G C C C C G A G C T G C T G C A G G G C C T G G C C C A C T T C C C T G A G A C C A T C
G C C G G C T C T G A T G C A C C T T C C C T G G C C A C T G T G G C C G G C A C C T G T G T G G A C C A T G C C G T G
G T G C C A C C G G G G G G T G A A G A G C C C C G T A T G C A C T G T G C A G T G G A T G G C G A G T G G C T G G T
G C C C A T T G G G C A G T G C C T G T G C C A G G C A G G C T A C G A G A A G G T G G A G G A T G C C T G C C A G G
C C T G C T C G C C T G G A T T T T T T A A G T T T G A G G C A T C T G A G A G C C C C T G C T T G G A G T G C C C T G
A G C A C A C G C T G C C A T C C C C T G A G G G T G C C A C C T C C T G C G A G T G T G A G G A A G G C T T C T T C C
G G G C A C C T C A G G A C C C A G C G T C G A T G C C T T G C A C A C G A C C C C C C T C C G C C C C A C A C T A C C
T C A C A G C C G T G G G C A T G G G T G C C A A G G T G G A G C T G C G C T G G A C G C C C C C T C A G G A C A G C
G G G G G C C G C G A G G A C A T T G T C T A C A G C G T C A C C T G C G A A C A G T G C T G G C C C G A G T C T G G
G G A A T G C G G G C C G T G T G A G G C C A G T G T G C G C T A C T C G G A G C C T C C T C A C G G A C T G A C C C
G C A C C A G T G T G A C A G T G A G C G A C C T G G A G C C C C A C A T G A A C T A C A C C T T C A C C G T G G A G G
C C C G C A A T G G C G T C T C A G G C C T G G T A A C C A G C C G C A G C T T C C G T A C T G C C A G T G T C A G C A
T C A A C C A G A C A G A G C C C C C C A A G G T G A G G C T G G A G G G C C G C A G C A C C A C C T C G C T T A G C G
T C T C C T G G A G C A T C C C C C C G C C G C A G C A G A G C C G A G T G T G G A A G T A C G A G G T C A C T T A C C
G C A A G A A G G G A G A C T C C A A C A G C T A C A A T G T G C G C C G C A C C G A G G G T T T C T C C G T G A C C C
T G G A C G A C C T G G C C C C A G A C A C C A C C T A C C T G G T C C A G G T G C A G G C A C T G A C G C A G G A G
G G C C A G G G G G C C G G C A G C A A G G T G C A C G A A T T C C A G A C G C T G T C C C C G G A G G G A T C T G G
C A A C T T G G C G G T G A T T G G C G G C G T G G C T G T C G G T G T G G T C C T G C T T C T G G T G C T G G C A G
G A G T T G G C T T C T T T A T C C A C C G C A G G A G G A A G A A C C A G C G T G C C C G C C A G T C C C C G G A G G
A C G T T T A C T T C T C C A A G T C A G A A C A A C T G A A G C C C C T G A A G A C A T A C G T G G A C C C C C A C A
C A T A T G A G G A C C C C A A C C A G G C T G T G T T G A A G T T C A C T A C C G A G A T C C A T C C A T C C T G T G
T C A C T C G G C A G A A G G T G A T C G G A G C A G G A G A G T T T G G G G A G G T G T A C A A G G G C A T G C T G
A A G A C A T C C T C G G G G A A G A A G G A G G T G C C G G T G G C C A T C A A G A C G C T G A A A G C C G G C T A
C A C A G A G A A G C A G C G A G T G G A C T T C C T C G G C G A G G C C G G C A T C A T G G G C C A G T T C A G C C
A C C A C A A C A T C A T C C G C C T A G A G G G C G T C A T C T C C A A A T A C A A G C C C A T G A T G A T C A T C A C
T G A G T A C A T G G A G A A T G G G G C C C T G G A C A A G T T C C T T C G G G A G A A G G A T G G C G A G T T C A
G C G T G C T G C A G C T G G T G G G C A T G C T G C G G G G C A T C G C A G C T G G C A T G A A G T A C C T G G C C
A A C A T G A A C T A T G T G C A C C G T G A C C T G G C T G C C C G C A A C A T C C T C G T C A A C A G C A A C C T G
G T C T G C A A G G T G T C T G A C T T T G G C C T G T C C C G C G T G C T G G A G G A C G A C C C C G A G G C C A C
C T A C A C C A C C A G T G G C G G C A A G A T C C C C A T C C G C T G G A C C G C C C C G G A G G C C A T T T C C T A
C C G G A A G T T C A C C T C T G C C A G C G A C G T G T G G A G C T T T G G C A T T G T C A T G T G G G A G G T G A
T G A C C T A T G G C G A G C G G C C C T A C T G G G A G T T G T C C A A C C A C G A G G T G A T G A A A G C C A T C A
A T G A T G G C T T C C G G C T C C C C A C A C C C A T G G A C T G C C C C T C C G C C A T C T A C C A G C T C A T G A T
G C A G T G C T G G C A G C A G G A G C G T G C C C G C C G C C C C A A G T T C G C T G A C A T C G T C A G C A T C C T
G G A C A A G C T C A T T C G T G C C C C T G A C T C C C T C A A G A C C C T G G C T G A C T T T G A C C C C C G C G T
G T C T A T C C G G C T C C C C A G C A C G A G C G G C T C G G A G G G G G T G C C C T T C C G C A C G G T G T C C G
A G T G G C T G G A G T C C A T C A A G A T G C A G C A G T A T A C G G A G C A C T T C A T G G C G G C C G G C T A C A
C T G C C A T C G A G A A G G T G G T G C A G A T G A C C A A C G A C G A C A T C A A G A G G A T T G G G G T G C G G
C T G C C C G G C C A C C A G A A G C G C A T C G C C T A C A G C C T G C T G G G A C T C A A G G A C C A G G T G A A C
A C T G T G G G G A T C C C C A T C C T G T C G A C C C C

Sequence of Rab6B cloned into pEGFP-C3

A A A G A A T T C A T G T C C G C A G G G G G A G A T T T T G G G A A T C C A C T G A G A A A
A T T C A A G T T T G G T G T T C T T G G G G G A G C A G A G C G T C G G G A A G A C G T C
T C T G A T T A C G A G G T T C A T G T A C G A C A G C T T C G A C A A C A C A T A C C A
G G C A A C C A T T G G G A T T G A C T T C T T G T C A A A A A C C A T G T A C T T G G A G
G A C C G C A C G G T G C G A C T G C A G C T C T G G G A C A C A G C T G G T C A G G A G
A G G T T C C G C A G C C T G A T C C C C A G C T A C A T C C G G G A C T C C A C G G T G G
C T G T G G T G G T G T A C G A C A T C A C A A A T C T C A A C T C C T T C C A A C A G A C
C T C T A A G T G G A T C G A C G A C G T C A G G A C A G A G A G G G G C A G T G A T G T
T A T C A T C A T G C T G G T G G G C A A C A A G A C G G A C C T G G C T G A T A A G A G
G C A G A T A A C C A T C G A G G A G G G G G A G C A G C G C G C C A A A G A A C T G A G
C G T C A T G T T C A T T G A G A C C A G T G C G A A G A C T G G C T A C A A C G T G A A G
C A G C T T T T T C G A C G T G T G G C G T C G G C T C T A C C C G G A A T G G A G A A T
G T C C A G G A G A A A A G C A A A G A A G G G A T G A T C G A C A T C A A G C T G G A C
A A A C C C C A G G A G C C C C C G G C C A G C C A G C T G A A A

Sequence of Rab6A in pEGFP-C2

ATGTCCACGGGCGGAGACTTCGGGAATCCGCTGAGGAAATTCAAGCTGGTGTTCCTGGG
GGAGCAAAGCGTTGGAAAGACATCTTTGATCACCAGATTCATGTATGACAGTTTTGACAA
CACCTATCAGGCAACAATTGGCATTGACTTTTTATCAAAAACTATGTACTTGGAGGATCG
AACAGTACGATTGCAATTATGGGACACAGCAGGTCAAGAGCGGTTCAGGAGCTTGATTCC
TAGCTACATTCGTGACTCCACTGTGGCAGTTGTTGTTATGATATCACAAATGTTAACTCAT
TCCAGCAAACTACAAAGTGGATTGATGATGTCAGAACAGAAAGAGGAAGTGATGTTATCA
TCATGCTAGTAGGAAATAAAACAGATCTTGCTGACAAGAGGCAAGTGTCAATTGAGGAGG
GAGAGAGGAAAGCCAAAGAGCTGAATGTTATGTTTATTGAAACTAGTGCAAAAGCTGGAT
ACAATGTAAAGCAGCTCTTTCGACGTGTAGCAGCAGCTTTGCCGGGAATGGAAAGCACAC
AGGACAGAAGCAGAGAAGATATGATTGACATAAAACTGGAAAAGCCTCAGGAGCAACCAG
TCAGTGAAGGAGGCTGTTCCTGCTAA

Sequence of Rab14 in pEGFP-C2

ATGGCAACTGCACCATACAACTACTCTTACATCTTTAAATATATTATTATTGGGGACATGG
GAGTAGGAAAATCTTGCTTGCTTCATCAATTTACAGAAAAAAAATTTATGGCTGATTGTCC
TCACACAATTGGTGTTGAATTTGGTACAAGAATAATCGAAGTTAGTGGCCAAAAAATAAA
ACTGCAGATTTGGGATACGGCAGGACAGGAGCGATTTAGGGCTGTTACACGGAGCTACTA
CAGAGGAGCTGCGGGAGCTCTTATGGTCTATGATATCACTAGAAGAAGTACATATAACCA
CTTAAGCAGCTGGTTGACAGATGCAAGGAATCTCACCAATCCAAATACTGTAATAATTCTC
ATAGGAAATAAAGCAGATTTGGAGGCACAGAGAGATGTTACATATGAAGAAGCCAAACAG
TTTGCTGAAGAAAATGGCTTATTGTTCCTCGAAGCGAGTGCAAAAACGGGAGAGAATGTA
GAAGATGCCTTCCTTGAGGCTGCCAAGAAAATCTATCAGAACATTCAGGATGGAAGCTTG
GATCTGAATGCTGCTGAGTCTGGTGTACAACACAAACCTTCAGCCCCGCAGGGAGGCCGG
CTAACCAGTGAACCCCAACCCCAGAGAGAAGGCTGTGGCTGCTAG

Sequence of RCP in pEGFP-C3

AGTGTTATCGTCACCATGTCCCTAATGGTCTCGGCTGGCCGGGGCCTGGGGGCCGTGTG
GTCCCCAACCCACGTGCAGGTGACGGTGCTGCAGGCGCGGGGCCTGCGGGCCAAGGGCC
CCGGGGGCACGAGCGACGCGTACGCGGTGATCCAGGTGGGCAAGGAGAAGTACGCCACC
TCCGTGTCGGAGCGCAGCCTGGGCGCGCCCGTGTGGCGCGAGGAGGCCACCTTCGAGCT
GCCATCGCTGCTGTCCTCCGGACCCGCGGCCGCCGCCACCCTGCAGCTCACCGTGCTGCA
CCGCGCGCTGCTCGGCCTCGACAAGTTCCTGGGCCGCGCCGAGGTGGACCTGCGGGATC
TGCACCGCGACCAGGGCCGCAGGAAGACGCAGTGGTATAAGTTGAAATCCAAACCAGGAA
AGAAGGACAAGGAGCGAGGAGAAATTGAGGTTGACATCCAGTTTATGAGAAACAACATGA
CTGCCAGCATGTTTGACCTTTCTATGAAAGACAAGTCTCGGAATCCATTTGGAAAGCTGA
AGGACAAGATCAAGGGGAAGAATAAGGACAGTGGGTCAGACACCGCCTCCGCCATCATCC
CTAGCACGACACCTTCGGTCGACAGTGATGATGAGTCTGTGGTTAAAGACAAGAAAAAGA
AATCAAAGATCAAGACCTTACTTTCCAAGTCAAATTTGCAGAAGACGCCTCTTTCCCAGTC
CATGTCTGTCCTGCCGACTTCAAAGCCAGAAAAAGTGCTGCTTCGTCCCGGAGACTTTCA
GTCCCAGTGGGATGAAGATGACAATGAGGATGAGTCCTCCTCGGCCTCGGATGTCATGTC
TCACAAGAGAACAGCGAGTACGGATCTTAAGCAACTGAACCAGGTCAACTTTACCCTTCC
CAAGAAGGAAGGACTTTCCTTTCTTGGTGGCCTTCGGTCTAAGAATGATGTCCTTTCCCG
CTCTAATGTCTGCATCAATGGGAACCATGTTTACCTGGAGCAGCCAGAAGCCAAGGGTGA
GATCAAGGATAGCAGCCCGTCCTCCTCCCCATCCCCCAAGGGCTTCAGAAAGAAGCATTT
GTTCTCTTCTACAGAGAACCTGGCGGCTGGGTCTTGGAAGGAGCCTGCTGAAGGAGGTG
GGCTGTCTTCTGACAGGCAGCTCTCCGAATCTTCCACCAAGGACTCCTTGAAGTCTATGA
CCCTGCCGTCCTACCGACCTGCCCCACTGGTCAGTGGGGACCTCAGGGAAAACATGGCCC
CCGCAAACTCAGAGGCCACAAAAGAAGCTAAGGAGAGCAAGAAGCCAGAGAGCAGGAGGT
CCTCTTTGCTGTCTCTGATGACGGGGAAGAAGGATGTGGCTAAGGGCAGTGAAGGTGAA
AACCCTCTCACGGTCCCAGGGAGGGAGAAGGAAGGCATGCTGATGGGGGTTAAGCCGGG
GGAGGACGCATCGGGGCCTGCTGAAGACCTTGTGAGAAGATCTGAGAAAGATACTGCAG
CTGTTGTCTCCAGACAGGGCAGCTCCC TGAACCTCTTTGAAGATGTGCAGATCACAGAAC
CAGAAGCTGAGCCAGAGTCCAAGTCTGAACCGAGACCTCCAATTTCCTCTCCGAGGGCTC
CCCAGACCAGAGCTGTCAAGCCCCGACTTCATCCTGTGAAGCCAATGAATGCAATGGCCA
CCAAGGTTGCTAACTGCAGCTTGGGAACTGCCACCATCATCAGTGAGAACTTGAACAATG
AGGTCATGATGAAGAAATACAGCCCCTCGGACCCTGCATTTGCATATGCGCAGCTGACCC
ACGATGAGCTGATTCAGCTGGTCCTCA AACAGAAGGAAACGATAAGCAAGAAGGAGTTCC
AGGTCCGCGAGCTGGAAGACTACATTGACAACCTGCTTGTCAGGGTCATGGAAGAAACCC
CCAATATCCTCCGCATCCCGACTCAGGTTGGCAAAAAAGCAGGAAAGATGTAA

Sequence of Fip2 in pEGFP-C3

ATGATGCTGTCCGAGCAAGCCCAAAAGTGGTTTCCAACCCACGTGCAGGTCACAGTGCTC
CAAGCCAAAGATCTGAAGCCAAAAGGCAAAAGTGGTACCAATGACACATACACTATAATT
CAGCTGGGCAAGGAAAAGTACTCCACCTCTGTAGCTGAGAAAACCCTTGAGCCAGTTTGG
AAGGAGGAGGCCTCTTTCGAGCTACCTGGATTGCTAATTCAGGGAAGTCCAGAGAAATAC
ATTCTTTTCCTTATAGTTATGCACAGGTCCCTGGTGGGTCTGGATAAATTTTTAGGGCAG
GTGGCAATCAATCTCAATGACATCTTTGAGGACAAACAAAGAAGGAAAACAGAGTGGTTT
AGATTAGAATCCAAACAAGGAAAACGAATCAAAAACAGGGGTGAGATAAAGGTCAATATT
CAGTTTATGAGGAACAATATGACCGCAAGTATGTTTGACTTATCAATGAAGGACAAAACC
AGATCTCCTTTTGCAAAGTTAAAAGATAAGATGAAGGGTAGAAAAAATGATGGAACATTT
TCTGATACGTCTTCTGCAATCATTCCAAGTACTCACATGCCCGATGCCAATAGTGAATTTT
CAAGTGGTGAAATACAGATGAAATCCAAACCAAAAAAGCCTTTTCTCTTGGGTCCTCAGC
GACTCTCGTCAGCGCATTCAATGTCTGATTTATCTGGGTCCCATATGTCTTCTGAGAAAC
TGAAGGCTGGCACCATAGGTCAAACACATCTTCTCGGAC ACCAGTTAGATTCCTTTGGAA
CAGTTCCAGAAAGTGGAAGTCTCAAATCTCCACACAGAAGAACATTAAGCTTTGATACTTC
TAAAATGAACCAACCTGACAGCATTGTGGATGAAGGTGAATTGTGTTTCGGAAGACAAAA
TGACCCATTTACAAATGTGACTGCTTCATTACCCCAAAAATTTGCAACACTGCCAAGGAAG
AAAAATCCATTTGAAGAAAGCAGCGAAACATGGGACAGCAGCATGAATTTATTTTCAAAA
CCAATTGAAATAAGAAAAGAAAATAAAAGAGAGAAAAGGGAGAAAGTTAGCCTGTTTGAA
AGAGTGACTGGAAAAAAAGATAGCAGAAGATCTGATAAACTTAACAATGGGGGATCTGAT
AGCCCTTGTGACTTGAAATCACCTAATGCATTTAGTGAAAATCGCCAGGACTATTTTGAT
TATGAGTCAACCAATCCATTTACAGCAAAATTCAGGGCTTCAAATATAATGCCATCTTCAA
GTTTTCATATGAGTCCAACAAGCAATGAAGACCTCAGGAAAATCCCGGACAGCAACCCCT
TTGATGCCACTGCAGGGTATCGTAGTCTGACCTATGAAGAGGTTCTACAGGAGCTGGTGA
AACACAAAGAACTCCTTAGGAGGAAAGACACCCACATCCGGGAACTCGAGGACTACATCG
ACAACCTCCTTGTAAGGGTAATGGAAGAAACGCCCAGTATTCTCAGAGTGCCGTATGAAC
CATCCAGGAAAGCTGGCAAATTCTCTAACAGTTAATAAAGCCAATTGTATTGTATTGATAA
TTGGACAAAGAGAGAGAAAGAAAGAAGGAAGGAAGGAAAAACTTGTTACTGAAAGAGACT
ACACTATCAGGTTTCATTACATATTCTCCTTTAT

Sequence of Rip11 in pEGFP-C3

AGGTCCTGGGGTCTGCACCGGCTCGGCCAGACCTCGCCCCCCGCTTCTCCGCCATGGCCC
TGGTGCGGGGCGCGGAGCCGGCGGCGGGGCCTTCCCGCTGGCTGCCCACGCACGTCCAG
GTGACGGTGCTGCGGGCCCGCGGGCTGCGGGGCAAGAGCTCGGGAGCGGGCAGCACCAG
CGACGCGTACACGGTGATCCAGGTGGGCCGCGAGAAGTACAGTACGTCGGTGGTGGAGA
AGACGCACGGCTGCCCCGAGTGGCGTGAGGAGTGCTCCTTCGAGCTGCCGCCGGGGGCC
CTGGATGGCCTGCTGCGGGCGCAGGAGGCCGACGCGGGCCCGGCGCCCTGGGCCGCGAG
CTCCGCCGCCGCCTGCGAGCTGGTGCTCACCACCATGCACCGCTCGCTCATCGGCGTCGA
CAAGTTCCTGGGCCAGGCCACGGTGGCGCTGGACGAGGTCTTCGGCGCAGGCCGCGCCC
AGCACACGCAGTGGTACAAGCTGCACTCCAAGCCAGGCAAGAAGGAGAAGGAACGCGG C
GAGATTGAAGTCACCATCCAGTTCACGCGCAACAACCTGAGCGCCAGTATGTTTGACCTG
TCCATGAAGGACAAGCCAAGGTCTCCCTTCAGCAAGATCAGGGACAAGATGAAGGGCAAG
AAGAAGTATGATCTGGAATCTGCCTCTGCCATCCTCCCAAGCAGCGCCATAGAGGATCCT
GACCTGGGCAGCCTGGGCAAGATGGGCAAAGCCAAAGGCTTCTTCCTCCGCAACAAGCTG
CGCAAGTCGTCCCTGACCCAGTCCAACACCTCGCTGGGCTCGGACAGCACCCTGTCCTCA
GCCAGCGGGAGCTTGGCCTACCAGGGACCTGGCGCCGAACTCCTCACCCGCTCACCAAGC
CGTAGCAGCTGGCTGTCCACTGAAGGGGGCAGGGACTCTGCACAGTCCCCCAAGCTGTTC
ACCCATAAGAGGACCTACAGCGATGAGGCCAACCAGATGCGAGTGGCTCCTCCTCGGGCC
CTTCTGGACCTTCAGGGCCACCTGGATGCTGCCTCCCGCTCTTCGCTCTGTGTCAATGGG
AGCCACATTTACAATGAGGAGCCCCAGGGCCCTGTGCGGCACCGCAGCTCCATCTCGGGC
TCGCTTCCATCCTCTGGCTCCTTGCAAGCTGTCTCTTCCCGGTTCTCCGAGGAGGGGCCT
CGTTCCACAGATGACACCTGGCCCAGAGGCAGTCGTAGCAACAGCAGCTCAGAGGCAGTG
CTTGGACAGGAGGAGCTGAGTGCTCAGGCTAAAGTCCTGGCCCCTGGGGCCAGCCACCC
TGGAGAGGAGGAGGGGGCCCGGCTACCAGAGGGCAAGCCAGTCCAGGTTGCCACACCCA
TAGTGGCCTCCTCTGAGGCTGTGGCAGAGAAGGAGGGAGCCCGGAAGGAGGAACGCAAG
CCCCGGATGGGTCTCTTCCACCACCACCACCAAGGCCTAAGTCGGAGCGAGTTGGGTCGC
CGAAGCTCTCTGGGGGAAAAGGGGGGTCCCATCCTGGGGGCCTCCCCACATCACTCATCC
AGTGGGGAGGAAAAGGCCAAGAGTAGCTGGTTTGGCTTGAGAGAAGCCAAGGACCCGAC
TCAGAAACCCAGTCCCCACCCCGTGAAGCCCCTCAGTGCCGCCCCTGTGGAGGGCAGCCC
CGA CAGGAAGCAGTCCCGCTCCAGTCTGAGCATAGCCCTGAGCAGTGGGCTGGAGAAGC
TCAAAACAGTCACATCTGGGAGCATTCAGCCTGTGACCCAGGCCCCCCAGGCTGGCCAGA
TGGTGGACACCAAAAGGCTGAAGGACTCAGCTGTGCTGGACCAGTCGGCCAAGTACTACC
ACCTGACCCACGATGAGCTCATCAGCCTGCTCCTGCAGCGGGAGCGGGAGCTGAGCCAGC
GGGACGAGCATGTGCAGGAGCTGGAGAGCTACATCGACCGGCTGCTGGTGCGGATCATG
GAGACCTCACCCACGCTGCTGCAGATCCCCCCGGGCCCCCCCAAATAG

Sequence of Fip3 in pEGFP-C3

ATGGCGTCGGCCCCGCCGGCCTCGCCCCCGGGCTCGGAGCCGCCGGGGCCCGACCCGGA
GCCGGGCGGGCCGGACGGGCCGGGGGCGGCACAACTGGCTCCGGGCCCTGCGGAGCTAC
GCCTCGGAGCGCCCGTCGGCGGCCCCGACCCGCAGTCCCCGGGCCTGGATGAGCCTGCG
CCCGGGGCCGCTGCAGATGGCGGGGCGCGTTGGAGCGCCGGGCCGGCCCCGGGGCTGG
AGGGAGGCCCGCGAGACCCCGGGCCGTCCGCCCCGCCGCCGCGCTCCGGCCCGCGGGGG
CAGCTTGCGAGCCCCGACGCCCCGGGCCCAGGGCCGCGCTCCGAAGCGCCGCTTCCAGA
ACTCGACCCGTTGTTCTCCTGGACTGAGGAGCCCGAGGAGTGTGGCCCCGCGAGCTGCC
CGGAGAGCGCGCCTTTCCGCTTGCAGGGGTCCAGCAGCAGCCACCGAGCGCGGGGCGAG
GTCGACGTCTTCTCTCCCTTCCCCGCGCCCACGGCGGGCGAGCTGGCGCTGGAGCAAGG
TCCCGGGTCCCCGCCGCAGCCCTCGGACCTCAGCCAGACCCACCCCCTTCCGAGCGAGCC
CGTGGGGAGTCAGGAGGACGGCCCCCGCCTCCGAGCCGTGTTCGATGCCCTGGACGGGG
ATGGGGACGGTTTCGTCCGCATCGAGGACTTCATCCAGTTTGCTACGGTCTACGGGGCAG
AGCAGGTGAAGGACTTAACTAAGTACTTGGATCCCAGTGGGCTCGGCGTGATCAGCTTTG
AAGACTTCTACCAAGGGATCACAGCCATCAGAAACGGAGATCCTGATGGCCAGTGCTACG
GTGGTGTCGCTTCTGCCCAAGATGAGGAGCCCCTGGCCTGCCCGGACGAGTTCGATGAC
TTCGTCACCTATGAGGCCAACGAGGTGACGGACAGCGCGTACATGGGCTCCGAGAGCACC
TACAGTGAGTGTGAGACCTTCACGGACGAGGACACCAGCACCCTGGTGCACCCTGAGCTG
CAACCTGAAGGGGACGCAGACAGTGCCGGCGGCTCGGCCGTGCCCTCTGAGTGCCTGGA
CGCCATGGAGGAGCCCGACCATGGTGCCCTGCTGCTGCTCCCAGGCAGGCCTCACCCCCA
TGGCCAGTCTGTCATCACGGTGATCGGGGGCGAGGAGCACTTTGAGGACTACGGTGAAG
GCAGTGAGGCGGAGCTGTCCCCAGAGACCCTATGCAACGGGCAGCTGGGCTGCAGTGAC
CCCGCTTTCCTCACGCCCAGTCCGACAAAGCGGCTCTCCAGCAAGAAGGTGGCAAGGTAC
CTGCACCAGTCAGGGGCCCTGACCATGGAGGCCCTGGAGGACCCTTCCCCCGAGCTCATG
GAGGGCCCAGAGGAGGACATTGCTGACAAGGTTGTCTTCCTGGAAAGGCGTGTGCTGGA
GCTGGAAAAGGACACGGCAGCCACCGGTGAGCAACACAGCCGCCTGAGGCAGGAGAACC
TGCAGCTGGTGCACAGAGCAAACGCCCTGGAGGAGCAGCTGAAGGAGCAGGAGCTGAGA
GCCTGCGAGATGGTCCTGGAAGAGACCCGGCGTCAGAAGGAGCTCCTGTGCAAGATGGA
GAGGGAGAAGAGCATTGAGATCGAGAACCTGCAGACCAGGCTACAGCAACTGGACGAGG
AGAACAGTGAACTCCGGTCCTGCACGCCCTGTCTGAAGGCCAACATTGAGCGTCTGGAGG
AGGAGAAGCAGAAGCTGTTGGATGAGATAGAGTCGCTGACGCTGCGGCTCAGTGAAGAG
CAGGAGAACAAGAGGAGAATGGGGGACAGGCTGAGTCACGAGAGGCACCAGTTCCAGAG
GGACAAGGAGGCCACCCAGGAGCTGATCGAGGACCTCCGAAAGCAGCTGGAGCACCTGC
AGCTCCTCAAGCTGGAGGCCGAGCAGCGGCGGGGCCGCAGCAGCAGCATGGGCCTGCAG
GAGTACCACAGCCGCGCCCGGGAGAGCGAGCTGGAGCAGGAGGTCCGCAGGCTGAAGCA
GGACAACCGCAACCTGAAGGAGCAGAACGAGGAGCTGAACGGGCAGATCATTACCCTCAG
CATCCAGGGCGCCAAGAGCCTCTTCTCCACAGCCTTCTCTGAGTCCCTGGCTGCAGAGAT
CAGCTCCGTCTCCCGAGATGAGCTCATGGAGGCGATTCAGAAGCAGGAGGAGATCAACTT
CCGCCTGCAGGACTACATCGACAGGATCATCGTGGCCATCATGGAGACCAACCCGTCCAT
CCTGGAGGTCAAGTAG

Sequence of Fip4 in pEGFP-C3

ATGGCGGGCGGCGCGGGCTGGTCGGGCGCCCCCGCGGCTCTGCTGCGCTCCGTGCGCCG
CCTGCGCGAGGTGTTCGAGGTGTGCGGCCGCGACCCCGACGGCTTCCTGCGCGTGGAGC
GCGTCGCGGCGCTCGGACTGCGCTTCGGCCAGGGCGAGGAGGTGGAAAAACTTGTGAAA
TATTTGGATCCCAACGACCTGGGGAGAATCAACTTCAAGGACTTTTGCCGGGGGGGTGTTC
GCCATGAAAGGGTGCGAGGAGCTGCTGAAGGATGTGCTGTCGGTGGAGAGCGCGGGGAC
GCTGCCGTGCGCGCCAGAGATCCCAGACTGCGTGGAGCAGGGCAGCGAGGTCACAGGCC
CCACCTTTGCTGATGGCGAGCTCATCCCCAGGGAACCCGGCTTTTTTCCCGAGGACGAGG
AGGAGGCTATGACGCTGGCGCCACCTGAGGGCCCCCAGGAGTTGTACACAGACAGCCCCA
TGGAGAGCACTCAGAGCCTGGAGGGGTCTGTCGGGAGTCCTGCCGAGAAGGACGGGGGA
CTTGGGGGCCTGTTTCTGCCAGAAGACAAGTCCCTGGTCCACACTCCATCCATGACGACC
TCAGACCTTTCTACACACTCCACCACCTCGCTCATCAGCAATGAGGAGCAGTTTGAAGAC
TATGGGGAGGGTGACGATGTGGACTGTGCCCCCAGCAGCCCTTGCCCCGATGATGAGAC
CAGGACCAACGTCTACTCGGACCTGGGGTCTTCGGTGTCTTCCAGTGCGGGGCAGACGC
CTAGGAAAATGCGGCACGTGTACAACAGCGAATTGCTAGATGTTTACTGCTCTCAATGCT
GCAAGAAAATCAACCTGCTCAATGACTTGGAAGCCCGACTGAAAAACCTGAAGGCCAACA
GCCCCAACCGAAAGATCTCCAGCACGGCCTTTGGACGGCAGCTCATGCACAGCAGCAACT
TCAGCAGCAGCAATGGCAGCACCGAAGACCTGTTCCGGGACAGCATTGACTCTTGCGACA
ATGACATCACAGAGAAGGTAAGCTTCCTGGAAAAGAAGGTGACAGAGCTGGAGAATGACA
GCCTGACCAATGGGGACCTGAAGAGCAAGCTGAAGCAAGAGAACACACAGCTGGTGCACA
GGGTGCATGAGCTGGAGGAGATGGTGAAGGATCAGGAGACCACGGCCGAGCAGGCTCTG
GAGGAGGAGGCGCGGCGCCACCGCGAGGCCTACGGCAAGCTGGAGAGGGAGAAGGCTAC
CGAGGTGGAGCTGCTCAATGCCAGGGTGCAGCAGTTGGAGGAAGAAAATACAGAGCTTA
GAACAACAGTGACTCGGCTCAAGTCTCAAACAGAGAAACTGGATGAGGAGCGGCAGCGCA
TGTCTGACCGTCTGGAGGACACCAGCCTGCGGCTCAAAGATGAGATGGACCTGTACAAGC
GCATGATGGACAAGCTGCGACAGAACCGCCTTGAGTTCCAGAAGGAGCGGGAGGCGACG
CAGGAGCTCATCGAGGACTTGCGGAAGGAGCTGGAGCACCTGCAGATGTACAAGCTGGA
CTGCGAGCGGCCAGGCAGGGGCCGCAGTGCCTCCTCTGGCCTAGGCGAGTTCAATGCCA
GGGCCCGCGAGGTGGAGCTCGAGCACGAGGTCAAGCGGCTCAAGCAGGAGAATTATAAG
CTGCGGGATCAGAACGACGACTTGAATGGGCAGATTTTGAGCCTCAGCCTCTACGAAGCA
AAAAACCTCTTTGCTGCCCAGACTAAAGCCCAGTCTCTGGCTGCGGAGATAGACACCGCC
TCGCGCGATGAGCTAATGGAAGCCCTGAAGGAGCAGGAGGAGATCAACTTCCGGCTGAG
GCAGTACATGGACAAGATTATCCTCGCCATCCTGGACCACAATCCCTCCATCCTCGAGAT
CAAACACTAA

References

Abercrombie, M. (1970). Contact inhibition in tissue culture. In vitro *6*, 128-142.

Abercrombie, M. (1979). Contact inhibition and malignancy. Nature *281*, 259-262.

Abercrombie, M., and Dunn, G. A. (1975). Adhesions of fibroblasts to substratum during contact inhibition observed by interference reflection microscopy. Exp Cell Res *92*, 57-62.

Abercrombie, M., and Heaysman, J. E. (1954). Observations on the social behaviour of cells in tissue culture. II. Monolayering of fibroblasts. Experimental cell research *6*, 293-306.

Abercrombie, M., and Turner, A. A. (1978). Contact reactions influencing cell locomotion of a mouse sarcoma in culture. Medical biology *56*, 299-303.

Abraham, S., Yeo, M., Montero-Balaguer, M., and Paterson…, H. (2009). VE-Cadherin-mediated cell-cell interaction suppresses sprouting via signaling to MLC2 phosphorylation. Current biology.

Adams, R. H., Diella, F., Hennig, S., Helmbacher, F., Deutsch, U., and Klein, R. (2001). The cytoplasmic domain of the ligand ephrinB2 is required for vascular morphogenesis but not cranial neural crest migration. Cell *104*, 57-69.

Adorno, M., Cordenonsi, M., Montagner, M., Dupont, S., Wong, C., Hann, B., Solari, A., Bobisse, S., Rondina, M., Guzzardo, V.*, et al.* (2009). A Mutant-p53/Smad complex opposes p63 to empower TGFbeta-induced metastasis. Cell *137*, 87-98.

Alazzouzi, H., Davalos, V., Kokko, A., Domingo, E., Woerner, S. M., Wilson, A. J., Konrad, L., Laiho, P., Espín, E., Armengol, M.*, et al.* (2005). Mechanisms of inactivation of the receptor tyrosine kinase EPHB2 in colorectal tumors. Cancer research *65*, 10170-10173.

Anear, E., and Parish, R. W. (2012). The effects of modifying RhoA and Rac1 activities on heterotypic contact inhibition of locomotion. FEBS letters *586*, 1330-1335.

Arvanitis, D. N., and Davy, A. (2012). Regulation and misregulation of Eph/ephrin expression. Cell adhesion & migration *6*, 131-137.

Astin, J., Batson, J., Kadir, S., Charlet, J., Persad, R., Gillatt, D., Oxley, J., and Nobes, C. (2010). Competition amongst Eph receptors regulates contact inhibition of locomotion and invasiveness in prostate cancer cells. Nature cell biology *12*, 1194-1204.

Baetz, N. W., and Goldenring, J. R. (2013). Rab11-family interacting proteins define spatially and temporally distinct regions within the dynamic Rab11a-dependent recycling system. Molecular biology of the cell *24*, 643-658.

Balsara, B., Sonoda, G., du Manoir, S., Siegfried, J., Gabrielson, E., and Testa, J. (1997). Comparative genomic hybridization analysis detects frequent, often high-level, overrepresentation of DNA sequences at 3q, 5p, 7p, and 8q in human non-small cell lung carcinomas. Cancer research *57*, 2116-2120.

Barbero, P., Bittova, L., and Pfeffer, S. R. (2002). Visualization of Rab9-mediated vesicle transport from endosomes to the trans-Golgi in living cells. J Cell Biol *156*, 511-518.

Barrios, A., Poole, R. J., Durbin, L., Brennan, C., Holder, N., and Wilson, S. W. (2003). Eph/Ephrin signaling regulates the mesenchymal-to-epithelial transition of the paraxial mesoderm during somite morphogenesis. Current biology : CB *13*, 1571-1582.

Batlle, E., Henderson, J. T., Beghtel, H., van den Born, M. M., Sancho, E., Huls, G., Meeldijk, J., Robertson, J., van de Wetering, M., Pawson, T., and Clevers, H. (2002). Beta-catenin and TCF mediate cell positioning in the intestinal epithelium by controlling the expression of EphB/ephrinB. Cell *111*, 251-263.

Batson, J., Maccarthy-Morrogh, L., Archer, A., Tanton, H., and Nobes, C. D. (2014). EphA receptors regulate prostate cancer cell dissemination through Vav2-RhoA mediated cell-cell repulsion. Biology open *3*, 453-462.

Bernatchez, P., Sharma, A., Kodaman, P., and Sessa, W. (2009). Myoferlin is critical for endocytosis in endothelial cells. American journal of physiology Cell physiology *297*, 92.

Biankin, A. V., Waddell, N., Kassahn, K. S., Gingras, M.-C. C., Muthuswamy, L. B., Johns, A. L., Miller, D. K., Wilson, P. J., Patch, A.-M. M., Wu, J.*, et al.* (2012). Pancreatic cancer genomes reveal aberrations in axon guidance pathway genes. Nature *491*, 399-405.

Binda, E., Visioli, A., Giani, F., Lamorte, G., Copetti, M., Pitter, K. L., Huse, J. T., Cajola, L., Zanetti, N., DiMeco, F.*, et al.* (2012). The EphA2 receptor drives self-renewal and tumorigenicity in stem-like tumor-propagating cells from human glioblastomas. Cancer cell *22*, 765-780.

Binns, K. L., Taylor, P. P., Sicheri, F., Pawson, T., and Holland, S. J. (2000). Phosphorylation of tyrosine residues in the kinase domain and juxtamembrane region regulates the biological and catalytic activities of Eph receptors. Molecular and cellular biology *20*, 4791-4805.

Blumer, J., Rey, J., Dehmelt, L., Mazel, T., Wu, Y. W., Bastiaens, P., Goody, R. S., and Itzen, A. (2013). RabGEFs are a major determinant for specific Rab membrane targeting. J Cell Biol *200*, 287-300.

Bogan, C., Chen, J., O'Sullivan, M. G., and Cormier, R. T. (2009). Loss of EphA2 receptor tyrosine kinase reduces ApcMin/+ tumorigenesis. International journal of cancer Journal international du cancer *124*, 1366-1371.

Boissier, P., Chen, J., and Huynh-Do, U. (2013). EphA2 signaling following endocytosis: role of Tiam1. Traffic (Copenhagen, Denmark) *14*, 1255-1271.

Bonanomi, D., Chivatakarn, O., Bai, G., Abdesselem, H., Lettieri, K., Marquardt, T., Pierchala, B. A., and Pfaff, S. L. (2012). Ret is a multifunctional coreceptor that integrates diffusible- and contact-axon guidance signals. Cell *148*, 568-582.

Böttcher, R. T., Stremmel, C., Meves, A., Meyer, H., Widmaier, M., Tseng, H.-Y. Y., and Fässler, R. (2012). Sorting nexin 17 prevents lysosomal degradation of ß1 integrins by binding to the ß1-integrin tail. Nature cell biology *14*, 584-592.

Bourgin, C., Murai, K. K., Richter, M., and Pasquale, E. B. (2007). The EphA4 receptor regulates dendritic spine remodeling by affecting beta1-integrin signaling pathways. The Journal of cell biology *178*, 1295-1307.

Bouvier, D., Tremblay, M.-E. E., Riad, M., Corera, A. T., Gingras, D., Horn, K. E., Fotouhi, M., Girard, M., Murai, K. K., Kennedy, T. E.*, et al.* (2010). EphA4 is localized in clathrin-coated and synaptic vesicles in adult mouse brain. Journal of neurochemistry *113*, 153-165.

Bracke, M. E., Depypere, H., Labit, C., Van Marck, V., Vennekens, K., Vermeulen, S. J., Maelfait, I., Philippé, J., Serreyn, R., and Mareel, M. M. (1997). Functional downregulation of the E-cadherin/catenin complex leads to loss of contact inhibition of motility and of mitochondrial activity, but not of growth in confluent epithelial cell cultures. European journal of cell biology *74*, 342-349.

Brantley-Sieders, D. M., Caughron, J., Hicks, D., Pozzi, A., Ruiz, J. C., and Chen, J. (2004). EphA2 receptor tyrosine kinase regulates endothelial cell migration and vascular assembly through phosphoinositide 3-kinase-mediated Rac1 GTPase activation. Journal of cell science *117*, 2037-2049.

Brantley-Sieders, D. M., Fang, W., Hicks, D. J., Zhuang, G., Shyr, Y., and Chen, J. (2005). Impaired tumor microenvironment in EphA2-deficient mice inhibits tumor angiogenesis and metastatic progression. The FASEB journal *19*, 1884-1886.

Brantley-Sieders, D. M., Zhuang, G., Hicks, D., Fang, W. B., Hwang, Y., Cates, J. M. M., Coffman, K., Jackson, D., Bruckheimer, E., Muraoka-Cook, R. S., and Chen, J. (2008). The receptor tyrosine kinase EphA2 promotes mammary adenocarcinoma tumorigenesis and metastatic progression in mice by amplifying ErbB2 signaling. The Journal of clinical investigation *118*, 64-78.

Brass, A., Dykxhoorn, D., Benita, Y., Yan, N., Engelman, A., Xavier, R., Lieberman, J., and Elledge, S. (2008). Identification of host proteins required for HIV infection through a functional genomic screen. Science (New York, NY) *319*, 921-926.

Bronsert, P., Enderle-Ammour, K., Bader, M., Timme, S., Kuehs, M., Csanadi, A., Kayser, G., Kohler, I., Bausch, D., Hoeppner, J.*, et al.* (2014). Cancer cell invasion and EMT marker expression: a three-dimensional study of the human cancer-host interface. The Journal of pathology *234*, 410-422.

Brown, A., Yates, P. A., Burrola, P., Ortuño, D., Vaidya, A., Jessell, T. M., Pfaff, S. L., O'Leary, D. D., and Lemke, G. (2000). Topographic mapping from the retina to the midbrain is controlled by relative but not absolute levels of EphA receptor signaling. Cell *102*, 77-88.

Brückner, K., Pablo Labrador, J., Scheiffele, P., Herb, A., Seeburg, P. H., and Klein, R. (1999). EphrinB ligands recruit GRIP family PDZ adaptor proteins into raft membrane microdomains. Neuron *22*, 511-524.

Buricchi, F., Giannoni, E., Grimaldi, G., Parri, M., Raugei, G., Ramponi, G., and Chiarugi, P. (2007). Redox regulation of ephrin/integrin cross-talk. Cell adhesion & migration *1*, 33-42.

Campbell, T. N., Attwell, S., Arcellana-Panlilio, M., and Robbins, S. M. (2006). Ephrin A5 expression promotes invasion and transformation of murine fibroblasts. Biochemical and biophysical research communications *350*, 623-628.

Carmona-Fontaine, C., Matthews, H. K., Kuriyama, S., Moreno, M., Dunn, G. A., Parsons, M., Stern, C. D., and Mayor, R. (2008). Contact inhibition of locomotion in vivo controls neural crest directional migration. Nature *456*, 957-961.

Carter, N., Nakamoto, T., Hirai, H., and Hunter, T. (2002). EphrinA1-induced cytoskeletal re-organization requires FAK and p130(cas). Nature cell biology *4*, 565-573.

Carvalho, R. F., Beutler, M., Marler, K. J., Knöll, B., Becker-Barroso, E., Heintzmann, R., Ng, T., and Drescher, U. (2006). Silencing of EphA3 through a cis interaction with ephrinA5. Nature neuroscience *9*, 322-330.

Casanova, J. E., Wang, X., Kumar, R., Bhartur, S. G., Navarre, J., Woodrum, J. E., Altschuler, Y., Ray, G. S., and Goldenring, J. R. (1999). Association of Rab25 and Rab11a with the apical recycling system of polarized Madin-Darby canine kidney cells. Mol Biol Cell *10*, 47-61.

Caswell, P., Chan, M., Lindsay, A., McCaffrey, M., Boettiger, D., and Norman, J. (2008). Rab-coupling protein coordinates recycling of alpha5beta1 integrin and EGFR1 to promote cell migration in 3D microenvironments. The Journal of cell biology *183*, 143-155.

Caswell, P., Spence, H., Parsons, M., White, D., Clark, K., Cheng, K., Mills, G., Humphries, M., Messent, A., Anderson, K.*, et al.* (2007). Rab25 associates with alpha5beta1 integrin to promote invasive migration in 3D microenvironments. Developmental cell *13*, 496-510.

Caswell, P. T., and Norman, J. C. (2006). Integrin trafficking and the control of cell migration. Traffic (Copenhagen, Denmark) *7*, 14-21.

Chang, Q., Jorgensen, C., Pawson, T., and Hedley, D. W. (2008). Effects of dasatinib on EphA2 receptor tyrosine kinase activity and downstream signalling in pancreatic cancer. British journal of cancer *99*, 1074-1082.

Chen, P., Huang, Y., Zhang, B., Wang, Q., and Bai, P. (2014). EphA2 enhances the proliferation and invasion ability of LNCaP prostate cancer cells. Oncology letters *8*, 41-46.

Cheng, J.-M. M., Ding, M., Aribi, A., Shah, P., and Rao, K. (2006). Loss of RAB25 expression in breast cancer. International journal of cancer Journal international du cancer *118*, 2957-2964.

Cheng, J.-M. M., Volk, L., Janaki, D. K., Vyakaranam, S., Ran, S., and Rao, K. A. (2010). Tumor suppressor function of Rab25 in triple-negative breast cancer. International journal of cancer Journal international du cancer *126*, 2799-2812.

Cheng, K., Lahad, J., Gray, J., and Mills, G. (2005). Emerging role of RAB GTPases in cancer and human disease. Cancer research *65*, 2516-2519.

Cheng, N., Brantley, D. M., Liu, H., Lin, Q., Enriquez, M., Gale, N., Yancopoulos, G., Cerretti, D. P., Daniel, T. O., and Chen, J. (2002). Blockade of EphA receptor tyrosine kinase activation inhibits vascular endothelial cell growth factor-induced angiogenesis. Molecular cancer research : MCR *1*, 2-11.

Chia, W. J., and Tang, B. L. (2009). Emerging roles for Rab family GTPases in human cancer. Biochimica et biophysica acta *1795*, 110-116.

Choi, S., and Park, S. (1999). Phosphorylation at Tyr-838 in the kinase domain of EphA8 modulates Fyn binding to the Tyr-615 site by enhancing tyrosine kinase activity. Oncogene *18*, 5413-5422.

Christiansen, J. J., and Rajasekaran, A. K. (2006). Reassessing epithelial to mesenchymal transition as a prerequisite for carcinoma invasion and metastasis. Cancer research *66*, 8319-8326.

Christoforides, C., Rainero, E., Brown, K. K., Norman, J. C., and Toker, A. (2012). PKD controls αvβ3 integrin recycling and tumor cell invasive migration through its substrate Rabaptin-5. Developmental cell *23*, 560-572.

Christoforidis, S., McBride, H. M., Burgoyne, R. D., and Zerial, M. (1999). The Rab5 effector EEA1 is a core component of endosome docking. Nature *397*, 621-625.

Cortina, C., Palomo-Ponce, S., Iglesias, M., Fernández-Masip, J. L., Vivancos, A., Whissell, G., Humà, M., Peiró, N., Gallego, L., Jonkheer, S*., et al.* (2007). EphB-ephrin-B interactions suppress colorectal cancer progression by compartmentalizing tumor cells. Nature genetics *39*, 1376-1383.

Cowan, C. A., and Henkemeyer, M. (2001). The SH2/SH3 adaptor Grb4 transduces B-ephrin reverse signals. Nature *413*, 174-179.

Cowan, C. W., Shao, Y. R., Sahin, M., Shamah, S. M., Lin, M. Z., Greer, P. L., Gao, S., Griffith, E. C., Brugge, J. S., and Greenberg, M. E. (2005). Vav family GEFs link activated Ephs to endocytosis and axon guidance. Neuron *46*, 205-217.

Crowner, D., Gall, M., Gates, M. A., and Giniger, E. (2003). Notch Steers< i> Drosophila</i> ISNb Motor Axons by Regulating the Abl Signaling Pathway. Current biology *13*, 967-972.

Cuif, M. H., Possmayer, F., Zander, H., Bordes, N., Jollivet, F., Couedel-Courteille, A., Janoueix-Lerosey, I., Langsley, G., Bornens, M., and Goud, B. (1999). Characterization of GAPCenA, a GTPase activating protein for Rab6, part of which associates with the centrosome. The EMBO journal *18*, 1772-1782.

Dai, Y., Liu, Y., Huang, D., Yu, C., Cai, G., Pi, L., Ren, C., Chen, G., Tian, Y., and Zhang, X. (2012). Increased expression of Rab coupling protein in squamous cell carcinoma of the head and neck and its clinical significance. Oncology letters *3*, 1231-1236.

Dalva, M. B., Takasu, M. A., Lin, M. Z., Shamah, S. M., Hu, L., Gale, N. W., and Greenberg, M. E. (2000). EphB receptors interact with NMDA receptors and regulate excitatory synapse formation. Cell *103*, 945-956.

Damiani, M. T., Pavarotti, M., Leiva, N., Lindsay, A. J., McCaffrey, M. W., and Colombo, M. I. (2004). Rab coupling protein associates with phagosomes and regulates recycling from the phagosomal compartment. Traffic (Copenhagen, Denmark) *5*, 785-797.

Davies, H., Hunter, C., Smith, R., Stephens, P., Greenman, C., Bignell, G., Teague, J., Butler, A., Edkins, S., Stevens, C.*, et al.* (2005a). Somatic mutations of the protein kinase gene family in human lung cancer. Cancer research *65*, 7591-7595.

Davies, M., Robinson, M., Smith, E., Huntley, S., Prime, S., and Paterson, I. (2005b). Induction of an epithelial to mesenchymal transition in human immortal and malignant keratinocytes by TGF-beta1 involves MAPK, Smad and AP-1 signalling pathways. Journal of cellular biochemistry *95*, 918-931.

Davis, J. R., Huang, C.-Y. Y., Zanet, J., Harrison, S., Rosten, E., Cox, S., Soong, D. Y., Dunn, G. A., and Stramer, B. M. (2012). Emergence of embryonic pattern through contact inhibition of locomotion. Development (Cambridge, England) *139*, 4555-4560.

Davy, A., Gale, N. W., Murray, E. W., Klinghoffer, R. A., Soriano, P., Feuerstein, C., and Robbins, S. M. (1999). Compartmentalized signaling by GPI-anchored ephrin-A5 requires the Fyn tyrosine kinase to regulate cellular adhesion. Genes Dev *13*, 3125-3135.

Davy, A., and Robbins, S. M. (2000). Ephrin-A5 modulates cell adhesion and morphology in an integrin-dependent manner. The EMBO journal *19*, 5396-5405.

Day, B. W., Stringer, B. W., Al-Ejeh, F., Ting, M. J., Wilson, J., Ensbey, K. S., Jamieson, P. R., Bruce, Z. C., Lim, Y. C., Offenhäuser, C.*, et al.* (2013). EphA3 maintains tumorigenicity and is a therapeutic target in glioblastoma multiforme. Cancer cell *23*, 238-248.

Dechantsreiter, M., Planker, E., Mathä, B., Lohof, E., Hölzemann, G., Jonczyk, A., Goodman, S., and Kessler, H. (1999). N-Methylated cyclic RGD peptides as highly active and selective alpha(V)beta(3) integrin antagonists. Journal of medicinal chemistry *42*, 3033-3040.

Deininger, K., Eder, M., Kramer, E. R., Zieglgänsberger, W., Dodt, H.-U. U., Dornmair, K., Colicelli, J., and Klein, R. (2008). The Rab5 guanylate exchange factor Rin1 regulates endocytosis of the EphA4 receptor in mature excitatory neurons. Proceedings of the National Academy of Sciences of the United States of America *105*, 12539-12544.

Del Nery, E., Miserey-Lenkei, S., Falguières, T., Nizak, C., Johannes, L., Perez, F., and Goud, B. (2006). Rab6A and Rab6A' GTPases play non-overlapping roles in membrane trafficking. Traffic (Copenhagen, Denmark) *7*, 394-407.

Demory Beckler, M., Higginbotham, J. N., Franklin, J. L., Ham, A.-J. J., Halvey, P. J., Imasuen, I. E., Whitwell, C., Li, M., Liebler, D. C., and Coffey, R. J. (2013). Proteomic analysis of exosomes from mutant KRAS colon cancer cells identifies intercellular transfer of mutant KRAS. Molecular & cellular proteomics : MCP *12*, 343-355.

DePina, A., and Langford, G. (1999). Vesicle transport: the role of actin filaments and myosin motors. Microscopy research and technique *47*, 93-106.

Ding, L., Getz, G., Wheeler, D. A., Mardis, E. R., McLellan, M. D., Cibulskis, K., Sougnez, C., Greulich, H., Muzny, D. M., Morgan, M. B.*, et al.* (2008). Somatic mutations affect key pathways in lung adenocarcinoma. Nature *455*, 1069-1075.

Dozynkiewicz, M. A., Jamieson, N. B., Macpherson, I., Grindlay, J., van den Berghe, P. V., von Thun, A., Morton, J. P., Gourley, C., Timpson, P., Nixon, C.*, et al.* (2012). Rab25 and CLIC3 collaborate to promote integrin recycling from late endosomes/lysosomes and drive cancer progression. Developmental cell *22*, 131-145.

Drescher, U. (2002). Eph family functions from an evolutionary perspective. Current opinion in genetics & development *12*, 397-402.

Drescher, U., Kremoser, C., Handwerker, C., Löschinger, J., Noda, M., and Bonhoeffer, F. (1995). In vitro guidance of retinal ganglion cell axons by RAGS, a 25 kDa tectal protein related to ligands for Eph receptor tyrosine kinases. Cell *82*, 359-370.

Duffy, S. L., Steiner, K. A., Tam, P. P., and Boyd, A. W. (2006). Expression analysis of the Epha1 receptor tyrosine kinase and its high-affinity ligands Efna1 and Efna3 during early mouse development. Gene expression patterns : GEP *6*, 719-723.

Durbin, L., Brennan, C., Shiomi, K., Cooke, J., Barrios, A., Shanmugalingam, S., Guthrie, B., Lindberg, R., and Holder, N. (1998). Eph signaling is required for segmentation and differentiation of the somites. Genes & development *12*, 3096-3109.

Duxbury, M. S., Ito, H., Zinner, M. J., Ashley, S. W., and Whang, E. E. (2004). EphA2: a determinant of malignant cellular behavior and a potential therapeutic target in pancreatic adenocarcinoma. Oncogene *23*, 1448-1456.

Easty, D. J., Herlyn, M., and Bennett, D. C. (1995). Abnormal protein tyrosine kinase gene expression during melanoma progression and metastasis. International journal of cancer Journal international du cancer *60*, 129-136.

Echard, A., Jollivet, F., Martinez, O., Lacapère, J. J., Rousselet, A., Janoueix-Lerosey, I., and Goud, B. (1998). Interaction of a Golgi-associated kinesin-like protein with Rab6. Science (New York, NY) *279*, 580-585.

Echard, A., Opdam, F., de Leeuw, H., Jollivet, F., Savelkoul, P., Hendriks, W., Voorberg, J., Goud, B., and Fransen, J. (2000). Alternative splicing of the human Rab6A gene generates two close but functionally different isoforms. Molecular biology of the cell *11*, 3819-3833.

Elfrink, H., Zwart, R., Cavanillas, M., Schindler, A., Baas, F., and Scheper, W. (2012). Rab6 is a modulator of the unfolded protein response: implications for Alzheimer's disease. Journal of Alzheimer's disease : JAD *28*, 917-929.

Elowe, S., Holland, S. J., Kulkarni, S., and Pawson, T. (2001). Downregulation of the Ras-mitogen-activated protein kinase pathway by the EphB2 receptor tyrosine kinase is required for ephrin-induced neurite retraction. Molecular and cellular biology *21*, 7429-7441.

Ethell, I. M., Irie, F., Kalo, M. S., Couchman, J. R., Pasquale, E. B., and Yamaguchi, Y. (2001). EphB/syndecan-2 signaling in dendritic spine morphogenesis. Neuron *31*, 1001-1013.

Ewald, A. J., Brenot, A., Duong, M., Chan, B. S., and Werb, Z. (2008). Collective epithelial migration and cell rearrangements drive mammary branching morphogenesis. Developmental cell *14*, 570-581.

Falivelli, G., Lisabeth, E. M., Rubio de la Torre, E., Perez-Tenorio, G., Tosato, G., Salvucci, O., and Pasquale, E. B. (2013). Attenuation of eph receptor kinase activation in cancer cells by coexpressed ephrin ligands. PloS one *8*.

Fan, G.-H. H., Lapierre, L. A., Goldenring, J. R., Sai, J., and Richmond, A. (2004). Rab11-family interacting protein 2 and myosin Vb are required for CXCR2 recycling and receptor-mediated chemotaxis. Molecular biology of the cell *15*, 2456-2469.

Faoro, L., Singleton, P. A., Cervantes, G. M., Lennon, F. E., Choong, N. W., Kanteti, R., Ferguson, B. D., Husain, A. N., Tretiakova, M. S., Ramnath, N., *et al.* (2010). EphA2 mutation in lung squamous cell carcinoma promotes increased cell survival, cell invasion, focal adhesions, and mammalian target of rapamycin activation. The Journal of biological chemistry *285*, 18575-18585.

Fasen, K., Cerretti, D. P., and Huynh-Do, U. (2008). Ligand binding induces Cbl-dependent EphB1 receptor degradation through the lysosomal pathway. Traffic (Copenhagen, Denmark) *9*, 251-266.

Feldheim, D. A., Kim, Y. I., Bergemann, A. D., Frisén, J., Barbacid, M., and Flanagan, J. G. (2000). Genetic analysis of ephrin-A2 and ephrin-A5 shows their requirement in multiple aspects of retinocollicular mapping. Neuron *25*, 563-574.

Fielding, A. B., Schonteich, E., Matheson, J., Wilson, G., Yu, X., Hickson, G. R., Srivastava, S., Baldwin, S. A., Prekeris, R., and Gould, G. W. (2005). Rab11-FIP3 and FIP4 interact with Arf6 and the exocyst to control membrane traffic in cytokinesis. The EMBO journal *24*, 3389-3399.

Forcet, C., Stein, E., Pays, L., Corset, V., Llambi, F., Tessier-Lavigne, M., and Mehlen, P. (2002). Netrin-1-mediated axon outgrowth requires deleted in colorectal cancer-dependent MAPK activation. Nature *417*, 443-447.

Friedl, P., Borgmann, S., and Bröcker, E. B. (2001). Amoeboid leukocyte crawling through extracellular matrix: lessons from the Dictyostelium paradigm of cell movement. Journal of leukocyte biology *70*, 491-509.

Friedl, P., Locker, J., Sahai, E., and Segall, J. E. (2012). Classifying collective cancer cell invasion. Nature cell biology *14*, 777-783.

Fujito, T., Ikeda, W., Kakunaga, S., Minami, Y., Kajita, M., Sakamoto, Y., Monden, M., and Takai, Y. (2005). Inhibition of cell movement and proliferation by cell-cell contact-induced interaction of Necl-5 with nectin-3. The Journal of cell biology *171*, 165-173.

Fukai, J., Yokote, H., Yamanaka, R., Arao, T., Nishio, K., and Itakura, T. (2008). EphA4 promotes cell proliferation and migration through a novel EphA4-FGFR1 signaling pathway in the human glioma U251 cell line. Molecular cancer therapeutics *7*, 2768-2778.

Gammill, L. S., Gonzalez, C., and Bronner-Fraser, M. (2007). Neuropilin 2/semaphorin 3F signaling is essential for cranial neural crest migration and trigeminal ganglion condensation. Developmental neurobiology *67*, 47-56.

Gao, Q., Liu, W., Cai, J., Li, M., Gao, Y., Lin, W., and Li, Z. (2014). EphB2 promotes cervical cancer progression by inducing epithelial-mesenchymal transition. Human pathology *45*, 372-381.

Garcia, M. J., Pole, J. C., Chin, S.-F. F., Teschendorff, A., Naderi, A., Ozdag, H., Vias, M., Kranjac, T., Subkhankulova, T., Paish, C.*, et al.* (2005). A 1 Mb minimal amplicon at 8p11-12 in breast cancer identifies new candidate oncogenes. Oncogene *24*, 5235-5245.

Georgakopoulos, A., Litterst, C., Ghersi, E., Baki, L., Xu, C., Serban, G., and Robakis, N. K. (2006). Metalloproteinase/Presenilin1 processing of ephrinB regulates EphB-induced Src phosphorylation and signaling. The EMBO journal *25*, 1242-1252.

George, S. E., Simokat, K., Hardin, J., and Chisholm, A. D. (1998). The VAB-1 Eph receptor tyrosine kinase functions in neural and epithelial morphogenesis in C. elegans. Cell *92*, 633-643.

Gerety, S. S., Wang, H. U., Chen, Z. F., and Anderson, D. J. (1999). Symmetrical mutant phenotypes of the receptor EphB4 and its specific transmembrane ligand ephrin-B2 in cardiovascular development. Molecular cell *4*, 403-414.

Gerhardt, H., Golding, M., and Fruttiger…, M. (2003). VEGF guides angiogenic sprouting utilizing endothelial tip cell filopodia. The Journal of cell ….

Gerondopoulos, A., Langemeyer, L., Liang, J. R., Linford, A., and Barr, F. A. (2012). BLOC-3 mutated in Hermansky-Pudlak syndrome is a Rab32/38 guanine nucleotide exchange factor. Curr Biol *22*, 2135-2139.

Giamas, G., Filipović, A., Jacob, J., Messier, W., Zhang, H., Yang, D., Zhang, W., Shifa, B. A., Photiou, A., Tralau-Stewart, C.*, et al.* (2011). Kinome screening for regulators of

the estrogen receptor identifies LMTK3 as a new therapeutic target in breast cancer. Nature medicine *17*, 715-719.

Giampieri, S., Manning, C., Hooper, S., Jones, L., Hill, C. S., and Sahai, E. (2009). Localized and reversible TGFbeta signalling switches breast cancer cells from cohesive to single cell motility. Nature cell biology *11*, 1287-1296.

Giordano, S., Ponzetto, C., Di Renzo, M. F., Cooper, C. S., and Comoglio, P. M. (1989). Tyrosine kinase receptor indistinguishable from the c-met protein. Nature *339*, 155-156.

Goldenring, J. R., and Nam, K. T. (2011). Rab25 as a tumour suppressor in colon carcinogenesis. British journal of cancer *104*, 33-36.

Goud, B., Zahraoui, A., Tavitian, A., and Saraste, J. (1990). Small GTP-binding protein associated with Golgi cisternae. Nature *345*, 553-556.

Graveel, C. R., Tolbert, D., and Vande Woude, G. F. (2013). MET: a critical player in tumorigenesis and therapeutic target. Cold Spring Harbor perspectives in biology *5*.

Grigoriev, I., Splinter, D., Keijzer, N., Wulf, P. S., Demmers, J., Ohtsuka, T., Modesti, M., Maly, I. V., Grosveld, F., Hoogenraad, C. C., and Akhmanova, A. (2007). Rab6 regulates transport and targeting of exocytotic carriers. Dev Cell *13*, 305-314.

Grigoriev, I., Yu, K. L., Martinez-Sanchez, E., Serra-Marques, A., Smal, I., Meijering, E., Demmers, J., Peranen, J., Pasterkamp, R. J., van der Sluijs, P.*, et al.* (2011). Rab6, Rab8, and MICAL3 cooperate in controlling docking and fusion of exocytotic carriers. Curr Biol *21*, 967-974.

Grosshans, B. L., Andreeva, A., Gangar, A., Niessen, S., Yates, J. R., Brennwald, P., and Novick, P. (2006). The yeast lgl family member Sro7p is an effector of the secretory Rab GTPase Sec4p. The Journal of cell biology *172*, 55-66.

Gu, C., and Park, S. (2001). The EphA8 receptor regulates integrin activity through p110gamma phosphatidylinositol-3 kinase in a tyrosine kinase activity-independent manner. Molecular and cellular biology *21*, 4579-4597.

Hafner, C., Becker, B., Landthaler, M., and Vogt, T. (2006). Expression profile of Eph receptors and ephrin ligands in human skin and downregulation of EphA1 in nonmelanoma skin cancer. Modern pathology : an official journal of the United States and Canadian Academy of Pathology, Inc *19*, 1369-1377.

Hales, C., Griner, R., Hobdy-Henderson, K., Dorn, M., Hardy, D., Kumar, R., Navarre, J., Chan, E., Lapierre, L., and Goldenring, J. (2001). Identification and characterization of a family of Rab11-interacting proteins. The Journal of biological chemistry *276*, 39067-39075.

Hanahan, D., and Weinberg, R. A. (2000). The hallmarks of cancer. Cell *100*, 57-70.

Hanahan, D., and Weinberg, R. A. (2011). Hallmarks of cancer: the next generation. Cell *144*, 646-674.

Hansen, M. J., Dallal, G. E., and Flanagan, J. G. (2004). Retinal axon response to ephrin-as shows a graded, concentration-dependent transition from growth promotion to inhibition. Neuron *42*, 717-730.

Harris, E., and Cardelli, J. (2002). RabD, a Dictyostelium Rab14-related GTPase, regulates phagocytosis and homotypic phagosome and lysosome fusion. Journal of cell science *115*, 3703-3713.

Hattori, M., Osterfield, M., and Flanagan, J. G. (2000). Regulated cleavage of a contact-mediated axon repellent. Science (New York, NY) *289*, 1360-1365.

Hegerfeldt, Y., Tusch, M., Bröcker, E.-B. B., and Friedl, P. (2002). Collective cell movement in primary melanoma explants: plasticity of cell-cell interaction, beta1-integrin function, and migration strategies. Cancer research *62*, 2125-2130.

Hennigan, R. F., Hawker, K. L., and Ozanne, B. W. (1994). Fos-transformation activates genes associated with invasion. Oncogene *9*, 3591-3600.

Herath, N. I., and Boyd, A. W. (2010). The role of Eph receptors and ephrin ligands in colorectal cancer. International journal of cancer Journal international du cancer *126*, 2003-2011.

Herath, N. I., Doecke, J., Spanevello, M. D., Leggett, B. A., and Boyd, A. W. (2009). Epigenetic silencing of EphA1 expression in colorectal cancer is correlated with poor survival. British journal of cancer *100*, 1095-1102.

Himanen, J. P., Henkemeyer, M., and Nikolov, D. B. (1998). Crystal structure of the ligand-binding domain of the receptor tyrosine kinase EphB2. Nature *396*, 486-491.

Himanen, J. P., and Nikolov, D. B. (2002). Purification, crystallization and preliminary characterization of an Eph-B2/ephrin-B2 complex. Acta crystallographica Section D, Biological crystallography *58*, 533-535.

Himanen, J. P., Rajashankar, K. R., Lackmann, M., Cowan, C. A., Henkemeyer, M., and Nikolov, D. B. (2001). Crystal structure of an Eph receptor-ephrin complex. Nature *414*, 933-938.

Hingorani, S. R., Wang, L., Multani, A. S., Combs, C., Deramaudt, T. B., Hruban, R. H., Rustgi, A. K., Chang, S., and Tuveson, D. A. (2005). Trp53R172H and KrasG12D cooperate to promote chromosomal instability and widely metastatic pancreatic ductal adenocarcinoma in mice. Cancer cell *7*, 469-483.

Hirai, H., Maru, Y., Hagiwara, K., Nishida, J., and Takaku, F. (1987). A novel putative tyrosine kinase receptor encoded by the eph gene. Science (New York, NY) *238*, 1717-1720.

Hou, F., Yuan, W., Huang, J., Qian, L., Chen, Z., Ge, J., Wu, S., Chen, J., Wang, J., and Chen, Z. (2012). Overexpression of EphA2 correlates with epithelial-mesenchymal transition-related proteins in gastric cancer and their prognostic importance for postoperative patients. Medical oncology (Northwood, London, England) *29*, 2691-2700.

Hruban, R. H., Goggins, M., Parsons, J., and Kern, S. E. (2000). Progression model for pancreatic cancer. Clinical cancer research : an official journal of the American Association for Cancer Research *6*, 2969-2972.

Huai, J., and Drescher, U. (2001). An ephrin-A-dependent signaling pathway controls integrin function and is linked to the tyrosine phosphorylation of a 120-kDa protein. The Journal of biological chemistry *276*, 6689-6694.

Huang, J., Xiao, D., Li, G., Ma, J., Chen, P., Yuan, W., Hou, F., Ge, J., Zhong, M., and Tang, Y. (2014). EphA2 promotes epithelial–mesenchymal transition through the Wnt/ -catenin pathway in gastric cancer cells. Oncogene *33*, 2737-2747.

Huttenlocher, A., Lakonishok, M., Kinder, M., Wu, S., Truong, T., Knudsen, K. A., and Horwitz, A. F. (1998). Integrin and cadherin synergy regulates contact inhibition of migration and motile activity. The Journal of cell biology *141*, 515-526.

Huynh-Do, U., Vindis, C., Liu, H., Cerretti, D. P., McGrew, J. T., Enriquez, M., Chen, J., and Daniel, T. O. (2002). Ephrin-B1 transduces signals to activate integrin-mediated migration, attachment and angiogenesis. Journal of cell science *115*, 3073-3081.

Hwang, Y.-S. S., Lee, H.-S. S., Kamata, T., Mood, K., Cho, H. J., Winterbottom, E., Ji, Y. J., Singh, A., and Daar, I. O. (2013). The Smurf ubiquitin ligases regulate tissue separation via antagonistic interactions with ephrinB1. Genes & development *27*, 491-503.

Ieguchi, K., Tomita, T., Omori, T., Komatsu, A., Deguchi, A., Masuda, J., Duffy, S. L., Coulthard, M. G., Boyd, A., and Maru, Y. (2014). ADAM12-cleaved ephrin-A1 contributes to lung metastasis. Oncogene *33*, 2179-2190.

Inoue, E., Deguchi-Tawarada, M., Togawa, A., Matsui, C., Arita, K., Katahira-Tayama, S., Sato, T., Yamauchi, E., Oda, Y., and Takai, Y. (2009). Synaptic activity prompts gamma-secretase-mediated cleavage of EphA4 and dendritic spine formation. The Journal of cell biology *185*, 551-564.

Inoue, T., Hoshina, N., Nakazawa, T., Kiyama, Y., Kobayashi, S., Abe, T., Yamamoto, T., Manabe, T., and Yamamoto, T. (2014). LMTK3 deficiency causes pronounced locomotor hyperactivity and impairs endocytic trafficking. The Journal of neuroscience : the official journal of the Society for Neuroscience *34*, 5927-5937.

Irie, F., Okuno, M., Pasquale, E. B., and Yamaguchi, Y. (2005). EphrinB-EphB signalling regulates clathrin-mediated endocytosis through tyrosine phosphorylation of synaptojanin 1. Nature cell biology *7*, 501-509.

Irie, F., and Yamaguchi, Y. (2002). EphB receptors regulate dendritic spine development via intersectin, Cdc42 and N-WASP. Nature neuroscience *5*, 1117-1118.

Ivaska, J., Vuoriluoto, K., Huovinen, T., Izawa, I., Inagaki, M., and Parker, P. J. (2005). PKCepsilon-mediated phosphorylation of vimentin controls integrin recycling and motility. The EMBO journal *24*, 3834-3845.

Jacquemet, G., Green, D., Bridgewater, R., von Kriegsheim, A., Humphries, M., Norman, J., and Caswell, P. (2013). RCP-driven α5β1 recycling suppresses Rac and promotes RhoA activity via the RacGAP1-IQGAP1 complex. The Journal of cell biology *202*, 917-935.

Jagoe, W. N., Lindsay, A. J., Read, R. J., McCoy, A. J., McCaffrey, M. W., and Khan, A. R. (2006). Crystal structure of rab11 in complex with rab11 family interacting protein 2. Structure (London, England : 1993) *14*, 1273-1283.

Janes, P. W., Saha, N., Barton, W. A., Kolev, M. V., Wimmer-Kleikamp, S. H., Nievergall, E., Blobel, C. P., Himanen, J.-P. P., Lackmann, M., and Nikolov, D. B. (2005). Adam meets Eph: an ADAM substrate recognition module acts as a molecular switch for ephrin cleavage in trans. Cell *123*, 291-304.

Janes, P. W., Wimmer-Kleikamp, S. H., Frangakis, A. S., Treble, K., Griesshaber, B., Sabet, O., Grabenbauer, M., Ting, A. Y., Saftig, P., Bastiaens, P. I., and Lackmann, M. (2009). Cytoplasmic relaxation of active Eph controls ephrin shedding by ADAM10. PLoS biology *7*.

Jin, M., and Goldenring, J. R. (2006). The Rab11-FIP1/RCP gene codes for multiple protein transcripts related to the plasma membrane recycling system. Biochimica et biophysica acta *1759*, 281-295.

Jing, J., Junutula, J., Wu, C., Burden, J., Matern, H., Peden, A., and Prekeris, R. (2010). FIP1/RCP binding to Golgin-97 regulates retrograde transport from recycling endosomes to the trans-Golgi network. Molecular biology of the cell *21*, 3041-3053.

Jing, J., Tarbutton, E., Wilson, G., and Prekeris, R. (2009). Rab11-FIP3 is a Rab11-binding protein that regulates breast cancer cell motility by modulating the actin cytoskeleton. European journal of cell biology *88*, 325-341.

Joffre, C., Barrow, R., Ménard, L., Calleja, V., Hart, I. R., and Kermorgant, S. (2011). A direct role for Met endocytosis in tumorigenesis. Nature cell biology *13*, 827-837.

Johns, H., Gonzalez-Lopez, C., Sayers, C., Hollinshead, M., and Elliott, G. (2014). Rab6 dependent post-Golgi trafficking of HSV1 envelope proteins to sites of virus envelopment. Traffic (Copenhagen, Denmark) *15*, 157-178.

Johnson, L., Mercer, K., Greenbaum, D., Bronson, R. T., Crowley, D., Tuveson, D. A., and Jacks, T. (2001). Somatic activation of the K-ras oncogene causes early onset lung cancer in mice. Nature *410*, 1111-1116.

Jørgensen, C., Sherman, A., Chen, G. I., Pasculescu, A., Poliakov, A., Hsiung, M., Larsen, B., Wilkinson, D. G., Linding, R., and Pawson, T. (2009). Cell-specific

information processing in segregating populations of Eph receptor ephrin-expressing cells. Science (New York, NY) *326*, 1502-1509.

Jülich, D., Mould, A. P., Koper, E., and Holley, S. A. (2009). Control of extracellular matrix assembly along tissue boundaries via Integrin and Eph/Ephrin signaling. Development (Cambridge, England) *136*, 2913-2921.

Jung, J. J., Tiwari, A., Inamdar, S. M., Thomas, C. P., Goel, A., and Choudhury, A. (2012). Secretion of soluble vascular endothelial growth factor receptor 1 (sVEGFR1/sFlt1) requires Arf1, Arf6, and Rab11 GTPases. PloS one *7*, e44572.

Junutula, J., De Maziére, A., Peden, A., Ervin, K., Advani, R., van Dijk, S., Klumperman, J., and Scheller, R. (2004). Rab14 is involved in membrane trafficking between the Golgi complex and endosomes. Molecular biology of the cell *15*, 2218-2229.

Kadir, S., Astin, J. W., Tahtamouni, L., Martin, P., and Nobes, C. D. (2011). Microtubule remodelling is required for the front-rear polarity switch during contact inhibition of locomotion. Journal of cell science *124*, 2642-2653.

Kalluri, R., and Zeisberg, M. (2006). Fibroblasts in cancer. Nature reviews Cancer *6*, 392-401.

Kalo, M. S., and Pasquale, E. B. (1999). Signal transfer by eph receptors. Cell and tissue research *298*, 1-9.

Kapfhammer, J. P., and Raper, J. A. (1987). Collapse of growth cone structure on contact with specific neurites in culture. The Journal of neuroscience : the official journal of the Society for Neuroscience *7*, 201-212.

Kataoka, H., Igarashi, H., Kanamori, M., and Ihara…, M. (2004). Correlation of EPHA2 overexpression with high microvessel count in human primary colorectal cancer. Cancer ….

Kelly, E., Horgan, C., Adams, C., Patzer, T., Ní Shúilleabháin, D., Norman, J., and McCaffrey, M. (2010). Class I Rab11-family interacting proteins are binding targets for the Rab14 GTPase. Biology of the cell / under the auspices of the European Cell Biology Organization *102*, 51-62.

Kermorgant, S., Zicha, D., and Parker, P. J. (2004). PKC controls HGF-dependent c-Met traffic, signalling and cell migration. The EMBO journal *23*, 3721-3734.

Kikawa, K. D., Vidale, D. R., Van Etten, R. L., and Kinch, M. S. (2002). Regulation of the EphA2 kinase by the low molecular weight tyrosine phosphatase induces transformation. The Journal of biological chemistry *277*, 39274-39279.

Kim, J., Lee, H., Kim, Y., Yoo, S., Park, E., and Park, S. (2010). The SAM domains of Anks family proteins are critically involved in modulating the degradation of EphA receptors. Molecular and cellular biology *30*, 1582-1592.

Kimura, K., and Kimura, A. (2012). Rab6 is required for the exocytosis of cortical granules and the recruitment of separase to the granules during the oocyte-to-embryo transition in Caenorhabditis elegans. J Cell Sci *125*, 5897-5905.

Kitt, K. N., Hernández-Deviez, D., Ballantyne, S. D., Spiliotis, E. T., Casanova, J. E., and Wilson, J. M. (2008). Rab14 regulates apical targeting in polarized epithelial cells. Traffic (Copenhagen, Denmark) *9*, 1218-1231.

Koropouli, E., and Kolodkin, A. L. (2014). Semaphorins and the dynamic regulation of synapse assembly, refinement, and function. Current opinion in neurobiology *27C*, 1-7.

Krull, C. E., Lansford, R., Gale, N. W., Collazo, A., Marcelle, C., Yancopoulos, G. D., Fraser, S. E., and Bronner-Fraser, M. (1997). Interactions of Eph-related receptors and ligands confer rostrocaudal pattern to trunk neural crest migration. Current biology : CB *7*, 571-580.

Kulesa, P. M., and Fraser, S. E. (2000). In ovo time-lapse analysis of chick hindbrain neural crest cell migration shows cell interactions during migration to the branchial arches. Development (Cambridge, England) *127*, 1161-1172.

Laflamme, C., Assaker, G., Ramel, D., Dorn, J. F., She, D., Maddox, P. S., and Emery, G. (2012). Evi5 promotes collective cell migration through its Rab-GAP activity. J Cell Biol *198*, 57-67.

Lane, A. A., Cerretti, D. P., and Schoecklmann…, H. O. (1998). Eph receptors discriminate specific ligand oligomers to determine alternative signaling complexes, attachment, and assembly responses. … & development.

Lapierre, L. A., Kumar, R., Hales, C. M., Navarre, J., Bhartur, S. G., Burnette, J. O., Provance, D. W., Jr., Mercer, J. A., Bahler, M., and Goldenring, J. R. (2001). Myosin vb is associated with plasma membrane recycling systems. Mol Biol Cell *12*, 1843-1857.

Larsen, A. B., Pedersen, M. W., Stockhausen, M.-T. T., Grandal, M. V., van Deurs, B., and Poulsen, H. S. (2007). Activation of the EGFR gene target EphA2 inhibits epidermal growth factor-induced cancer cell motility. Molecular cancer research : MCR *5*, 283-293.

Larsen, A. B., Stockhausen, M.-T. T., and Poulsen, H. S. (2010). Cell adhesion and EGFR activation regulate EphA2 expression in cancer. Cellular signalling *22*, 636-644.

Larsson, A., Nodin, B., Syk, I., Palmquist, I., Uhlén, M., Eberhard, J., and Jirström, K. (2013). Podocalyxin-like protein expression in primary colorectal cancer and synchronous lymph node metastases. Diagnostic pathology *8*, 109.

Leber, M. F., and Efferth, T. (2009). Molecular principles of cancer invasion and metastasis (review). International journal of oncology *34*, 881-895.

Lee, H.-S. S., Mood, K., Battu, G., Ji, Y. J., Singh, A., and Daar, I. O. (2009). Fibroblast growth factor receptor-induced phosphorylation of ephrinB1 modulates its interaction with Dishevelled. Molecular biology of the cell *20*, 124-133.

Lemke, G. (2013). Biology of the TAM receptors. Cold Spring Harbor perspectives in biology *5*.

Levental, K. R., Yu, H., Kass, L., Lakins, J. N., Egeblad, M., Erler, J. T., Fong, S. F., Csiszar, K., Giaccia, A., Weninger, W.*, et al.* (2009). Matrix crosslinking forces tumor progression by enhancing integrin signaling. Cell *139*, 891-906.

Li, J., Peters, P. J., Bai, M., Dai, J., Bos, E., Kirchhausen, T., Kandror, K. V., and Hsu, V. W. (2007). An ACAP1-containing clathrin coat complex for endocytic recycling. The Journal of cell biology *178*, 453-464.

Li, J. J. J., Liu, D. P. P., Liu, G. T. T., and Xie, D. (2009). EphrinA5 acts as a tumor suppressor in glioma by negative regulation of epidermal growth factor receptor. Oncogene *28*, 1759-1768.

Liebig, C., Ayala, G., Wilks, J. A., Berger, D. H., and Albo, D. (2009). Perineural invasion in cancer: a review of the literature. Cancer *115*, 3379-3391.

Lindsay, A., Hendrick, A., Cantalupo, G., Senic-Matuglia, F., Goud, B., Bucci, C., and McCaffrey, M. (2002). Rab coupling protein (RCP), a novel Rab4 and Rab11 effector protein. The Journal of biological chemistry *277*, 12190-12199.

Lindsay, A., and McCaffrey, M. (2004). Characterisation of the Rab binding properties of Rab coupling protein (RCP) by site-directed mutagenesis. FEBS letters *571*, 86-92.

Linford, A., Yoshimura, S.-i., Nunes Bastos, R., Langemeyer, L., Gerondopoulos, A., Rigden, D., and Barr, F. (2012). Rab14 and its exchange factor FAM116 link endocytic recycling and adherens junction stability in migrating cells. Developmental cell *22*, 952-966.

Lisabeth, E. M., Fernandez, C., and Pasquale, E. B. (2012). Cancer somatic mutations disrupt functions of the EphA3 receptor tyrosine kinase through multiple mechanisms. Biochemistry *51*, 1464-1475.

Liu, C., Huang, H., Wang, C., Kong, Y., and Zhang, H. (2014). Involvement of ephrin receptor A4 in pancreatic cancer cell motility and invasion. Oncology letters *7*, 2165-2169.

Lobert, V. H., Brech, A., Pedersen, N. M., Wesche, J., Oppelt, A., Malerød, L., and Stenmark, H. (2010). Ubiquitination of alpha 5 beta 1 integrin controls fibroblast migration through lysosomal degradation of fibronectin-integrin complexes. Developmental cell *19*, 148-159.

Lu, R., Dalgalan, D., Mandell, E. K., Parker, S. S., Ghosh, S., and Wilson, J. M. (2015). PKCiota interacts with Rab14 and modulates epithelial barrier function through regulation of claudin-2 levels. Mol Biol Cell.

Lu, R., Johnson, D. L., Stewart, L., Waite, K., Elliott, D., and Wilson, J. M. (2014). Rab14 regulation of claudin-2 trafficking modulates epithelial permeability and lumen morphogenesis. Mol Biol Cell *25*, 1744-1754.

Luz, S., Cihil, K. M., Brautigan, D. L., Amaral, M. D., Farinha, C. M., and Swiatecka-Urban, A. (2014). LMTK2 Mediated Phosphorylation Regulates CFTR Endocytosis in Human Airway Epithelial Cells. The Journal of biological chemistry.

Macrae, M., Neve, R. M., Rodriguez-Viciana, P., Haqq, C., Yeh, J., Chen, C., Gray, J. W., and McCormick, F. (2005). A conditional feedback loop regulates Ras activity through EphA2. Cancer cell *8*, 111-118.

Maddigan, A., Truitt, L., Arsenault, R., Freywald, T., Allonby, O., Dean, J., Narendran, A., Xiang, J., Weng, A., Napper, S., and Freywald, A. (2011). EphB receptors trigger Akt activation and suppress Fas receptor-induced apoptosis in malignant T lymphocytes. Journal of immunology (Baltimore, Md : 1950) *187*, 5983-5994.

Makarov, A., Ylivinkka, I., Nyman, T. A., Hyytiäinen, M., and Keski-Oja, J. (2013). Ephrin-As, Eph receptors and integrin α3 interact and colocalise at membrane protrusions of U251MG glioblastoma cells. Cell biology international *37*, 1080-1088.

Mallard, F., Tang, B., Galli, T., Tenza, D., Saint-Pol, A., Yue, X., Antony, C., Hong, W., Goud, B., and Johannes, L. (2002). Early/recycling endosomes-to-TGN transport involves two SNARE complexes and a Rab6 isoform. The Journal of cell biology *156*, 653-664.

Mammoto, A., Ohtsuka, T., Hotta, I., Sasaki, T., and Takai, Y. (1999). Rab11BP/Rabphilin-11, a downstream target of rab11 small G protein implicated in vesicle recycling. The Journal of biological chemistry *274*, 25517-25524.

Marie, N., Lindsay, A., and McCaffrey, M. (2005). Rab coupling protein is selectively degraded by calpain in a Ca2+-dependent manner. The Biochemical journal *389*, 223-231.

Marston, D. J., Dickinson, S., and Nobes, C. D. (2003). Rac-dependent trans-endocytosis of ephrinBs regulates Eph-ephrin contact repulsion. Nature cell biology *5*, 879-888.

Martinez, O., Schmidt, A., Salaméro, J., Hoflack, B., Roa, M., and Goud, B. (1994). The small GTP-binding protein rab6 functions in intra-Golgi transport. The Journal of cell biology *127*, 1575-1588.

Matthews, H. K., Marchant, L., Carmona-Fontaine, C., Kuriyama, S., Larraín, J., Holt, M. R., Parsons, M., and Mayor, R. (2008). Directional migration of neural crest cells in vivo is regulated by Syndecan-4/Rac1 and non-canonical Wnt signaling/RhoA. Development (Cambridge, England) *135*, 1771-1780.

Mayor, R., and Carmona-Fontaine, C. (2010). Keeping in touch with contact inhibition of locomotion. Trends in cell biology *20*, 319-328.

Menges, C. W., and McCance, D. J. (2008). Constitutive activation of the Raf-MAPK pathway causes negative feedback inhibition of Ras-PI3K-AKT and cellular arrest through the EphA2 receptor. Oncogene *27*, 2934-2940.

Miao, H., Burnett, E., Kinch, M., Simon, E., and Wang, B. (2000). Activation of EphA2 kinase suppresses integrin function and causes focal-adhesion-kinase dephosphorylation. Nature cell biology *2*, 62-69.

Miao, H., Li, D.-Q. Q., Mukherjee, A., Guo, H., Petty, A., Cutter, J., Basilion, J. P., Sedor, J., Wu, J., Danielpour, D.*, et al.* (2009). EphA2 mediates ligand-dependent inhibition and ligand-independent promotion of cell migration and invasion via a reciprocal regulatory loop with Akt. Cancer cell *16*, 9-20.

Miao, H., Wei, B. R., Peehl, D. M., Li, Q., Alexandrou, T., Schelling, J. R., Rhim, J. S., Sedor, J. R., Burnett, E., and Wang, B. (2001). Activation of EphA receptor tyrosine kinase inhibits the Ras/MAPK pathway. Nature cell biology *3*, 527-530.

Micaroni, M., Stanley, A., Khromykh, T., Venturato, J., Wong, C., Lim, J., Marsh, B., Storrie, B., Gleeson, P., and Stow, J. (2013). Rab6a/a' are important Golgi regulators of pro-inflammatory TNF secretion in macrophages. PloS one *8*.

Mills, G., Jurisica, I., Yarden, Y., and Norman, J. (2009). Genomic amplicons target vesicle recycling in breast cancer. The Journal of clinical investigation *119*, 2123-2127.

Miserey-Lenkei, S., Waharte, F., Boulet, A., Cuif, M.-H., Tenza, D., El Marjou, A., Raposo, G., Salamero, J., Héliot, L., Goud, B., and Monier, S. (2007). Rab6-interacting protein 1 links Rab6 and Rab11 function. Traffic (Copenhagen, Denmark) *8*, 1385-1403.

Miura, K., Nam, J.-M. M., Kojima, C., Mochizuki, N., and Sabe, H. (2009). EphA2 engages Git1 to suppress Arf6 activity modulating epithelial cell-cell contacts. Molecular biology of the cell *20*, 1949-1959.

Miyazaki, T., Kato, H., Fukuchi, M., Nakajima, M., and Kuwano, H. (2003). EphA2 overexpression correlates with poor prognosis in esophageal squamous cell carcinoma. International journal of cancer Journal international du cancer *103*, 657-663.

Moore, R., Theveneau, E., Pozzi, S., Alexandre, P., Richardson, J., Merks, A., Parsons, M., Kashef, J., Linker, C., and Mayor, R. (2013). Par3 controls neural crest migration by promoting microtubule catastrophe during contact inhibition of locomotion. Development (Cambridge, England) *140*, 4763-4775.

Morello, V., Cabodi, S., Sigismund, S., Camacho-Leal, M., Repetto, D., Volante, M., Papotti, M., Turco, E., and Defilippi, P. (2011). β1 integrin controls EGFR signaling and tumorigenic properties of lung cancer cells. Oncogene *30*, 4087-4096.

Morton, J., Timpson, P., Karim, S., Ridgway, R., Athineos, D., Doyle, B., Jamieson, N., Oien, K., Lowy, A., Brunton, V.*, et al.* (2010). Mutant p53 drives metastasis and overcomes growth arrest/senescence in pancreatic cancer. Proceedings of the National Academy of Sciences of the United States of America *107*, 246-251.

Mudali, S. V., Fu, B., Lakkur, S. S., Luo, M., Embuscado, E. E., and Iacobuzio-Donahue, C. A. (2006). Patterns of EphA2 protein expression in primary and metastatic pancreatic carcinoma and correlation with genetic status. Clinical & experimental metastasis *23*, 357-365.

Mueller, B. K., Yamashita, T., Schaffar, G., and Mueller, R. (2006). The role of repulsive guidance molecules in the embryonic and adult vertebrate central nervous system. Philosophical transactions of the Royal Society of London Series B, Biological sciences *361*, 1513-1529.

Muller, P., Caswell, P., Doyle, B., Iwanicki, M., Tan, E., Karim, S., Lukashchuk, N., Gillespie, D., Ludwig, R., Gosselin, P.*, et al.* (2009). Mutant p53 drives invasion by promoting integrin recycling. Cell *139*, 1327-1341.

Muller, P., Trinidad, A., Timpson, P., Morton, J., Zanivan, S., van den Berghe, P., Nixon, C., Karim, S., Caswell, P., Noll, J., *et al.* (2013). Mutant p53 enhances MET trafficking and signalling to drive cell scattering and invasion. Oncogene *32*, 1252-1265.

Munarini, N., Jäger, R., Abderhalden, S., Zuercher, G., Rohrbach, V., Loercher, S., Pfanner-Meyer, B., Andres, A.-C. C., and Ziemiecki, A. (2002). Altered mammary epithelial development, pattern formation and involution in transgenic mice expressing the EphB4 receptor tyrosine kinase. Journal of cell science *115*, 25-37.

Murai, K. K., Nguyen, L. N., Irie, F., Yamaguchi, Y., and Pasquale, E. B. (2003). Control of hippocampal dendritic spine morphology through ephrin-A3/EphA4 signaling. Nature neuroscience *6*, 153-160.

Nakamura, T., Sakai, K., Nakamura, T., and Matsumoto, K. (2011). Hepatocyte growth factor twenty years on: Much more than a growth factor. Journal of gastroenterology and hepatology *26 Suppl 1*, 188-202.

Nakao, K., Mehta, K. R., Fridlyand, J., Moore, D. H., Jain, A. N., Lafuente, A., Wiencke, J. W., Terdiman, J. P., and Waldman, F. M. (2004). High-resolution analysis of DNA copy number alterations in colorectal cancer by array-based comparative genomic hybridization. Carcinogenesis *25*, 1345-1357.

Nasarre, P., Potiron, V., Drabkin, H., and Roche, J. (2010). Guidance molecules in lung cancer. Cell adhesion & migration *4*, 130-145.

Naslavsky, N., Rahajeng, J., Sharma, M., Jovic, M., and Caplan, S. (2006). Interactions between EHD proteins and Rab11-FIP2: a role for EHD3 in early endosomal transport. Molecular biology of the cell *17*, 163-177.

Nehls, V., Herrmann, R., and Hühnken…, M. (1998). Contact-dependent inhibition of angiogenesis by cardiac fibroblasts in three-dimensional fibrin gels in vitro: implications for microvascular network remodeling and …. Cell and tissue ….

Nikolova, Z., Djonov, V., Zuercher, G., Andres, A. C., and Ziemiecki, A. (1998). Cell-type specific and estrogen dependent expression of the receptor tyrosine kinase EphB4 and its ligand ephrin-B2 during mammary gland morphogenesis. Journal of cell science *111 (Pt 18)*, 2741-2751.

Noren, N. K., Yang, N.-Y. Y., Silldorff, M., Mutyala, R., and Pasquale, E. B. (2009). Ephrin-independent regulation of cell substrate adhesion by the EphB4 receptor. The Biochemical journal *422*, 433-442.

Oakley, R. A., and Tosney, K. W. (1993). Contact-mediated mechanisms of motor axon segmentation. The Journal of neuroscience : the official journal of the Society for Neuroscience *13*, 3773-3792.

Okazaki, T., Ni, A., Baluk, P., Ayeni, O. A., Kearley, J., Coyle, A. J., Humbles, A., and McDonald, D. M. (2009). Capillary defects and exaggerated inflammatory response in the airways of EphA2-deficient mice. The American journal of pathology *174*, 2388-2399.

Olive, K., Tuveson, D., Ruhe, Z., Yin, B., Willis, N., Bronson, R., Crowley, D., and Jacks, T. (2004). Mutant p53 gain of function in two mouse models of Li-Fraumeni syndrome. Cell *119*, 847-860.

Opdam, F., Echard, A., Croes, H., van den Hurk, J., van de Vorstenbosch, R., Ginsel, L., Goud, B., and Fransen, J. (2000). The small GTPase Rab6B, a novel Rab6 subfamily member, is cell-type specifically expressed and localised to the Golgi apparatus. Journal of cell science *113 (Pt 15)*, 2725-2735.

Oricchio, E., Nanjangud, G., Wolfe, A. L., Schatz, J. H., Mavrakis, K. J., Jiang, M., Liu, X., Bruno, J., Heguy, A., Olshen, A. B., *et al.* (2011). The Eph-receptor A7 is a soluble tumor suppressor for follicular lymphoma. Cell *147*, 554-564.

Orimo, A., Gupta, P. B., Sgroi, D. C., and Arenzana-Seisdedos…, F. (2005). Stromal fibroblasts present in invasive human breast carcinomas promote tumor growth and angiogenesis through elevated SDF-1/CXCL12 secretion. Cell.

Orsulic, S., and Kemler, R. (2000). Expression of Eph receptors and ephrins is differentially regulated by E-cadherin. Journal of cell science *113 (Pt 10)*, 1793-1802.

Paddock, S. W., and Dunn, G. A. (1986). Analysing collisions between fibroblasts and fibrosarcoma cells: fibrosarcoma cells show an active invasionary response. Journal of cell science *81*, 163-187.

Palamidessi, A., Frittoli, E., Garré, M., Faretta, M., Mione, M., Testa, I., Diaspro, A., Lanzetti, L., Scita, G., and Di Fiore, P. P. (2008). Endocytic trafficking of Rac is required for the spatial restriction of signaling in cell migration. Cell *134*, 135-147.

Palmer, A., Zimmer, M., Erdmann, K. S., Eulenburg, V., Porthin, A., Heumann, R., Deutsch, U., and Klein, R. (2002). EphrinB phosphorylation and reverse signaling: regulation by Src kinases and PTP-BL phosphatase. Molecular cell *9*, 725-737.

Pandey, A., Shao, H., Marks, R. M., Polverini, P. J., and Dixit, V. M. (1995). Role of B61, the ligand for the Eck receptor tyrosine kinase, in TNF-alpha-induced angiogenesis. Science (New York, NY) *268*, 567-569.

Parachoniak, C. A., Luo, Y., Abella, J. V., Keen, J. H., and Park, M. (2011). GGA3 functions as a switch to promote Met receptor recycling, essential for sustained ERK and cell migration. Developmental cell *20*, 751-763.

Parker, M., Roberts, R., Enriquez, M., Zhao, X., Takahashi, T., Pat Cerretti, D., Daniel, T., and Chen, J. (2004). Reverse endocytosis of transmembrane ephrin-B ligands via a clathrin-mediated pathway. Biochemical and biophysical research communications *323*, 17-23.

Parri, M., Buricchi, F., Giannoni, E., Grimaldi, G., Mello, T., Raugei, G., Ramponi, G., and Chiarugi, P. (2007). EphrinA1 activates a Src/focal adhesion kinase-mediated motility response leading to rho-dependent actino/myosin contractility. The Journal of biological chemistry *282*, 19619-19628.

Pasquale, E. (2010). Eph receptors and ephrins in cancer: bidirectional signalling and beyond. Nature reviews Cancer *10*, 165-180.

Peden, A., Schonteich, E., Chun, J., Junutula, J., Scheller, R., and Prekeris, R. (2004). The RCP-Rab11 complex regulates endocytic protein sorting. Molecular biology of the cell *15*, 3530-3541.

Pellinen, T., Arjonen, A., Vuoriluoto, K., Kallio, K., Fransen, J. A., and Ivaska, J. (2006). Small GTPase Rab21 regulates cell adhesion and controls endosomal traffic of beta1-integrins. The Journal of cell biology *173*, 767-780.

Penzes, P., Beeser, A., Chernoff, J., Schiller, M. R., Eipper, B. A., Mains, R. E., and Huganir, R. L. (2003). Rapid induction of dendritic spine morphogenesis by trans-synaptic ephrinB-EphB receptor activation of the Rho-GEF kalirin. Neuron *37*, 263-274.

Petrelli, A., Gilestro, G. F., Lanzardo, S., Comoglio, P. M., Migone, N., and Giordano, S. (2002). The endophilin-CIN85-Cbl complex mediates ligand-dependent downregulation of c-Met. Nature *416*, 187-190.

Pfeffer, S., and Aivazian, D. (2004). Targeting Rab GTPases to distinct membrane compartments. Nature reviews Molecular cell biology *5*, 886-896.

Pia, H., Damaris, P.-J., Maija, W., Jeff, A. K., David, O. A., Sukru, T., Don, W., Christiane, R., Tracy, M., Minna, A.*, et al.* (2004). Nonsense-mediated decay microarray analysis identifies mutations of EPHB2 in human prostate cancer. Nature genetics.

Piazza, F., Manni, S., Ruzzene, M., Pinna, L. A., Gurrieri, C., and Semenzato, G. (2012). Protein kinase CK2 in hematologic malignancies: reliance on a pivotal cell survival regulator by oncogenic signaling pathways. Leukemia *26*, 1174-1179.

Poliakov, A., Cotrina, M. L., Pasini, A., and Wilkinson, D. G. (2008). Regulation of EphB2 activation and cell repulsion by feedback control of the MAPK pathway. The Journal of cell biology *183*, 933-947.

Prekeris, R., Klumperman, J., and Scheller, R. H. (2000). A Rab11/Rip11 protein complex regulates apical membrane trafficking via recycling endosomes. Molecular cell *6*, 1437-1448.

Prévost, N., Woulfe, D. S., Jiang, H., Stalker, T. J., Marchese, P., Ruggeri, Z. M., and Brass, L. F. (2005). Eph kinases and ephrins support thrombus growth and stability by regulating integrin outside-in signaling in platelets. Proceedings of the National Academy of Sciences of the United States of America *102*, 9820-9825.

Prickett, T. D., Agrawal, N. S., Wei, X., Yates, K. E., Lin, J. C., Wunderlich, J. R., Cronin, J. C., Cruz, P., Rosenberg, S. A., and Samuels, Y. (2009). Analysis of the tyrosine kinome in melanoma reveals recurrent mutations in ERBB4. Nature genetics *41*, 1127-1132.

Qi, M., Williams, J., Chu, H., Chen, X., Wang, J.-J., Ding, L., Akhirome, E., Wen, X., Lapierre, L., Goldenring, J., and Spearman, P. (2013). Rab11-FIP1C and Rab14 direct plasma membrane sorting and particle incorporation of the HIV-1 envelope glycoprotein complex. PLoS pathogens *9*.

Qin, H., Noberini, R., Huan, X., Shi, J., Pasquale, E. B., and Song, J. (2010). Structural characterization of the EphA4-Ephrin-B2 complex reveals new features enabling Eph-ephrin binding promiscuity. The Journal of biological chemistry *285*, 644-654.

Rainero, E., Caswell, P., Muller, P., Grindlay, J., McCaffrey, M., Zhang, Q., Wakelam, M., Vousden, K., Graziani, A., and Norman, J. (2012). Diacylglycerol kinase α controls RCP-dependent integrin trafficking to promote invasive migration. The Journal of cell biology *196*, 277-295.

Rangaswami, H., Bulbule, A., and Kundu, G. C. (2006). Osteopontin: role in cell signaling and cancer progression. Trends in cell biology *16*, 79-87.

Ribatti, D., and Crivellato, E. (2012). "Sprouting angiogenesis", a reappraisal. Developmental biology.

Ridley, A. J., Schwartz, M. A., Burridge, K., Firtel, R. A., Ginsberg, M. H., Borisy, G., Parsons, J. T., and Horwitz, A. R. (2003). Cell migration: integrating signals from front to back. Science (New York, NY) *302*, 1704-1709.

Roberts, M., Barry, S., Woods, A., van der Sluijs, P., and Norman, J. (2001). PDGF-regulated rab4-dependent recycling of alphavbeta3 integrin from early endosomes is necessary for cell adhesion and spreading. Current biology : CB *11*, 1392-1402.

Roberts, M. S., Woods, A. J., Dale, T. C., Van Der Sluijs, P., and Norman, J. C. (2004). Protein kinase B/Akt acts via glycogen synthase kinase 3 to regulate recycling of alpha v beta 3 and alpha 5 beta 1 integrins. Molecular and cellular biology *24*, 1505-1515.

Rothschild, B. M., Tanke, D. H., Helbling, M., and Martin, L. D. (2003). Epidemiologic study of tumors in dinosaurs. Die Naturwissenschaften *90*, 495-500.

Roussos, E. T., Balsamo, M., Alford, S. K., Wyckoff, J. B., Gligorijevic, B., Wang, Y., Pozzuto, M., Stobezki, R., Goswami, S., Segall, J. E.*, et al.* (2011). Mena invasive (MenaINV) promotes multicellular streaming motility and transendothelial migration in a mouse model of breast cancer. Journal of cell science *124*, 2120-2131.

Saito, M., Tucker, D., Kohlhorst, D., Niessen, C., and Kowalczyk, A. (2012). Classical and desmosomal cadherins at a glance. Journal of cell science *125*, 2547-2552.

Santiago, A., and Erickson, C. A. (2002). Ephrin-B ligands play a dual role in the control of neural crest cell migration. Development (Cambridge, England) *129*, 3621-3632.

Sanz-Moreno, V., Gadea, G., Ahn, J., Paterson, H., Marra, P., Pinner, S., Sahai, E., and Marshall, C. J. (2008). Rac activation and inactivation control plasticity of tumor cell movement. Cell *135*, 510-523.

Sanz-Moreno, V., and Marshall, C. J. (2010). The plasticity of cytoskeletal dynamics underlying neoplastic cell migration. Current opinion in cell biology *22*, 690-696.

Sawamiphak, S., Seidel, S., Essmann, C. L., Wilkinson, G. A., Pitulescu, M. E., Acker, T., and Acker-Palmer, A. (2010). Ephrin-B2 regulates VEGFR2 function in developmental and tumour angiogenesis. Nature *465*, 487-491.

Schafer, J. C., Baetz, N. W., Lapierre, L. A., McRae, R. E., Roland, J. T., and Goldenring, J. R. (2014). Rab11-FIP2 interaction with MYO5B regulates movement of Rab11a-containing recycling vesicles. Traffic (Copenhagen, Denmark) *15*, 292-308.

Schaner, M. E., Ross, D. T., Ciaravino, G., Sorlie, T., Troyanskaya, O., Diehn, M., Wang, Y. C., Duran, G. E., Sikic, T. L., Caldeira, S.*, et al.* (2003). Gene expression patterns in ovarian carcinomas. Molecular biology of the cell *14*, 4376-4386.

Schwenk, R. W., Luiken, J. J., and Eckel, J. (2007). FIP2 and Rip11 specify Rab11a-mediated cellular distribution of GLUT4 and FAT/CD36 in H9c2-hIR cells. Biochemical and biophysical research communications *363*, 119-125.

Šestan, N., Artavanis-Tsakonas, S., and Rakic, P. (1999). Contact-dependent inhibition of cortical neurite growth mediated by notch signaling. Science.

Shamah, S. M., Lin, M. Z., Goldberg, J. L., Estrach, S., Sahin, M., Hu, L., Bazalakova, M., Neve, R. L., Corfas, G., Debant, A., and Greenberg, M. E. (2001). EphA receptors regulate growth cone dynamics through the novel guanine nucleotide exchange factor ephexin. Cell *105*, 233-244.

Sheen, V. (2014). Filamin A and Big2: A shared endocytic pathway. Bioarchitecture *4*.

Shiba, T., Koga, H., Shin, H.-W. W., Kawasaki, M., Kato, R., Nakayama, K., and Wakatsuki, S. (2006). Structural basis for Rab11-dependent membrane recruitment of a family of Rab11-interacting protein 3 (FIP3)/Arfophilin-1. Proceedings of the National Academy of Sciences of the United States of America *103*, 15416-15421.

Shintani, T., Ihara, M., Sakuta, H., Takahashi, H., Watakabe, I., and Noda, M. (2006). Eph receptors are negatively controlled by protein tyrosine phosphatase receptor type O. Nature neuroscience *9*, 761-769.

Sigismund, S., Argenzio, E., Tosoni, D., Cavallaro, E., Polo, S., and Di Fiore, P. P. (2008). Clathrin-mediated internalization is essential for sustained EGFR signaling but dispensable for degradation. Developmental cell *15*, 209-219.

Simon, G. C., Schonteich, E., Wu, C. C., Piekny, A., Ekiert, D., Yu, X., Gould, G. W., Glotzer, M., and Prekeris, R. (2008). Sequential Cyk-4 binding to ECT2 and FIP3 regulates cleavage furrow ingression and abscission during cytokinesis. The EMBO journal *27*, 1791-1803.

Simon, R., Richter, J., Wagner, U., Fijan, A., Bruderer, J., Schmid, U., Ackermann, D., Maurer, R., Alund, G., Knönagel, H.*, et al.* (2001). High-throughput tissue microarray analysis of 3p25 (RAF1) and 8p12 (FGFR1) copy number alterations in urinary bladder cancer. Cancer research *61*, 4514-4519.

Smith, A., Robinson, V., Patel, K., and Wilkinson, D. G. (1997). The EphA4 and EphB1 receptor tyrosine kinases and ephrin-B2 ligand regulate targeted migration of branchial neural crest cells. Current biology : CB *7*, 561-570.

Solanas, G., Cortina, C., Sevillano, M., and Batlle, E. (2011). Cleavage of E-cadherin by ADAM10 mediates epithelial cell sorting downstream of EphB signalling. Nature cell biology *13*, 1100-1107.

Song, W., Apodaca, G., and Mostov, K. (1994). Transcytosis of the polymeric immunoglobulin receptor is regulated in multiple intracellular compartments. J Biol Chem *269*, 29474-29480.

Song, W., Ma, Y., Wang, J., Brantley-Sieders, D., and Chen, J. (2014). JNK signaling mediates EPHA2-dependent tumor cell proliferation, motility, and cancer stem cell-like properties in non-small cell lung cancer. Cancer research *74*, 2444-2454.

Sonnichsen, B., De Renzis, S., Nielsen, E., Rietdorf, J., and Zerial, M. (2000). Distinct membrane domains on endosomes in the recycling pathway visualized by multicolor imaging of Rab4, Rab5, and Rab11. J Cell Biol *149*, 901-914.

Sorlie, T., Tibshirani, R., Parker, J., Hastie, T., Marron, J. S., Nobel, A., Deng, S., Johnsen, H., Pesich, R., Geisler, S.*, et al.* (2003). Repeated observation of breast tumor subtypes in independent gene expression data sets. Proceedings of the National Academy of Sciences of the United States of America *100*, 8418-8423.

Spacek, J., and Harris, K. M. (2004). Trans-endocytosis via spinules in adult rat hippocampus. The Journal of neuroscience : the official journal of the Society for Neuroscience *24*, 4233-4241.

Stanger, B. Z., and Dor, Y. (2006). Dissecting the cellular origins of pancreatic cancer. Cell cycle (Georgetown, Tex) *5*, 43-46.

Stenmark, H., Parton, R. G., Steele-Mortimer, O., Lutcke, A., Gruenberg, J., and Zerial, M. (1994). Inhibition of rab5 GTPase activity stimulates membrane fusion in endocytosis. EMBO J *13*, 1287-1296.

Storrie, B., Micaroni, M., Morgan, G., Jones, N., Kamykowski, J., Wilkins, N., Pan, T., and Marsh, B. (2012). Electron tomography reveals Rab6 is essential to the trafficking of trans-Golgi clathrin and COPI-coated vesicles and the maintenance of Golgi cisternal number. Traffic (Copenhagen, Denmark) *13*, 727-744.

Strachan, L. R., and Condic, M. L. (2004). Cranial neural crest recycle surface integrins in a substratum-dependent manner to promote rapid motility. The Journal of cell biology *167*, 545-554.

Stramer, B., Moreira, S., Millard, T., Evans, I., Huang, C.-Y. Y., Sabet, O., Milner, M., Dunn, G., Martin, P., and Wood, W. (2010). Clasp-mediated microtubule bundling regulates persistent motility and contact repulsion in Drosophila macrophages in vivo. The Journal of cell biology *189*, 681-689.

Sturge, J., Wienke, D., and Isacke, C. M. (2006). Endosomes generate localized Rho-ROCK-MLC2-based contractile signals via Endo180 to promote adhesion disassembly. The Journal of cell biology *175*, 337-347.

Sugiyama, N., Gucciardo, E., Tatti, O., Varjosalo, M., Hyytiäinen, M., Gstaiger, M., and Lehti, K. (2013). EphA2 cleavage by MT1-MMP triggers single cancer cell invasion via homotypic cell repulsion. The Journal of cell biology *201*, 467-484.

Takai, Y., Miyoshi, J., Ikeda, W., and Ogita, H. (2008). Nectins and nectin-like molecules: roles in contact inhibition of cell movement and proliferation. Nature reviews Molecular cell biology *9*, 603-615.

Takano, T., Tomomura, M., Yoshioka, N., Tsutsumi, K., Terasawa, Y., Saito, T., Kawano, H., Kamiguchi, H., Fukuda, M., and Hisanaga, S.-i. (2012). LMTK1/AATYK1 is a novel regulator of axonal outgrowth that acts via Rab11 in a Cdk5-dependent manner. The Journal of neuroscience : the official journal of the Society for Neuroscience *32*, 6587-6599.

Tanaka, M., Kuriyama, S., and Aiba, N. (2012). Nm23-H1 regulates contact inhibition of locomotion, which is affected by ephrin-B1. Journal of cell science *125*, 4343-4353.

Teddy, J. M., and Kulesa, P. M. (2004). In vivo evidence for short- and long-range cell communication in cranial neural crest cells. Development (Cambridge, England) *131*, 6141-6151.

Tepper, C., Gregg, J., Shi, X.-B., Vinall, R., Baron, C., Ryan, P., Desprez, P.-Y., Kung, H.-J., and deVere White, R. (2005). Profiling of gene expression changes caused by p53 gain-of-function mutant alleles in prostate cancer cells. The Prostate *65*, 375-389.

Thanos, C. D., Goodwill, K. E., and Bowie, J. U. (1999). Oligomeric structure of the human EphB2 receptor SAM domain. Science (New York, NY) *283*, 833-836.

Theveneau, E., and Mayor, R. (2012). Cadherins in collective cell migration of mesenchymal cells. Current opinion in cell biology *24*, 677-684.

Tolias, K. F., Bikoff, J. B., Kane, C. G., Tolias, C. S., Hu, L., and Greenberg, M. E. (2007). The Rac1 guanine nucleotide exchange factor Tiam1 mediates EphB receptor-dependent dendritic spine development. Proceedings of the National Academy of Sciences of the United States of America *104*, 7265-7270.

Tomita, T., Tanaka, S., Morohashi, Y., and Iwatsubo, T. (2006). Presenilin-dependent intramembrane cleavage of ephrin-B1. Molecular neurodegeneration *1*, 2.

Torres, R., Firestein, B. L., Dong, H., Staudinger, J., Olson, E. N., Huganir, R. L., Bredt, D. S., Gale, N. W., and Yancopoulos, G. D. (1998). PDZ proteins bind, cluster, and synaptically colocalize with Eph receptors and their ephrin ligands. Neuron *21*, 1453-1463.

Ullrich, O., Stenmark, H., Alexandrov, K., Huber, L. A., Kaibuchi, K., Sasaki, T., Takai, Y., and Zerial, M. (1993). Rab GDP dissociation inhibitor as a general regulator for the membrane association of rab proteins. J Biol Chem *268*, 18143-18150.

van de Wetering, M., Sancho, E., Verweij, C., de Lau, W., Oving, I., Hurlstone, A., van der Horn, K., Batlle, E., Coudreuse, D., Haramis, A. P.*, et al.* (2002). The beta-catenin/TCF-4 complex imposes a crypt progenitor phenotype on colorectal cancer cells. Cell *111*, 241-250.

Van den Broeck, A., Vankelecom, H., Van Eijsden, R., Govaere, O., and Topal, B. (2012). Molecular markers associated with outcome and metastasis in human pancreatic cancer. Journal of experimental & clinical cancer research : CR *31*, 68.

Vaught, D., Chen, J., and Brantley-Sieders, D. M. (2009). Regulation of mammary gland branching morphogenesis by EphA2 receptor tyrosine kinase. Molecular biology of the cell *20*, 2572-2581.

Veselý, P., and Weiss, R. A. (1973). Cell locomotion and contact inhibition of normal and neoplastic rat cells. International journal of cancer Journal international du cancer *11*, 64-76.

Vihanto, M. M., Vindis, C., Djonov, V., Cerretti, D. P., and Huynh-Do, U. (2006). Caveolin-1 is required for signaling and membrane targeting of EphB1 receptor tyrosine kinase. Journal of cell science *119*, 2299-2309.

Vindis, C., Cerretti, D. P., Daniel, T. O., and Huynh-Do, U. (2003). EphB1 recruits c-Src and p52Shc to activate MAPK/ERK and promote chemotaxis. The Journal of cell biology *162*, 661-671.

Vindis, C., Teli, T., Cerretti, D. P., Turner, C. E., and Huynh-Do, U. (2004). EphB1-mediated cell migration requires the phosphorylation of paxillin at Tyr-31/Tyr-118. The Journal of biological chemistry *279*, 27965-27970.

Vogelstein, B., Lane, D., and Levine, A. (2000). Surfing the p53 network. Nature *408*, 307-310.

Wahl, S., Barth, H., Ciossek, T., Aktories, K., and Mueller, B. K. (2000). Ephrin-A5 induces collapse of growth cones by activating Rho and Rho kinase. The Journal of cell biology *149*, 263-270.

Wang, H., and Brautigan, D. L. (2006). Peptide microarray analysis of substrate specificity of the transmembrane Ser/Thr kinase KPI-2 reveals reactivity with cystic fibrosis transmembrane conductance regulator and phosphorylase. Molecular & cellular proteomics : MCP *5*, 2124-2130.

Wang, H. U., and Anderson, D. J. (1997). Eph family transmembrane ligands can mediate repulsive guidance of trunk neural crest migration and motor axon outgrowth. Neuron *18*, 383-396.

Wang, H. U., Chen, Z. F., and Anderson, D. J. (1998). Molecular distinction and angiogenic interaction between embryonic arteries and veins revealed by ephrin-B2 and its receptor Eph-B4. Cell *93*, 741-753.

Wang, Y., Nakayama, M., Pitulescu, M. E., Schmidt, T. S., Bochenek, M. L., Sakakibara, A., Adams, S., Davy, A., Deutsch, U., Lüthi, U.*, et al.* (2010). Ephrin-B2 controls VEGF-induced angiogenesis and lymphangiogenesis. Nature *465*, 483-486.

Wang, Y. j., Ota, S., Kataoka, H., Kanamori, M., Li, Z. y., Band, H., Tanaka, M., and Sugimura, H. (2002). Negative regulation of EphA2 receptor by Cbl. Biochemical and biophysical research communications *296*, 214-220.

Warshaw, A. L., and Fernández-del Castillo, C. (1992). Pancreatic carcinoma. The New England journal of medicine *326*, 455-465.

Wei, M. C., Zong, W. X., Cheng, E. H., Lindsten, T., Panoutsakopoulou, V., Ross, A. J., Roth, K. A., MacGregor, G. R., Thompson, C. B., and Korsmeyer, S. J. (2001). Proapoptotic BAX and BAK: a requisite gateway to mitochondrial dysfunction and death. Science (New York, NY) *292*, 727-730.

Weinberg, R. (2007). The nature of Cancer in The Biology of Cancer: Garland Science).

Welz, T., Wellbourne-Wood, J., and Kerkhoff, E. (2014). Orchestration of cell surface proteins by Rab11. Trends Cell Biol *24*, 407-415.

White, D., Caswell, P., and Norman, J. (2007). alpha v beta3 and alpha5beta1 integrin recycling pathways dictate downstream Rho kinase signaling to regulate persistent cell migration. The Journal of cell biology *177*, 515-525.

White, J., Johannes, L., Mallard, F., Girod, A., Grill, S., Reinsch, S., Keller, P., Tzschaschel, B., Echard, A., Goud, B., and Stelzer, E. (1999). Rab6 coordinates a novel Golgi to ER retrograde transport pathway in live cells. The Journal of cell biology *147*, 743-760.

Wimmer-Kleikamp, S. H., Janes, P. W., Squire, A., Bastiaens, P. I., and Lackmann, M. (2004). Recruitment of Eph receptors into signaling clusters does not require ephrin contact. The Journal of cell biology *164*, 661-666.

Wolf, K., Wu, Y. I., Liu, Y., Geiger, J., Tam, E., Overall, C., Stack, M. S., and Friedl, P. (2007). Multi-step pericellular proteolysis controls the transition from individual to collective cancer cell invasion. Nature cell biology *9*, 893-904.

Wybenga-Groot, L. E., Baskin, B., Ong, S. H., Tong, J., Pawson, T., and Sicheri, F. (2001). Structural basis for autoinhibition of the Ephb2 receptor tyrosine kinase by the unphosphorylated juxtamembrane region. Cell *106*, 745-757.

Wykosky, J., Palma, E., Gibo, D. M., Ringler, S., Turner, C. P., and Debinski, W. (2008). Soluble monomeric EphrinA1 is released from tumor cells and is a functional ligand for the EphA2 receptor. Oncogene *27*, 7260-7273.

Xiong, B., Bayat, V., Jaiswal, M., Zhang, K., Sandoval, H., Charng, W. L., Li, T., David, G., Duraine, L., Lin, Y. Q.*, et al.* (2012). Crag is a GEF for Rab11 required for rhodopsin trafficking and maintenance of adult photoreceptor cells. PLoS Biol *10*, e1001438.

Xu, K., Tzvetkova-Robev, D., Xu, Y., Goldgur, Y., Chan, Y.-P. P., Himanen, J. P., and Nikolov, D. B. (2013). Insights into Eph receptor tyrosine kinase activation from crystal

structures of the EphA4 ectodomain and its complex with ephrin-A5. Proceedings of the National Academy of Sciences of the United States of America *110*, 14634-14639.

Xu, Y., Zhang, H., Lit, L. C., Grothey, A., Athanasiadou, M., Kiritsi, M., Lombardo, Y., Frampton, A. E., Green, A. R., Ellis, I. O.*, et al.* (2014). The kinase LMTK3 promotes invasion in breast cancer through GRB2-mediated induction of integrin $ß_1$. Science signaling *7*.

Yamamoto, H., Koga, H., Katoh, Y., Takahashi, S., Nakayama, K., and Shin, H.-W. (2010). Functional cross-talk between Rab14 and Rab4 through a dual effector, RUFY1/Rabip4. Molecular biology of the cell *21*, 2746-2755.

Yamashita, T., Ohneda, K., Nagano, M., Miyoshi, C., Kaneko, N., Miwa, Y., Yamamoto, M., Ohneda, O., and Fujii-Kuriyama, Y. (2008). Hypoxia-inducible transcription factor-2alpha in endothelial cells regulates tumor neovascularization through activation of ephrin A1. The Journal of biological chemistry *283*, 18926-18936.

Yan, Q., Sun, W., Kujala, P., Lotfi, Y., Vida, T., and Bean, A. (2005). CART: an Hrs/actinin-4/BERP/myosin V protein complex required for efficient receptor recycling. Molecular biology of the cell *16*, 2470-2482.

Yates, P. A., Roskies, A. L., McLaughlin, T., and O'Leary, D. D. (2001). Topographic-specific axon branching controlled by ephrin-As is the critical event in retinotectal map development. The Journal of neuroscience : the official journal of the Society for Neuroscience *21*, 8548-8563.

Yazaki, Y., Hara, Y., Tamaki, H., Fukaya, M., and Sakagami, H. (2014). Endosomal localization of FIP3/Arfophilin-1 and its involvement in dendritic formation of mouse hippocampal neurons. Brain research *1557*, 55-65.

Yin, Y., Yamashita, Y., Noda, H., Okafuji, T., Go, M. J., and Tanaka, H. (2004). EphA receptor tyrosine kinases interact with co-expressed ephrin-A ligands in cis. Neuroscience research *48*, 285-296.

Yoo, S., Shin, J., and Park, S. (2010). EphA8-ephrinA5 signaling and clathrin-mediated endocytosis is regulated by Tiam-1, a Rac-specific guanine nucleotide exchange factor. Molecules and cells *29*, 603-609.

Yoon, S.-O. O., Shin, S., and Mercurio, A. M. (2005). Hypoxia stimulates carcinoma invasion by stabilizing microtubules and promoting the Rab11 trafficking of the alpha6beta4 integrin. Cancer research *65*, 2761-2769.

Yu, H. H., Zisch, A. H., Dodelet, V. C., and Pasquale, E. B. (2001). Multiple signaling interactions of Abl and Arg kinases with the EphB2 receptor. Oncogene *20*, 3995-4006.

Zantek, N. D., Azimi, M., Fedor-Chaiken, M., Wang, B., Brackenbury, R., and Kinch, M. S. (1999). E-cadherin regulates the function of the EphA2 receptor tyrosine kinase. Cell growth & differentiation : the molecular biology journal of the American Association for Cancer Research *10*, 629-638.

Zerial, M., and McBride, H. (2001). Rab proteins as membrane organizers. Nature reviews Molecular cell biology *2*, 107-117.

Zhang, J., Liu, X., Datta, A., Govindarajan, K., Tam, W., Han, J., George, J., Wong, C., Ramnarayanan, K., Phua, T.*, et al.* (2009). RCP is a human breast cancer-promoting gene with Ras-activating function. The Journal of clinical investigation *119*, 2171-2183.

Zhuang, G., Hunter, S., Hwang, Y., and Chen, J. (2007). Regulation of EphA2 receptor endocytosis by SHIP2 lipid phosphatase via phosphatidylinositol 3-Kinase-dependent Rac1 activation. The Journal of biological chemistry *282*, 2683-2694.

Zhuang, G., Song, W., Amato, K., Hwang, Y., Lee, K., Boothby, M., Ye, F., Guo, Y., Shyr, Y., Lin, L.*, et al.* (2012). Effects of cancer-associated EPHA3 mutations on lung cancer. Journal of the National Cancer Institute *104*, 1182-1197.

Zimmer, M., Palmer, A., Köhler, J., and Klein, R. (2003). EphB-ephrinB bi-directional endocytosis terminates adhesion allowing contact mediated repulsion. Nature cell biology *5*, 869-878.

Zou, J. X., Wang, B., Kalo, M. S., Zisch, A. H., Pasquale, E. B., and Ruoslahti, E. (1999). An Eph receptor regulates integrin activity through R-Ras. Proceedings of the National Academy of Sciences of the United States of America *96*, 13813-13818.